



UNIVERSIDAD DE OVIEDO

DEPARTAMENTO DE INGENIERÍA QUÍMICA Y TECNOLOGÍA DEL MEDIO

AMBIENTE

Programa de Doctorado en Ingeniería Química, Ambiental y Bioalimentaria

INTEGRACIÓN DE TECNOLOGÍAS DE ADSORCIÓN Y ELECTROQUÍMICAS PARA LA ELIMINACIÓN DE CONTAMINANTES EMERGENTES EN AGUAS

TESIS DOCTORAL POR

Yolanda Patiño Menéndez

2016

Índice

Índice.....	I
Resumen	V
Abstract.....	IX
Lista de tablas	XIII
Lista de figuras.....	XV
Difusión de la Tesis Doctoral.....	XVII
1. Introducción.....	1
1.1. Contaminantes emergentes.....	3
1.2. Clasificación de los contaminantes emergentes.....	6
1.2.1. Retardantes de llama bromados	6
1.2.2. Parafinas cloradas.....	7
1.2.3. Pesticidas polares	7
1.2.4. Compuestos perfluorados.....	9
1.2.5. Fármacos y productos de higiene personal	9
1.2.6. Drogas.....	10
1.3. Contaminantes emergentes en España.....	10
1.4. Métodos de eliminación de contaminantes emergentes.....	12
1.4.1. Métodos físico-químicos	13
1.4.2. Procesos de oxidación avanzada.....	14
1.4.3. Tratamientos biológicos	17

1.4.4. Tecnologías híbridas.....	17
1.5. Alternativa propuesta para la eliminación de contaminantes emergentes.....	18
1.6. Fundamentos teóricos del proceso de adsorción	21
1.6.1. Factores que influyen en el proceso de adsorción.....	23
1.6.2. Adsorción por lotes (discontinuo).....	23
1.6.3. Adsorción en lecho fijo.....	25
1.6.4. Regeneración del adsorbente.....	28
1.6.5. Materiales carbonosos empleados como adsorbentes	29
1.7. Fundamentos teóricos de las técnicas voltamperométricas	32
.....	
1.7.1. Técnicas voltamperométricas de barrido	33
1.7.2. Celda de trabajo.....	35
1.7.3. Electrodos de trabajo basados en carbono.....	36
1.8. Bibliografía.....	38
2. Objetivos	49
3. Metodología experimental	53
3.1. Técnicas de caracterización de materiales	55
3.1.1. Técnicas de microscopía electrónica.....	55
3.1.2. Espectroscopía fotoelectrónica de Rayos-X (XPS)	56
3.1.3. Fisisorción de nitrógeno	57
3.1.4. Potencial zeta: punto isoeléctrico	58
3.1.5. Desorción a temperatura programada (TPD)	59
3.1.6. Termogravimetría	59
3.2. Ensayos de adsorción	60
3.2.1. Ensayos de adsorción en discontinuo	60
3.2.2. Ensayos de adsorción/desorción en continuo	61
3.3. Degradación electroquímica.....	62
3.4. Análisis de muestras.....	63
3.4.1. Cromatografía líquida	63
3.4.2. Cromatografía de gases.....	63
3.4.3. Espectrofotometría.....	63

4. Pre-concentración	65
4.1. Adsorción en discontinuo.....	67
4.1.1. Publicación I	69
4.1.2. Publicación II	79
4.2. Estudios de adsorción-desorción en lecho fijo	89
4.2.1. Publicación III.....	91
4.2.2. Publicación IV.....	103
5. Degradación electroquímica.....	131
5.1. Publicación V	137
5.2. Publicación VI.....	157
6. Conclusiones	177
7. Conclusions	183

Resumen

Cada día, la industria, la agricultura y la actividad humana, liberan muchas sustancias químicas a los efluentes acuosos. Con los años, estas prácticas han ido generando diferentes contaminantes y han alterado el ciclo del agua, lo que ha causado una preocupación mundial por sus posibles efectos sobre la vida acuática y humana. Estos nuevos compuestos presentes en el agua, se denominan “contaminantes emergentes” (CEs) y han sido detectados en el medio ambiente en un intervalo de concentraciones de ngL^{-1} a μgL^{-1} . La Agencia de Protección Medioambiental de Estados Unidos (US EPA) define los contaminantes emergentes como nuevos compuestos químicos sin regular y cuyo impacto sobre el medio ambiente y la salud humana son escasamente conocidos a día de hoy.

El principal problema acerca de estos contaminantes, es la ineficiencia de las plantas de tratamiento de aguas residuales para su eliminación. Por ello, la importancia de desarrollar tecnologías eficaces para su eliminación es una necesidad ambiental. Estos compuestos están presentes en agua a bajas concentraciones, por lo que es necesario procesar una gran cantidad de agua para eliminar una pequeña cantidad de contaminantes, por lo que el proceso sería costoso. Por esta razón, en esta Tesis, se propone una nueva estrategia basada en dos etapas: pre-concentración mediante adsorción-desorción y degradación mediante tecnologías electroquímicas.

Tres contaminantes emergentes pertenecientes a tres de las familias más importantes, han sido seleccionados como representativos para evaluar la viabilidad del método propuesto. Ácido nalidixico (NAL) como representativo de productos farmacéuticos, 1,8-diclorooctano (DCO) como representativo de las parafinas cloradas de cadena corta (SCCPs), y dentro de los disruptores endocrino, el 2-(4-metilfenoxi)etanol (MPET) ha sido elegido como representante del Triton X-100 ($\text{C}_{14}\text{H}_{22}\text{O}(\text{C}_2\text{H}_4\text{O})_n$), debido a la facilidad de análisis.

Para el primer paso, se llevaron a cabo experimentos de adsorción en discontinuo con el fin de explorar el comportamiento y mecanismo de adsorción, ajustando los resultados a los modelos de Langmuir y Freundlich. Se seleccionaron diferentes adsorbentes carbonosos: carbones activos, como material amorgo (GC-900 y GF-40), nanofibras de carbono (CNF) como material microporoso, grafito de alta superficie específica (HSAG-500) por su carácter mesoporoso y nanotubos de carbono (MWCNT) como nuevo material carbonoso.

La capacidad de adsorción, es en todos los casos, un orden de magnitud mayor para DCO que para NAL y MPET, debido a su elevada hidrofobicidad. La cantidad de adsorbato retenido, por lo general, sigue el orden: GC-900 > GF-40 > HSAG-500 > MWCNT > CNF, coincidente con el área superficial externa de los materiales, con la excepción de los carbones activados.

Se estudió la influencia de la temperatura mediante adsorción a tres temperaturas diferentes, obteniendo los parámetros termodinámicos. ΔH° es negativa en todos los casos, lo que indica la naturaleza exotérmica del proceso de adsorción. La naturaleza espontánea ha sido confirmada mediante la energía libre de Gibbs ($\Delta G^\circ < 0$), y los valores negativos de entropía, muy próximos a cero, indican que la adsorción tiene poco efecto en el orden de las especies adsorbidas.

Con el fin de estudiar el efecto de la química superficial en el rendimiento de la adsorción, se estudiaron tres nanotubos de carbono funcionalizados -MWCNT-COOH, MWCNT-NH₂ and N-CNT -. Para DCO y NAL, los MWCNT presentan la mayor capacidad de adsorción, mientras que el valor más bajo, se corresponde con MWCNT-COOH. Por el contrario, para MPET, el orden es: N-CNT > MWCNT-NH₂> MWCNT-COOH > MWCNT, siendo la capacidad de adsorción obtenida por los nanotubos modificados, incluso mayor que para los carbones activos.

Se ha demostrado que la capacidad de adsorción depende tanto de las propiedades del adsorbato como de la morfología del adsorbente.

Una vez que se realizaron los experimentos en batch, se llevó a cabo la pre-concentración mediante adsorción en lecho fijo usando como adsorbentes: GF-40, HSAG-500 and MWCNT. Se obtuvieron las curvas de ruptura y se evaluó la capacidad de pre-concentración y la eficiencia de la regeneración. En todos los casos, las curvas de ruptura fueron ajustadas a tres modelos: BDST, Thomas y Yoon-Nelson, permitiendo así una estimación de los parámetros de adsorción, muy útil para el diseño a gran escala. Las capacidades de adsorción en el punto de ruptura y saturación, sigue el orden: GF-40 > MWCNT > HSAG-500. La morfología y la superficie química justifican estas diferencias. Teniendo en cuenta la capacidad de adsorción normalizada (mg adsorbato / m² adsorbente), la tendencia es: MWCNT > GF-40 > HSAG-500, debido al elevado volumen de mesoporos de MWCNT.

Se llevó a cabo la desorción con agua a mayor temperatura que el proceso de adsorción con el fin de obtener una concentración más elevada en el efluente. La concentración obtenida para los tres compuestos sigue el orden: DCO > MPET > NAL. Esto puede ser debido a la interacción π - π del MPET y NAL con los materiales carbonosos, ya que esto dificulta la adsorción. Aunque GF-40 presenta una elevada capacidad de adsorción, no es posible la pre-concentración con este adsorbente. Para los otros adsorbentes, la pre-concentración obtenida con MWCNT es mayor que la obtenida con HSAG-500. En resumen, MWCNT presenta la mayor capacidad de adsorción normalizada y el mayor poder de concentración, con un factor de concentración que sigue el orden: DCO (3.4) > MPET (2.8) > NAL (2.1).

Para la segunda etapa, se lleva a cabo la degradación mediante técnicas electroquímicas, utilizando un sistema convencional de tres electrodos, consistente en un electrodo de carbón vitreo (GCE) como electrodo de trabajo, de calomelanos saturado (SCE) como electrodo de referencia y de platino (Pt) como electrodo auxiliar. Es posible mejorar la sensibilidad y selectividad mediante modificación del electrodo de trabajo, por lo que se estudió el efecto de la modificación del GCE con nanotubos de carbono (MWCNT-GCE). La respuesta electroquímica del electrodo modificado está fuertemente influenciada por los grupos funcionales presentes en su estructura, por ello se estudió el efecto de nanotubos de carbono funcionalizados con grupos carboxilo (MWCNT-COOH) y grupos amino (MWCNT-NH₂).

En el caso del DCO, no ha sido posible la degradación mediante esta técnica, ya que no se obtuvieron picos de reducción u oxidación, probablemente debido a que esta molécula no presenta grupos funcionales electroquímicamente activos. EN el caso de NAL, se obtuvo un pico de reducción irreversible, mientras que para el MPET se obtuvo un pico de oxidación irreversible. La degradación de NAL se llevó a cabo por voltamperometría de pulso diferencial (DPV), mientras que la degradación de MPET se llevó a cabo por voltamperometría cíclica (CV). La corriente de pico obtenida mejora cuando la superficie del GCE se modifica con MWCNTs, lo que indica que los MWCNTs presentan una elevada actividad hacia la reducción y oxidación de NAL y MPET respectivamente. En el caso del NAL aunque la respuesta con electrodo GCE modificado con nanotubos de carbono funcionalizados es mejor que para GCE, es menor que para MWCNT-GCE, debido a una menor adsorción sobre la superficie del electrodo. Por el contrario, para MPET, la tendencia sigue el orden: MWCNT > MWCNT-NH₂ > MWCNT-COOH, coincidente con la fuerza de interacción entre la superficie del electrodo y el MPET.

Se obtuvo una degradación completa para ambos compuestos, NAL y MPET, bajo las condiciones óptimas obtenidas para cada compuesto (pH, velocidad de barrido y tiempo de deposición). En el caso del NAL, se han identificada dos sub-productos de degradación, mientras que en el caso del MPET, la degradación tuvo lugar sin observar la formación de ningún subproducto. Por lo tanto se obtuvo una degradación completa para el MPET obteniendo como productos finales dióxido de carbono y agua.

Abstract

Every day, industry, agriculture and human activity, release many chemicals into the water streams. Over the years, these practices have generated different pollutants and altered the water cycle, which has caused global concern about its possible effects on aquatic and human life. These new compounds present in water are called "emerging pollutants" (EPs) and have been detected in the environment in a concentration range from ngL^{-1} to μgL^{-1} . The US EPA (United States – Environmental Protection Agency) defines emerging pollutants as new chemicals without regulatory status and whose impact on environment and human health is nowadays poorly understood.

The main problem about these pollutants, is the inefficiency of wastewater treatment plants for their removal. Thus, the importance of developing effective technologies for their removal is an urgent environmental need. They are present in water at very low concentration, so it is necessary to process a large amount of water to remove a small amount of pollutant and the process would be costly. For this reason, in this Thesis, a new strategy is proposed based on two steps: pre-concentration by adsorption-desorption process and degradation by electrochemical technologies.

Three different emerging pollutants belonging to three of the most important families have been selected as representatives to evaluate the feasibility of the proposed method. Nalidixic acid (NAL) as representative of pharmaceutical products. 1,8-dichlorooctane (DCO) as representative of Short Chain Chlorinated Paraffin (SCCPs), and within endocrine disruptors, 2-(4-methylphenoxy)ethanol (MPET) has been chosen as representative of Triton X-100 ($\text{C}_{14}\text{H}_{22}\text{O}(\text{C}_2\text{H}_4\text{O})_n$) due to the easiness of analysis.

For the first step, batch adsorption experiments were carried out in order to explore the adsorption behavior and mechanism, fitting the results to both Langmuir and Freundlich models.

Abstract

Different carbonaceous adsorbents have been selected as adsorbents: activated carbon as amorphous materials (GC-900 and GF-40), carbon nanofiber (CNF) as microporous material, high surface area graphite (HSAG-500) for its mesoporous character and multiwall carbon nanotube (MWCNT) as a new carbon material.

The adsorption capacity is in all cases, one order of magnitude higher for DCO than for NAL and MPET, due to the higher hydrophobicity of DCO. The amount of adsorbate retained, generally follows the order: GC-900 > GF-40 > HSAG-500 > MWCNT > CNF, coincident with the external surface area of the materials, with the exception of the activated carbons.

The influence of the temperature was studied at three different temperatures and the thermodynamic parameters were obtained. ΔH° is negative in all cases, indicating the exothermic nature of the adsorption process. The spontaneous nature is confirmed ($\Delta G^\circ < 0$) and the entropy is negative, but close to zero, indicating that the adsorption has little effect in the order of the adsorbed species.

In order to study the effect of surface chemistry on adsorption performance, three functionalized carbon nanotubes -MWCNT-COOH, MWCNT-NH₂ and N-CNT - were considered. For DCO and NAL, MWCNT presents the highest adsorption capacity and the lowest value is for MWCNT-COOH. Contrary, for MPET, the order is: N-CNT > MWCNT-NH₂> MWCNT-COOH > MWCNT; and, in this case, the adsorption capacity presented by modified-MWCNT is even better than this of activated carbon.

It has been shown that the adsorption capacity depends on both, the adsorbate properties and the adsorbent morphology.

Once batch experiments were done, the pre-concentration was carried out by fixed bed adsorption onto GF-40, HSAG-500 and MWCNT. The breakthrough curves have been recorded and the pre-concentration capacity and regeneration efficiency were evaluated. In all cases the breakthrough curves were modelled by the three models – BDST, Thomas and Yoon-Nelson – allowing to obtain an estimation of the adsorption parameters, very useful for further designing and scaling-up purposes. The adsorption capacities at breakthrough time and saturation time follow the order: GF-40 > MWCNT > HSAG-500. The morphology and chemistry surface justified these differences. Taking into account the normalized adsorption capacity, (mg adsorbate / m² adsorbent), the trend is: MWCNT > GF-40 > HSAG-500, due to the highest mesoporous volume of MWCNT.

Desorption with water at higher temperature than the adsorption process was carried out in order to obtain a higher effluent concentration after desorption. The concentration obtained for the three adsorbates follows the order: DCO > MPET > NAL. It can be due to the π - π interaction of MPET and NAL with the carbon materials since this interaction hinders desorption. Although

GF-40 presents a high adsorption capacity, it is no possible to pre-concentrate the pollutant with this adsorbent. For the other adsorbents, the pre-concentration obtained onto MWCNT is higher than the obtained for HSAG-500. In summary, MWCNT presents the highest normalized adsorption capacity and the greatest concentration power, with a pre-concentration factor, which follows the order: DCO (3.4) > MPET (2.8) > NAL (2.1)

For the second step, the degradation is carried out by electrochemical techniques, using a conventional three electrodes system, consisting of a glassy carbon (GCE) as working electrode, saturated calomel (SCE) as the reference electrode and platinum (Pt) as an auxiliary electrode. The sensitivity and selectivity can be improved by modification of the working electrode, so MWCNT modified GCE has been tested. The electrochemical response of the MWCNT modified electrode is greatly influenced by the functional groups present in its structure; that is why functionalized MWCNT by carboxylic (MWCNT-COOH) and by amine (MWCNT-NH₂) groups were also checked.

In the case of DCO, degradation was not possible by this technique, since no reduction/oxidation peaks was obtained, probably because this molecule does not present electrochemically active functional groups. In the case of NAL, an irreversible reduction peak was obtained. Contrary in the case of MPET, an irreversible oxidation peak was achieved. The NAL degradation was carried out by differential pulse voltammetry (DPV), while MPET was implemented by cyclic voltammetry (CV). The peak current improved when the surface of GCE is modified with MWCNTs, which indicates that MWCNTs possessed high activity toward NAL reduction and MPET oxidation. In the case of NAL, although the response of modified-GCE with functionalized MWCNT is better than for bare-GCE, it is less than for MWCNT-GCE, due to a less adsorption on the electrode surface. Contrary, for MPET, the trend follows the order: MWCNT > MWCNT-NH₂ > MWCNT-COOH, coincident with the strength of interaction between the electrode surface and MPET.

A complete degradation was obtained for both, NAL and MPET under the optimal conditions obtained for each compound (pH, scan rate and deposition time). In the case of NAL, two different sub-products were identified, while in the case of MPET the degradation takes place without observing the formation of any new compound. Therefore the MPET oxidation was completed, having as end products carbon dioxide and water.

Lista de tablas

Tabla 1.1. Clasificación de los pesticidas en función de su toxicidad, vida media de efectividad y familia química.....	8
Tabla 1.2. Niveles de contaminantes emergentes en España, (●) niveles significativos, (○) cantidades mínimas (Adaptada de la OCU, 2013)	11
Tabla 1.3. Eliminación de contaminantes emergentes mediante adsorción.....	13
Tabla 1.4. Ventajas e inconvenientes de los procesos de oxidación avanzada (AOPs)	16
Tabla 1.5. Propiedades físico-químicas del ácido nalidíxico, 1,8-diclorooctano y 2-(4-metilfenoxi)etanol	21
Tabla 1.6. Principales diferencias entre fisisorción y quimisorción.....	22
Tabla 1.7. Tecnologías de regeneración del adsorbente.....	28
Tabla 1.8. Disposición de los planos de grafeno en las nanofibras de carbono	31

Lista de figuras

Figura 1.1. Publicaciones en las últimas décadas sobre CEs en aguas (Expert Research en Science Direct: "emerging contaminant or emerging pollutant")	5
Figura 1.2. Estado de la calidad de las aguas en río y lagos de los países miembro de la Unión Europea (Fuente: Agencia Europa de Medio Ambiente).....	11
Figura 1.3. Clasificación de las técnicas de oxidación avanzada homogéneas.....	15
Figura 1.4. Sistemas de tratamiento biológico (Adaptada de Fernández-Alba <i>et al.</i>).....	17
Figura 1.5. Esquema del método de eliminación propuesto	19
Figura 1.6. Estructura química del ácido nalidíxico.....	20
Figura 1.7. Estructura química del 1,8-diclorooctano	20
Figura 1.8. Estructura química del 2-(4-metilfenoxi)etanol	21
Figura 1.9. Curva de ruptura y avance de la zona de transferencia de masa	26
Figura 1.10. Tipos de carbón activo en función del tamaño de partícula. Carbón activado en polvo (CAP) y carbón activado granular (GAP)	30
Figura 1.11. Esquema de la estructura de nanotubos de carbono de pared simple (SWCNT) y de pared múltiple (MWCNT)	30
Figura 1.12. (a) Señal de perturbación y (b) voltamperograma al aplicar voltamperometría de pulso lineal	33
Figura 1.13. (a) Señal de perturbación y (b) voltamperograma al aplicar voltametría cíclica	33

Figura 1.14. (a) Señal de perturbación y (b) voltamperograma al aplicar voltametría normal de pulso	34
Figura 1.15. (a) Señal de perturbación y (b) voltamperograma al aplicar voltamperometría diferencial de pulso.....	34
Figura 1.16. (a) Señal de perturbación y (b) voltamperograma al aplicar voltamperometría de onda cuadrada.....	35
Figura 1.17. Esquema de una celda electroquímica	35
Figura 2.1. Clasificación de las isotermas de adsorción	58
Figura 2.2. Instalación de experimentos para adsorción en discontinuo.....	60
Figura 2.3. Dispositivo experimental para adsorción y desorción en continuo.....	61
Figura 2.4. Celda electroquímica con sistema de tres electrodos.....	62
Figura 4.1. Gráfico conceptual del proceso de adsorción en discontinuo.....	68
Figura 4.2. Gráfico conceptual del proceso de adsorción en continuo	89
Figura 5.1. Gráfico conceptual del proceso de degradación electroquímica	132

Difusión de la Tesis Doctoral

Artículos científicos

- ✓ “*Performance of different carbonaceous material for emerging pollutant adsorption*”, Yolanda Patiño, Eva Díaz, Salvador Ordóñez. Chemosphere 119 (2015) S124-S130.
- ✓ “*Adsorption of emerging pollutants on functionalized multiwall carbon nanotubes*” Yolanda Patiño, Eva Díaz, Salvador Ordóñez, Esteban Gallegos-Suarez, Antonio Guerrero-Ruiz, Inmaculada Rodríguez Ramos. Chemosphere 136 (2015) 174-180.
- ✓ “*Pre-concentration of nalidixic acid through adsorption-desorption cycles_ Adsorbent selection and modeling*”, Yolanda Patiño, Eva Díaz, Salvador Ordóñez. Chemical Engineering Journal 283 (2016) 486-494.

- ✓ “*Pre-concentration of emerging pollutants by adsorption-desorption onto carbonaceous materials: selection of the best adsorbent*”, Yolanda Patiño, Eva Díaz, Salvador Ordóñez. Chemical Engineering Journal, Enviada.
- ✓ “*Electrochemical reduction of nalidixic acid at glassy carbon electrode modified with multi-walled carbon nanotubes*”, Yolanda Patiño, Sanaz Pilehvar, Eva Díaz, Salvador Ordóñez, Karolien De Wael. ElectrochimicaActa, En preparación.
- ✓ “*Electrochemical oxidation of 2-(4-methylphenoxy)ethanol in water using glassy carbon electrode modified with multiwall carbon nanotubes sensor*”. Yolanda Patiño, Eva Díaz, Salvador Ordóñez. En preparación.

Artículos en revistas de divulgación científica:

- ✓ Y. Patiño, E. Díaz, S. Ordóñez, *Water micropollutants: classification and treatment technologies*, Avances en Ciencias e Ingeniería 5 (2) (2014) 1-20. ISSN. 0718-8706

Comunicaciones a congresos

1. Y. Patiño, E. Díaz, S. Ordóñez. *Utilización de técnicas de adsorción para la concentración de microcontaminantes en aguas*. XXXIV Reunión Bienal de la Real Sociedad Española de Química, Santander, 15-18 Septiembre 2013. Póster.
2. A. Guerrero-Ruiz, M. Almohalla, I. Rodríguez-Ramos, Y. Patiño, E. Díaz, S. Ordóñez. *Consequences of nitrogen surface groups on the performance of carbon nanotubes for the abatement of water emerging pollutants by adsorption and electrocatalytic methods*. 10th International Symposium on the Characterization of Porous Solids (COPS-X), Granada, 11-14 Mayo 2014. Póster.
3. Y. Patiño, E. Díaz, S. Ordóñez. *Funcionalización de nanotubos de carbono para su uso como adsorbentes y electrocatalizadores en la eliminación de microcontaminantes*. I Encuentro de Jóvenes Investigadores de la SECAT, Málaga, 22-24 Junio 2014. Oral + Poster.
4. Y. Patiño, E. Díaz, S. Ordóñez. *Estudio del efecto catalítico de los nanotubos de carbono en la reducción electrocatalítica de contaminantes emergentes*. SECAT'15, Barcelona, 13-15 Julio 2015. Poster.
5. Y. Patiño , S. Pilevar, K. De Wael , E. Diaz , S. Ordoñez. *Catalytic effect of carbon nanotubes in the electrochemical reduction of nalidixic acid*. XII European Congress on Catalysis, Kazan, 30 agosto- 4 Septiembre 2015. Póster.

Agradecimientos

Quiero expresar mis agradecimientos a todas las personas e Instituciones que han hecho posible el desarrollo de esta Tesis Doctoral:

A los doctores Eva Díaz y Salvador Ordóñez, por confiar en mi desde el principio, por su gran apoyo y ayuda.

A la Fundación para el Fomento de Asturias de la Investigación Científica Aplicada y la Tecnología (FICYT), sin cuya ayuda económica, mediante una beca "Severo Ochoa" y una beca de estancia breve, este trabajo no hubiera sido posible.

A la doctora Karolien de Wael, por permitirme realizar mi estancia doctoral en su grupo de investigación de la Universidad de Amberes, así como a todos los compañeros que conocí y con los que trabajé durante la misma.

Expresar todo mi agradecimiento también a todos mis compañeros del Departamento de Ingeniería Química, es especial a mis compañeros y amigos del grupos de "Reactores".

Finalmente a toda mi familia, y en especial a Marcos, por su gran apoyo, sobre todo en el último tirón.



Capítulo I

Introducción

En este capítulo se proporciona información sobre el problema medioambiental en relación a la presencia de contaminantes emergentes en agua. También incluye algún concepto teórico sobre los métodos de eliminación existentes. Se profundiza en técnicas de adsorción y electroquímicas, empleadas en esta investigación para hacer frente a la eliminación de este tipo de contaminantes

- 1.1. Contaminantes emergentes
- 1.2. Clasificación de los contaminantes emergentes
- 1.3. Contaminantes emergentes en España
- 1.4. Métodos de eliminación de contaminantes emergentes
- 1.5. Alternativa propuesta para la eliminación de contaminantes emergentes
- 1.6. Fundamentos teóricos del proceso de adsorción
- 1.7. Fundamentos teóricos de las técnicas voltamperométricas
- 1.8. Bibliografía

I. Introducción

A diario las diferentes industrias, la agricultura y ganadería, así como la población en general hacen uso del agua, liberando a la misma una gran cantidad de productos químicos que contribuyen al aumento de la contaminación de las aguas. Todo ello ha ido generando diversos contaminantes que han ido alterando el ciclo del agua, aumentando así la preocupación global sobre los posibles impactos sobre el medio ambiente y la salud humana.

Durante los últimos 25 años, y debido a la gran mejora de las técnicas analíticas, se ha descubierto la presencia de un gran número de sustancias químicas hasta ahora desconocidas tanto en vertidos residuales como en aguas naturales superficiales y subterráneas, [1-3]. Estos compuestos son los denominados “contaminantes emergentes” (CEs), o microcontaminantes. Su descubrimiento ha hecho que seamos conscientes de la posible presencia en nuestras aguas de otros compuestos, que aunque se denominen “emergentes”, es posible que lleven décadas o incluso siglos en nuestras aguas. Lo más preocupante es el desconocimiento para muchos de ellos, de las concentraciones que serían permisibles o de sus posibles efectos adversos sobre el medio ambiente y los seres vivos.

1.1. Contaminantes emergentes

Los contaminantes emergentes son microcontaminantes orgánicos de diverso origen y naturaleza química cuya presencia y posibles consecuencias sobre el medio ambiente y la salud humana habían pasado inadvertidos hasta hace poco [4]. Son considerados emergentes debido a que aún no se encuentran regulados o están siendo sometidos a un proceso de regulación [4]. Se encuentran presentes en aguas en concentraciones del orden de $\text{ng}\cdot\text{L}^{-1}$ a $\mu\text{g}\cdot\text{L}^{-1}$, pero a pesar de estas bajas concentraciones, son considerados muy perjudiciales ante la posibilidad de causar diversos efectos en los organismos.

Los efectos negativos más destacados de los contaminantes emergentes sobre los seres vivos, son su función como disruptores endocrinos, sus efectos carcinógenos, su posibilidad de bioacumulación y la toxicidad crónica de muchos de estos compuestos, etc. [5, 6]. Se ha demostrado la existencia de una relación directa entre la exposición a estos contaminantes y variaciones en el metabolismo, problemas de crecimiento y fertilidad, y feminización en diversos tipos de organismos [7, 8].

Las principales fuentes de CEs, son tanto las aguas residuales tipo doméstico, como las procedentes de las actividades ganaderas y agrícolas, así como los efluentes de las plantas de tratamiento de aguas residuales (EDAR), las cuales no están actualmente diseñadas para tratar este tipo de sustancias [9]. Entre los efluente que llegan a las EDAR y que son fuente de CEs se encuentran las aguas residuales domésticas, residuos hospitalarios o efluentes de plantas de fabricación de productos químicos [10, 11]. De este modo, una elevada cantidad de estos compuestos altamente tóxicos, entra al medio ambiente, contaminando los acuíferos y sistemas fluviales [11]. Por lo tanto, debido a su alta producción y consumo, y a su paso sin alteración alguna a través de las EDAR, no necesitan ser persistentes para ocasionar efectos negativos [9]. Los contaminantes emergentes, han sido detectados en ríos, mares, lagos, sedimentos, aguas subterráneas e incluso en el agua del grifo, por lo que son muchas las fuentes a partir de las cuales nos encontramos expuestos a estos compuestos [12-16].

La preocupación por la determinación de estos compuestos y por la búsqueda de técnicas que permitan su completa eliminación comenzó a mediados de los años 60, principios de los 70. Stumm-Zollinger y Fair [17] iniciaron el interés sobre determinados CEs como son los productos farmacéuticos y productos de higiene personal y sus posibles efectos sobre el medio ambiente. Continuando la preocupación con el trabajo realizado por Tabak y Bunch [18] sobre hormonas esteroideas como microcontaminantes presentes en agua. Uno de los primeros trabajos sobre la presencia de alquilfenoles etoxilados, se le atribuye a Lech et al, [19], estudiando la actividad estrogénica del nonilfenol, uno de los alquilfenoles etoxilados más preocupantes.

Con el paso de los años, la preocupación sobre los contaminantes emergentes ha ido en aumento, de tal manera que los estudios científicos sobre su determinación y métodos de eliminación en aguas han crecido de manera exponencial en los últimos años (Figura 1.1). Es tal la importancia de estos contaminantes, que los grandes organismos dedicados a la protección de la salud pública y medioambiental como son la Organización Mundial de la Salud (OMS), la Agencia de Protección Medioambiental de los Estados Unidos (USEPA) o la Agencia Europea de Medio Ambiente (AEMA), también han hecho eco de esta problemática y se encuentra entre sus principales líneas de investigación. En el caso de la OMS, son continuos sus estudios acerca de los posibles efectos sobre los CEs, incluyendo por ejemplo informes científicos confirmado el riesgo de ciertos CEs, los cuales a dosis muy bajas pueden producir alteraciones en el equilibrio hormonal, daños al sistema reproductor, cáncer, etc. [20]. Por otro lado, la EPA cuenta con un

programa de monitoreo de contaminantes emergentes con el fin de poder entender mejor estos productos químicos [21]. Así mismo, también son continuos los estudios que realiza la AEMA sobre los diferentes grupos de contaminantes emergentes, así como los posibles impactos sobre la vida y salud humana [22].

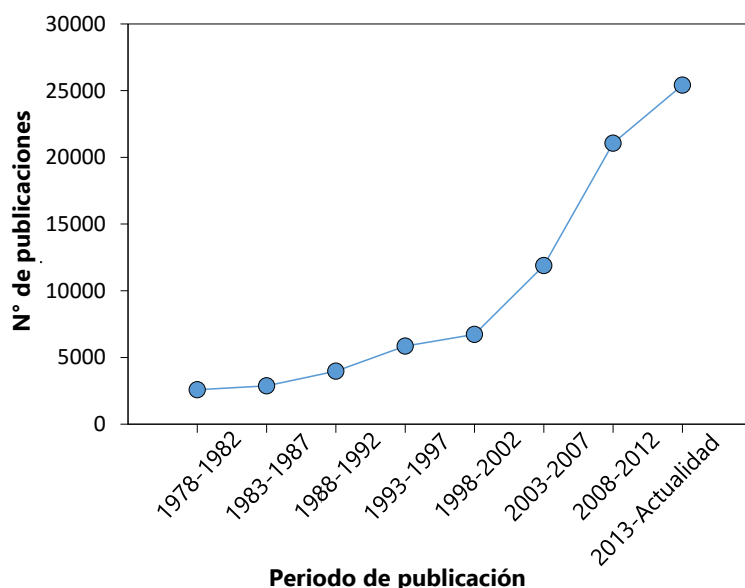


Figura 1.1. Publicaciones en las últimas décadas sobre CEs en aguas (Expert Research en Science Direct: “emerging contaminant or emerging pollutant”).

La creciente preocupación sobre la presencia de estos contaminantes en las aguas, que ponen en riesgo su calidad, hizo que la Comisión de la UE pusiera la protección del agua dentro de sus prioridades. De esta preocupación surge la Directiva Marco Europea del Agua (DMA) (Directiva 2000/60/CE, del 22 de Diciembre de 2000), con el fin de unificar las actuaciones en materia de gestión del agua en la Unión Europea [23]. Esta Directiva fue parcialmente modificada por la Directiva 2008/105/CE [24]. De este modo, la Unión Europea coordina la gestión de aguas superficiales, continentales de transición, aguas costeras y subterráneas, con el objetivo de prevenir y reducir su contaminación, promoviendo un uso sostenible que garantice su disponibilidad a largo plazo. Mediante esta Directiva se establece que para el 2015 debe de haberse alcanzado el buen estado de los ecosistemas acuáticos en todos los países de la UE. Con el fin de controlar la presencia de estos contaminantes, la Directiva Marco del Agua, presentó inicialmente una lista de 33 sustancias clasificadas como prioritarias, siendo 20 de ellas catalogadas como peligrosas. Esta lista puede ser revisada cada cuatro años, posibilitando la incorporación de nuevas sustancias que puedan suponer un riesgo para el medio acuático o a través del mismo; de hecho, mediante la Directiva 2013/39/CE, se añadieron 12 nuevos compuestos a la lista de sustancias prioritarias, formada finalmente por 45 compuestos.

1.2. Clasificación de los contaminantes emergentes

El término “contaminantes emergentes” abarca una gran variedad de productos de uso diario, tanto industrial como doméstico. Aunque por regla general son compuestos desconocidos hasta no hace mucho, en algunos casos se trata de compuestos ampliamente utilizados, como por ejemplo el caso de los plaguicidas, para los que se ha descubierto que presentan productos de degradación altamente tóxicos.

Según la bibliografía, puede hacerse una clasificación de los CEs en seis grandes grupos:

- Retardantes de llama bromados
- Cloroalcanos
- Pesticidas polares
- Compuestos perfluorados
- Fármacos y productos de higiene personal
- Drogas

1.2.1. Retardantes de llama bromados

Los retardantes de llama bromados (BFRs) se emplean en una gran variedad de productos comerciales. Se usan como aditivos o reactivos de una amplia variedad de polímeros (espumas de poliestireno, poliestireno de elevado impacto y resinas epoxy). Forman parte también de un elevado número de materiales de construcción y material electrónico. Se producen en la actualidad unas 20-25 clases de BFRs, destacando: tetrabromobisfenol A, Hexabromociclohexano y Difenil-éteres plobrominados [25].

Se ha encontrado presencia de BFRs en muestras humanas, animales y medioambientales, observándose como sus concentraciones son crecientes según se avanza en la cadena alimenticia, así como se detectó mayor presencia en sitios cercanos a puntos de reciclaje de residuos electrónicos [26].

En cuanto a sus efectos adversos, no están completamente demostrados sus efectos carcinogénicos así como su comportamiento como disruptores endocrinos [4]. Por ello se ha aplicado para estos compuestos el principio de precaución, basado en tomar medidas preventivas antes de esperar a obtener pruebas de la causa y efecto del contaminante en cuestión. No obstante ya existen estudios acerca de los daños provocados por algunos PFRs; Darnerud et al. observaron efectos carcinogénicos en varios BFRs, así como efectos para la tiroides y el hígado [27].

1.2.2. Parafinas cloradas

Las parafinas cloradas (CPs) son formulaciones industriales formadas por mezclas muy complejas de alcanos de cadena lineal policlorados (PCAs), con un contenido en cloro de entre un 30-70% de su masa [28]. Existen unas 200 formulaciones comerciales. Se clasifican en función de la longitud de la cadena carbonosa en parafinas cloradas de cadena corta (10 a 13 átomos de carbono), de cadena media (14 a 17 átomos de carbono) o de cadena larga (18-30 átomos de carbono). La mayor peligrosidad la presentan las CPs de cadena corta con un contenido en cloro del 60%, que han sido catalogadas por la Agencia de la Investigación del Cáncer como posibles carcinógenos humanos [4]. Son compuestos altamente tóxicos, con un elevado poder de bioacumulación y una alta persistencia en el medio, pudiendo incluso a permanecer más de un año en sedimentos [29, 30].

Su presencia en el medio ambiente es debida exclusivamente a su producción y uso, ya que no existe un origen natural conocido. Se emplean en una amplia gama de aplicaciones, tales como aditivos a elevada presión en el trabajo de metales, retardantes de llama, en plásticos, pinturas, revestimientos, etc. [31]

La gran dificultad radica en el análisis de las CPs por ser mezclas muy complejas con miles de congéneres individuales y propiedades físico-químicas muy diversas. Por ello hasta el momento es muy difícil disponer de datos exactos de concentración de CPs en medios, obteniendo principalmente estimaciones globales de su presencia [32].

1.2.3. Pesticidas polares

El uso extendido de pesticidas es debido a sus efectos positivos en la agricultura. Su elevado y continuado uso ha acarreado graves problemas de contaminación y efectos perjudiciales para la salud humana. Son compuestos orgánicos de carácter antropogénico, con estructura química muy diversa. Existen diversas clasificaciones de pesticidas en función de su toxicidad, vida media de efectividad o según la familia química a la que pertenece (Tabla 1.1).

Actualmente se conocen alrededor de 16 millones de pesticidas diferentes, y cada año se sintetizan unos 250 000 nuevos compuestos. Éstos se regularon hace décadas y han sido ampliamente estudiados, por lo que se dispone ya de un amplio conocimiento sobre su presencia en el medio ambiente. No obstante, en los últimos años ha aumentado la preocupación debido a sus productos de degradación, la gran mayoría polares, que en ocasiones pueden resultar más tóxicos y persistentes que los productos de partida.

En cuanto a los efectos de los pesticidas, se han encontrado evidencias de graves daños para la salud humana. Así, el dicloro-difenil-tricloroetano (DDT), empleado como insecticida, ha

causado efectos hormonales y problemas en el sistema reproductor [34]. El lindano, usado como insecticida y fungicida, puede afectar a la tiroides y a la próstata [35].

Tabla 1.1. Clasificación de los pesticidas en función de su toxicidad, vida media de efectividad y familia química [33].

Según toxicidad		
Clase	Toxicidad	Ejemplos
Clase IA	Extremadamente peligrosos	Paratión, dieldrín
Clase IB	Altamente peligrosos	Eldrín, diclorvos
Clase II	Moderadamente peligrosos	DDT, clordano
Clase III	Ligeramente peligrosos	Malatión, Isoproturón

Según vida media de efectividad		
Persistencia	Vida media	Ejemplos
No persistente	De días hasta doce semanas	Malatión, diazinón, carbarilo, diametrín
Moderadamente persistente	De 1 a 18 meses	Paratión, Iannate
Persistente	De meses a 20 años	DDT, aldrín, dieldrín
Permanente	Indefinidamente	Productos hechos a partir de mercurio, plomo o arsénico

Según su familia química	
Familia química	Ejemplos
Organoclorados	DDT, aldrín, endosulfán, dieldrín, heptacloro, lindane
Organofosforados	Bromophos, diclorvos, malatión, paratión
Carbamatos	Carbaryl, methomyl, propoxur
Triazinas y derivados	Atrazine, ametryn, desmetryn, simazine, metamitron
Ureas	Diuron, isoproturon
Compuestos inorgánicos	Fosfato de magnesio, cloruro de mercurio, arsenato de plomo, bromuro de metilo, antimonio, mercurio, selenio, talio, fósforo blanco

1.2.4. Compuestos perfluorados

Los compuestos perfluorados (PFCs) son sustancias químicas con cadena lineal hidrofóbica lineal de carbonos completamente fluorados, unida a diversos grupos hidrofílicos. Dentro de los PFCs las investigaciones se han centrado en el perfluorooctano sulfonato (PFOS) y ácido perfluorooctanoico (PFOA), por ser estos los más dañinos [13]. Se emplean para diversas aplicaciones industriales; el PFOS se ha usado como refrigerante, detergente y polímero en preparados farmacéuticos, retardantes de llama, insecticidas, etc. y el PFOA se emplea en la fabricación de fluoropolímeros (PTFE) y fluoroelastómeros (PVDF).

Estudios recientes han demostrado que estos compuestos son tóxicos y persistentes, destacando además el carácter carcinogénica del PFOA y el poder de bioacumulación del PFOS [36]. Hay trabajos recientes que evidencian los efectos de los PFCs como disruptores endocrinos [37].

1.2.5. Fármacos y productos de higiene personal

Los productos farmacéuticos y de higiene personal (PPCPs) son un amplio y variado grupo de compuestos químicos para el cuidado de la salud humana y animal. Son quizás el grupo de contaminantes emergentes que suscitan una mayor preocupación y han sido objeto de un estudio más exhaustivo. Aunque las primeras evidencias de fármacos en aguas se remontan a los años 70, no fue hasta principio de los 90 cuando adquirieron más fuerza y se empezó a probar ya su interferencia con el medioambiente [38].

De entre los aproximadamente 3000 tipos de fármacos que existen, los más prescritos en medicina son los analgésicos/antiinflamatorios, como ibuprofeno, diclofenaco, los antiepilepticos como la carbamacepina, antibióticos como la amoxicilina y sulfametazol o los β -bloqueantes como el metoprolol y atenolol [39-41]. No hay que olvidarse tampoco el extenso uso de productos farmacéuticos en veterinaria, ganadería, etc. el cual ha ido en aumento en los últimos años. Asimismo, estos compuestos pueden aparecer en las aguas domésticas al ser evacuados directamente a los desagües y por las excreciones humanas, ya que son sólo parcialmente metabolizados por el ser humano. Todo esto hace que sea muy difícil poder controlar los vertidos de productos farmacéuticos [6].

Debido a las propiedades físico-químicas y a las características de los suelos, estas sustancias pueden alcanzar fácilmente aguas subterráneas, contaminando acuíferos y en otros casos, quedando retenidos en los suelos. Pueden persistir durante largos períodos de tiempo, por lo que llegan a alcanzar concentraciones elevadas. Pero la gran problemática de los compuestos farmacéuticos radica en que algunos compuestos han llegado incluso a ser detectados en agua potable, presentando un riesgo para la salud humana [42]. Antibióticos como la penicilina, sulfonamidas y tetraciclinas provocan resistencia sobre patógenos bacterianos [43]. El Integración de tecnologías de adsorción y electroquímicas para la eliminación de contaminantes emergentes en aguas

diclofenaco crea alteraciones en el hígado y riñones de mamíferos y peces [44]. Además, muchos fármacos se acumulan en los tejidos animales, por lo que ante exposición prolongada, pueden encontrarse en concentraciones elevadas en organismos vivos. Como es el caso de gemfibrozil, diclofenaco e ibuprofeno, que han sido encontrados en altas concentraciones en el hígado, riñones y plasma de peces [45, 46]. Es importante destacar que en muchas ocasiones los distintos productos farmacéuticos se encuentran mezclados, por lo que pueden producirse efectos sinérgicos [47]. González-Pleiter et al. [48], estudiaron la toxicidad de cinco antibióticos (amoxicilina, eritromicina, tetraciclina, norfloxacín y levofloxacín) de manera individual y combinada, pudiendo detectar un efecto sinérgico tanto en mezclas binarias como multicomponente, el cual es más pronunciado ante la presencia de tetraciclina en las mezclas.

1.2.6. Drogas

Las drogas han destacado en los últimos años como contaminantes emergentes. Los estudios sobre la presencia de drogas, permiten determinar su presencia y posibles efectos tanto de las drogas más consumidas, como de sus principales metabolitos. Son pocos los estudios acerca de la presencia de drogas en diversas aguas, centrándose los trabajos en la presencia de cocaína, estimulantes anfetámicos, opiáceos y cannabis [9]. Aunque estos compuestos se encuentran principalmente en muy bajas concentraciones, sus posibles efectos adversos sobre la fauna y la salud humana no pueden descartarse.

1.3. Contaminantes emergentes en España

Según un informe realizado en 2010 por la Agencia Europea de Medio Ambiente, la calidad de los ríos de España, se encuentra por debajo de los estándares considerados como óptimos (Figura 1.2). Teniendo en cuenta el estado de las aguas de todos los países miembros de la Unión Europea, son los países de Europa central y del noroeste, los que presentan peores calidades del agua; coincidente con zonas en las que se realizan prácticas de agricultura intensiva, y que además cuentan con alta densidad de población [22]. Aunque los datos no parecen nada optimistas, hay que remarcar que las aguas se encontraban mucho más contaminadas años, cuando no existía un control a nivel europeo y elevadas cantidades de aguas residuales urbanas e industriales sin tratar o parcialmente tratadas eran vertidas de manera indiscriminada en las aguas [22].

Si tenemos en cuenta el estado de las aguas en España en particular, son varios los estudio sobre CEs que indican la presencia de contaminantes emergentes a niveles de concentración significativos, siendo más destacada su presencia en las cuencas del Mediterráneo [4, 49]. En la Tabla 1.2 puede verse la situación de los cauces analizados por la Organización de Consumidores

y Usuarios (OCU). Los CEs más ampliamente detectados son los productos farmacéuticos, pesticidas y productos de higiene personal.

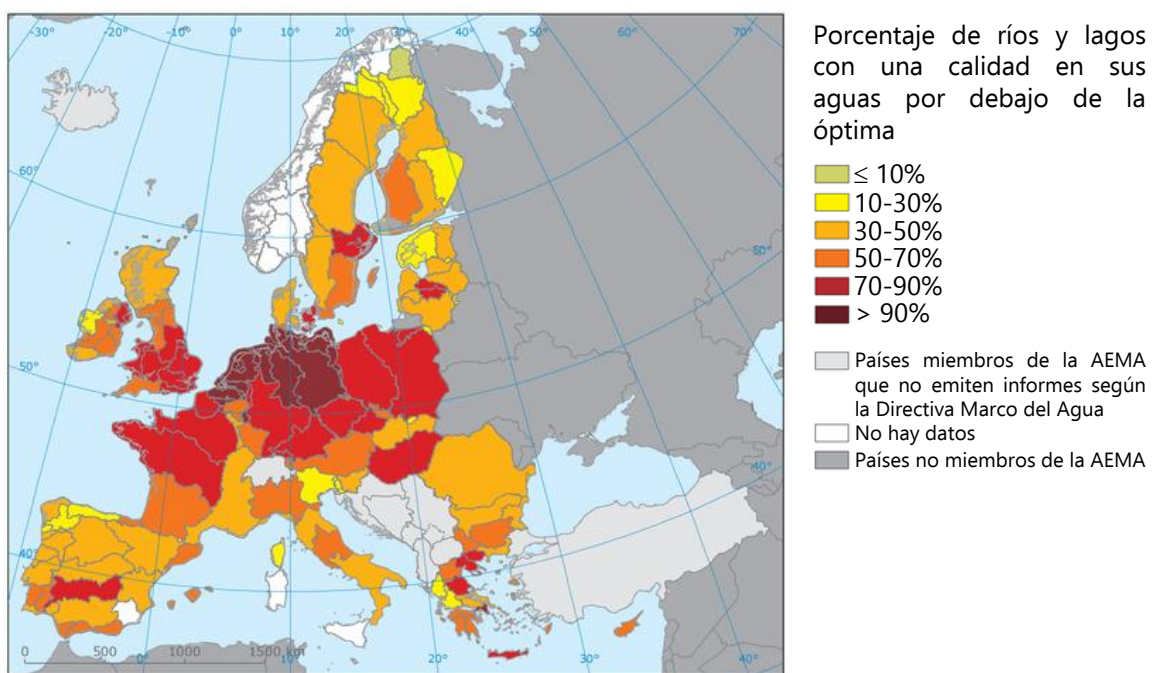


Figura 1.2. Estado de la calidad de las aguas en río y lagos de los países miembro de la Unión Europea (Fuente: Agencia Europa de Medio Ambiente [22]).

Tabla 1.2. Niveles de contaminantes emergentes en España, (●) niveles significativos, (○) cantidades mínimas (Adaptada de la OCU, 2013).

	Medicamentos	Plaguicidas	Jabones	Aditivos
Besaya	●			○
Ebro		○		
Turia		○		
Segura	●			
Genil	●			
Miño		○		
Tormes		○	○	
Guadiana		○		
Pisuerga	●			○
Manzanares	●		○	○
Tajo	●			○

Varios estudios han determinado la presencia de estos contaminantes en varias cuencas españolas, en el área mediterránea, norte penínsulas, zona central de España y las Islas.

En el área Mediterránea, mediante el proyecto AQUATERRA, se encontró la presencia de diversos fármacos en el río Ebro, destacando analgésicos y antiinflamatorios como el ibuprofeno o la codeína, fármacos de psiquiatría como el diazepam o la fluoxetina, antihistamínicos como la loratadina, antibióticos como el cloranfenicol o la ciprofloxacina y betabloqueantes como el pindolol o el propanolol. En el río Llobregat se ha observado la feminización de peces debido a la presencia de alquilenoles etoxilados, los cuales actúan como disruptores endocrinos [9, 50]. También fueron detectadas cloroparafinas de cadena corta, así como drogas de abuso y productos farmacéuticos [51]. En cuanto al río Ter, cabe destacar la presencia de detergentes tipo nonilfenol etoxilado [4].

En el norte peninsular se detectaron diversos contaminantes emergentes en ríos gallegos. Se observó la presencia de gran cantidad de productos farmacéuticos y pesticidas [52, 53]. Llama la atención, que aunque en el río Miño los niveles de pesticidas son muy bajos, las aguas subterráneas de la misma zona poseen niveles muy superiores [54].

En la zona central de España se determinó la presencia de diversos disruptores endocrinos, así como productos farmacéuticos, destacando analgésicos, antipirépticos y antiinflamatorios [55].

En cuanto a las Islas Canarias, también fueron detectados productos farmacéuticos y pesticidas, incluso en aguas subterráneas. Destacar que incluso se encontraron plaguicidas en concentraciones que exceden los límites fijados [56].

1.4. Métodos de eliminación de contaminantes emergentes

Las plantas de tratamiento de aguas residuales se componen de un sistema de pretratamientos, tratamiento primarios (métodos físico-químicos) y de un sistema secundario (reactor biológico). Estas plantas han sido diseñadas para la eliminación de parámetros convencionales tales como DBO₅, DQO, sólidos suspendidos totales o nutrientes, teniendo una capacidad limitada en cuanto a la eliminación de contaminantes emergentes presentes en las aguas residuales urbanas [57]. Muchos de los CEs persisten sin alteración alguna tras estos tratamientos, por lo que es necesario evaluar nuevas tecnologías mediante tratamientos avanzados, para garantizar su eliminación con el menor coste energético y ambiental posible.

En comparación con otros problemas ambientales, cabe destacar que en el caso de los CEs deben tratarse caudales muy elevados con concentraciones muy bajas, lo que supone un desafío para el diseño de procesos físicos y químicos.

Los métodos para el tratamiento de contaminantes emergentes pueden clasificarse en tres familias: tratamientos físico-químicos, biológicos y tecnologías híbridas. Dentro de los procesos físico-químicos se encuentran los procesos de oxidación avanzada (AOPs) los cuales serán tratados por separado dada su gran importancia y eficacia.

1.4.1. Métodos físico-químicos

Tratamientos físico-químicos como coagulación/flocculación se han utilizado para la eliminación de contaminantes emergentes en aguas. Se adicionan coagulantes o flocculantes a las aguas con el fin de desestabilizar las partículas coloidales, permitiendo su agregación y posterior sedimentación [58]. Los agentes químicos más utilizados son aluminio, sales de hierro y polímeros. Pero estos métodos resultan ineficientes para muchos de los contaminantes emergentes [58, 59]. Adams et al., [58] estudiaron el tratamiento de siete antibióticos mediante coagulación/flocculación, sin observar eliminación significativa para ninguno de los compuestos. Huerta-Fontela et al., [59] llevaron a cabo la eliminación de 35 productos farmacéuticos y hormonas mediante coagulación/flocculación combinado a un filtro de arena, obteniendo una eliminación superior al 50% en tan sólo ocho de los compuestos estudiados.

Los procesos de adsorción son una de las técnicas más estudiadas para el tratamiento de aguas; por ello su aplicación se ha extendido a la eliminación de contaminantes emergentes. El carbón activo es el adsorbente más ampliamente utilizado por su elevada capacidad de adsorción [60]. La eficacia de adsorción depende de las propiedades del adsorbente empleado, como pueden ser al área superficial, morfología y química superficial, por lo que la selección de un buen adsorbente en un parámetro clave para obtener unas buenas capacidades de eliminación [61]. En la Tabla 1.3, se muestran varios ejemplos de eliminación de contaminantes emergentes mediante adsorción, pudiendo observar la variación en la eficacia de eliminación en función del adsorbente seleccionado.

Tabla 1.3. Eliminación de contaminantes emergentes mediante adsorción

Compuesto/s	Adsorbente/s	Eficacia (%)	Referencia
Sulfonamidas	Carbón activo	90	Adams et al. [58]
Amoxicilina	Carbón activo	95	Putra et al. [62]
	Bentonita	88	
Ofloxacino	Nanotubos de carbono	>80	Peng et al. [63]
	Carbón activo	60	
Triclosán	Caolinita	32	Behera et al. [64]
	Montmorillonita	10	

Pueden emplearse diversos tipos de procesos de membrana tales como la microfiltración, ultrafiltración, nanofiltración, electrodiálisis y ósmosis inversa (RO) para la eliminación de contaminantes emergente de aguas residuales. Éstas técnicas presentan eliminaciones muy variadas en función del material del que esté compuesto la membrana, pudiendo varias la eficacia de eliminación entre el 30-90% [65]. La microfiltración y ultrafiltración no resultan eficaces debido a su limitada capacidad de retención, así como por fenómenos de ensuciamiento [66]. Yoon et al., [67] estudiaron la eliminación de varias familias de contaminantes emergentes mediante nanofiltración y ultrafiltración. Los porcentajes de eliminación fueron distintos en función de la naturaleza del adsorbato. Para los compuestos más polares y menos volátiles las retenciones fueron menores al 70%, mientras que para los más volátiles éstas son superiores al 75%.

Bodzek y Dudziak, [68] realizaron un estudio comparativo de varios tratamientos físico-químicos, como son la coagulación/flocculación, adsorción con carbón activo y nanofiltración. Seleccionaron seis estrógeno para llevar a cabo la eliminación, obteniendo el siguiente orden de eficacias: coagulación/flocculación (5-35%) < nanofiltración (65-100%) < adsorción con carbón activo (\approx 100%).

1.4.2. Procesos de oxidación avanzada

Debido a la ineficacia de los métodos de tratamiento convencionales, se han realizado en los últimos años estudios sobre nuevas tecnologías, conocidas como procesos de oxidación avanzada (AOPs), las cuales resultan eficaces para la oxidación de un gran número de compuestos. Estas técnicas incluyen aquellos procesos que producen *in situ* especies altamente activas, principalmente el radical hidróxilo. El radical hidróxilo es un radical no selectivo, capaz de atacar a un gran número de compuestos orgánicos, transformándolos en productos menos complejos y perjudiciales [69]. Existen también otras especies oxidantes reactivas como el peróxido de hidrógeno que pueden contribuir a la eliminación de contaminantes persistentes. Los AOPs pueden clasificarse en procesos homogéneos y heterogéneos. Dentro de estos últimos se encontraría la ozonización catalítica ($O_3/Cat.$), ozonización fotocatalítica ($O_3/TiO_2/UV$) y fotocatálisis heterogénea ($H_2O_2/TiO_2/UV$)[70]. La clasificación de los procesos homogéneos puede verse en la Fig. 1.3.

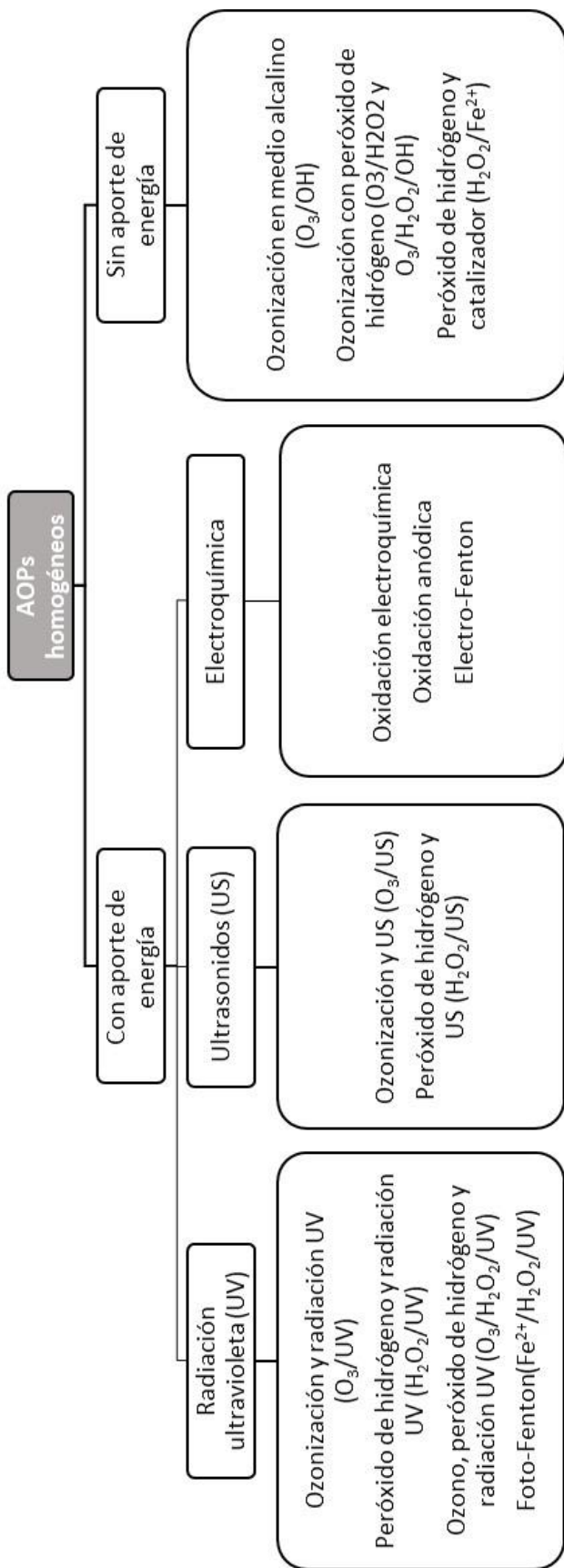


Figura 1.3. Clasificación de las técnicas de oxidación avanzada homogéneas [70].

De los procesos de AOPs, sobre el que existe un mayor número de estudios es la ozonización. Debido al alto potencial de oxidación del ozono, es empleado para la desinfección de agua potable, consiguiendo una reducción en los productos de desinfección y una mayor biodegradabilidad [71]. El ozono reacciona particularmente con moléculas que presentan anillos aromáticos en su estructura, enlaces insaturados y grupos amino [72]. Por lo general se obtienen eficacias superiores al 90% mediante ozonización, pero tiene la desventaja del alto coste y mantenimiento [73]. Adams et al. [58] realizaron la oxidación con ozono de siete compuestos farmacéuticos alcanzando un 100% de eliminación. Rivas et al. [74] obtuvieron la degradación completa de diversos productos farmacéuticos, pero sin embargo, la reducción en el contenido en carbono orgánico total (TOC) limitada. Rivas et al. [74] consiguieron una mejora del 55% en cuanto a la reducción del TOC, al combinar ozonización con UV.

Aunque puede tener lugar la oxidación de contaminantes emergentes mediante oxidación con UV, no suele dar lugar a elevadas eficacias de eliminación, pudiendo mejorarse su rendimiento al acoplarla a otros procesos como puede ser la ozonización, en presencia de H_2O_2 , etc. Si se tiene en cuenta la degradación mediante UV en presencia de H_2O_2 , se observan diferencias significativas. Neamtu et al. [75] estudiaron la degradación de octilfenol mediante UV con eficacias que rondan el 20%, llegando al 80% en presencia de H_2O_2 , ya que acelera la degradación del contaminante con la generación de $\cdot\text{OH}$ a partir de la fotólisis del H_2O_2 .

Los procesos Fenton y foto-Fenton también han sido empleados para el tratamiento de contaminantes emergentes. La oxidación Fenton tiene lugar empleando como agente oxidante Fenton ($\text{H}_2\text{O}_2/\text{Fe}^{3+}$), pudiendo combinarse con radiación UV (foto-Fenton). Normalmente los resultados son mejores mediante foto-Fenton, excepto cuando se tratan aguas con un alto contenido en materia orgánica, ya que la turbidez evita la penetración de la radiación UV [73]. Elmolla y Chaudhuri [76] realizaron estudios de optimización para ambas técnicas para la eliminación de antibióticos, consiguiendo una degradación del 100% mediante ambas técnicas.

Los AOPs presentan ciertas ventajas respecto a las técnicas convencionales de tratamiento de aguas. La Tabla 1.4 presenta un resumen de las principales ventajas y desventajas de los AOPs.

Tabla 1.4. Ventajas e inconvenientes de los procesos de oxidación avanzada (AOPs) [77].

Ventajas	Inconvenientes
Velocidades de reacción elevadas.	Producción de productos de transformación desconocidos
Posibilidad de mineralización completa	La calidad del agua puede interferir en la eficacia
No generan residuos	Es una técnica costosa
Potencial para reducir la toxicidad.	
Son técnicas no selectivas	

1.4.3. Tratamientos biológicos

Los tratamientos biológicos son uno de los principales métodos de tratamiento de contaminantes acuosos, pero su capacidad es limitada en cuanto a la eliminación de contaminantes emergentes. La Figura 1.4 muestra una clasificación de los distintos métodos de tratamiento biológico.

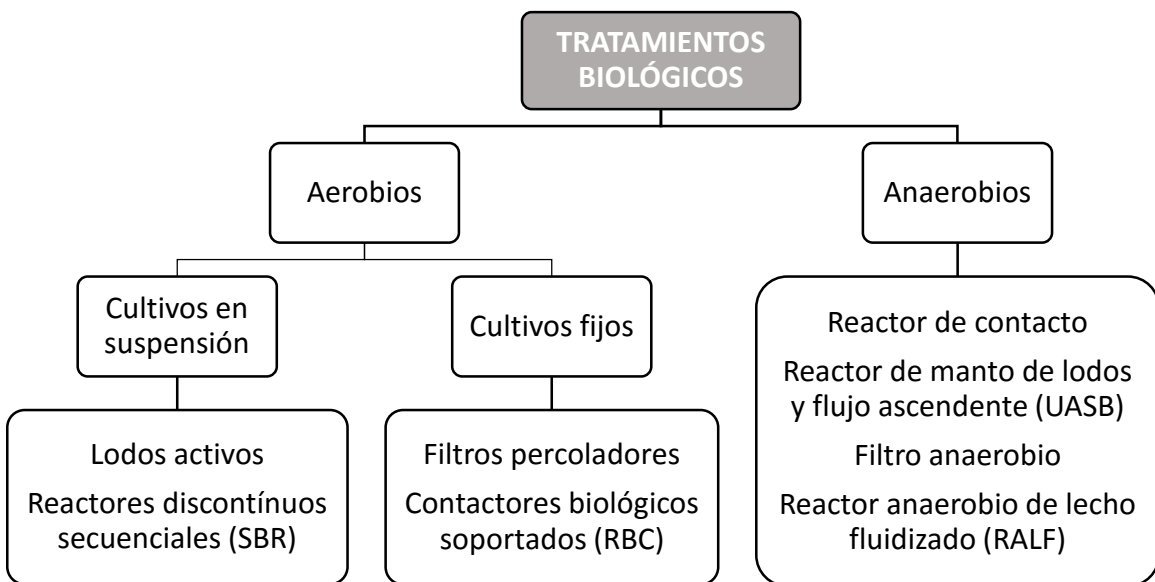


Fig. 1.4. Sistemas de tratamiento biológico (Adaptada de Fernández-Alba et al. [78])

Las actuales plantas de tratamiento de aguas residuales ya disponen en el tratamiento secundario de un reactor biológico y en muchas de ellas se han encontrado restos de contaminantes emergentes en sus efluentes, demostrando la ineeficacia de esta tecnología para su eliminación. Urase y Kikuta [79] estudiaron la eliminación con lodos activos de 14 contaminantes emergentes mediante ensayos en discontinuo, siendo el porcentaje de eliminación inferior al 30% para $\frac{3}{4}$ partes de los compuestos. Narumiya et al., [80] estudiaron la eliminación de productos farmacéuticos con eliminaciones inferiores al 50% para la mitad de los compuestos seleccionados.

1.4.4. Tecnologías híbridas

Otra alternativa para la eliminación de contaminantes emergentes, es mediante el empleo de tecnologías híbridas, que no es más que la combinación de dos o más de las técnicas ya mencionadas. Un claro ejemplo son los bioreactores de membrana (MBR) que a su vez pueden combinarse también con otros métodos de eliminación.

Los bioreactores de membrana que compaganan métodos biológicos y tecnología de membrana, resultan eficaces para la eliminación de contaminantes orgánicos hidrófobos y fácilmente biodegradables [81]. Es importante también tener en cuenta que los procesos mediante MBR resultan costosos debido al ensuciamiento de las membranas que obligan a una parada en la producción para su limpieza [82]. Existen dos configuraciones posibles en función de si la situación de la membrana es externa o sumergida en el reactor biológico. Sipma et al., [83] llevaron a cabo la eliminación de 30 compuestos farmacéuticos mediante tratamiento con lodos activos y mediante el empleo de MBR. No sólo las eficacias de eliminación fueron superiores con el tratamiento mediante MBR, sino que incluso para casi 1/3 de los compuestos se duplicaron las eficacias de eliminación.

Es posible mejorar las eficacias si se añade al tratamiento con MBR un sistema en serie de tratamiento con membranas. Cartajena et al. [82] evaluaron la eliminación de diez contaminantes emergentes a la salida del MBR y a la salida del proceso con membranas situado en serie. Obtuvieron en la mayoría de los casos una mayor reducción de las concentraciones tras el tratamiento con membranas, aumentando las eficacias entre un 10-40%.

Otra alternativa es la combinación de MBR con tratamiento mediante UV. Nguyen et al.[84], estudiaron ambas técnicas combinadas, obteniendo mejoras de hasta el 60% en comparación con la eliminación sólo mediante MBR.

Es posible también completar el tratamiento de un MBR con adsorción en carbón activo - MBR-GAC – mejorando la eliminación de los compuestos hidrofílicos y persistentes. La adsorción de contaminantes emergentes en niveles de trazas disminuye debido a la competición con los gruesos de materia orgánica, por lo que es importante que la alimentación al GAC tenga baja concentración de gruesos de materia orgánica. Esto se consigue empleando la adsorción como post-tratamiento alimentando el permeado obtenido tras el tratamiento en un MBR [85]. Nguyen et al. [84], estudiaron la aplicación de esta técnica a la eliminación de 22 contaminantes emergentes, obteniendo que aquellos compuestos que habían sido eliminados mediante MBR con eficacias inferiores al 40%, presentaban eficacias superiores al 98% tras el tratamiento con GAC.

1.5. Alternativa propuesta para la eliminación de contaminantes emergentes

Ha sido demostrado que procesos convencionales tales como métodos biológicos y tratamientos físico-químicos no son eficaces para la eliminación de contaminantes emergentes. Aunque los procesos de oxidación avanzada son un mecanismo de eliminación prometedor, son técnicas de elevado coste, en las cuales la elección del reactivo es un parámetro crítico por la posible formación de subproductos. Por otra parte hay que tener en cuenta las bajas

concentraciones a las que se encuentran estos contaminantes, para las que muchas técnicas convencionales pueden no ser lo suficientemente eficaces.

Es importante remarcar que debido a esa baja concentración será necesario procesar un volumen muy grande de agua para eliminar una pequeña cantidad de contaminante, lo que hace que el proceso sea muy costoso. Por esta razón, en el presente trabajo se propone una nueva estrategia basada en un proceso en dos etapas (Fig. 1.5): una pre-concentración del contaminante, seguido del proceso de degradación.

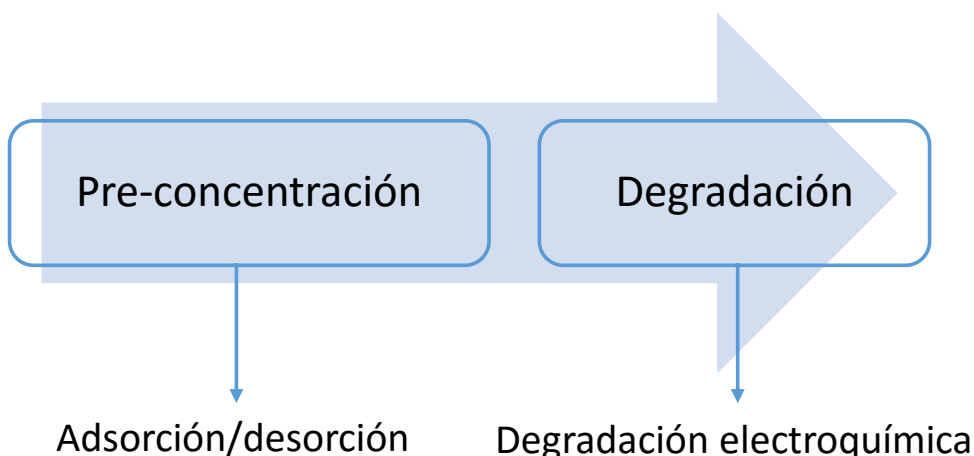


Figura 1.5. Esquema del método de eliminación propuesto

Los procesos de adsorción han sido ampliamente empleados en la industria para la eliminación de contaminantes. Presentan la ventaja de que no transforman el contaminante, por lo que no existe riesgo de formación de sub-productos. Por otra parte, con isotermas de adsorción favorables, esta técnica permite la retención de contaminantes cuando este se encuentra en concentraciones muy bajas, como es el caso de los CEs. Además instrumentalmente son técnicas sencillas con costes moderados y con la posibilidad de trabajar a temperatura y presión ambientales. Por estas ventajas, en este trabajo se seleccionó el proceso de adsorción para llevar a cabo la pre-concentración del contaminante mediante ciclos de adsorción/desorción, obteniendo una corriente al final del ciclo, más concentrada que la corriente de partida. Algunos estudios emplean un regenerante químico, pero implicaría un problema adicional; por ello en este trabajo la regeneración se llevará a cabo con agua a contracorriente para evitar modificar químicamente la corriente a ser tratada.

Una vez conseguida la pre-concentración del contaminante, se lleva a cabo la degradación del mismo mediante tratamiento electroquímico, ya que esta tecnología ofrece ventajas como la simplicidad instrumental, costes moderados y no emplea reactivos químicos ya que son electrones los encargados de llevar a cabo la degradación. Además ofrece la posibilidad de operar en condiciones de presión y temperatura ambiente.

Para el estudio de la viabilidad de la alternativa propuesta para la eliminación de contaminantes emergentes en agua, se han seleccionado tres compuestos modelo, pertenecientes a tres familias de contaminantes emergentes: un compuesto farmacéutico, un cloroalcano de cadena corta y un alquilfenol etoxilado. Son compuestos que han sido seleccionados debido a su presencia tanto en aguas superficiales como subterráneas (Tabla 1.2). Por lo general, están presentes en bajas concentraciones, del orden de $\mu\text{g}\cdot\text{L}^{-1}$, por lo que el proceso propuesto, con una primera etapa de pre-concentración resulta interesante [86-89].

El objetivo es proponer una alternativa de eliminación, que pueda ser aplicable a un gran intervalo de contaminantes emergentes; es por ello que los tres compuestos seleccionados presentan diferentes funcionalidades. De este modo es posible verificar la idoneidad de la técnica para un amplio intervalo de contaminantes.

Los contaminantes modelo seleccionados son: ácido nalidíxico (antibiótico), 1,8-diclorooctano (cloroalcano) y 2-(4-metilfenoxi)etanol (MPET) (alquilfenol etoxilado), cuyas características principales se exponen a continuación.

Ácido nalidíxico (NAL) (Figura 1.6). Producto farmacéutico sintetizado por Lesher et al., en 1960, el cual actúa como agente antibacteriano. Pertece al grupo de los antibióticos, es usado para el tratamiento de infecciones urinarias. Cuando se encuentra presente a bajas concentraciones, actúa como bacteriostático, inhibiendo el crecimiento bacteriano, mientras que a altas concentraciones presenta efecto bactericida [90]. Además ha sido demostrado que presenta toxicidad crónica y efectos carcinogénicos [91].

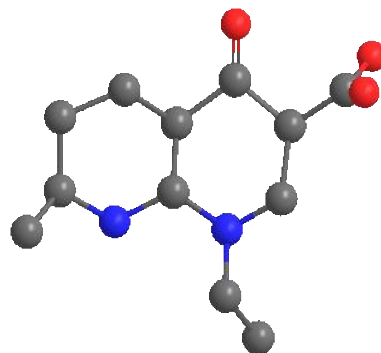


Figura 1.6. Estructura química del ácido nalidíxico

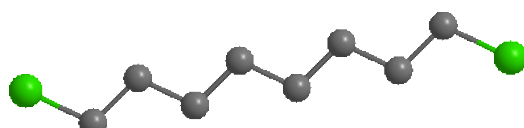


Figura 1.7. Estructura química del 1,8-diclorooctano

1,8-diclorooctano (DCO) (Figura 1.7). n-alcano policlorado de cadena corta, como representativo de cloroparafinas de cadena corta (SCCPs) consideradas como las más perjudiciales. Empleadas en aditivos en lubricantes, pinturas, aislantes y también como retardantes de llama en plásticos [92, 93]. Las SCCPs están consideradas como posibles compuestos carcinógenos [92, 94].

2-(4-metilfenoxi)etanol (MPET) (Figura 1.8).

Seleccionado como molécula modelo dentro de los alquilfenoles etoxilados (APEs), debido a su facilidad en cuanto a análisis. Los APEs se emplean como agentes humectantes, solubilizantes o detergentes.

Este tipo de compuestos actúan como disruptores endocrinos, interfiriendo en el sistema endocrino (hormonal), produciendo problemas de fertilidad, feminización, etc.

Las propiedades físico-químicas de los tres compuestos seleccionados se encuentran en la Tabla 1.5.

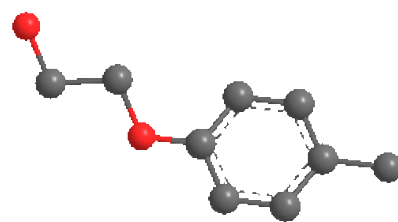


Figura 1.8. Estructura química del 2-(4-metilfenoxi)etanol

Tabla 1.5. Propiedades físico-químicas del ácido nalidíxico, 1,8-diclorooctano y 2-(4-metilfenoxi)etanol

	Ácido nalidíxico	1,8-diclorooctano	2-(4-metilfenoxi)etanol
nºCAS	2162-99-4	389-08-2	15149-10-7
Peso molecular	183.12	232.23	152.19
Volumen molecular (Å ³)	174.12	229.76	151.21
Log K _{ow}	4.086	0.228	1.811
TPSA	0	69.6	29.4
Solubilidad (g·L ⁻¹)	0.17	0.10	9.40

1.6. Fundamentos teóricos del proceso de adsorción

La adsorción implica la acumulación o concentración de una sustancia en la región existente entre dos fases, denominada: interfase. Mediante la adsorción se extrae una sustancia de una fase y se concentra en la superficie de la otra fase, por lo que es considerado un fenómeno superficial. El adsorbato es la sustancia que se concentra o adsorbe en la superficie y el adsorbente la fase sólida sobre la que se adsorbe.

La adsorción es el resultado de la presencia de fuerzas moleculares existentes en el seno de un fluido o de un sólido. En el interior de una fase, las fuerzas que la mantienen unida se encuentran compensadas en toda la fase, excepto en su superficie, donde tiene lugar una fuerza atractiva

neta, normal a la superficie. Esta fuerza es la que hace que se produzca el acercamiento de las moléculas de la otra fase, produciéndose la adsorción. La energía que posea dicha adsorción va a determinar el tiempo que van a permanecer en la superficie del adsorbente las diferentes especies.

Existen dos tipos de adsorción en función del tipo de interacción entre ambas fases: adsorción física o adsorción química.

- Adsorción física (fisisorción): la adsorción se produce mediante fuerzas intermoleculares relativamente débiles, tipo Van der Waals.
- Adsorción química (quimisorción): se produce una reacción química en la superficie del sólido y el adsorbato se mantiene unido mediante enlaces químicos fuertes.

En condiciones favorables, ambos procesos tienen lugar de manera simultánea o alternativa, aunque fisisorción parece ser el mecanismo predominante. La Tabla 1.6 se resumen las principales diferencias entre ambos procesos de adsorción.

Tabla 1.6. Principales diferencias entre fisisorción y quimisorción [95]

Adsorción física	Adsorción química
Proceso exotérmico	Endotérmico
Interacción no específica	Interacción altamente específica
Monocapa o multicapa	Sólo monocapa
La molécula fisisorbida mantiene su identidad	Disociación de las moléculas adsorvidas
Significativa a bajas temperaturas	Amplio intervalo de temperatura
Rápida y reversible	Puede ser lenta e irreversible
No hay transferencia de electrones	Transferencia de electrones y formación de enlace adsorbato/adsorbente

Cuando se trata de adsorción sólido-líquido, el proceso es más complejo, ya que pueden tener lugar además de las interacciones adsorbente-adsorbato, interacciones adsorbente-disolvente o adsorbato-disolvente. Por lo que la afinidad del adsorbato por el adsorbente va a depender también de la naturaleza del disolvente.

1.6.1. Factores que influyen en el proceso de adsorción

Son varios los factores que afectan a la extensión y velocidad del proceso de adsorción, de entre los que cabe destacar:

- **Propiedades del adsorbente.** La adsorción es un fenómeno superficial, por lo que generalmente, a mayor área superficial, mayor será la capacidad de adsorción del adsorbente. Por ello suelen emplearse sólidos porosos con elevada superficie específica. El volumen de poros y la distribución de tamaño de poro afectan a la capacidad de adsorción y a la velocidad del proceso [96]. La naturaleza del adsorbente afecta a la velocidad y capacidad de adsorción [97].
- **Propiedades del adsorbato.** Las características físico-químicas del adsorbato como son su peso molecular y tamaño, presencia de grupos funcionales o solubilidad condicionan el proceso de adsorción [98, 99]. La afinidad de un compuesto a ser adsorbido aumenta con su peso molecular por regla general. La presencia de dobles enlaces, anillos aromáticos, grupos halogenados, etc. varían la capacidad de adsorción. Existe además una relación inversa entre la solubilidad del medio y la capacidad de adsorción.
- **Condiciones del medio.** Factores como el pH o temperatura del medio, afectan a las capacidades de adsorción. La influencia del pH en el proceso de adsorción está relacionado con la naturaleza de la superficie adsorbente, punto isoeléctrico del adsorbente y grado de ionización del adsorbato [100]. En cuanto a la temperatura, por lo general la adsorción es fenómeno exotérmico, por lo que un aumento de temperatura provoca una disminución en la capacidad de adsorción [101].
- **Presencia de otros compuestos.** Cuando se trabaja con mezclas multicomponentes puede tener lugar competencia entre adsorbatos, la cual no sólo afecta a la velocidad de adsorción, sino también a la velocidad de difusión dentro de las partículas del adsorbente.

1.6.2. Adsorción por lotes (discontínuo)

La adsorción mediante experimentos por lotes o también denominada en discontínuo, permite obtener una medida de la eficacia de adsorción, así como calcular la capacidad máxima de adsorción. Para ello es necesario colocar una cantidad determinada de adsorbente en contacto con la disolución que contiene el adsorbato, manteniéndola en agitación el tiempo necesario para alcanzar el equilibrio.

La forma típica de representar el equilibrio de adsorción es mediante las determinadas isotermas de adsorción, las cuales representan la cantidad adsorbida y la presión relativa a una temperatura dada.

La capacidad de adsorción puede expresarse según la siguiente ecuación:

$$q_e = \frac{(C_0 - C_e) \cdot V}{m} \quad \text{Ec. 1.1}$$

donde q_e es la cantidad adsorbida por unidad de masa de adsorbente ($\text{mg}\cdot\text{g}^{-1}$), C_0 y C_e son la concentración inicial y de equilibrio del adsorbato ($\text{mg}\cdot\text{L}^{-1}$), V es el volumen de disolución (L) y m es la masa de adsorbente (g).

Son varios los modelos existentes para la descripción de las isotermas de adsorción, que difieren entre sí en las hipótesis de partida y en el número de parámetros característicos. Los más empleados para adsorción sólido-líquido de un solo componente son los modelos de Langmuir, Freundlich, Dubinin-Radushkevich y Brunauer-Teller (BET).

- **Modelo de Langmuir.** Es un modelo termodinámico basado en las siguientes suposiciones:
(i) tiene lugar adsorción en monocapa, (ii) la superficie del adsorbente es energéticamente homogénea, (iii) no existe migración del adsorbato sobre la superficie del adsorbente [102]. El modelo se corresponde con la siguiente expresión matemática:

$$q_e = \frac{q_{sat} \cdot K_L \cdot C_e}{1 + K_L \cdot C_e} \quad \text{Ec. 1.2}$$

donde q_{sat} es la máxima capacidad de adsorción en la monocapa ($\text{mg}\cdot\text{g}^{-1}$) y K_L es una constante de equilibrio relacionada con la afinidad adsorbato-adsorbente ($\text{L}\cdot\text{mg}^{-1}$).

- **Modelo de Freundlich.** Es un modelo empírico que puede aplicarse a procesos de adsorción en multicapa, donde la distribución de los sitios de adsorción es uniforme y la superficie del material se considera enérgicamente heterogénea. Supone que al aumentar la energía libre de adsorción el número de centros de adsorción disminuyen exponencialmente [103]. La expresión matemática del modelo se expone a continuación:

$$q_e = k_F \cdot C_e^{1/n} \quad \text{Ec. 1.3}$$

donde k_F y n son parámetros característicos del modelo. El valor de $1/n$ es un indicador de la intensidad del proceso de adsorción o la heterogeneidad de la superficie [103].

- **Modelo de Dubinin-Radushkevich (D-R).** El mecanismo de adsorción se representa mediante una distribución gaussiana de energía sobre superficies heterogéneas [104, 105].

$$q_e = Q_m \cdot \exp(-K \cdot \varepsilon^2) \quad \text{Ec. 1.4}$$

donde Qm es la máxima capacidad de adsorción ($\text{mg}\cdot\text{g}^{-1}$), K es el coeficiente de actividad relacionada con la energía de adsorción (mol^2/kJ^2) y ε es el potencial Polanyi.

- **Modelo de Brauner-Emmet-Teller (BET).** Supone la formación de varias capas de adsorbato en la superficie, aplicando el modelo de Langmuir a cada una de las capas. Todas las capas se unen con una energía idéntica e excepción de la primera, que se adhiere con una energía comparable al calor de adsorción [106]. La ecuación BET se expresa de la siguiente manera:

$$q_e = \frac{q_s \cdot C_{BET} \cdot C_e}{(C_s - C_e) \cdot [1 + (C_{BET} - 1) \cdot (C_e / C_s)]} \quad \text{Ec. 1.5}$$

donde C_{BET} es un parámetro característico del modelo ($\text{L}\cdot\text{mg}^{-1}$), C_s es la concentración de saturación en la monocapa ($\text{mg}\cdot\text{L}^{-1}$) y q_s es la capacidad de adsorción teórica según la ecuación BET ($\text{mg}\cdot\text{g}^{-1}$).

1.6.3. Adsorción en lecho fijo

Los estudios de adsorción en una columna de lecho fijo no se llevan a cabo en condiciones de equilibrio, ya que la disolución de alimentación atraviesa de manera continua la columna, donde tiene lugar un proceso de transferencia de masa permanente entre la alimentación y el adsorbente. Generalmente en la industria se trabaja en continuo, por lo que este tipo de estudios son una aplicación más práctica desde el punto de vista industrial.

Cuando se alimenta un fluido con una concentración C_0 de adsorbato a una columna de lecho fijo, el adsorbato comienza a ser retenido por el adsorbente en la zona de entrada, por lo que inicialmente el fluido que sale de la columna está prácticamente libre del adsorbato. Existe una zona de lecho donde está teniendo lugar la adsorción (zona de transferencia de masa, MTZ), que se va desplazando a medida que se continúa alimentando a la columna y por lo tanto la concentración del adsorbato a la salida irá aumentando con el tiempo. El tamaño de esta zona es un indicador de la rapidez del proceso (Figura 1.9).

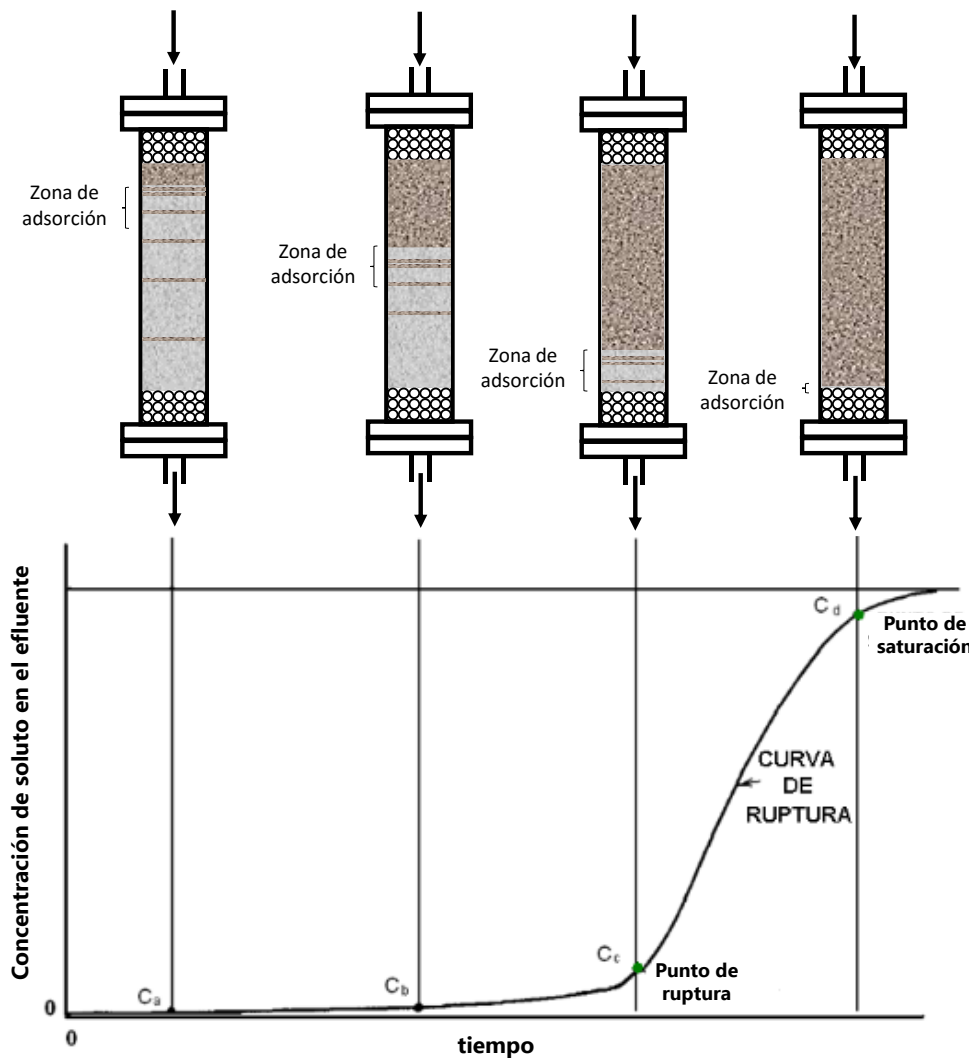


Figura 1.9. Curva de ruptura y avance de la zona de transferencia de masa

En una situación ideal donde las transferencias de materia externa e interna del lecho ocurrieran a velocidades muy elevadas, la MTZ debería de ser próxima a cero, condición para la cual el tiempo de ruptura coincidiría con el tiempo de saturación. En un instante dado del proceso, se distinguirán fundamentalmente tres zonas:

- **Zona saturada.** No se produce adsorción, ya que se ha alcanzado la saturación del adsorbente, por lo que la concentración de la disolución es igual a la de alimentación.
- **Zona de adsorción o de transferencia de materia (MTZ).** Es la zona en la que tiene lugar el proceso de adsorción donde el adsorbente está parcialmente saturado.
- **Zona de adsorbente virgen.** Se corresponde con la región de lecho más alejada al punto de alimentación que aún no ha sido alcanzada por el frente de adsorción y por lo tanto, el adsorbente se encuentra libre de adsorbato.

La representación de la variación de la concentración (C/C_0) con el tiempo, determina la denominada curva de ruptura (Figura 1.9). La curva de ruptura presenta forma sigmoidea. El tiempo al que empieza a salir una concentración significativa de adsorbato, considerada como $C/C_0=0.05$, se denomina tiempo de ruptura. A $C/C_0=1$, se alcanza el tiempo de saturación, correspondiente al momento en el que todo el lecho se encuentra saturado. Las curvas de ruptura se emplean para el diseño de torres de adsorción en lecho fijo a escala piloto e industrial. Por ello es necesario primeramente llevar a cabo operaciones en lecho fijo a escala de laboratorio.

Existen modelos matemáticos que permiten predecir el proceso de adsorción en lecho fijo.

- **Modelo del tiempo de servicio de la altura de un lecho (BDST).** Supone que la difusión intraparticular y la resistencia de masa externa son insignificantes y que la cinética de adsorción está controlada por la reacción superficial entre el adsorbato y el adsorbente que no ha sido usado [107]. Su expresión es la siguiente:

$$\ln\left(\frac{C_0}{C} - 1\right) = \ln\left[e^{(K \cdot N_0 \cdot \frac{Z}{u})} - 1\right] - K \cdot C_0 \cdot t \quad \text{Ec 1.6}$$

donde C_0 y C son la concentración de adsorbato a la entrada y salida del lecho ($\text{mg} \cdot \text{L}^{-1}$), K es la constante de velocidad de adsorción ($\text{L} \cdot \text{mg}^{-1} \cdot \text{min}^{-1}$), N_0 es la capacidad dinámica del lecho ($\text{mg} \cdot \text{L}^{-1}$), Z es la longitud del lecho (cm), u es la velocidad de flujo lineal ($\text{cm} \cdot \text{min}^{-1}$) y t el tiempo de servicio de la columna (min)

- **Modelo de Thomas.** Es uno de los métodos más empleados, asume la isoterma de Langmuir para el equilibrio. Su principal limitación es que se basa en una cinética de segundo orden y que la adsorción está controlada por la transferencia de materia en la interfase [108]. Viene dado por la siguiente expresión:

$$\ln\left(\frac{C}{C_0} - 1\right) = \frac{K_T \cdot q_0 \cdot m}{Q} - K_T \cdot C_0 \cdot t \quad \text{Ec 1.7}$$

donde K_T es la constante de velocidad de Thomas ($\text{L} \cdot \text{min}^{-1} \cdot \text{mg}^{-1}$), q_0 es la máxima capacidad de adsorción ($\text{mg} \cdot \text{g}^{-1}$), m es la masa de adsorbente (g) y Q es el flujo volumétrico ($\text{L} \cdot \text{min}^{-1}$).

- **Modelo Yoon-Nelson.** Considera que la velocidad de disminución de la probabilidad de adsorción es proporcional a la probabilidad de adsorción del adsorbato y a la probabilidad de que no se adsorba sobre el adsorbente [109]. Es menos complejo que el resto de modelos y se representa por la siguiente ecuación:

$$\ln\left(\frac{C}{C_0 - C}\right) = K_{YN} \cdot t - \tau \cdot K_{YN} \quad \text{Ec 1.8}$$

donde K_{YN} es la constante de Yoon-Nelson (min^{-1}) y τ es el tiempo necesario para retener el 50% del adsorbato (min).

- **Modelo de Clark.** Clark empleó el coeficiente de transferencia de masa en combinación con la isoterma de Freundlich definiendo una nueva curva de ruptura [110]:

$$\ln \left[\left(\frac{C_0}{C} \right)^{n-1} - 1 \right] = -r \cdot t + \ln A \quad \text{Ec 1.9}$$

n es el parámetro de Freundlich y A y $r(\text{min}^{-1})$ de Clark.

1.6.4. Regeneración del adsorbente

Una vez que se alcanza la saturación del lecho, es posible su regeneración para su posterior uso en sucesivos ciclos de adsorción. Existen diversos métodos de regeneración del adsorbente, cuyas ventajas y desventajas pueden verse en la Tabla 1.7.

Si nos centramos en el proceso de desorción propiamente dicho, éste se logra a través de variaciones de temperatura o de presión. La adsorción normalmente es un proceso exotérmico favorecido por la disminución de la temperatura, por lo que la desorción se verá favorecida a altas temperaturas. En cuanto a la presión, por regla general un aumento de la presión, favorece la desorción del contaminante [95].

Tabla 1.7. Tecnologías de regeneración del adsorbente [95, 111, 112]

Método de desorción	Fundamento	Ventajas	Inconvenientes
Térmico	Gas a elevada temperatura	Recuperación de sustancia en alta concentración	Elevado coste Pérdida de capacidad
Oxidación húmeda	Alta T y P en presencia de aire	No emisión de partículas Moderado coste	Pérdidas de masa por oxidación del adsorbente Alteraciones químicas en la superficie del adsorbente
Biológico	Bacterias en los poros del adsorbente	Elevada eficacia	Possible superproducción de biomasa Posterior desinfección
Extracción con disolvente	Desplazamiento del adsorbato con corriente liq. o gas	Ciclos rápidos	En ocasiones disolventes caros y tóxicos

1.6.5. Materiales carbonosos empleados como adsorbentes

Existen multitud de materiales que pueden ser utilizados como adsorbentes, los cuales deben cumplir una serie de características. Debido a que la acumulación de adsorbato por unidad de superficie es muy pequeña, suelen seleccionarse materiales porosos para el proceso de adsorción, con elevada superficie específica y volumen de poros, lo que dotará al adsorbente de una elevada capacidad de adsorción. Además es importante que el adsorbente sea de bajo coste, abundancia, fácil regeneración, etc.

Entre los adsorbentes más ampliamente utilizados se encuentran la alúmina, gel de sílice, carbón activo, zeolitas y adsorbentes poliméricos. Muchos de estos adsorbentes son de origen sintético, pero en otros casos, como el de la zeolita, son de origen natural. Adsorbentes como la alumina, gel de sílice y carbón son amorfos, y contienen redes complejas de microporos, mesoporos y macroporos interconectados [113]. Por el contrario, los poros presentes en las zeolitas son de dimensiones precisas [113]. Por regla general, los adsorbentes de origen sintético presentan mayores capacidades de adsorción, aunque en ocasiones pueden resultar costosos.

Los adsorbentes carbonosos han sido ampliamente utilizados para el tratamiento de aguas, contando con muy buenas capacidades de adsorción para la gran mayoría de los contaminantes orgánicos presentes en las mismas [114]. Existe gran variedad de adsorbentes carbonos, los cuales se nombran a continuación.

Carbón activo. Es un material carbonoso no grafitizable, constituido por un conjunto irregular y generalmente desordenado de capas de carbono. Su estructura cristalina difiere bastante de la de un cristal de grafito, con distancias entre planos superiores a las del grafito. Todo ello hace que posean una estructura porosa interna altamente desarrollada, accesible para los procesos de adsorción [115, 116]. La adecuada elección de las variables que afectan al proceso de síntesis (temperatura, caudal de gas, precursor, etc.) permiten controlar y adaptar las propiedades finales del carbón activado.

Podemos clasificar el carbón activo en polvo (CAP) y granular (CAG), dependiendo del tamaño de grano del mismo; grano fino o grueso (Figura 1.10).

- Carbón activado en polvo (CAP). Carbón pulverizado con un tamaño inferior a 100 µm, siendo el tamaño habitual entre 15 y 25 µm. Se emplea para aplicaciones en fase líquida y sobre todo en el tratamiento de aguas residuales.
- Carbón activado granular (CAG). Son partículas de forma irregular y cuyo tamaño medio está comprendido entre 1 y 5 mm. Se emplea tanto en fase gas como líquida.

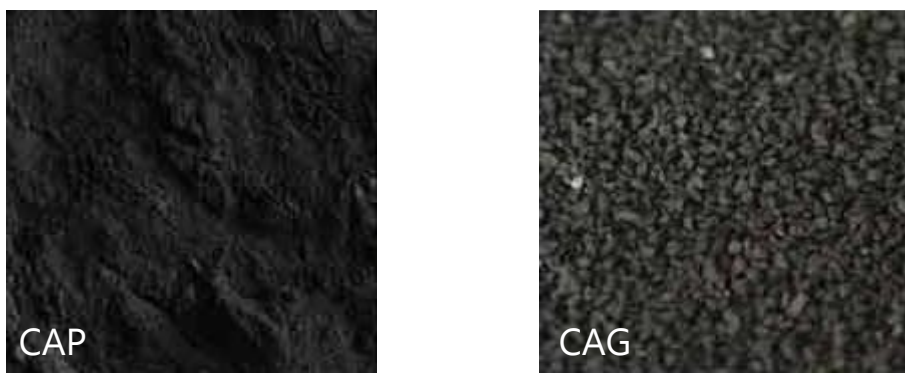


Figura 1.10. Tipos de carbón activo en función del tamaño de partícula. Carbón activado en polvo (CAP) y carbón activado granular (GAP)

- **Nanotubos de carbono (CNT).** Los nanotubos de carbono constan de una o varias láminas de grafito enrolladas sobre sí mismas, formando así nanotubos de pared simple (single wall carbon nanotube, SWCNT) o de pared múltiple (multi wall carbon nanotube, MWCNT) (Figura 1.11). En el caso de SWCNT, cada átomo de carbono está unido a otros tres mediante hibridación sp^2 , quedando el cuarto enlace del carbono deslocalizado entre los demás átomos, por lo que la capa exterior presenta un arreglo hexagonal de átomos de carbono [117]. En el caso de MWCNT, presenta también una hibridación sp^2 , pero el cuarto enlace de carbono forma enlaces débiles tipo Van der Waals con las demás láminas de grafito [118]. La perfecta estructura cristalina de los CNT se va perdiendo al aumentar el número de láminas de grafito de la estructura [119].

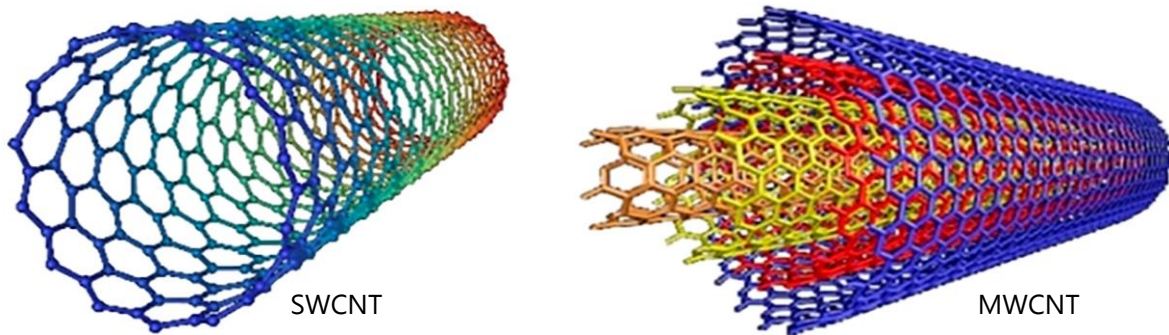


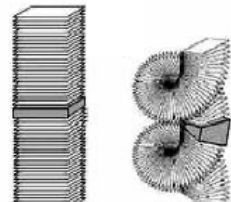
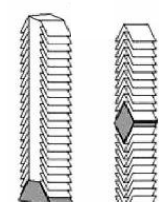
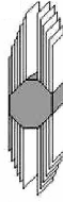
Figura 1.11. Esquema de la estructura de nanotubos de carbono de pared simple (SWCNT) y de pared múltiple (MWCNT).

La estructura de los CNT les confiere de propiedades diversas, como pueden ser la dureza y rigidez, elasticidad, resistencia térmica y mecánica, elevada superficie específica, etc. En cuanto a su aplicación como adsorbentes, se presentan como una gran alternativa debido a su gran área superficial.

- **Nanofibras de carbono (NF).** Son filamentos compuestos principalmente por carbono de naturaleza grafítica, con diámetros entre 20 y 80 nm, presentando en ocasiones un hueco en su interior. En función del ángulo con el que los planos de grafito estén orientados respecto al eje de la fibra, tendrán lugar cuatro tipos de NF (Tabla 1.8).

Podrían considerarse como una variedad de los nanotubos de carbono, pero presentan una mayor cantidad de defectos en su estructura [119]. Las propiedades de las NF dependerán de su estructura atómica y de su ordenamiento electrónico y molecular [121]. Presentan un gran número de bordes que constituyen sitios fácilmente accesibles para interacción química o física, particularmente para la adsorción [122].

Tabla 1.8. Disposición de los planos de grafeno en las nanofibras de carbono [120]

Tipo	Posición de los planos	Estructura
<i>Platelet</i>	Perpendiculares al eje	
<i>Fishbone</i>	Inclinados respecto al eje	
<i>Ribbon</i>	Paralelos al eje	
<i>Stacked cup</i>	Inclinados respecto al eje y son huecas	

- **Grafito de elevada área superficial (HSAG).** Está constituido por láminas paralelas de carbón dispuestas de forma hexagonal. El grafito es un material cristalino no poroso a partir del cual puede obtenerse grafito de alta superficie por un proceso especial de molido. De este modo, pueden obtenerse áreas superficiales de entre $100\text{-}500 \text{ m}^2\cdot\text{g}^{-1}$, lo que hacen que sea un material interesante para su uso como adsorbente. El HSAG no presenta prácticamente microposidad, por lo que su contribución a la porosidad es prácticamente debida a los mesoporos.
- **Materiales carbonosos funcionalizados.** Una de las ventajas que presentan los materiales carbonosos es la posibilidad de incorporar heteroátomos a su estructura, permitiendo así su funcionalización. Con esto, podrán mejorarse las propiedades de estos materiales para su empleo como adsorbentes para determinados tipos de contaminantes. Es posible adicionar grupos oxigenados, comúnmente de naturaleza hidrófila, los cuales son capaces de adsorber fácilmente las especies polares, además de aumentar la humectabilidad [123-125]. Es posible también la modificación con átomos de nitrógeno, con el objetivo de aumentar las propiedades básicas [123]. Con la modificación química de los materiales carbonosos es posible aumentar su poder de adsorción y modificar su selectividad hacia determinados grupos de contaminantes.

1.7. Fundamentos teóricos de las técnicas voltamperométricas

La voltamperometría engloba a un grupo de técnicas comúnmente usadas para el análisis químico de diversos compuestos, así como para establecer el punto de equivalencia en las valoraciones; presentando una sensibilidad que oscila entre 10^{-8} y $10^{11} \text{ mol}\cdot\text{L}^{-1}$ [126]. Una novedosa aplicación de las técnicas voltamperometricas, sería su empleo como técnica de degradación; particularmente para la eliminación de contaminantes emergentes, dadas las grandes ventajas que ofrecen estas técnicas. Presentan facilidad de operación, así como la opción de trabajar a presión y temperatura ambientales, pudiendo además alcanzar una completa mineralización del compuesto a degradar [127, 128].

En las técnicas voltamperométricas se aplica un determinado potencial eléctrico a un electrodo de trabajo sumergido en una disolución que contiene una especie electroactiva, midiendo la intensidad de corriente que circula por dicho electrodo. Se aplica un programa de potencial en función del tiempo y se obtiene un gráfica de corriente-potencial, denominado voltamperograma.

1.7.1. Técnicas voltamperométricas de barrido

- **Voltamperometría de barrido lineal.** Es uno de los métodos más sencillos en el que se aumenta o disminuye el potencial del electrodo de trabajo de manera lineal con el tiempo [129].

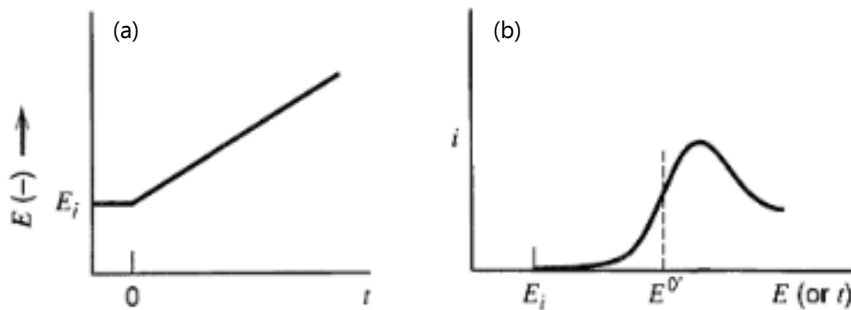


Figura 1.12. (a) Señal de perturbación y (b) voltamperograma al aplicar voltamperometría de pulso lineal.

- **Voltamperometría cíclica (CV).** Se diferencia de la voltamperometría de barrido lineal en que una vez que se alcanza el potencial máximo, se lleva a cabo un nuevo barrido en sentido contrario, hasta alcanzar el valor inicial (Figura 1.13). El barrido inicial se realiza hacia potenciales positivos, de manera que el compuesto presente en el electrolito, será oxidado. Al invertir la corriente, el compuesto es reducido de nuevo. En el caso de procesos reversibles, obtendremos un pico tanto de oxidación como de reducción, mientras que para un sistema irreversible tendremos sólo uno de los dos picos [129]. Hay que destacar que es una de las técnicas voltamperométricas más rápidas.

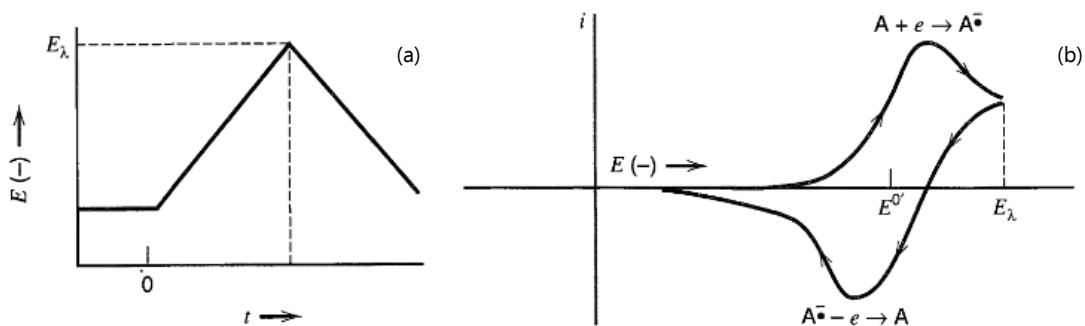


Figura 1.13. (a) Señal de perturbación y (b) voltamperograma al aplicar voltametría cíclica.

- **Voltamperometría normal de pulso (NPV).** Se basa en aplicar sucesivos pulsos de potencial de diferente valor. El potencial aplicado en cada pulso controla la reacción electroquímica [129]. El voltamperograma correspondiente a NPV tiene forma sigmoidal (Figura 1.14).

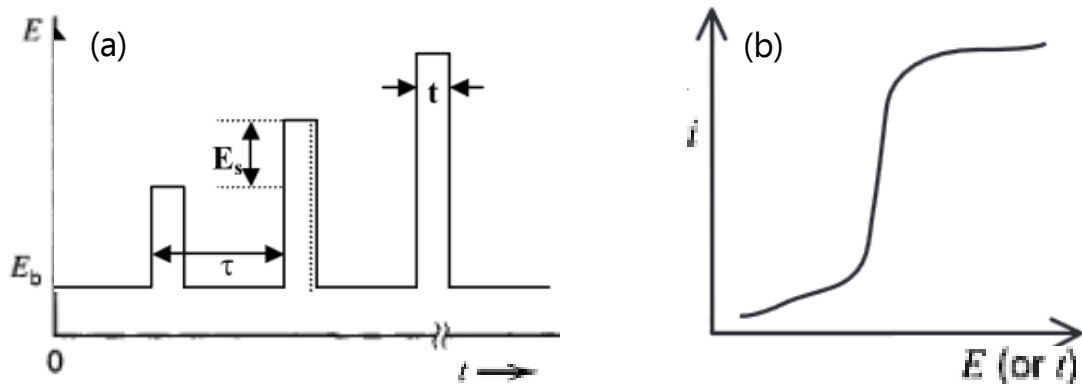


Figura 1.14. (a) Señal de perturbación y (b) voltamperograma al aplicar voltametría normal de pulso.

- **Voltampermetría diferencial de pulso (DPV).** Esta técnica es más sensible y tiene una diferenciación de especies más eficiente, cuando se aplica con propósitos analíticos. Se diferencia de la NPV en que en este caso, el potencial aplicado no retorna en cada pulso al mismo potencial. Esto permite disminuir la corriente de carga en cada pulso y hace más rápida la obtención del voltamperograma. El voltamperograma que se obtiene es aproximadamente la derivada del obtenido mediante NPV, lo que hace que mejore cualitativa y cuantitativamente la técnica [129].

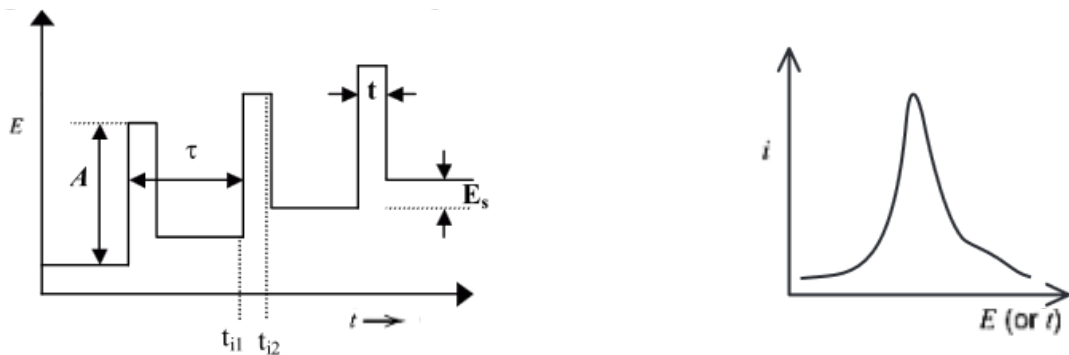


Figura 1.15. (a) Señal de perturbación y (b) voltamperograma al aplicar voltamperometría diferencial de pulso.

- **Voltamperometría de onda cuadrada (SWV).** La corriente es medida durante intervalos muy cortos de tiempo, aplicando una señal en forma de escalón al igual que NPV y DPV, partiendo cada vez de un potencial menor, sin retornar al punto inicial. Es una técnica aún más rápida que DPV y presenta una sensibilidad de dos a tres veces superior a la de DPV [130] [131].

Dada la rapidez de la técnica resulta adecuada para ser acoplada con otras técnicas instrumentales como por ejemplo técnicas cromatográficas [132].

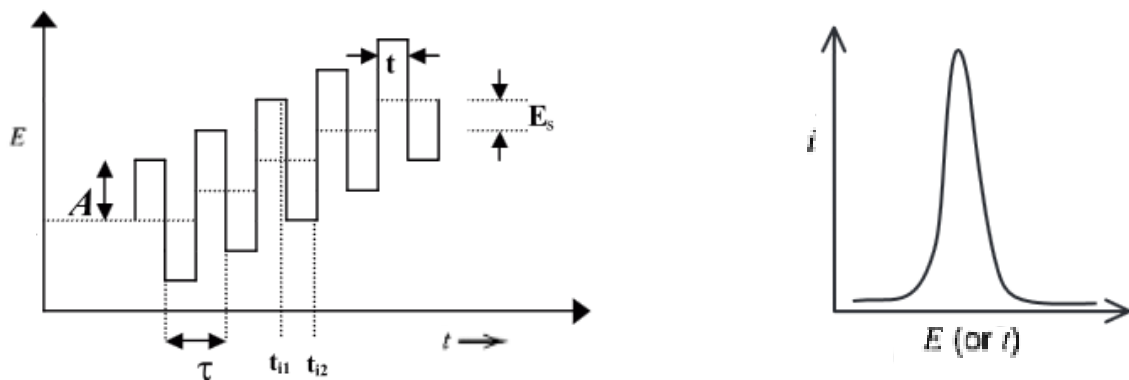


Figura 1.16. (a) Señal de perturbación y (b) voltamperograma al aplicar voltamperometría de onda cuadrada.

1.7.2. Celda de trabajo

La disposición típica consta de una celda electroquímica, el electrolito y tres electrodos: el electrodo auxiliar, el de referencia y el electrodo de trabajo (Figura 1.11).

- Electrodo auxiliar. Permite la circulación de la corriente hacia el electrodo de trabajo. La caída de potencial que en él se produce no es importante para el funcionamiento del sistema.
- Electrodo de referencia. Ha de estar conectado a una entrada de alta impedancia del potenciómetro, para que no se produzca circulación de corriente por el mismo. Ha de ser muy estable ante cambios de concentración de la disolución.
- Electrodo de trabajo. Electrodo sobre el que se realizan las medidas. Al aplicarle una tensión controlada, se medirá la corriente que circula por él.

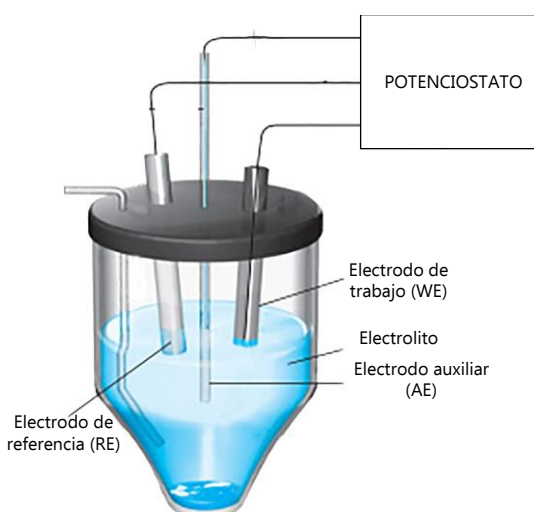


Figura 1.17. Esquema de una celda electroquímica

1.7.3. Electrodos de trabajo basados en carbono

El electrodo de trabajo (working electrode, WE) es el componente más importante de la celda electroquímica. La transferencia de electrones tiene lugar entre la superficie del electrodo de trabajo y el electrolito que contiene al compuesto objeto de estudio, por lo tanto la correcta elección del WE es un parámetro crítico en el desarrollo experimental de técnicas voltamperométricas. Los WE más comúnmente empleados en las diversas técnicas electroquímicas son de platino, oro, carbón y mercurio.

Los electrodos de platino además de ser costosos, ante la presencia de pequeñas cantidades de agua o ácido en el electrolito producen la reducción del ión hidrógeno, formando hidrógeno gas, pudiendo interferir en la señal analítica de los compuestos de estudio.

Los electrodos de oro son también costosos y presentan la desventaja de que sólo pueden emplearse en un rango positivo de potencial, debido a la oxidación de su superficie.

Los electrodos de carbón permiten barridos de potencial a valores negativos. El electrodo más común de carbón es el electrodo de carbón vítreo (glassy carbon electrode, GCE). Presentan el inconveniente de que son difíciles de fabricar.

Los electrodos de mercurio han sido ampliamente empleados. Presentan un gran rango de potenciales en la dirección catódica, pero limitado en la anódica. La alta toxicidad del mercurio ha limitado su uso hoy en día.

Debido a la toxicidad del mercurio y a que tanto los electrodos de platino como oro suelen ser empleados en medios no acuosos, los electrodos basados en carbón se presentan como la mejor alternativa para el tratamiento de contaminantes acuosos [133]. Los electrodos de carbón representan un amplio rango de electrodos donde cabe destacar lo de grafito pirolítico, grafito policristalino, carbón vítreo y fibras de carbono.

- **Electrodo de grafito pirolítico (PG).** Producidos por la pirolisis de hidrocarburos ligeros a elevada temperatura (800 °C). Está formado por sucesivas capas grafíticas orientadas de forma paralela unas con otras [134]. La relativa dificultad en el manejo del material, ha impedido su aplicación generalizada .
- **Electrodo de grafito policristalino.** El carbón es grafitizado con microcristales de varios cientos de angstroms. Éste puede ser en forma de polvo de grafito, sólido con orientación cristalina aleatoria, carbón grafitizado o una película de carbón pirolizado [134]. Este tipo de electrodos suelen presentar alta porosidad, siendo necesario reducirla ya que si no, la solución entrará en el electrodo y provocará una corriente de fondo muy elevada, perjudicando a la señal de los compuestos[134].

- **Electrodo de carbón vítreo (GC).** Fabricado a partir de polímero carbonáceo de alto peso molecular. Ha sido ampliamente estudiado debido a sus buenas características. Es impermeable a gases y líquidos, por lo que la porosidad en este caso no supone un problema, además de ser compatible con la gran mayoría de disolventes[134]. Es probablemente el electrodo más empleado.

- **Fibras de carbono.** Son fibras de carbono con diámetro en el rango de unas pocas micras. La gran mayoría son obtenidas a partir de brea de petróleo o poliacrilonitrilo (PAN). Es un material relativamente novedoso, que aún no ha sido ampliamente estudiado.

Generalmente los electrodos comerciales presentan bajas sensibilidades, por lo que con el fin de mejorar las propiedades y respuesta de los electrodos convencionales, es posible modificar la superficie del electrodo. Los nanotubos de carbono (CNT) se emplean para la modificación dadas sus buenas propiedades en electroquímica, como son los bajos límites de detección que presenta, aumento de la sensibilidad y disminución de sobretensiones [135]. La primera modificación mediante CNT fue realizada por Britto et al., en 1996 [136]. Emplearon el electrodo modificado para la oxidación electroquímica de dopamina, obteniendo una mejora en su degradación. En la actualidad son numerosos los estudios sobre la modificación de GCE mediante una película o capa de nanotubos de carbono, mejorando los resultados frente al empleo de electrodos de carbón vítreo sin modificar [137-142].

Para la modificación es necesario dispersar los CNT en un disolvente orgánico y pipetejar un volumen conocido de la suspensión sobre la superficie del electrodo, dejando que el disolvente se volatilice quedando depositada una fina capa de CNT sobre la superficie del electrodo [135]. De este modo se consigue tras la modificación un incremento del área superficial del electrodo, lo que provocará una mejora en la respuesta electroquímica, sumado a la habilidad de los CNT de promover reacciones de transferencia de electrones.

1.8. Bibliografía

- [1] T.-T. Pham, S. Proulx, PCBs and PAHs in the Montreal Urban Community (Quebec, Canada) wastewater treatment plant and in the effluent plume in the St Lawrence River, *Water Research*, 31 (1997) 1887-1896.
- [2] R. Rosal, A. Rodríguez, J.A. Perdigón-Melón, A. Petre, E. García-Calvo, M.J. Gómez, A. Agüera, A.R. Fernández-Alba, Occurrence of emerging pollutants in urban wastewater and their removal through biological treatment followed by ozonation, *Water Research*, 44 (2010) 578-588.
- [3] S. SA, Occurrence, treatment, and toxicological relevance of EDCs and pharmaceuticals in water, *Ozone Sci. Eng.*, 30 (2008) 65-69.
- [4] D. Barceló, López de Alda M J . , Contaminación y calidad química del agua: el problema de los contaminantes emergentes, Instituto de Investigaciones Químicas y Ambientales-CSIC (Barcelona), (2008).
- [5] J. Virkutyte, Varma, R.S. & Jegatheesan, V., Treatment of Micropollutants in Water and Wastewater, London, 2010.
- [6] M.I. Farré, S. Pérez, L. Kantiani, D. Barceló, Fate and toxicity of emerging pollutants, their metabolites and transformation products in the aquatic environment, *TrAC Trends in Analytical Chemistry*, 27 (2008) 991-1007.
- [7] S.R. Jackson J., Sources of endocrine-disrupting chemicals in urban wastewater, Oakland, CA, *Science of the Total Environment*, 405 (2008) 153-160.
- [8] G.K.Y. Pal A., Reinhard M., Impact of emerging organic contaminants onfresh-water resources: review of recent occurrences, sources, fate and effects. *Science of the Total Environment Science of the Total Environment*, 408 (2010) 6062-6069.
- [9] M. Petrović, S. Gonzalez, D. Barceló, Analysis and removal of emerging contaminants in wastewater and drinking water, *TrAC Trends in Analytical Chemistry*, 22 (2003) 685-696.
- [10] A. Pal, K.Y.-H. Gin, A.Y.-C. Lin, M. Reinhard, Impacts of emerging organic contaminants on freshwater resources: Review of recent occurrences, sources, fate and effects, *Science of The Total Environment*, 408 (2010) 6062-6069.
- [11] S.P. Dougherty JA, Dinicola RS, Reinhard M. Occurrence of herbicides and pharmaceutical and personal care products in surface water and groundwater around Liberty Bay, Puget Sound, Washington., *J Environ Qual*, (2010) 1173-1180.
- [12] J.L. Zhou, Z.L. Zhang, E. Banks, D. Grover, J.Q. Jiang, Pharmaceutical residues in wastewater treatment works effluents and their impact on receiving river water, *Journal of Hazardous Materials*, 166 (2009) 655-661.
- [13] H. Fromme, S.A. Tittlemier, W. Völkel, M. Wilhelm, D. Twardella, Perfluorinated compounds – Exposure assessment for the general population in western countries, *International Journal of Hygiene and Environmental Health*, 212 (2009) 239-270.

- [14] D. Voutsas, P. Hartmann, C. Schaffner, W. Giger, Benzotriazoles, Alkylphenols and Bisphenol A in Municipal Wastewaters and in the Glatt River, Switzerland, Environmental Science and Pollution Research, 13 (2006) 333-341.
- [15] M.F. Rahman, E.K. Yanful, S.Y. Jasim, L.M. Bragg, M.R. Servos, S. Ndiongue, D. Borikar, Advanced Oxidation Treatment of Drinking Water: Part I. Occurrence and Removal of Pharmaceuticals and Endocrine-Disrupting Compounds from Lake Huron Water, Ozone: Science & Engineering, 32 (2010) 217-229.
- [16] M.J. Benotti, R.A. Trenholm, B.J. Vanderford, J.C. Holady, B.D. Stanford, S.A. Snyder, Pharmaceuticals and Endocrine Disrupting Compounds in U.S. Drinking Water, Environmental science & technology, 43 (2009) 597-603.
- [17] E. Stumm-Zollinger and G.M. Fair, Biodegradation of steroid hormones, Water Pollution Control Federation, 37 (1965) 1506-1510.
- [18] H.H. Tabak and R.L. Bunch, Steroid hormones as water pollutants I. Metabolism of natural and synthetic ovulation-inhibiting hormones by microorganism of activated sludge and primary settles sewage, Dev. Ind. Microbiol., 11 (1970) 367-376.
- [19] J.J. Lech, S.K. Lewis, L. Ren, In vivo estrogenic activity of nonylphenol in rainbow trout, Fundamental and applied toxicology : official journal of the Society of Toxicology, 30 (1996) 229-232.
- [20] http://www.who.int/ipcs/publications/new_issues/endocrine_disruptors/en/. Visitada en Diciembre 2015.
- [21] <http://www.epa.gov/dwucmr>. Visitada en Diciembre 2015.
- [22] <http://www.eea.europa.eu/es>. Visitada en Diciembre 2015.
- [23] Directive 2000/60/EC of the European Parliament and of the Council of 23 October 2000 establishing a framework for Community action in the field of water policy. Official Journal of the European Union; L 327, 22.12.2000, 1-73. Directiva 2008/105/CE del Parlamento Europeo y del Consejo, relativa a las normas de calidad ambiental en el ámbito de la política de aguas, por la que se modifican y derogan ulteriormente las Directivas 82/176/CEE, 83/513/CEE, 84/156/CEE, 84/491/CEE y 86/280/CEE del Consejo, y por la que se modifica la Directiva 2000/60/CE. 348, 24.10.2008, 84-97.
- [24] C.A. de Wit, An overview of brominated flame retardants in the environment, Chemosphere, 46 (2002) 583-624.
- [25] L.S. Birnbaum, D.F. Staskal, Brominated flame retardants: cause for concern, Environmental health perspectives, 112 (2004) 9-17.
- [26] P.O. Darnerud, Toxic effects of brominated flame retardants in man and in wildlife, Environment International, 29 (2003) 841-853.
- [27] K.A. Kenne, U.G. (1996). Environmental Health Criteria 181, Chlorinated Paraffins. Recuperado, Diciembre 1, 2013, de International Programme on Chemical Safety. Sitio web:<http://www.inchem.org/documents/ehc/ehc181.htm>.
- [28] D. Muir, Environmental levels and fate in, Berlin, Heidelberg, 2010.

- [29] S.D. Shaw, A. Blum, R. Weber, K. Kannan, D. Rich, D. Lucas, C.P. Koshland, D. Dobraca, S. Hanson, L.S. Birnbaum, Halogenated flame retardants: Do the fire safety benefits justify the risks?, *Reviews on Environmental Health*, 25 (2010) 261-305.
- [30] Short-chained chlorinated paraffins: revised draft risk profile UNEP/POP/PORC.8/6. United Nations Environmental Programme Stockholm Convention on Persistent Organic Pollutants, Geneva.
- [31] E. Eljarrat, D. Barceló, Quantitative analysis of polychlorinated n-alkanes in environmental samples, *TrAC Trends in Analytical Chemistry*, 25 (2006) 421-434.
- [32] Organización Mundial de la Salud (OMS), Organización Panamericana de la Salud (OPS), División Salud y Ambiente. Plaguicidas y salud en las Américas, Washington: OMS/OPS, 1993.
- [33] T. Colborn, Pesticides--how research has succeeded and failed to translate science into policy: endocrinological effects on wildlife, *Environmental health perspectives*, 103 Suppl 6 (1995) 81-85.
- [34] J.D. McKinney y C.L. Waller, Polychlorinates biphenyls as hormonally active structural analogues, *Environmental health perspectives*, 107 (1994) 63-38.
- [35] B.D. Schultz MM, Field JA, Fluorinated alkyl surfactants, *Environmental Engineering Science*, 20 (2003) 487-501.
- [36] C. Liu, Y. Du, B. Zhou, Evaluation of estrogenic activities and mechanism of action of perfluorinated chemicals determined by vitellogenin induction in primary cultured tilapia hepatocytes, *Aquatic toxicology* (Amsterdam, Netherlands), 85 (2007) 267-277.
- [37] T. Heberer, Occurrence, fate, and removal of pharmaceutical residues in the aquatic environment: a review of recent research data, *Toxicology Letters*, 131 (2002) 5-17.
- [38] K. Kümmerer, Pharmaceuticals in the environment. Sources, fate, effects and risks, Heidelberg, Berlin, 2001.
- [39] A.J. T.A. Ternes, Human Pharmaceuticals, Hormones and Fragrances. The challenge of micropollutants in urban water management, 2006.
- [40] J. Lienert, T. Burki, B.I. Escher, Reducing micropollutants with source control: substance flow analysis of 212 pharmaceuticals in faeces and urine, *Water science and technology: a journal of the International Association on Water Pollution Research*, 56 (2007) 87-96.
- [41] M. Bedner, W.A. MacCrehan, Transformation of acetaminophen by chlorination produces the toxicants 1,4-benzoquinone and N-acetyl-p-benzoquinone imine, *Environmental science & technology*, 40 (2006) 516-522.
- [42] W. Witte, Medical consequences of antibiotic use in agriculture, *Science* (New York, N.Y.), 279 (1998) 996-997.
- [43] R. Triebeskorn, H. Casper, A. Heyd, R. Eikemper, H.R. Kohler, J. Schwaiger, Toxic effects of the non-steroidal anti-inflammatory drug diclofenac. Part II: cytological effects in liver, kidney, gills and intestine of rainbow trout (*Oncorhynchus mykiss*), *Aquatic toxicology* (Amsterdam, Netherlands), 68 (2004) 151-166.

- [44] J.N. Brown, N. Paxéus, L. Förlin, D.G.J. Larsson, Variations in bioconcentration of human pharmaceuticals from sewage effluents into fish blood plasma, *Environmental Toxicology and Pharmacology*, 24 (2007) 267-274.
- [45] H.F. J. Schwaiger, U. Mallow, H. Wintermayr, R.D. Negele, Toxic effects of the non-steroidal anti-inflammatory drug diclofenac, part 1: Histopathological alterations and bioaccumulation in rainbow trout, *Aquat. Toxicol.* 68 (2004) 405-410.
- [46] F.G. B. Quinn, C. Blaise, Evaluation of the acute, chronic and teratogenic effects of a mixture of eleven pharmaceuticals on the cnidarians, *Hydra attenuata*, *Sci. Total Environ.* , 407 (2009) 1072-1079.
- [47] M. González-Pleiter, S. Gonzalo, I. Rodea-Palomares, F. Leganés, R. Rosal, K. Boltes, E. Marco, F. Fernández-Piñas, Toxicity of five antibiotics and their mixtures towards photosynthetic aquatic organisms: Implications for environmental risk assessment, *Water Research*, 47 (2013) 2050-2064.
- [48] G. Teijon, L. Candela, K. Tamoh, A. Molina-Díaz, A.R. Fernandez-Alba, Occurrence of emerging contaminants, priority substances (2008/105/CE) and heavy metals in treated wastewater and groundwater at Depurbaix facility (Barcelona, Spain), *The Science of the total environment*, 408 (2010) 3584-3595.
- [49] M. Solé, Porte, C., Barcelo, D. & Albaiges, J, Bivalves Residue Analysis for the Assessment of Coastal Pollution in the Ebro Delta (NW Mediterranean), *Mar. Pollut. Bull.*, 40 (2000) 746-753.
- [50] M. Kuster, A. De la Cal, E. Eljarrat, M.J. López de Alda, D. Barceló, Evaluation of two aquatic passive sampling configurations for their suitability in the analysis of estrogens in water, *Talanta*, 83 (2010) 493-499.
- [51] C. Salgado-Penital, Llompart, M., García-Jares, C., García-Chao, M. & Cela, R., Simple approach for the determination of brominated flame retardants in environmental solid samples based on solvent extraction and solid-phase microextraction followed by gas chromatography–tandem mass spectrometry, *J. of Chromatogr. A*, 1124 (2006) 139-147.
- [52] R. Rodil, J.B. Quintana, E. Concha-Graña, P. López-Mahía, S. Muniategui-Lorenzo, D. Prada-Rodríguez, Emerging pollutants in sewage, surface and drinking water in Galicia (NW Spain), *Chemosphere*, 86 (2012) 1040-1049.
- [53] A. Hildebrandt, M. Guillamón, S. Lacorte, R. Tauler, D. Barceló, Impact of pesticides used in agriculture and vineyards to surface and groundwater quality (North Spain), *Water Research*, 42 (2008) 3315-3326.
- [54] Y. Valcarcel, S.G. Alonso, J.L. Rodriguez-Gil, R.R. Maroto, A. Gil, M. Catala, Analysis of the presence of cardiovascular and analgesic/anti-inflammatory/antipyretic pharmaceuticals in river- and drinking-water of the Madrid Region in Spain, *Chemosphere*, 82 (2011) 1062-1071.
- [55] E. Estevez, C. Cabrera Mdel, A. Molina-Díaz, J. Robles-Molina, P. Palacios-Díaz Mdel, Screening of emerging contaminants and priority substances (2008/105/EC) in reclaimed water for irrigation and groundwater in a volcanic aquifer (Gran Canaria, Canary Islands, Spain), *The Science of the total environment*, 433 (2012) 538-546.

- [56] N. Ratola, A. Cincinelli, A. Alves, A. Katsoyiannis, Occurrence of organic microcontaminants in the wastewater treatment process. A mini review, *Journal of Hazardous Materials*, 239–240 (2012) 1-18.
- [57] C. Adams, ASCE, M., Wang, Y., Loftin, K. & Meyer, M., Removal of antibiotics from surface and distilled water in conventional water treatment processes, *J. Environ. Eng.*, 128 (2002) 253-259.
- [58] M. Huerta-Fontela, M.T. Galceran, F. Ventura, Occurrence and removal of pharmaceuticals and hormones through drinking water treatment, *Water Research*, 45 (2011) 1432-1442.
- [59] B.N. Estevinho, Martins, I., Ratola, N., Alves, A. & Santos, L. , Removal of 2,4.dichlorophenol and pentachlorophenol from waters by sorption using coal fly ash from Portuguese thermal power plant, *J. Hazard. Mater.*, 143 (2007) 533-540.
- [60] J. Rivera-Utrilla, M. Sánchez-Polo, M.Á. Ferro-García, G. Prados-Joya, R. Ocampo-Pérez, Pharmaceuticals as emerging contaminants and their removal from water. A review, *Chemosphere*, 93 (2013) 1268-1287.
- [61] E.K. Putra, R. Pranowo, J. Sunarso, N. Indraswati, S. Ismadji, Performance of activated carbon and bentonite for adsorption of amoxicillin from wastewater: Mechanisms, isotherms and kinetics, *Water Research*, 43 (2009) 2419-2430.
- [62] H. Peng, B. Pan, M. Wu, Y. Liu, D. Zhang, B. Xing, Adsorption of ofloxacin and norfloxacin on carbon nanotubes: Hydrophobicity- and structure-controlled process, *Journal of Hazardous Materials*, 233–234 (2012) 89-96.
- [63] S.K. Behera, S.-Y. Oh, H.-S. Park, Sorption of triclosan onto activated carbon, kaolinite and montmorillonite: Effects of pH, ionic strength, and humic acid, *Journal of Hazardous Materials*, 179 (2010) 684-691.
- [64] K. Kimura, S. Toshima, G. Amy, Y. Watanabe, Rejection of neutral endocrine disrupting compounds (EDCs) and pharmaceutical active compounds (PhACs) by RO membranes, *Journal of Membrane Science*, 245 (2004) 71-78.
- [65] J.L. Acero, F.J. Benitez, F. Teva, A.I. Leal, Retention of emerging micropollutants from UP water and a municipal secondary effluent by ultrafiltration and nanofiltration, *Chemical Engineering Journal*, 163 (2010) 264-272.
- [66] Y. Yoon, P. Westerhoff, S.A. Snyder, E.C. Wert, Nanofiltration and ultrafiltration of endocrine disrupting compounds, pharmaceuticals and personal care products, *Journal of Membrane Science*, 270 (2006) 88-100.
- [67] M. Bodzek, M. Dudziak, Elimination of steroid sex hormones by conventional water treatment and membrane processes, *Desalination*, 198 (2006) 24-32.
- [68] S.A.W. Parsons, M., Advanced Oxidation Processes for Water and Wastewater Treatment, London, 2004.
- [69] J.C.T.R. Francisco Osorio Robles, Mercedes Sánchez Blas, Tratamiento de aguas para la eliminación de microorganismos y agentes contaminantes. Aplicación de procesos industriales a la reutilización de aguas residuales, Madrid, 2010.

- [70] R. Broséus, S. Vincent, K. Aboufadl, A. Daneshvar, S. Sauvé, B. Barbeau, M. Prévost, Ozone oxidation of pharmaceuticals, endocrine disruptors and pesticides during drinking water treatment, *Water Research*, 43 (2009) 4707-4717.
- [71] U. Von Gunten, Ozonation of drinking water: part I. Oxidation kinetics and product formation, *Water Research*, 37 (2003) 1443-1467.
- [72] V. Homem, L. Santos, Degradation and removal methods of antibiotics from aqueous matrices – A review, *Journal of Environmental Management*, 92 (2011) 2304-2347.
- [73] F.J. Rivas, F.J. Beltrán, A. Encinas, Removal of emergent contaminants: Integration of ozone and photocatalysis, *Journal of Environmental Management*, 100 (2012) 10-15.
- [74] M. Neamțu, D.-M. Popa, F.H. Frimmel, Simulated solar UV-irradiation of endocrine disrupting chemical octylphenol, *Journal of Hazardous Materials*, 164 (2009) 1561-1567.
- [75] E.S. Elmolla, M. Chaudhuri, Degradation of the antibiotics amoxicillin, ampicillin and cloxacillin in aqueous solution by the photo-Fenton process, *Journal of Hazardous Materials*, 172 (2009) 1476-1481.
- [76] K.G. Linden, M. Mohseni, 2.8 - Advanced Oxidation Processes: Applications in Drinking Water Treatment, in: S. Ahuja (Ed.) *Comprehensive Water Quality and Purification*, Elsevier, Waltham, 2014, pp. 148-172.
- [77] A.R. Fernández-Alba, Letón, P., Rosal, R., Dorado, M., Villar, S. & Sanz J.M. , Tratamientos avanzados de aguas residuales industriales, pp .. Cap. 2, Madrid, (2006) 30-43.
- [78] T. Urase y T. Kikuta, Separated estimation of adsorption and degradation of pharmaceuticals substances and strogens in the activates sludge process, *Water Res.*, 39 (2005) 1283-1300.
- [79] M. Narumiya, Nakada, N., Yamashita, N. & Tanaka H. , Phase distribution and removal of pharmaceuticals and personal care products during anaerobic sludge digestion, *J. Hazard. Mater.*, 260 (2013) 305-3012.
- [80] N. Tadkaew, Hai, F.I., McDonald, J.A., Khan, S.J.& Nghiem, L.D. , Removal of trace organics by MBR treatment: the role of molecular properties, *Water Research*, 45 (2011) 2439-2451.
- [81] P. Cartajena, El Kaddouri, M., Cases, V., Trapote, A. & Prats, D., Reduction of emerging micropollutants, organic matter, nutrients and salinity from real wastewater by combined MBR-NF/RO treatment, *Sep. Purif. Technol.*, 110 (2013) 132-143.
- [82] J. Sipma, B. Osuna, N. Collado, H. Monclús, G. Ferrero, J. Comas, I. Rodriguez-Roda, Comparison of removal of pharmaceuticals in MBR and activated sludge systems, *Desalination*, 250 (2010) 653-659.
- [83] L.N. Nguyen, Hai, F.I., Kang, J., Price, W.E.& Nghiem, L.D. , Removal of trace organic contaminants by a membrane bioreactor-granular activated carbon (MBR-GAC) system, *Bioresource Technol.*, 113 (2012) 169-173.
- [84] T. Melin, Jefferson, B., Bixio, D., Thoeye, C., De Wilde, W., De Koning, J., Membrane bioreactor technology for wastewater treatment and reuse, *Desalination*, 187 (2006) 271–282.

- [85] M.A. Blackburn, S.J. Kirby, M.J. Waldock, Concentrations of alkylphenol polyethoxylates entering UK estuaries, *Marine Pollution Bulletin*, 38 (1999) 109-118.
- [86] A.J. Watkinson, E.J. Murby, D.W. Kolpin, S.D. Costanzo, The occurrence of antibiotics in an urban watershed: From wastewater to drinking water, *Science of The Total Environment*, 407 (2009) 2711-2723.
- [87] Y. Xiao, H. Chang, A. Jia, J. Hu, Trace analysis of quinolone and fluoroquinolone antibiotics from wastewaters by liquid chromatography-electrospray tandem mass spectrometry, *Journal of Chromatography A*, 1214 (2008) 100-108.
- [88] L. Zeng, T. Wang, T. Ruan, Q. Liu, Y. Wang, G. Jiang, Levels and distribution patterns of short chain chlorinated paraffins in sewage sludge of wastewater treatment plants in China, *Environmental Pollution*, 160 (2012) 88-94.
- [89] A. Pollice, G. Laera, D. Cassano, S. Diomede, A. Pinto, A. Lopez, G. Mascolo, Removal of nalidixic acid and its degradation products by an integrated MBR-ozonation system, *Journal of Hazardous Materials*, 203–204 (2012) 46-52.
- [90] M.S. Ibrahim, I.S. Shehatta, M.R. Sultan, Cathodic adsorptive stripping voltammetric determination of nalidixic acid in pharmaceuticals, human urine and serum, *Talanta*, 56 (2002) 471-479.
- [91] P. Castells, F.J. Santos, M.T. Galceran, Solid-phase microextraction for the analysis of short-chain chlorinated paraffins in water samples, *Journal of chromatography. A*, 984 (2003) 1-8.
- [92] S. Bayen, J.P. Obbard, G.O. Thomas, Chlorinated paraffins: A review of analysis and environmental occurrence, *Environment International*, 32 (2006) 915-929.
- [93] U.S.E.P.A. (USEPA), *Chlorinated Paraffins. Environmental and Risk Assessment*, Washington DC, 1991.
- [94] D.M. Ruthven, *Principles of adsorption and adsorption processes*, Nueva York, 1984.
- [95] M. Suzuki, *Adsorption engineering*, TOKIO, Japan, 1990.
- [96] P.L. Walker, S.K. Verma, J. Rivera-Utrilla, A. Davis, Densities, porosities and surface areas of coal macerals as measured by their interaction with gases, vapours and liquids, *Fuel*, 67 (1988) 1615-1623.
- [97] F. Ahnert, H.A. Arafat, N.G. Pinto, A Study of the Influence of Hydrophobicity of Activated Carbon on the Adsorption Equilibrium of Aromatics in Non-Aqueous Media, *Adsorption*, 9 311-319.
- [98] N.P. Cheremisinoff, *Handbook of water and wastewater treatment technologies*, Woburn, MA, USA, 2002.
- [99] Y. Yoon, P. Westerhoff, S.A. Snyder, M. Esparza, HPLC-fluorescence detection and adsorption of bisphenol A, 17 β -estradiol, and 17 α -ethynodiol estradiol on powdered activated carbon, *Water Research*, 37 (2003) 3530-3537.

- [100] A.H. El-Sheikh, A.P. Newman, H.K. Al-Daffaee, S. Phull, N. Cresswell, Characterization of activated carbon prepared from a single cultivar of Jordanian Olive stones by chemical and physicochemical techniques, *Journal of Analytical and Applied Pyrolysis*, 71 (2004) 151-164.
- [101] I. Langmuir, THE ADSORPTION OF GASES ON PLANE SURFACES OF GLASS, MICA AND PLATINUM, *Journal of the American Chemical Society*, 40 (1918) 1361-1403.
- [102] H. Freundlich, H. Hatfield, *Colloid & capillary chemistry*, E.P. Dutton, New York, 1922.
- [103] D. MM, The potential theory of adsorption of gases and vapours for adsorbents with energetically non-uniform surface, *Chem. Rev.*, 60 (1960) 235-241.
- [104] D. MM, Microporous structures of carbonaceous adsorbents, *Carbon*, 6 (1968) 183-192.
- [105] S. Brunauer, P.H. Emmett, E. Teller, Adsorption of Gases in Multimolecular Layers, *Journal of the American Chemical Society*, 60 (1938) 309-319.
- [106] E.A. G. Bohart, Some aspects of the behavior of charcoal with respect to chlorine, *J. Am. Chem. Soc* 42 (1920) 523-544.
- [107] H.C. Thomas, Heterogeneous ion exchange in a flowing system, *J. Am. Chem. Soc.*, 66 (1944) 1466–1664.
- [108] J.H.N. Y.H. Yoon. Application of gas adsorption kinetics. I. A theoretical model for respirator cartridge service life, *Am. Ind. Hyg. Assoc. J.*, 45 (1984) 509–516.
- [109] R.M. Clark, Evaluating the cost and performance of field-scale granular activated carbon systems, *Environmental science & technology*, 21 (1987) 573-580.
- [110] H.L. B.B. Pruden, Wet air oxidation of soluble components in waste water, *Can. J. Chem. Eng.*, 54 (1976) 319-325.
- [111] M. Scholz, R.J. Martin, Ecological equilibrium on biological activated carbon, *Water Research*, 31 (1997) 2959-2968.
- [112] E. Worch, *Adsorption Technology in water treatment. Fundamentals, processes and modeling*, Berlin/Boston, 2012.
- [113] A.B.y.A.K. Minocha, Conventional and non-conventional adsorbents for removal of pollutants from water-A review, *Indian Journal of Chemical Technology*, 13 (2006) 203-217.
- [114] F.R.R. H. Marsh, *Activated carbon*, Amsterdam, 2006.
- [115] J.M.D. Tascón, *Novel carbon adsorbents*, Amsterdam, 2012.
- [116] P.M. Ajayan, Nanotubes from Carbon, *Chemical reviews*, 99 (1999) 1787-1800.
- [117] V.J. Cruz-Delgado, C. A. Ávila-Orta, O. Pérez-Camacho, M. García-Zamora, V. E. Comparán-Padilla y F. J. Medellín-Rodríguez Funcionalización de Nanotubos de Carbono para la Preparación de Nanocompuestos Poliméricos, *Ide@s CONCYTEG*, 6 (2011) 675-692.

- [118] M.S. Dresselhaus, G. Dresselhaus y P. Avouris Carbon nanotubes: synthesis, structure, properties and applications, New York, 2001.
- [119] N.M. Rodriguez, A review of catalytically grown carbon nanofibers, Journal of Materials Research, 8 (1993) 3233-3250.
- [120] R.L.M. Tzu-Chi Kuo, and Greg M. Swain, Electrochemical Modification of Boron-Doped Chemical Vapor Deposited Diamond Surfaces with Covalently Bonded Monolayers, Electrochemical & Solid State Lett, (1999) 288-290.
- [121] J. Shi, Y. F. Lu, K.F. Tan, y X. W. Wang, Catalytical growth of carbon nanotubes/fibers from nanocatalysts prepared by laser pulverization of nickel sulfate, J. Appl. Phys., 99 (2006).
- [122] L. Faba, Criado, Y.A., Gallegos-Suárez, E., Pérez-Cadenas, M., Díaz, E., Rodríguez-Ramos, I., Guerrero-Ruiz, A., Ordóñez, S., Preparation of nitrogencontaining carbon nanotubes and study of their performance as basic catalysts, Appl. Catal. A 458 (2013) 155–161.
- [123] J.K. Chinthaginjala, Seshan, K., Lefferts, L., Preparation and application of carbon-nanofiber based microstructured materials as catalyst supports, Ind. Eng. Chem. Res. , 46 (2007) 3968–3978.
- [124] D. Banerjee, U. Sarkar, S. Chakraborty, D. Roy, Removal of a cationic bisbiguanide using Functionalized Activated Carbons (FACs), Process Safety and Environmental Protection, 92 (2014) 957-972.
- [125] S.R.M. Marc J. Madou, Chemical sensing with solid state devices, London, 1989.
- [126] J. Kim, G.V. Korshin, A.B. Velichenko, Comparative study of electrochemical degradation and ozonation of nonylphenol, Water Research, 39 (2005) 2527-2534.
- [127] A.M. Polcaro, S. Palmas, Electrochemical Oxidation of Chlorophenols, Industrial & Engineering Chemistry Research, 36 (1997) 1791-1798.
- [128] J.W. A. J. Bard and L. R. Faulkner, Electrochemical methods: fundamentals and applications, New York, 1980.
- [129] A.J. Bard, Faulkner L.R., Controlled Potential Microelectrode Techniques Potential Step Methods. In Electrochemical Methods, Fundamentals and Applications, New York, EE. UU, 1980.
- [130] T.M.G.E.B. Florence, Electrochemical Techniques for Trace Element Speciation in Waters. In Trace Element Speciation: Analytical Methods and Problems, Florida, EE. UU, 1986.
- [131] J.R. Pretty, E.A. Blubaugh, J.A. Caruso, Determination of arsenic(III) and selenium(IV) using an on-line anodic stripping voltammetry flow cell with detection by inductively coupled plasma atomic emission spectrometry and inductively coupled plasma mass spectrometry, Analytical Chemistry, 65 (1993) 3396-3403.
- [132] E. Pungor, A practical guide to Instrumental Analysis, Florida, 1995.
- [133] W.R.H. Peter Kissinger, Laboratory techniques in electroanalytical chemistry, Nueva York, 1996.

- [134] C.E.Banks y R.G. Compton, New electrodes for old: from carbon nanotubes to edge plane pyrolytic graphite, *Analyst*, 131 (2006) 15-21.
- [135] K.S.V.S.a.P.M.A. P. J. Britto, *Bioelectrochem, Bioenergy*, 41 (1996) 121.
- [136] G. Paimard, M.B. Gholivand, M. Shamsipur, Determination of ganciclovir as an antiviral drug and its interaction with DNA at Fe₃O₄/carboxylated multi-walled carbon nanotubes modified glassy carbon electrode, *Measurement*, 77 (2016) 269-277.
- [137] S. Cerovac, V. Guzsvány, Z. Kónya, A.M. Ashrafi, I. Švancara, S. Rončević, Á. Kukovecz, B. Dalmacija, K. Vytrás, Trace level voltammetric determination of lead and cadmium in sediment pore water by a bismuth-oxychloride particle-multiwalled carbon nanotube composite modified glassy carbon electrode, *Talanta*, 134 (2015) 640-649.
- [138] F.A. Gutierrez, M.D. Rubianes, G.A. Rivas, Electrochemical sensor for amino acids and glucose based on glassy carbon electrodes modified with multi-walled carbon nanotubes and copper microparticles dispersed in polyethylenimine, *Journal of Electroanalytical Chemistry*.
- [139] A. Hatefi-Mehrjardi, M.A. Karimi, S. kamalabadi-khorasani, Electrocatalytic Oxidation and Determination of Insulin at Rhodamine B –Multi-walled Carbon Nanotubes Modified Glassy Carbon Electrode, *Procedia Materials Science*, 11 (2015) 162-165.
- [140] R. Gupta, J. Gamare, M.K. Sharma, J.V. Kamat, Electrochemical investigations of Pu(IV)/Pu(III) redox reaction using graphene modified glassy carbon electrodes and a comparison to the performance of SWCNTs modified glassy carbon electrodes, *Electrochimica Acta*.
- [141] J. Hubalek, J. Prasek, D. Huska, M. Adamek, O. Jasek, V. Adam, L. Trnkova, A. Horna, R. Kizek, Modification of Working Electrode Surface with Carbon Nanotubes as an Electrochemical Sensor for Estimation of Melting Points of DNA, *Procedia Chemistry*, 1 (2009) 1011-1014.



Capítulo II

Objetivos

En este capítulo se presenta el objetivo principal de la presente Tesis Doctoral, así como los objetivos específicos de cada uno de los bloques que la componen

II. Objetivos

Dado el interés creciente en la eliminación de los contaminantes emergentes en las aguas y la problemática de las bajas concentraciones a las que se encuentran, se plantea como objetivo general de la tesis, el desarrollo de una alternativa novedosa para su eliminación, basada en un proceso en dos etapas. Una primera etapa de pre-concentración, basada en la adsorción, y una segunda etapa de degradación del contaminante, mediante técnicas electroquímicas.

El estudio de dicho objetivo se ha estructurado en tres bloques diferenciados, dando lugar a los siguientes objetivos específicos:

1. Adsorción en discontinuo. El objetivo de este bloque es la selección de los adsorbentes óptimos para la pre-concentración de cada contaminante modelo estudiado (ácido nalidíxico, 1,8-diclorooctano y 2-(4-metilfenoxi)etanol). Con dicho fin, se estudia el comportamiento de diferentes materiales carbonosos, tanto mesoporosos como microporosos, analizando las isotermas de adsorción obtenidas con cada uno de ellos y las consiguientes capacidades máximas de adsorción. De igual forma, se realizaron estudios a diferentes temperaturas con la finalidad de determinar los parámetros termodinámicos necesarios para caracterizar completamente el proceso de adsorción en cada uno de los casos.

2. Adsorción en continuo. Una vez identificados los adsorbentes óptimos para cada contaminante emergente, se ha abordado la etapa de pre-concentración, mediante ciclos de adsorción-desorción. Con estos estudios se determina el adsorbente que proporciona una óptima pre-concentración para cada compuesto modelo, analizando los resultados desde un

doble punto de vista: maximizar el factor de concentración y también la regenerabilidad, de forma que se garantice su eficacia en posteriores ciclos. Estos estudios están basados en la comparación y análisis de las consiguientes curvas de ruptura, incluyendo la modelización de las mismas.

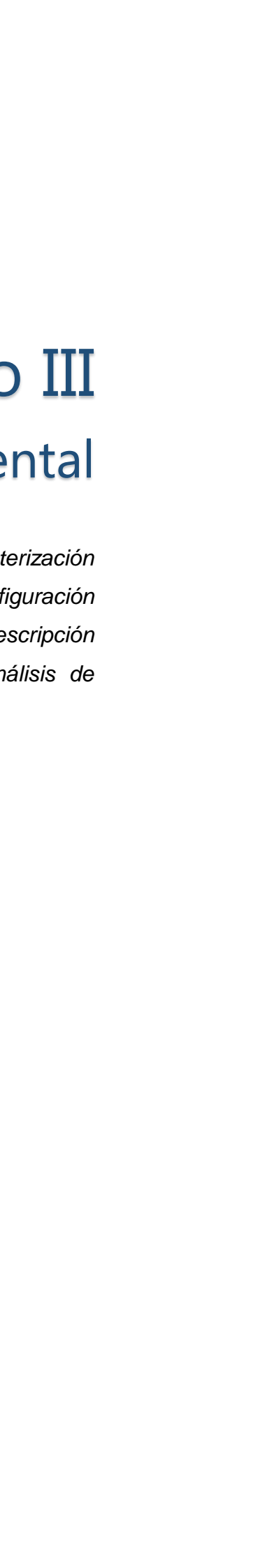
3. Degradación electroquímica. La finalidad del último bloque es el desarrollo de un método electroquímico que permita la degradación de los contaminantes modelo. Se estudiará la influencia de los parámetros típicos que afectan a este tipo de procesos ampliando el estudio a la modificación del electrodo de trabajo con nanotubos de carbono sin funcionalizar y funcionalizados con grupos amino y carboxilo. Se busca así maximizar la adsorción y posterior degradación de los compuestos, aumentando el área superficial y los centros activos de adsorción del electrodo.



Capítulo III

Metodología experimental

En este capítulo se describen las técnicas de caracterización empleadas, así como los procedimientos y configuración experimental utilizados. Cuenta también con una descripción de las distintas técnicas empleadas para el análisis de muestras

- 
- 3.1. Técnicas de caracterización de materiales
 - 3.2. Ensayos de adsorción
 - 3.3. Degradación electroquímica
 - 3.4. Análisis de muestras

III. Metodología experimental

En este capítulo se describen los procedimientos experimentales empleados en las diferentes técnicas de caracterización de materiales, técnicas de adsorción, así como las técnicas electroquímicas.

En las técnicas electroquímicas, se nombrarán dos equipos experimentales diferentes, ya que parte de estos estudios fueron realizados en la Universidad de Amberes (Bélgica), durante la estancia predoctoral.

3.1. Técnicas de caracterización de materiales

3.1.1. Técnicas de microscopía electrónica

La microscopía electrónica realiza el estudio de imágenes a gran aumento, empleando para generarlas haces de electrones que barren la superficie del material (microscopía electrónica de barrido) o atraviesan el espesor (microscopía electrónica de transmisión).

- **Microscopía electrónica de barrido.** La microscopía electrónica de barrido (SEM) da información de la morfología y topografías de los sólidos objeto de estudio. La superficie de la muestra es barrida por un haz de electrones enfocado con precisión. La imagen es barrida en una serie de líneas y redes, construyéndose una imagen de la superficie. Esta imagen es formada a partir de los electrones secundarios, emitidos como consecuencia de las ionizaciones surgidas de las interacciones inelásticas entre la materia y el haz, por lo que poseen baja energía. Como consecuencia de su baja energía, los electrones tienen un camino libre medio corto, por lo que se asegura que la señal proviene de la región superficial de la muestra. El número de electrones

emitidos depende del ángulo de la superficie de la muestra respecto al haz de electrones y al detector.

El número de electrones secundarios producidos depende del material y de su forma. A mayor número atómico mayor emisión y además, ésta será diferente en función de la zona. La emisión en una zona rugosa, borde o arista será mayor debido a la mayor concentración de carga en esos puntos.

La superficie de la muestra debe ser conductora de la electricidad. En caso de que no lo sea, es necesario recubrir la superficie con una fina capa conductora, generalmente de oro o carbono, para evitar que la superficie se cargue, lo que ocasionaría distorsión en la imagen.

Para los análisis SEM se empleó un microscopio QUANTA 250 FEG SEM (FEI, Hillsboro, Oregon, USA). La técnica fue empleada para la caracterización de los electrodos de trabajo en las técnicas electroquímicas. No fue necesario recubrir la muestra por ser ésta conductora.

- **Microscopía electrónica de transmisión.** La microscopía electrónica de transmisión (TEM) ofrece información acerca de la microestructura del material (tanto si es amorfa como cristalina) y de las distancias interplanares de un material cristalino. La muestra debe de ser muy fina para penetrar los electrones. Cuando éstos colisionan con la muestra, en función el grosor y de los átomos que la forman, una parte de los electrones rebotan o son absorbidos por el objeto y otros lo atraviesan formando una imagen aumentada. La imagen final que puede tener miles de aumentos. Se obtendrá una imagen con diferentes intensidades de gris en función del grado de dispersión de los electrones incidentes.

Para los análisis TEM se utilizó un microscopio modelo JEOL JEM-2100F a 200 kV. Las muestras fueron preparadas por molienda y posterior dispersión ultrasónica en una solución de acetona.

3.1.2. Espectroscopía fotoelectrónica de Rayos-X (XPS). El análisis más básico XPS permite el análisis cuantitativo y cualitativo de todos los elementos, excepto el hidrógeno y helio. Con aplicaciones más sofisticadas, es posible obtener información detallada de la química, organización y morfología de la superficie. Esta técnica proporciona información del estado de oxidación, entorno químico, orbitales moleculares, información sobre estructuras aromáticas o insaturadas, etc. Es el método de caracterización de superficies más ampliamente utilizado.

La técnica está basada en la interacción de fotones de luz con la superficie del sólido. Los fotones incidentes han de tener una energía superior a la energía necesaria para desprender un electrón del átomo en el que se encuentra (energía de ligadura). La energía de los fotones incidentes,

pasa a ser adsorbida por el electrón, por lo que la medida de la energía cinética de los electrones permite calcular la energía de ligadura de estos. Esta energía es propia de cada elemento en cada estado de oxidación.

El análisis se llevó a cabo con un espectrómetro ESCA-PROBE P (Omicron) mediante el uso de la radiación Mgk no monocromática (1253,6 eV). La presión de fondo en la cámara de análisis se mantuvo por debajo de 5×10^{-9} mbar durante la adquisición de datos. Todas las energías de enlace hacen referencia a la línea de (1s) a 284,6 eV.

3.1.3. Fisisorción de nitrógeno. Es un proceso de adsorción y desorción de gases, empleado para la determinación de propiedades superficiales de sólidos. La técnica de fisisorción de gases es la más empleada para la determinación de áreas superficiales y distribución de tamaños de poro.

Al poner el gas en contacto con el sólido desgasificado, la velocidad de adsorción será rápida, disminuyendo a medida que se va cubriendo la superficie, momento en el que aumenta la desorción. Llega un punto en el que se alcanza el equilibrio dinámico donde el número de moléculas adsorbidas y desorbidas es igual, momento en el cual, el sólido está en equilibrio de adsorción con el gas. El equilibrio entre las moléculas adsorbidas y las moléculas en fase gaseosa depende de la presión del gas y de la temperatura. La relación entre las moléculas que han sido adsorbidas y la presión a temperatura constante, se traduce en isotermas de adsorción. El eje de abscisas de la isoterma de adsorción viene representado por (p/p^0) , donde p^0 es la presión de vapor del adsorbato a la temperatura de trabajo. En función de la forma de la gráfica obtenida, podemos tener seis tipos de isotermas de adsorción (Fig. 2.1):

- **Isoterma tipo I.** Cónica hacia el eje de abscisas. Se corresponden con sólidos microporosos, donde se produce la adsorción en monocapa en la primera zona, mientras que la zona de pendiente suave se corresponde con la adsorción en multicapa.
- **Isoterma tipo II.** Forma de isoterma correspondiente con un sólido no poroso o macroporoso. Representa una adsorción en monocapa y multicapa sin restricciones. El punto B (Figura 2.1) indica el valor de la presión relativa para el cual se ha producido el recubrimiento completo de la monocapa, por lo que indica el principio de la adsorción en multicapa.
- **Isoterma tipo III.** Convexa hacia el eje de abscisas. Típica de materiales macroporosos o no porosos cuando la interacción entre el adsorbato y adsorbente es débil.
- **Isoterma tipo IV.** Presenta un ciclo de histéresis por la condensación capilar dada por la adsorción/desorción en mesoporos. Esta isoterma la presentan los sólidos mesoporosos. En la parte inicial, al igual que en la isoterma tipo II tiene lugar la adsorción en monocapa.

- **Isoterma tipo V.** Es una isoterma muy poco frecuente que tiene lugar en materiales mesoporosos (por ello el ciclo de histéresis) con poca afinidad entre el adsorbato y el adsorbente.
- **Isoterma tipo VI.** Es una adsorción en multicapa escalonada, sobre una superficie uniforme no porosa. Cada escalón obtenido se corresponde con una capa adsorbida.

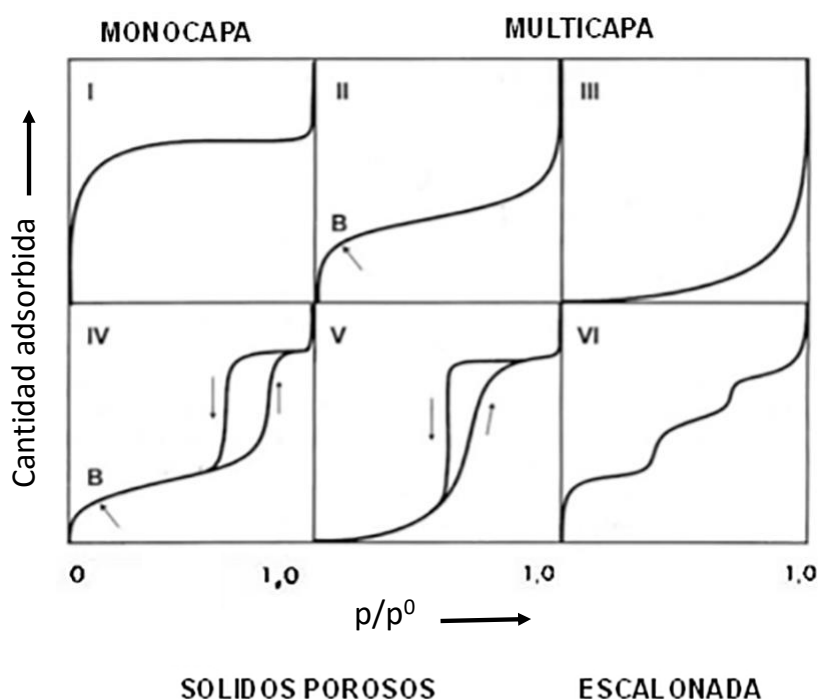


Figura 2.1. Clasificación de las isothermas de adsorción

Los análisis de fisisorción de este trabajo fueron realizados mediante un procedimiento volumétrico estático en un Micromeritics ASAP 2010. Previo al análisis de adsorción, las muestras fueron desgasificadas durante 2 horas a 110 °C. Se aplicó la ecuación de Brunauer, Emmet y Teller (BET) para obtener valores del área superficial (sección transversal de adsorción de N₂ de 0.16 nm²), la cual tiene en cuenta la formación de multicapas y se aplica en materiales mesoporosos. Las distribuciones de tamaño de volumen de mesoporos y poros se obtuvo mediante la aplicación del modelo Barret, Joyner y Halenda (BJH) a la rema de desorción de la isoterma de nitrógeno.

3.1.4. Potencial zeta: punto isoeléctrico

La carga superficial de un material puede afectar a las propiedades y comportamiento de cualquier material. El potencial zeta (ζ) es un indicador de la carga superficial. Dado que la adsorción de cualquier ion depende de su estructura química, de su concentración en disolución y de la estructura superficial. Las medidas del potencial ζ pueden realizarse con diversos fines,

como son el cálculo del punto isoeléctrico, caracterización de la estructura química superficial de sólidos, determinación de energía libre de adsorción de tensioactivos sobre sólidos, etc.

Cuando dos fases están en contacto, existe una diferencia de potencial entre ambas. Sobre la superficie del sólido existe un exceso de carga de un determinado signo, neutralizada por la carga de signo contrario distribuida a lo largo de la disolución. El potencial ξ es el potencial que se encuentra entre la superficie cargada y la disolución.

El pH es el factor más importante que afecta al potencial ξ . Una medida de éste a diferentes pHs permite obtener el punto isoeléctrico, definido como el pH al cual el potencial ξ es cero, siendo el punto donde el sistema coloidal es menos estable.

Las medias de punto isoeléctrico de los distintos materiales se realizaron en un Zetasizer Nano series (Malvern Instruments, UK). Para su medida se preparó una suspensión perfectamente estable de los distintos materiales en agua.

3.1.5. Desorción a temperatura programada (TPD)

La TPD da información sobre la cantidad de grupos oxigenados de la superficie de materiales carbonosos, su estabilidad térmica y su naturaleza. Es una de las técnicas más empleadas para evaluar la química superficial de diversos materiales,

Se basa en el estudio de las especies desorbidas en un material sólido cuando se somete éste a un programa de temperatura. Los grupos funcionales oxigenados del material serán desprendidos generando CO y/o CO₂ a diferentes temperaturas.

La naturaleza química de los distintos materiales fue evaluada mediante TPD acoplado a un espectrómetro de masas: TPD-MS en un equipo convencional de vacío acoplado a un espectrómetro SRS RGA-200. La muestra fue evacuada durante 30 minutos a temperatura ambiente, seguido de una rampa de 10 K/min hasta alcanzar 1023 K, bajo un flujo de He a 20 mL·min⁻¹. La cantidad de carboxilo puede ser estimada por la pérdida de peso hasta 723 K, mientras que los grupos fenol-carbonilo corresponden a la pérdida de masa de 723 hasta 1100 K.

3.1.6. Termogravimetría (TG)

Es una técnica de análisis térmico, donde se mide una propiedad física de una sustancia y/o de sus productos de reacción en función de la temperatura, sometiendo a la muestra a un programa de temperatura controlado. Mediante un análisis termogravimétrico se registra de manera continua la masa de la muestra a analizar, colocada en una atmósfera controlada, en función de la temperatura. Con la representación de la masa o porcentaje de masa en función del tiempo

se obtiene el denominado termograma, permitiendo estudiar reacciones de descomposición y de oxidación, así como procesos de desorción, vaporización o sublimación. El análisis temogravimétrico se lleva a cabo en una termobalanza, la cual ante el cambio de masa de la muestra.

Los análisis termogravimétricos fueron llevados a cabo bajo He en un equipo CI Electronics microbalance (MK2-MC5). Las muestras fueron calentadas mediante una rampa de 10 K/min hasta 1273 K, seguido por un estado isotermo a la máxima temperatura durante 30 min, todo ello bajo un flujo de He a $20 \text{ mL}\cdot\text{min}^{-1}$.

3.2. Ensayos de adsorción

3.2.1. Ensayos de adsorción en discontinuo

Se han llevado a cabo diversos ensayos en discontinuo con el objetivo de obtener la isoterma de adsorción y una medida de la capacidad de adsorción. Las distintas disoluciones de los compuestos a tratar fueron preparadas mediante dilución de disoluciones madre de concentración conocida, disponiéndolas en frascos de vidrio de 50 mL.

Las diferentes disoluciones se pusieron en contacto con diferentes masas de adsorbente seleccionadas para compuesto según su naturaleza. La disolución se puso en contacto con los distintos adsorbentes hasta alcanzar el equilibrio de adsorción, momento en el cual la concentración del adsorbato no varía con el tiempo.

Los experimentos se llevaron a cabo a temperatura y agitación constantes en un baño que permite controlar tanto la temperatura como la velocidad de agitación (Figura 2.2).



Figura 2.2. Instalación de experimentos para adsorción en discontinuo

3.2.2. Ensayos de adsorción/desorción en continuo

Los ensayos fueron realizados mediante adsorción/desorción en lecho fijo, mediante una instalación que dispone de una columna de adsorción según el esquema que puede verse en la Figura 2.3.

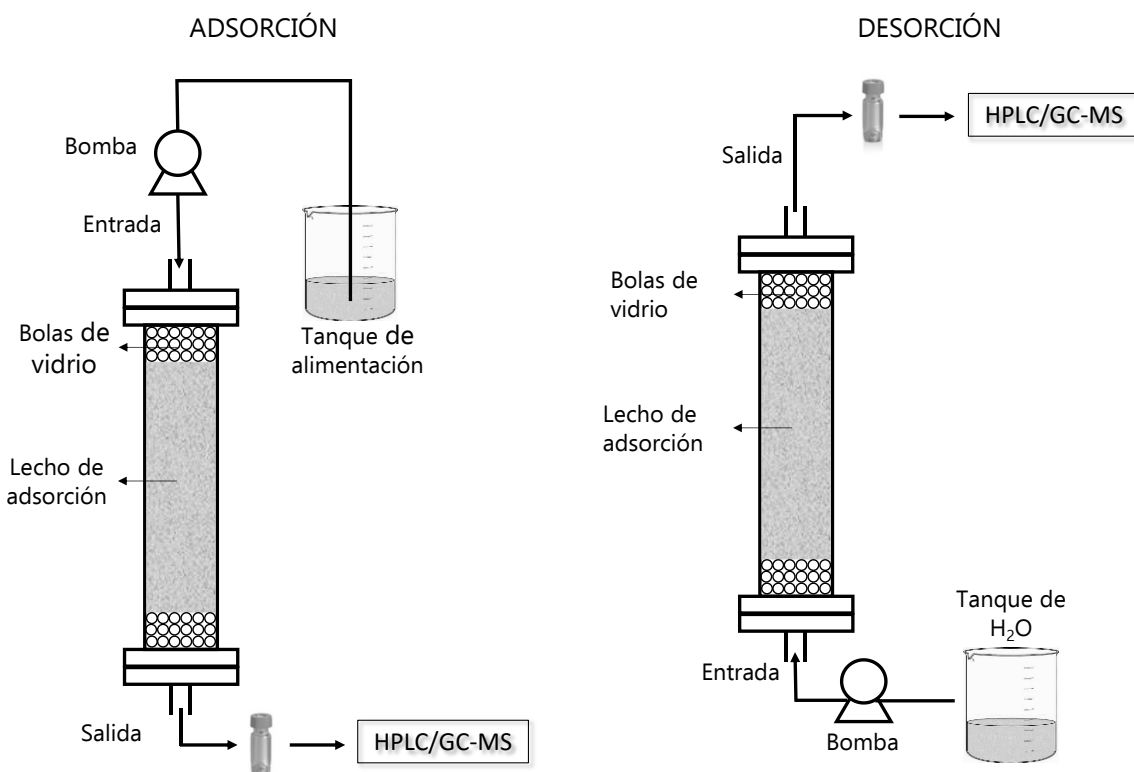


Figura 2.3. Dispositivo experimental para adsorción y desorción en continuo

La columna de adsorción de 3.3 mm de diámetro interno y 500 mm de longitud, está formada por el propio lecho donde se encuentra el adsorbente seleccionado (0.05g), con un diámetro de partícula comprendido entre 50-80 μm . Los extremos se rellenan con bolas de vidrio con el fin de evitar caminos preferenciales y volúmenes muertos. La disolución es mantenida a temperatura constante y alimentada a la columna mediante una bomba HPLC (LabAlliance, serie II) con un flujo volumétrico constante de $1 \text{ mL}\cdot\text{min}^{-1}$.

Una vez iniciado el experimento de adsorción se toman muestras a intervalos de tiempo constante en función del adsorbente y adsorbato, puesto que las velocidades de adsorción son diferentes en cada caso, hasta obtener una concentración de salida igual a la de alimentación, momento en el que se ha alcanzado la saturación del lecho.

Una vez alcanzada la saturación se lleva a cabo la desorción a contracorriente alimentando y tomando muestras de la salida a intervalos constantes de tiempo hasta que la concentración es cero o prácticamente despreciable

3.3. Degradación electroquímica

Los experimentos de voltamperometría cíclica (CV) y de voltamperometría de pulso diferencial (DPV) fueron llevados a cabo en dos equipos: un potenciómetro/galvanómetro μ -Autolab PGSTAT20, tipo II y un potenciómetro Zahner XPOT.

La degradación electroquímica fue llevada a cabo en una celda convencional de tres electrodos, carbón vítreo modificado o sin modificar como electrodo de trabajo, de calomelanos saturados con electrodo de referencia y electrodo de platino como electrodo auxiliar (Figura 2.4).



Figura 2.4. Celda electroquímica con sistema de tres electrodos

Previo a los ensayos de voltamperometría es necesario preparar el electrodo de trabajo. En el caso de electrodos de carbón vítreo sin modificar es necesario pulir la superficie del electrodo con alúmina y posteriormente eliminar los posibles restos de alúmina mediante sonicación. De este modo se obtendrá una superficie limpia tras dejar secar el electrodo a temperatura ambiente. En el caso de electrodos de carbón vítreo modificados con nanotubos de carbono (CNT) es necesario preparar previamente una suspensión estable de los CNT en un disolvente orgánico. Para la obtención de la suspensión es necesario mantener la mezcla de CNT y disolvente orgánico bajo sonicación durante al menos cuatro horas. Una vez que la suspensión es estable ha de depositarse sobre la superficie del electrodo y dejar evaporar el disolvente a temperatura ambiente. Estando ya listo el electrodo para su uso.

Antes de cada análisis, se purgaron las muestras con nitrógeno durante 20 minutos con el fin de desplazar el oxígeno disuelto en la misma.

3.4. Análisis de muestras

3.4.1. Cromatografía líquida

En este trabajo se ha utilizado para el análisis de las muestras de ácido nalidíxico en adsorción mediante cromatografía líquida de alta eficacia (HPLC), en un cromatógrafo Agilent 1200 con detector UV-vis y una columna de 150 mm Zorbax SB-Aqcolumn. Las fases móviles fueron acetonitrilo y agua en grado HPLC.

Para los estudios de degradación de ácido nalidíxico, los posibles subproductos fueron analizados mediante cromatografía líquida acoplada a un espectrómetro de masas (LC-MS) usando un equipo Agilent 6460.

3.4.2. Cromatografía de gases

Para el análisis de las muestras de 1,8-diclorooctano y 2-(4-metilfenoxi)etanol en adsorción y voltamperometría y para el estudio de los productos de degradación de 2-(4-metilfenoxi)etanol, se empleó un cromatógrafo de gases acoplado a un espectrómetro de masas (GC-MS). El equipo utilizado es un GC-MS Shimadzu QP 2010 Plus con una columna TRB-5MS de 30 m de longitud.

3.4.3. Espectrofotometría

Las muestras de ácido nalidíxico en los ensayos de voltamperometría, fueron llevadas a cabo mediante espectrofotometría en un espectrofotómetro Cary 100 UV-vis (Varian Inc. USA) a una longitud de onda de 258 nm.

Las muestras de ácido nalidíxico en voltamperometría no fueron llevadas a cabo en el mismo equipo que las de adsorción (GC-MS) por haber sido realizada esta parte en la Universidad de Amberes (Bélgica) durante la estancia doctoral.



Capítulo IV

Pre-concentración

En este capítulo se lleva a cabo pre-concentración de los contaminantes emergentes seleccionados mediante adsorción-desorción en lecho fijo, contando con un estudio previo que permite seleccionar los adsorbentes, así como las condiciones de operación.

- 4.1. Adsorción en discontinuo: Publicaciones I y II
- 4.2. Estudios de adsorción en lecho fijo: Publicaciones III y IV

IV. Pre-concentración

En esta sección se lleva a cabo la selección de adsorbentes y condiciones de operación para la pre-concentración de los contaminantes modelo seleccionados mediante técnicas de adsorción-desorción. Con el fin de poder diseñar un dispositivo experimental que permita la pre-concentración mediante un sistema en continuo, es necesario un estudio previo del comportamiento de cada uno de los adsorbentes seleccionados.

4.1. Adsorción en discontinuo

El comportamiento de cada uno de los adsorbentes es estudiado mediante ensayos de adsorción en discontinuo, a partir de los cuales se obtienen las isotermas de adsorción, obteniendo las capacidades de adsorción para cada uno de los adsorbentes seleccionados.

El esquema general se representa en la Figura 4.1, donde se parte de una disolución acuosa del contaminante en contacto con una masa determinada de adsorbente, procediendo a su adsorción en discontinuo a temperatura y agitación constantes, hasta alcanzar el equilibrio, lo que permitirá obtener una fase acuosa con una menor concentración del contaminante, ya que éste se encuentra concentrado en el sólido (adsorbente).

La capacidad de adsorción está influenciada por las propiedades físico-químicas del adsorbente, por lo tanto su selección es un parámetro clave en el proceso de adsorción. Para estudiar el efecto y comportamiento del adsorbente se seleccionaron diferentes materiales carbonosos: dos carbones activos con distinto volumen de poros (GC-900 y GF-40), nanofibras de carbono (CNF), grafito de alta superficie (HSAG-500) y nanotubos de carbono (CNT).

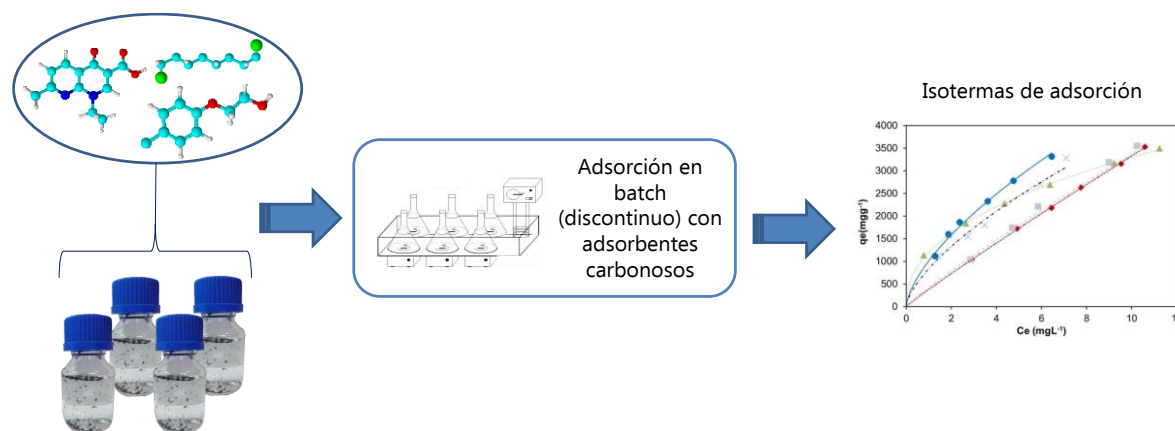


Figura 4.1. Gráfico conceptual del proceso de adsorción en discontinuo

Las diferencias que presentan los anteriores adsorbentes, se basan en parámetros morfológicos y estructurales, resultando también interesante el estudio del efecto de la química superficial. Con este propósito, se llevó a cabo la adsorción en discontinuo empleando como adsorbentes nanotubos de carbono modificados, a los que se les incorporó heteroátomos en su estructura. Se estudió la influencia de tres nanotubos de carbono funcionalizados: MWCNT-COOH, MWCNT-NH₂ y N-CNT. De este modo es posible ver el efecto tanto de las propiedades químicas como superficiales en el rendimiento del proceso de adsorción.

Los resultados obtenidos para cada uno de los adsorbentes se ajustan a los modelos matemáticos de Langmuir y Freundlich, los cuales describen el equilibrio de adsorción de un compuesto sobre una superficie determinada.

Es interesante también obtener la influencia de la temperatura en el proceso de adsorción, por lo que se lleva a cabo el proceso a tres temperaturas diferentes con el fin de obtener los parámetros termodinámicos: entalpía de adsorción (ΔH°), energía libre de Gibbs (ΔG°) y entropía de adsorción (ΔS°).

Los resultados obtenidos se presentan en los apartados 4.1.1 y 4.1.2, mediante las *Publicaciones I y II*.

- Y. Patiño, E. Díaz, S. Ordóñez. Performance of different carbonaceous materials for emerging pollutants adsorption, Chemosphere 119 (2015) S124-S130
- Y. Patiño, E. Díaz, S. Ordóñez, E. Gallegos-Suárez, A. Guerrero Ruiz, I. Rodríguez-Ramos. Adsorption of emerging pollutants on functionalized multiwall carbon nanotubes, Chemosphere 136 (2015) 174-180.

4.1.1. Publicación I

Performance of different carbonaceous material for emergin pollutants adsorption.

Autores: Y. Patiño, E. Díaz, S. Ordóñez

Publicado en:

Chemosphere

Volumen 119

Páginas S124-S130

Año 2015





Performance of different carbonaceous materials for emerging pollutants adsorption



Yolanda Patiño, Eva Díaz, Salvador Ordóñez*

Department of Chemical and Environmental Engineering, University of Oviedo, Faculty of Chemistry, Julián Clavería s/n, 33006 Oviedo, Spain

HIGHLIGHTS

- Micropollutants are removed from waters by adsorption on carbonaceous materials.
- Adsorbents tested: activated carbons, carbon nanofibers and nanotubes, and graphites.
- Equilibrium modeling and thermodynamic analysis.
- Morphology and physic-chemistry of pollutants determine their adsorption parameters.

ARTICLE INFO

Article history:

Received 24 January 2014

Received in revised form 8 May 2014

Accepted 9 May 2014

Available online 5 June 2014

Handling Editor: K. Kannan

Keywords:

Emerging water pollutants

Mesoporous carbons

CNFs

CNTs

Quinolones

Alkylphenoletoxilates

ABSTRACT

The adsorption of three representative emerging pollutants over different kinds of carbonaceous adsorbents has been studied in this work. The adsorbates were nalidixic acid (NAL, representative of a pharmaceutical), 1,8-dichlorooctane (DCO, a chloroparaffin) and methyl-phenoxy-ethanol (MPET, a surfactant). Activated carbons, carbon nanofibers, carbon nanotubes and high surface area graphites have been tested as adsorbents. Adsorption isotherms, carried out in a batch system, were fitted using both a Langmuir and a Freundlich model. It was shown that the capacity of adsorption follows the order DCO > NAL > MPET for all the adsorbents, and among the adsorbents, the external morphology (surface area and mesoporous volume) is the key parameter. The results from thermodynamic analysis show, however, that both morphological and chemical properties of both adsorbates and adsorbents influenced their behavior.

© 2014 Elsevier Ltd. All rights reserved.

1. Introduction

Emerging pollutants are a group of unregulated compounds presented in water, which are considered to be very harmful both for the human health and for the environment (Virkutyte et al., 2010). The origins of the emerging pollutants are very different, some of them having low reactivity- such as perfluorinated compounds-, which leads to relatively high exposure periods in the environment. Furthermore, they are water- and lipid-soluble enough to be introduced in natural waters and trophic cycles (Barceló and López de Alda, 2008). Their release into the environment is diverse and includes agricultural uses, municipal and industrial wastewater discharge or accidental spills (Mompelat et al., 2009). After the discharge, these compounds can be degraded

or distributed between different phases. Thus, different effects on organisms have been reported such as chronic toxicity, endocrine disruption, and bioaccumulation (Barceló and López de Alda, 2008; Bolong et al., 2009; Virkutyte et al., 2010).

The emerging pollutants have been divided into five groups: pharmaceuticals, steroid hormones, perfluorinated compounds, surfactants and personal care products (Virkutyte et al., 2010). In the group of pharmaceuticals alone, over a hundred compounds (excluding their metabolites) have been detected in effluents and surface waters: analgesics, anti-inflammatories, anti-depressants, anti-epileptics, lipid metabolism regulators, several classes of antibiotics, β -blockers, antineoplastics, and hormones (Monteiro and Boxall, 2009). Furthermore, since wastewater treatment plants are designed to remove organic matter and nutrients present at higher concentrations (g L^{-1}), these treatments are inefficient for the elimination of many emerging pollutants (Rivera-Utrilla et al., 2013). Partially, these compounds can

* Corresponding author. Tel.: +34 985 103 437; fax: +34 985 103 434.

E-mail address: sordonez@uniovi.es (S. Ordóñez).

be removed in conventional primary or secondary treatments or even by interaction effects, such as adsorption of emerging pollutants by biological sludge or into emulsified oils. However, a fraction of these compounds will be finally released into the environment and, via drinking water, constitute a major exposure pathway for humans (Bergman et al., 2012). In fact, recent works have evidenced the presence of these compounds in the treated drinking water (Vieno et al., 2007; Kumar and Xagoraraki, 2010; Wu et al., 2013). Furthermore, some transformations can occur through the different treatments, with the resulting chemicals exhibiting even higher toxicity than the parent ones (Farré et al., 2008). Thus, the importance of efficient technologies to remove these compounds in the wastewater treatment plants is evident.

In order to remove these pollutants, biological (Chang et al., 2009; Park et al., 2010), physico-chemical treatments, and hybrids techniques have been proposed. Among the physico-chemical procedures, the most common are membranes (Yoon et al., 2006) and coagulation (Kim et al., 2007); however these methods are not very effective in the removal of emerging pollutants. Other advanced methods, such as the UV irradiation in presence of H_2O_2 or advanced catalytic oxidation based either on cavitation, ozonation or Fenton processes have been studied with reasonable results (Esplugas et al., 2007). However, the main drawback is the low concentrations of the compounds to be removed.

In this way, adsorption has emerged as a feasible method for either the removal of the emerging pollutants from the water stream or as a method of concentrating the pollutants for further destructive treatments. Emerging pollutants adsorption has already been extensively studied, mainly on activated carbons (Nevskaya and Guerrero-Ruiz, 2001; Iwasaki et al., 2002; Yu et al., 2008; Ruiz et al., 2010; SlodobaRigobello et al., 2013) because of their good adsorption properties: high surface area and microporous structure. More recently, works on the adsorption of these emerging pollutants on carbon nanotubes (Wang et al., 2010; Zhang et al., 2013) have demonstrated their potential to control the presence of several contaminants in the environment due to unique physicochemical and electrical properties. From these works, the unique properties as adsorbents of carbonaceous materials stand out, indicating the possibility of tuning both the morphology and the surface chemistry. However, to the best of our knowledge, there are not systematic studies comparing the adsorption properties of these different kinds of carbon adsorbents.

The scope of this work is to explore the adsorption behavior on different carbonaceous materials (activated carbons, carbon nanofibers, carbon nanotubes and high surface area graphites) for emerging pollutants in waters. As emerging pollutants, three compounds representative of three groups (pharmaceuticals, surfactants and plasticizers) were chosen. More concretely, a quinolone, an alkylphenoletoxilate and a chlorinated paraffin. Quinolones are a group of antibacterial agents used as a human and veterinary drug. Among them, the nalidixic acid is an antibiotic which is effective against most Gram-negative bacteria (Velaga et al., 2008; Ulu, 2009). Chlorinated paraffins are flame retardants and chemical stabilizers in polymers and paints. They are usually considered as chloroparaffins molecules with a number of carbon atoms between 10 and 30 and a chlorine content ranging from 30% to 70% by mass (Zitko, 1980; Tomy et al., 1998). However, in this work, the 1,8-dichlorooctane molecule was chosen due to the easiness of the analysis. The alkylphenoletoxilates are used as detergents, pesticides and industrial products. One common compound of this family is the Triton X-100 ($C_{14}H_{22}O(C_2H_4O)_n$), used frequently as detergent. In this work, we have chosen a very similar molecule, 2-(4-Methylphenoxy)ethanol, due to the easiness of analysis.

2. Materials and methods

2.1. Materials

The three compounds used in this work as adsorbates are 1,8-dichlorooctane (Sigma-Aldrich, 98%), nalidixic acid (Duchefa, Biochemie B.V., 99.4%) and 2-(4-Methylphenoxy)ethanol (TCI Europe NV, 98%). The molecular structures of each adsorbate, as well as the physicochemical properties, are listed in Table 1.

The adsorbents used in this work were of carbonaceous nature, and were selected to be representative of the different morphologies: two activated carbons differing in morphology and surface chemistry (AC), carbon nanotubes (CNT), carbon nanofibers (CNF) and high surface area graphites (HSAG). The textural characterization of the materials was based on N_2 adsorption isotherms, measured in a Micromeritics ASAP 2000 surface analyzer. The point of zero charge was measured in a Zetasizer Nano ZS instrument (Malvern Instruments Ltd, UK), based on electrophoretic mobility measurements of aqueous suspensions of the catalysts at different pH values (Smoluchowski approximation). Table 2 summarizes the characterization data of the adsorbents (further details are given in Díaz et al., 2005; Cuervo et al., 2008, 2009). In all cases, the adsorbents were washed with distilled water to remove contaminants, and then dried at 373 K for 24 h before storage under vacuum in a desiccator until use. The experiments were conducted employing the particle diameter interval: $250\text{ }\mu\text{m} < D < 355\text{ }\mu\text{m}$. This interval was previously optimized in order to achieve the maximum adsorption capacity and avoid the flotation of the particles due to its low density.

2.2. Batch adsorption experiments

Batch adsorption experiments were performed in 50 mL glass bottles shaken in a water bath for 72 h at 100 opm (oscillations per minute). Preliminary tests were conducted at 298 K to determine the equilibrium time and to fix the optimum adsorbent amount, varying the amount of adsorbent between 1 and 10 mg in 50 mL of solution.

Adsorption isotherms were conducted at 298, 303 and 308 K for individual target compounds. A fixed amount of adsorbent – determined in preliminary studies –, was put in contact with 50 mL of solution of emerging pollutants of concentrations between 20 and 80 mg L⁻¹. Blank experiments were run under the same conditions to verify the losses by volatilization or adsorption on the bottle walls. After equilibration, the supernatants were filtered using a 0.22 μm glass fiber filter prior to analysis. Each adsorption experiment was repeated twice, with a deviation lower than 7%.

The initial and final concentrations of DCO and MPET were analyzed by GC-MS in a calibrated Shimadzu GC/MS QP2010 Plus instrument, using a 30 m long TRB-5MS capillary column as stationary phase. The samples, once filtered, were extracted in chloroform (using a volume ratio of 1:1). NAL solutions were analyzed using a HPLC apparatus (Agilent 1200 with an UV-vis detector and a 150 mm Zorbax SB-Aqcolumn).

3. Results and discussion

3.1. Influence of the adsorbent amount

The influence of adsorbent amount on the adsorption of the three chosen compounds is shown in Fig. 1A. The amount of adsorbate retained per unit of adsorbent decreased for DCO and MPET with increasing adsorbent mass, as it could be expected, due to the reduction in the adsorbate/adsorbent ratio. The amount of DCO retained (mg g⁻¹) is nearly the same for all the adsorbents,

Table 1

Physicochemical properties of the micropollutants used as adsorbates in this work.

Compound	Abbreviation	CAS No.	Molecular structure	MW	Molecular volume (Å ³) ^a	Log K _{ow} ^a	TPSA ^b	Water solubility (g L ⁻¹) ^c
1,8-Dichlorooctane	DCO	2162-99-4		183.12 232.23	174.121 229.762	4.086 0.228	0 69.635	0.17 (293 K) 0.1 (296 K)
Nalidixic acid	NAL	389-08-2						
2-(4-Methylphenoxy)ethanol	MPET	15149-10-7		152.19	151.211	1.811	29.462	9.407 (298 K)

^a Data obtained from <http://www.molinspiration.com>.^b Molecular polar surface area. Data obtained from <http://www.molinspiration.com>.^c Data obtained from <http://www.msds.com>.**Table 2**

Adsorption properties of the solids used in this work.

Adsorbent	Supplier	S _{BET} (m ² g ⁻¹)	V _{meso} (cm ³ g ⁻¹)	V _{micro} (cm ³ g ⁻¹)	PZC
AC GF-40	Norit	1248 ^a	0.29 ^a	0.18	1.36
AC GC-900	ChemiVall	1005 ^a	0.58 ^a	0.23	4.63
CNT	Dropsense	277	2.51	0.005	4.19
CNF	AppliedSciences	32 ^b	0.16 ^b	–	5.06
HSAG-500	Lonza	580	0.75	–	3.16

^a (Díaz et al., 2005).^b (Cuervo et al., 2008).

whereas in the case of MPET a higher adsorption capacity for the activated carbons was observed. However, in the case of NAL, the behavior is completely anomalous, increasing the amount of adsorbate retained per unit of adsorbent with the mass of adsorbent. This fact can be explained since the maximum amount of adsorbate retained for NAL is one order of magnitude lower than for the other compounds at the lowest adsorbent amount. Thus, if the affinity of adsorbents for NAL is very low, a higher amount of available surface area, increases the adsorption potential.

The Fig. 1B expressed the removal efficiency (% R), defined as:

$$\% R = \frac{(C_o - C_t) \cdot 100}{C_o} \quad (1)$$

where C_o and C_t (mg L⁻¹) are the liquid-phase adsorbate concentrations at initial and final times, respectively. Removal efficiency increased with the adsorbent amount, due to the increase in available active adsorption sites resulting from the increase of mass of adsorbent. In order to maximize adsorbate loading and removal efficiency, DCO and MPET remaining experiments were conducted with an adsorbent amount of 2 × 10⁻⁵ g L⁻¹ (1 mg of adsorbent/50 mL solution), whereas NAL trials were conducted at 2 × 10⁻⁴ g L⁻¹ (10 mg of adsorbent/50 mL solution).

These experimental results about the optimum solid/liquid ratio can be explained also from the physicochemical properties of the adsorbates. Although molecular weight and water solubility of NAL are the largest and lowest, respectively; their differences with respect to the other adsorbates are not so important as to justify its different behavior. However, the octanol–water partition coefficient- used in environmental fate modeling to characterize the partitioning of a molecules between large aqueous phases (rivers and lakes) and hydrophobic phases (organic fractions of sediments suspended in water)- is one order of magnitude lower for NAL (higher affinity for water) than for DCO and MPET (Table 1). The octanol–water partition coefficient can be related to bioaccumulation, that is increasing K_{ow} can be related to increasing bioaccumulation potential (Allen and Shonard, 2002). In the same way, the molecular polar surface area of NAL is considerably higher than

the other adsorbates (Table 1), especially than DCO, whose curves of adsorbent amount show more clear trends.

3.2. Adsorption isotherms

The adsorption isotherms of DCO, NAL and MPET over the five studied adsorbents are shown at 298 K for comparison, Fig. 2. The maximum amount of adsorbate retained (Table 3) is, in all cases, at least one order of magnitude larger for DCO than for NAL and MPET. The higher hydrophobicity of this molecule (octanol–water partition coefficient) could increase its affinity to the carbon adsorbents. The amount of adsorbate retained, at a same temperature, generally follows the order: GC-900 > GF-40 > HSAG-500 > CNT > CNF. This order is coincident with the external surface area of the materials (Table 2), with the exception of the activated carbons, where GC-900 has larger S_{BET} than GF-40. However, the main difference between these materials is the availability of mesoporous volume. In this way, it is remarkable that the size and the shape of the molecules avoid its entrance into the mesopores, favoring in this way the adsorption on the GC-900 activated carbon.

The adsorption isotherms obtained at 298, 303 and 308 K were fitted to Langmuir model and Freundlich equation. The equations are described as:

Langmuir model:

$$q = \frac{Q_0 k C_e}{1 + k C_e} \quad (2)$$

where q is the amount adsorbed per unit weight at equilibrium concentration (mg g⁻¹), Q₀ is the monolayer adsorption capacity (mg g⁻¹), C_e is the equilibrium concentration (mg L⁻¹) and k is a binding constant related to the heat of adsorption (L mg⁻¹).

Freundlich isotherm:

$$q_F = K_F C_e^{1/n} \quad (3)$$

where K_F and n are the adsorption isotherm parameters. K_F depends on the temperature, and is a function of the adsorption capacity of an adsorbent and 1/n determines the intensity of adsorption.

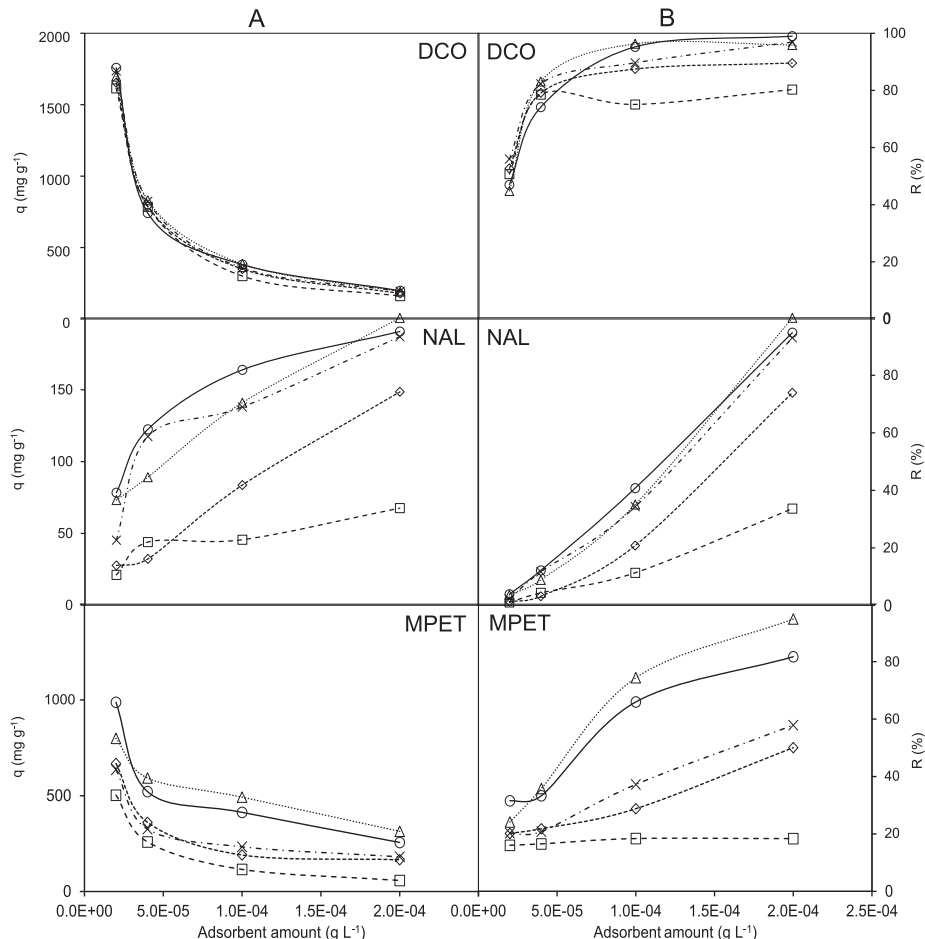


Fig. 1. Effect of adsorbent amount on different adsorbents on: A (left), the amount of adsorbate retained by adsorbent, and B (right), the removal percentage. Symbols: GF-40 (●), GC-900 (▲), CNT (◆), CNF (■), HSAG-500 – q (×) and HSAG-500 – $R\%$ (*).

The isothermal constants and the linear regression coefficients obtained from the experimental data are shown in Table S1. It was found that both models fit the adsorption behavior of NAL well (with the exception of CNF as adsorbent) and MPET. No constants for Langmuir isotherm are shown for DCO since this model failed completely in the fitting of the adsorption data for this compound. The isotherms of adsorption in these cases have a shape which is typical of an unfavorable isotherm, where the amount of adsorbate retained is very low at low concentrations and increases with the equilibrium of adsorbate in the liquid phase. In all cases, Freundlich isotherm gave a good fit, even in the case of DCO adsorption, where the capacity of adsorption is considerably high and thus the working conditions are closer to saturation. Thus, Freundlich isotherms are shown in Fig. 2. Likewise, discussion will be focused on the Freundlich model, for which more data is available in the literature. The K_F constant follows, in general, the same trend as the amount of adsorbate retained per unit mass of adsorbent, as could be expected. Concerning the n parameter, MPET adsorption isotherms are the most linear among the three adsorbates ($1.00 < n < 1.94$), suggesting the lowest strength of the interaction. On the contrary, NAL gives the highest variability of n constant, with values between 0.51 and 8.23. The higher values can be justi-

fied attending to the $\pi-\pi$ interaction of the benzene rings with the carbon materials (Woods et al., 2007; Lin and Xing, 2008). These results are in agreement with other works where the adsorption of aromatic compounds is studied: naproxen, carbamazepine and nonylphenol are adsorbed on activated carbons, with n values between 1.14 and 3.3 (Yu et al., 2008), and with the recovery of bisphenol F on MWCNT, with n constants between 3.1 and 3.5, depending on the temperature (Zhang et al., 2013).

However, n values less than 1 were observed for the NAL adsorption on CNF and DCO adsorption on CNT. These values, less common, justified the continuous increasing trend of the adsorption isotherms, as it can be observed for DCO (Fig. 2a) and mainly for NAL (Fig. 2b), where notorious differences with the other adsorbates are more evident. This behavior, where n values are lower than one and adsorption isotherms could be approximate to upswept curves, have already been observed for the adsorption of triclosan onto kaolinite (Behera et al., 2010) or phenylalanine on corn cobs (Alves et al., 2013).

Different aspects, both the surface chemistry and the morphology, influence the adsorption behavior of the molecules on the different adsorbents. The surface of all the adsorbents is negatively charged, since working pH (7) is higher in all cases than pH_{PZC}

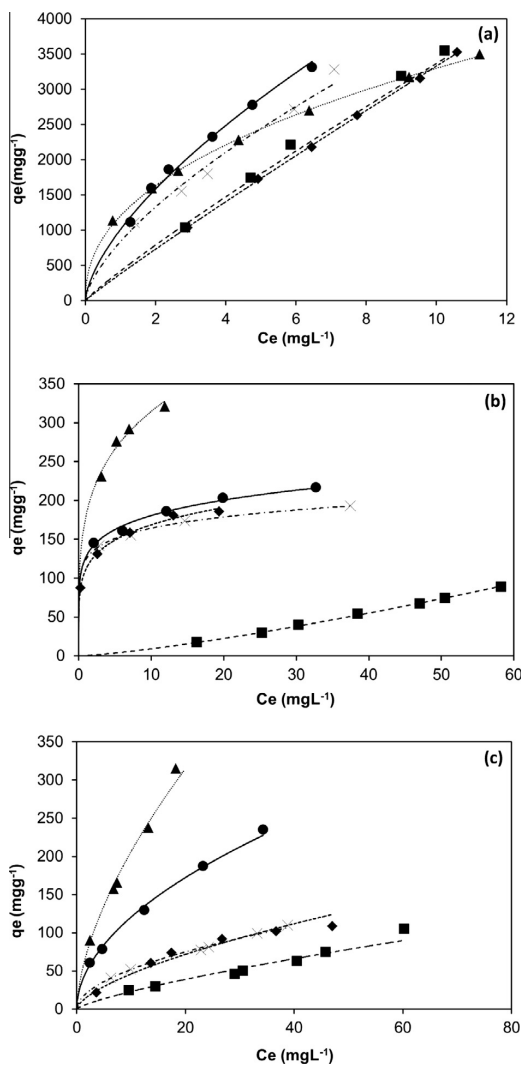


Fig. 2. Isotherms of adsorption at 298 K on different sorbents of: (a) DCO, (b) NAL, and (c) MPET. Symbols of adsorbents: the same as Fig. 1. Lines stand for the Freundlich model fitting of the adsorbents.

(Table 2). According to the dissociation constant of NAL ($pK_a = 5.95$ (Lorphenri et al., 2007) at operating conditions, this adsorbent is expected to be partially deprotonated, acquiring negative charge. The effect of the surface chemistry explains the poor behavior of AC GF-40 for the adsorption of NAL, since it presents the most negative surface charge at the operation conditions ($pH_{PZC} = 1.36$). Furthermore, among all the adsorbents, CNF is the material whose surface will be less charged due to its higher pH_{PZC} (5.06). Thus, CNF should be the best adsorbent for NAL, but Table 3 exhibits very low values of Freundlich constants for the adsorption of NAL on CNF and better values for the adsorption of DCO and MPET on the nanofibers. Thus, it is necessary to take into account the morphological constrictions. In this way, the S_{BET} of this material is very low in comparison with the other adsorbents, and even, the volume of the NAL molecule is considerably higher (Table 1), hindering in this way the adsorption.

Table 3
Adsorption capacity (mg g^{-1}) of DCO, NAL and MPET on the five adsorbents at the initial concentration of 60 ppm.

		DCO	NAL	MPET
298 K	GF-40	2779	203	210
	GC-900	2699	277	239
	CNT	2740	186	97
	CNF	2667	67	63
	HSAG-500	2760	179	99
303 K	GF-40	2766	195	160
	GC-900	2688	256	202
	CNT	2663	168	84
	CNF	2658	54	59
	HSAG-500	2739	165	89
308 K	GF-40	2686	184	135
	GC-900	2532	247	177
	CNT	2512	161	49
	CNF	2526	48	50
	HSAG-500	2639	149	69

In the case of MPET adsorption, it is expected to be in the protonated form ($pK_a \approx 14$, because of its similar structure with Triton X-series (Bai et al., 2010)), and the same it is expected for DCO. For these two compounds, no clear relationship between Freundlich constant and the pH_{PZC} is observed, the CNF being the adsorbent with the lower values of the Freundlich constant. Once again this effect is attributed to the scarce available surface area.

3.3. Thermodynamic studies

The influence temperature was studied at 298, 303 and 308 K, at different concentrations. Thermodynamic parameters were calculated by the following equations.

$$\Delta G^\circ = -RT \ln K_0, \text{ and} \quad (4)$$

$$\Delta G^\circ = \Delta H^\circ - T\Delta S^\circ \quad (5)$$

where T is temperature (K); K_0 the distribution coefficient (q_e/C_e) (mg g^{-1}), calculated in the Henry's law region of the isotherm; R the universal gas constant ($8.314 \times 10^{-3} \text{ kJ mol}^{-1} \text{ K}^{-1}$); ΔG° the standard Gibbs free energy (kJ mol^{-1}); ΔH° the standard enthalpy (kJ mol^{-1}) and ΔS° the standard entropy ($\text{kJ mol}^{-1} \text{ K}^{-1}$).

ΔH° and ΔS° were obtained from Eq. (4), taking the slope and intercept, respectively, of the linear plot of $\ln K_0$ versus $1/T$. The thermodynamic parameters were summarized in Table 4.

The ΔH° are negative in all cases, indicating the exothermic nature of the adsorption processes. Likewise, the values vary from -22 to -132 kJ mol^{-1} , indicating a stronger interaction than in other works reported in literature for the removal of bisphenol F on

Table 4
Thermodynamic parameters for the adsorption of DCO, NAL and MPET on the five adsorbents.

	AC	GF-40	AC	GC-900	CNT	CNF	HSAG-500
DCO							
$-\Delta H^\circ (\text{kJ mol}^{-1})$	49	40	37	35	44		
$-\Delta S^\circ (\text{kJ mol}^{-1} \text{ K}^{-1})$	0.11	0.08	0.07	0.07	0.10		
$-\Delta G^\circ (\text{kJ mol}^{-1})$ 298 K	16	15	14	15	15		
NAL							
$-\Delta H^\circ (\text{kJ mol}^{-1})$	91	23	132	27	103		
$-\Delta S^\circ (\text{kJ mol}^{-1} \text{ K}^{-1})$	0.27	0.04	0.39	0.08	0.31		
$-\Delta G^\circ (\text{kJ mol}^{-1})$ 298 K	11	11	15	0.88	9.7		
MPET							
$-\Delta H^\circ (\text{kJ mol}^{-1})$	24	24	88	31	29		
$-\Delta S^\circ (\text{kJ mol}^{-1} \text{ K}^{-1})$	0.01	0.05	0.28	0.12	0.01		
$-\Delta G^\circ (\text{kJ mol}^{-1})$ 298 K	5.1	7.3	3.3	1.3	2.8		

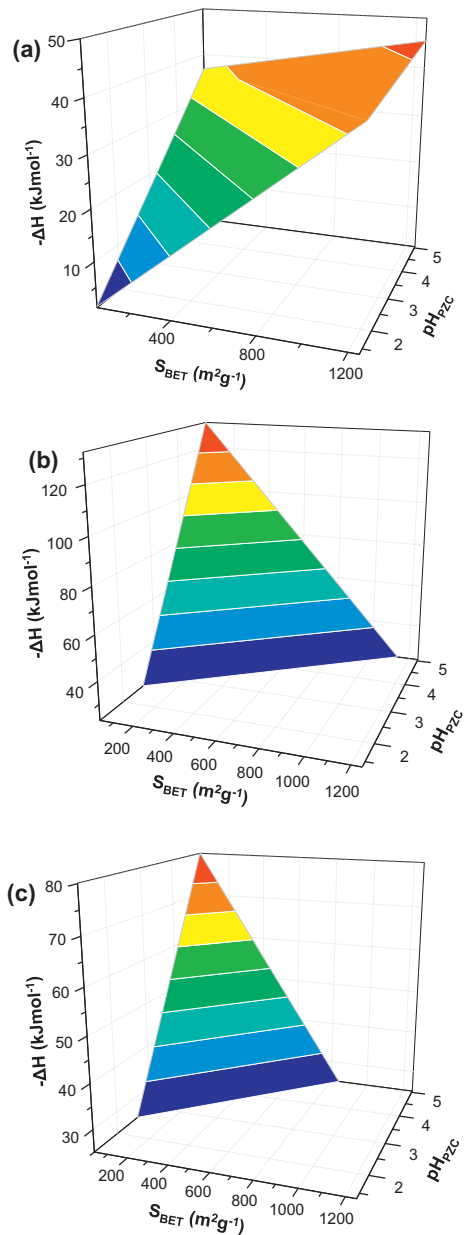


Fig. 3. Influence of S_{BET} and pH_{PZC} on the enthalpy of adsorption of the compounds under study in this work: (a) DCO, (b) NAL, and (c) MPET.

MWCNT (-16 kJ mol^{-1}) (Zhang et al., 2013) or the retention of chlorobenzenes on bentonite and kaolinite (from -4.57 to $-9.84 \text{ kJ mol}^{-1}$) (Shu et al., 2010). The ΔH° parameter can be related to the adsorbate characteristics: at high K_{ow} , the variations of ΔH° among the adsorbents are scarce, however, lower K_{ow} implies a higher ΔH° variation (Fig. S1).

Regarding the adsorbents, different behaviors are shown. In the case of AC GF-40 and HSAG-500, the strength of adsorption decreases in the order NAL > DCO > MPET, coincident with the molecular size (Table 1). For the CNF, the variation of ΔH° among

the different molecules is much lower. At this point, it is interesting to remark that CNF exhibits the highest pH_{PZC} value of all adsorbents, related to the absence of oxygen surface groups on the surface of this material (Cuervo et al., 2008, 2009). The surface of this material, without strong polar groups leads to "hydrophobic adsorption", a term used in the combination of London-Van der Waals interactions (Hulscher and Cornelissen, 1996). In the case of CNT, with acidid groups in the surface, the highest differences among the adsorbates are observed: $\Delta H^\circ_{NAL} > \Delta H^\circ_{MPET} > \Delta H^\circ_{DCO}$. At a first insight, the influence of the aromaticity is pointed out (NAL and MPET). The CNTs consist of curved graphene layers, thus the whole graphene planes are available for the adsorption of adsorbates. In this way, the double aromaticity of NAL enhances the intensity of the interaction. Finally, in the case of the adsorption on AC GC-900, the decreasing order in the enthalpy of adsorption ($\Delta H^\circ_{DCO} > \Delta H^\circ_{MPET} > \Delta H^\circ_{NAL}$) matches with the increasing order of TPSA (Table 1). Thus, the presence of functional groups in the adsorbate hinders the adsorption avoiding the entrance of the adsorbate into the micropores of the activated carbon.

To summarize, in Fig. 3, the influence of the morphology of the adsorbent (S_{BET}) and the surface chemistry (pH_{PZC}) on the enthalpy of adsorption is shown. The positive influence on the enthalpy of the adsorption of the highest values of pH_{PZC} , due to the lower charge of the surface is observed; and also of the elevated surface area, with the exception of the adsorption of NAL. The different behavior of NAL is attributed to the strongest interaction of the two aromatic rings with the graphene layers of CNT and HSAG-500, whereas in the case of AC GC-900, the presence of oxygen surface groups could hinder the adsorption.

The ΔG° and ΔS° values are also summarized in Table 4. Concerning ΔG° , the spontaneous nature of the reaction is confirmed ($\Delta G^\circ < 0$). The entropy values, negatives, but very close to zero, indicates that the adsorption does not increase appreciably the order of the adsorbed species. This fact contrasts with usual gas behavior, but it was already reported for liquid systems (Shu et al., 2010).

4. Conclusions

The adsorption of three pollutants was deeply studied on different kinds of carbonaceous materials: activated carbons, carbon nanofibers, carbon nanotubes and high surface area graphites. Both, adsorption isotherms and thermodynamic parameters (enthalpy and entropy of adsorption, and free energy) were calculated for the adsorption of a quinolone, a chlorinated paraffin and an alkylphenoletoxilate. The main conclusions obtained were:

1. The capacity of adsorption depends on both, the adsorbate properties and the adsorbent morphology. It was shown that the capacity of adsorption of DCO is one order of magnitude larger for DCO than for NAL and MPET, due to its hydrophobicity and hence, higher affinity for carbonaceous structures. Concerning the adsorbents, both the external surface area of the materials and the availability of mesoporous volume were shown to be decisive in the amount of adsorbate retained.
2. The enthalpy of adsorption depends on morphological constrictions (adsorbate molecular size and pore shape of the adsorbent) and also on the surface chemistry. In this way, for AC GF-40 and HSAG-500, the enthalpy of adsorption follows the order of the molecular size (NAL > DCO > MPET). However, on CNT with curve graphene layers, the influence of the aromaticity seems to be the most relevant parameter. In other cases, the functional groups seem to be the most relevant parameter.

In summary, it was shown that emerging pollutants resistant to conventional processes can be removed by adsorption after a meticulous selection of adsorbent and operating conditions.

Acknowledgements

This work was supported by the Spanish Government (contract CTQ2011-29272-C04-02). Y. Patiño thanks the Government of the Principality of Asturias for a Ph.D. fellowship (Severo Ochoa Program).

Appendix A. Supplementary material

Supplementary data associated with this article can be found, in the online version, at <http://dx.doi.org/10.1016/j.chemosphere.2014.05.025>.

References

- Allen, D.T., Shonnard, D.R., 2002. Environmentally Conscious Design of Chemical Processes, first ed. Green Engineering, New Jersey.
- Alves, C.C.O., Franca, A.S., Oliverira, L.S., 2013. Removal of phenylalanine from aqueous solutions with thermo-chemically modified corn cobs as adsorbents. *Food Sci. Technol.* 51, 1–8.
- Bai, Y., Lin, D., Wu, F., Wang, Z., Xing, B., 2010. Adsorption of Triton X-series surfactants and its role in stabilizing multi-walled carbon nanotube suspensions. *Chemosphere* 79, 362–367.
- Barceló, D., López de Alda, M.J., 2008. Contaminación y calidad química del agua: el problema de los contaminantes emergentes. Instituto de Investigaciones Químicas y Ambientales, CSIC, Barcelona.
- Behera, S.K., Oh, S.-Y., Park, H.-S., 2010. Sorption of tricosanontoactivatedcarbón, kaolinite and montmorillonite: effect of pH, ionicstrength, and humic acid. *J. Hazard. Mater.* 179, 684–691.
- Bergman, A., Heindel, J.J., Jobling, S., Kidd, K.A., Zoeller, R.T., 2012. State of the science of endocrine disrupting chemicals. *Toxicol. Lett.* 211, S3–S3.
- Bolong, N., Ismail, A.F., Salim, M.R., Matsuura, T., 2009. A review of the effects of emerging contaminants in wastewater and options for their removal. *Desalination* 239, 229–246.
- Chang, H.-S., Choo, K.-H., Lee, B., Choi, S.-J., 2009. The methods of identification, analysis, and removal of endocrine disrupting compounds (EDCs) in water. *J. Hazard. Mater.* 172, 1–12.
- Cuervo, M.R., Asedegbeaga-Nieto, E., Díaz, E., Vega, A., Ordóñez, S., Castillejos-López, E., Rodríguez-Ramos, I., 2008. Effect of carbon nanofiber functionalization on the adsorption properties of volatile organic compounds. *J. Chromatogr. A* 1188, 264–273.
- Cuervo, M.R., Asedegbeaga-Nieto, E., Díaz, E., Vega, A., Ordóñez, S., Dongil, B., Rodríguez-Ramos, I., 2009. Modification of the adsorption properties of high surface area graphites by oxygen functional groups. *Carbon* 46, 2096–2106.
- Díaz, E., Ordóñez, S., Vega, A., Coca, J., 2005. Comparison of adsorption properties of a chemically activated and a steam-activated carbon, using inverse gas chromatography. *Microp. Mesop. Mater.* 82, 173–181.
- Esplugas, S., Bila, D.M., Krause, L.G.T., Dezotti, M., 2007. Ozonation and advanced oxidation technologies to remove endocrine disrupting chemicals (EDCs) and pharmaceuticals and personal care products (PPCPs) in water effluents. *J. Hazard. Mater.* 149, 631–642.
- Farré, M.I., Pérez, S., Kantiani, L., Barceló, D., 2008. Fate and toxicity of emerging pollutants, their metabolites and transformation products in the aquatic environment. *TrAC Trends Anal. Chem.* 27, 991–1007.
- Hulscher, Th.E.M., Cornelissen, G., 1996. Effect of temperature on sorption equilibrium and sorption kinetics of organic micropollutants – a review. *Chemosphere* 32, 609–626.
- Iwasaki, S., Fukuhara, T., Abe, I., Yanagi, J., Mouri, M., Iwashima, Y., Tabuchi, T., Shinohara, O., 2002. Adsorption of alkylphenols onto microporous carbons prepared from coconut shell. *Synth. Met.* 125, 207–211.
- Kim, S.D., Cho, J., Kim, I.S., Vanderford, B.J., Snyder, S.A., 2007. Occurrence and removal of pharmaceuticals and endocrine disruptors in South Korean surface, drinking, and waste waters. *Water Res.* 41, 1013–1021.
- Kumar, A., Xagoraraki, I., 2010. Pharmaceuticals, personal care products and endocrine-disrupting chemicals in U.S. surface and finished drinking waters: a proposed ranking system. *Sci. Total Environ.* 408, 5972–5989.
- Lin, D.H., Xing, B.S., 2008. Adsorption of phenolic compounds by carbon nanotubes: role of aromaticity and substitution of hydroxyl groups. *Environ. Sci. Technol.* 42, 7254–7259.
- Lorhensri, O., Sabatini, D.A., Kibbey, T.C.G., Osathaphan, K., Saiwan, C., 2007. Sorption and transport of acetaminophen, 17 α -ethynodiol, nalidixic acid with low organic content aquifer sand. *Water Res.* 41, 2180–2188.
- Material Safety Data Sheet (MSDS). <http://www.msds.com/>.
- Mompelat, S., Le Bot, B., Thomas, O., 2009. Occurrence and fate of pharmaceutical products and by-products, from resource to drinking water. *Environ. Int.* 35, 803–814.
- Monteiro, S.C., Boxall, A.B.A., 2009. Factor affecting the degradation of pharmaceuticals in agricultural. *Environ. Toxicol. Chem.* 28, 2546–2554.
- Nevskaia, D.M., Guerrero-Ruiz, A., 2001. Comparative Study of the adsorption from aqueous solutions and the desorption of phenol and nonylphenol substrates on activated carbons. *J. Colloid Interface Sci.* 234, 316–321.
- Park, C., Fang, Y., Murthy, S.N., Novak, J.T., 2010. Effects of floc aluminum on activated sludge characteristics and removal of 17 α -ethynodiol in wastewater systems. *Water Res.* 44, 1335–1340.
- Rivera-Utrilla, J., Sánchez-Polo, M., Ferro-García, M.A., Prados-Joya, G., Ocampo-Pérez, R., 2013. Pharmaceuticals as emerging contaminants and their removal from water. A review. *Chemosphere* 93, 1268–1287.
- Ruiz, B., Cabrita, I., Mestre, A.S., Parra, J.B., Pires, J., Carvalho, A.P., Ania, C.O., 2010. Surface heterogeneity effects of activated carbons on the kinetics paracetamol removal from aqueous solution. *Appl. Surf. Sci.* 256, 5171–5175.
- Shu, Y., Li, L., Zhang, Q., Wu, H., 2010. Equilibrium, kinetics and thermodynamic studies for sorption of chlorobenzenes on CTMAB modified bentonite and kaolinite. *J. Hazard. Mater.* 173, 47–53.
- SlodobaRigobello, E., Di Bernardo Dantas, A., Di Bernardo, L., Vieira, E.M., 2013. Removal of diclofenac by conventional drinking water treatment processes and granular activated carbon filtration. *Chemosphere* 92, 184–191.
- Tomy, G.T., Fisk, A.T., Westmore, J.B., Muir, D.C.G., 1998. *Rev. Environ. Contam. Toxicol.* 158, 53.
- Ulu, S.T., 2009. Rapid and sensitive spectrofluorimetric determination of enrofloxacin, levofloxacin and ofloxacin with 2,3,5,6-tetrachloro-p-benzoquinone. *Spectrochim. Acta A* 72, 1038–1042.
- Velaga, S.P., Basavouj, S., Boström, D., 2008. Norfloxacin-saccharinate-saccharin dihydrateocrystal – a new pharmaceutical cocrystal with an organic counter ion. *J. Mol. Struct.* 889, 150–153.
- Vieno, N.M., Harkki, H., Tuhkanen, T., Kronberg, L., 2007. Occurrence of pharmaceuticals in river water and their elimination a pilot-scale drinking water treatment plant. *Environ. Sci. Technol.* 41, 5077–5084.
- Virkutyte, J., Varma, R.S., Jegatheesan, V., 2010. Treatment of Micropollutants in Water and Wastewater. IWA Publishing, London.
- Wang, Z., Yu, X., Pan, B., Xing, B., 2010. Norfloxacin sorption and its thermodynamics on surface-modified carbon nanotubes. *Environ. Sci. Technol.* 44, 978–984.
- Woods, L.M., Badescu, S.C., Reinecke, T.L., 2007. Adsorption of simple benzene derivatives on carbon nanotubes. *Phys. Rev. B* 75, 15.
- Wu, Y., Jia, Y., Lu, X., 2013. Assessment of semi-volatile organic compounds in drinking water sources in Jiangsu, China. *Ecotoxicol. Environ. Saf.* 94, 138–146.
- Yoon, Y., Westerhoff, P., Snyder, S.A., Wert, E.C., 2006. Nanofiltration and ultrafiltration of endocrine disrupting compounds, pharmaceuticals and personal care products. *J. Membr. Sci.* 270, 88–100.
- Yu, Z., Peldszusand, S., Huck, P.M., 2008. Adsorption characteristics of selected pharmaceuticals and an endocrine disrupting compound—Naproxen, carbamazepine and nonylphenol—on activated carbon. *Water Res.* 42, 2873–2882.
- Zhang, L., Pan, F., Liu, X., Yang, L., Jiang, X., Yang, J., Shi, W., 2013. Multi-walled carbon nanotubes as sorbent for recovery of endocrine disrupting compound-bisphenol F from wastewater. *Chem. Eng. J.* 218, 238–246.
- Zitko, V., 1980. The Handbook of Environmental Chemistry, Part A, Anthropogenic Compounds, first ed. Springer, Heidelberg.

4.1.2. Publicación II

Adsorption of emerging pollutants on functionalized multiwall carbon nanotubes

Autores: Y. Patiño, E. Díaz, S. Ordóñez, E. Gallegos-Suárez, A. Guerrero-Ruiz, I.

Rodríguez-Ramos

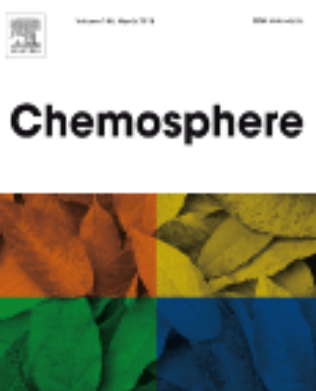
Publicado en:

Chemosphere

Volumen 136

Páginas 174-180

Año 2015





Adsorption of emerging pollutants on functionalized multiwall carbon nanotubes



Yolanda Patiño ^a, Eva Díaz ^a, Salvador Ordóñez ^{a,*}, Esteban Gallegos-Suarez ^{b,c}, Antonio Guerrero-Ruiz ^c, Inmaculada Rodríguez-Ramos ^b

^aDepartment of Chemical and Environmental Engineering, University of Oviedo, Faculty of Chemistry, Julián Clavería s/n, 33006 Oviedo, Spain

^bInstituto de Catálisis y Petroleoquímica, CSIC, c/Marie Curie No. 2, Cantoblanco, 28049 Madrid, Spain

^cDpto. Química Inorgánica y Técnica, Fac. de Ciencias, UNED, C/ Senda del Rey n° 9, 28040 Madrid, Spain

HIGHLIGHTS

- Adsorption of emerging pollutants on functionalized carbon nanotubes.
- Functionalization of carbon nanotubes tunes adsorption properties.
- Different functional groups tested (N- and O-containing groups), and compared with parent MWCNTs.
- Main factors affecting these effects: hydrophobicity, $\pi-\pi$ interaction, and morphology.

ARTICLE INFO

Article history:

Received 26 September 2014

Received in revised form 4 March 2015

Accepted 19 April 2015

Keywords:

Emerging water pollutants

Functionalized CNTs

Quinolones

Alkylphenoletoxilates

Chloroparaffins

ABSTRACT

Adsorption of three representative emerging pollutants – 1,8-dichlorooctane, nalidixic acid and 2-(4-methylphenoxy)ethanol- on different carbon nanotubes was studied in order to determine the influence of the morphological and chemical properties of the materials on their adsorption properties. As adsorbents, multiwall carbon nanotubes (MWCNTs) without functionalization and with oxygen or nitrogen surface groups, as well as carbon nanotubes doped with nitrogen were used. The adsorption was studied in aqueous phase using batch adsorption experiments, results being fitted to both Langmuir and Freundlich models. The adsorption capacity is strongly dependent on both the hydrophobicity of the adsorbates and the morphology of the adsorbents. Thermodynamic parameters were determined observing strong interactions between the aromatic rings of the emerging pollutant and the nitrogen modified adsorbents.

© 2015 Elsevier Ltd. All rights reserved.

1. Introduction

Emerging pollutants are defined as those no regulated pollutants presenting a significant risk for aquatic environments, and requiring future regulation (NORMAN, 2014). Emerging pollutants include not only compounds or substances in active or past production, but also their metabolites and other transformation products and chemical by-products generated during their production and use. European Union has prioritized the identification, prevention, monitoring and processing of pollutants and pathogens in European water bodies in order to protect human health and keep ecosystems quality (IRSTEA, 2014). In this way, the Water Framework Directive (EU, 2000) established Environmental

Quality Standards (EQS) for 33 priority pollutants. According to the directive, member states should implement measures to control their emissions in order to achieve "good chemical status" and accomplish the EQS for the priority pollutants in all water bodies before 2015. However, add to the priority pollutants, emerging pollutants may be included in the updated versions of the WFD. In fact, a working group of the European Commission (the sub-group on Chemical Monitoring and Emerging Pollutants) is focused on topics related to emerging pollutants, including analytical methods, levels in the environment and hazard information (Carere et al., 2012). The prevention of priority and emerging pollutants emissions through wastewater treatment plants effluents into the aqueous environment requires the development of treatment technologies that ensure the quality of receiving water bodies.

Unlike traditional priority pollutants, some emerging contaminants may not be toxic, persistent or bioaccumulative, but may

* Corresponding author.

E-mail address: sordonez@uniovi.es (S. Ordóñez).

produce subtle ecological effects, and there is uncertainty about their adverse ecological effects. These “emerging pollutants” are commonly derived from municipal and industrial wastewater treatment plants, which cannot eliminate it completely with conventional treatment technologies (Carballa et al., 2004; Rivera-Utrilla et al., 2013). Conventional biological wastewater treatment processes will attenuate at least some emerging pollutants, depending on the conditions (Omil et al., 2010). Alahmad and Alawi (2010) measured micropollutants concentrations in effluents from wastewater treatment plants, finding treatment efficiencies, which ranged from 25% to 100%, depending on the biological treatment facility. The use of membrane bioreactors (Sipma et al., 2010), photocatalysis and photolysis (Gamage and Zhang, 2010), or enzymatic treatments (Majeau et al., 2010) could be other options. Membrane separations have been widely studied, obtaining efficiencies of even 90% by nanofiltration (Dixon et al., 2010) or 100% by reverse osmosis (Boleda et al., 2010). An interesting alternative are the physicochemical separations by coagulation or adsorption, which could be a valuable pretreatment processes able to concentrate the emerging pollutants prior to further abatement treatments, decreasing in these way the cost of the overall treatment. Coagulation have been studied without significant removal for pharmaceuticals (Adams et al., 2002) or with removal rates lower than 30% (Huerta-Fontela et al., 2011), whereas adsorption on activated carbons are the most extended and known operation (Iwasaki et al., 2001; Nevskaia and Guerrero-Ruiz, 2001; Rigobello et al., 2013; Ruiz et al., 2010; Yu et al., 2008).

Recently, the use of carbon nanotubes (CNTs), mainly the multi-walled CNTs (MWCNTs), for the adsorption of these emerging pollutants (Wang et al., 2010; Zhang et al., 2013) has gained interest for the removal of different pollutants in the aqueous streams. They have been used for the sorption of a large number of contaminants, both inorganic (Fang and Chen, 2012; Yan et al., 2014) and organic (Bai et al., 2010; Joseph et al., 2011; Zhang et al., 2013). However, add to their chemically inert surface for physical adsorption and high specific surface area comparing with other carbon adsorbents (Kondratyuk and Yates Jr., 2007), CNTs presents surface sites, which can be tuned incorporating heteroatoms in their structure. In this way, nitrogen atoms are incorporated when the scope is the increase of basic properties (Faba et al., 2013), whereas oxygen surface groups, usually by oxidant treatments, are introduced with the aim of increasing the wettability properties of the surface, improving the adsorption properties for polar compounds (Chinthaginjala et al., 2007). Thus, CNTs allow the surface modification in order to maximize the selectivity of adsorption through families of compounds, add to improve the desorption behavior.

The aim of this work is to explore the sorption behavior and mechanism of the three emerging pollutants selected on different CNTs. Four types of CNTs, including functionalized CNTs – MWCNT, MWCNT-COOH, MWCNT-NH₂, N-CNT – were selected for studying the effect of the different chemical and surface properties on their adsorption performance. As emerging pollutants, three different compounds, representative from three groups (pharmaceuticals, surfactants and plasticizers), were chosen: a chlorinated paraffin (1,8-dichlorooctane), a quinolone (nalidixic acid) and an alkylphenoletoxilate (2-(4-methylphenoxy)ethanol).

2. Materials and methods

2.1. Materials

The three compounds used in this work as representative of emerging pollutants are: a chlorinated paraffin, 1,8-dichlorooctane (DCO, Sigma-Aldrich, 98%); a quinolone,

nalidixic acid (NAL, Duchefa, Biochemie B.V., 99.4%); and an alkylphenoletoxilate, 2-(4-methylphenoxy)ethanol (MPET, TCI Europe NV, 98%).

As adsorbents, four multiwalled carbon nanotubes have been used. Three of them are manufactured by DropSens: multi-wall non-functionalized nanotubes (MWCNT), functionalized with –COOH groups (MWCNT-COOH) and functionalized with –NH₂ groups (MWCNT-NH₂). Likewise, a fourth sample of carbon nanotubes was synthesized at laboratory scale by chemical vapor deposition in a fluidized bed reactor on Fe/SiO₂ catalyst from acetonitrile vapor at 1123 K (N-CNT) (Faba et al., 2013).

2.2. Characterization of carbon nanotubes

All the samples were characterized by N₂ adsorption at 77 K in an automatic Micromeritics ASAP 2010 volumetric system. The BET equation was applied to the N₂ isotherms to obtain surface area values. The mesopore volumes and pore size distributions were obtained by application of the Barret, Joyner and Halenda method (BJH) to the desorption branch of the N₂ isotherm. TEM micrographs were performed on a JEOL JEM-2100F microscope at 200 kV, the samples were prepared by grinding and ultrasonic dispersal in an acetone solution. Zeta potentials were measured in a Zetasizer Nano ZS instrument (Malvern Instruments Ltd., UK), with the carbon nanotubes suspensions at different pH. Thermogravimetric analyses (TGA) were conducted under He in an apparatus CI Electronics microbalance (MK2-MC5). The sample was heated with a 10 K/min ramp up to 1273 K, followed by an isotherm stage at that temperature for 30 min.

The surface functional groups were analyzed by temperature programmed desorption coupled with mass spectrometer (TPD-MS) experiments under vacuum in a conventional volumetric apparatus connected to a SRS RGA-200 mass spectrometer. The sample was evacuated for 30 min at room temperature and then, the temperature was increased until 1023 K at a 10 K/min. Considering that the gases evolved during the TGA experiment are CO₂ and CO, as it is evidenced from the TPD-MS, and that the range of temperatures at which the evolution takes place is different; the amount of carboxyl can be estimated by the weight loss up to 723 K while phenol-carbonyl groups correspond to the mass loss from 723 K up to 1100 K.

Elemental analysis of samples containing nitrogen was performed with a LECO CHNS-932 Chemical Analyzer. XPS analysis was performed with an ESCA-PROBE P (Omicron) spectrometer by using non-monochromatized Mg-K radiation (1253.6 eV). All binding energies (BE) were referenced to the C 1s line at 284.6 eV.

2.3. Adsorption experiments

Adsorption isotherms on CNTs were obtained using a batch equilibration technique at 298, 303 and 308 K for individual target compounds. The adsorption was carried out at neutral pH (pH = 7 ± 0.5) because this is a typical pH of water in treatment plants (Choi et al., 2005; Yu et al., 2008) and it is the pH for which the highest adsorption capacity values for this kind of pollutants were obtained in previous works (Bai et al., 2010; Peng et al., 2012). In all the reported experiments, measured pH values did not change during the adsorption experiment. A volume of 50 mL of each solution with different concentration (20–80 mg L⁻¹) were added to 50 mL glass bottles containing a weighed quantity of sorbents (1 mg for DCO and MPET and 10 mg for NAL), according to previous data on the influence of adsorbent dosage (Patiño et al., 2015). The bottles were shaken at 100 rpm (oscillations per minute) for 72 h – time required to reach equilibrium. Preliminary experiments showed that the equilibrium was achieved for all

pollutants and all CNTs after 72 h. After equilibration, the samples were filtered using a 0.22 µm glass fiber.

The initial concentration and the concentration in supernatant were analyzed by GC-MS in a calibrated Shimadzu GC/MS QP2010 Plus instrument, using a 30 m long TRB-5MS capillary column as stationary phase for DCO and MPET, and by HPLC (Agilent 1200 with an UV-vis detector and a 150 mm Zorbax SB-Aq column) in the case of NAL. Prior to analyze by GC/MS, the samples were extracted in chloroform with a 1:1 ratio.

Blank experiments were conducted under the same conditions to verify the losses by volatilization or adsorption on the bottle walls.

3. Results and discussions

3.1. Characteristics of CNTs

Table 1 gives the Brunauer, Emmett and Teller surface area (BET), the mean pore diameter obtained from Barret, Joyner and Halenda method (BJH) and internal and external diameter for the different CNTs samples obtained by TEM. BET surface areas were calculated from N₂ adsorption isotherms (**Fig. S1**) applying the equation in the same range of relative pressures (0.1 < p/p₀ < 0.3) for all samples. It was observed that all the CNTs samples have nearly the same type of isotherm, which is characteristic of mesoporous materials with cylindrical shaped porosities.

Low increase in nitrogen uptake at low relative pressure suggests the negligible presence of micropores in all these materials ([Faba et al., 2013](#)). Intermediate relative pressures show a surface adsorption corresponding to monolayer formation in mesopores, in which the nitrogen adsorption amount increased slowly. N-CNT shows a hysteresis loop at the relative pressure range of p/p₀ = 0.4–0.85 (**Fig. S1**), which is associated with capillarity in the inner hollow cavity of open-ended CNTs ([Eswaramoorthy et al., 1999](#)). Finally, a sharp adsorption at high relative pressures (values higher than 0.82), accompanied by hysteresis is indicating capillary condensation within large mesopores ([Yang et al., 2001](#)) which are constituted by aggregated particles (bundles) formed by interaction of isolated MWCNTs ([Gregg and Sing, 1982](#)). This fact is especially evident for the CNT sample. Functionalization of its surface, MWCNT-COOH and MWCNT-NH₂ samples reduces the interaction among CNTs and their association into bundles. **Table 1** also provides the pore widths, which is rather smaller for N-CNT, probably due to the absence of aggregation and the presence of deposited amorphous carbon.

TEM images (**Fig. S2**) show that N-CNT sample contains appreciable amounts of amorphous carbon, which explain the highest surface area of the sample. From the point of view of the morphology, it exhibits features of multiwall periodical bamboo-like carbon nanotubes ([Faba et al., 2013](#)), with inaccessible internal surface. The commercial samples display cylindrical shapes with the internal pore centered at the core of the CNTs. It is observed

that they have high graphitization (see high magnification inserted images), although certain amorphous carbon deposited on the external surface. For the MWCNT-COOH sample, some uncapped ends were observed, suggesting that the acid treatment could remove some caps of tubes. In agreement with the above discussed, the three commercial samples present large pores formed by aggregation of the small tubes in bundles in addition to the mesoporous opened tubes, while the small pores of the N-CNT sample likely comes from the amorphous carbon which accompanied the large bamboo structures. Thus, three possible adsorption sites can be identified: (i) the interior of the individual CNTs, which is accessible when the end of the CNTs is uncapped and unblocked; (ii) the cylindrical outer sidewall surface of the individual nanotube and (iii) some of the small grooves of the aggregated CNTs ([Agnihotri et al., 2005; Kang et al., 2008](#)).

The results of PZC measurements are also summarized in **Table 1**. From these results, it is evidenced the different surface chemistry of the CNTs. The MWCNT-COOH has the most acid surface, since it presents the lowest PZC value. It is remarkable that even MWCNT-NH₂ and N-CNT exhibit also values of pH_{PZC} < 7, probably from deprotonation of carboxyl or hydroxyl groups from the surface.

Table 1 shows the surface amounts of desorbed CO₂ and CO determined by thermogravimetry. The chemical nature of the surface functional groups was evaluated by temperature programmed desorption coupled with mass spectrometry (TPD-MS). The observed profiles are displayed in **Fig. S3**. It is well known that CO₂ results from the decomposition of carboxyl, anhydride and lactonic groups; whereas CO results from phenolic, carbonyl, quinine, pyrone and anhydride groups ([Castillejos and Serp, 2010](#)). The MWCNT and N-CNT samples present a small amount of surface oxygen functionalities, while the MWCNT-COOH shows a high concentration of surface oxygen groups confirming surface functionalization of the sample. For the MWCNT-NH₂ sample, the TPD experiment shows, in addition to masses m/z = 44 and 28 due to CO₂ and CO, a maximum of desorption at ca. 473 K due to the mass m/z = 17, which is in a much higher ratio than it would be as a result of water molecule fragmentation. This is the contribution of the amine thermal decomposition to the TPD profile ([Kinoshita, 1988](#)). For, the N-CNT sample no evolution of the mass m/z = 17 was observed.

The qualitative results obtained from TPD-MS were further checked by a surface analysis of these materials, so they were also studied by XPS. **Table 1** summarized the weight percentages of elements present in each sample. The inspection of the N 1s peak centered at 401 eV for sample N-CNT reveals that can be deconvoluted in three components: pyridinic nitrogen at 398.1 eV (26%), pyrrolic nitrogen at 400.1 eV (54%) and quaternary nitrogen at 401.8 eV (20%) ([Faba et al., 2013](#)). For the MWCNT-NH₂ the N 1s region shows a peak at 401.5 eV with a unique contribution due to amine groups ([Dongil et al., 2011](#)). Concerning the surface concentration of nitrogen is worth noting the good agreement between XPS

Table 1
Main physico-chemical properties of the different CNTs used for the adsorption studies.

CNTs	Din (nm)	Dext (nm)	Pore width (nm)	S _{BET} (m ² g ⁻¹)	Vmeso (cm ³ g ⁻¹)	Elemental analysis (%N)	XPS (%)		pH _{PZC}	TGA		
							N	O/C		CO ₂ (mmol/g)	CO (mmol/g)	[O] _{total} (mmol/m ²)
MWCNT	5 ± 1	10 ± 2	28.3	277	2.50	–	–	0.0077	4.19	0.22	0.48	0.0032
MWCNT-COOH	5 ± 1	10 ± 2	16.0	273	1.32	–	–	0.0707	0.64	0.97	3.08	0.0184
MWCNT-NH ₂	5 ± 1	11 ± 2	15.0	293	1.38	0.59 ± 0.02	0.60 ± 0.02	0.0172	4.70	0.09	1.02	0.0041
N-CNT	77 ± 46	120 ± 57	5.4	484	0.75	4.05 ± 0.02	3.74 ± 0.02	0.0234	5.46	0.50	1.40	0.0050

analysis and elemental analysis determinations. Likewise, Table 1 shows the relative content of functional groups in O1s, after deconvolution into surface oxygen complex contributions. The MWCNT-COOH, material with the highest O/C ratio, has half of the oxygen groups as C=O type oxygen (carboxylic oxygen in esters and anhydrides), and the other part split into C—O and COOH types. The N-CNT material has also as major peak the corresponding to C=O type, whereas the MWCNT-NH₂, exhibits the highest proportion of the second peak, corresponding to C—O type oxygen (hydroxyl groups, non-carbonyl-ether type-oxygen atoms in esters and anhydrides). Finally, for CNT, the highest peak corresponds to carboxylic groups, although it is important to remark the low content of oxygen in the surface of this material (Table 1) (Zhou et al., 2007).

3.2. Adsorption isotherms

Fig. 1 presents the adsorption isotherms of DCO, NAL and MPET on the four adsorbents at 298 K; whereas Langmuir and Freundlich regression parameters at 298, 303 and 308 K are shown in Table 2 and its fitting is shown in the supporting information (Fig. S4).

Concerning the Langmuir model, no constants for DCO are shown since LM failed especially in the fitting at low concentrations for this compound. DCO capacity of adsorption at very low adsorbate concentrations is unfavorable, as can be deduced from extrapolation to zero from the isotherms (Fig. 1). A similar behavior, although less pronounced, is observed for the MPET adsorption. In fact, from the *k* parameter, which measures the affinity

coefficient between CNTs and adsorbates (Table 2), it is evidenced the low affinity of this compound for all the adsorbents, especially for MWCNTs. Finally, NAL shows the highest affinity for the adsorbents, mainly for MWCNT-NH₂, although the monolayer adsorption capacity (*Q₀*) is slightly lower than for MWCNTs. This behavior can be understood since LM is usually applicable to describe monolayer adsorption on homogeneous surfaces (Yang and Xing, 2010), thus surface heterogeneities due to both morphologic constrictions, like the three previous identified different site adsorption on CNTs, or chemical modifications, such as the nitrogen or oxygen functionalities, could make it unsuitable. At this point, it should be pointed out that NAL, adsorbate with the lowest hydrophobicity (Patiño et al., 2015), exhibits the best fit to LM. However, the very low adsorption capacity, especially if it is compared to DCO, could justify this behavior.

The adsorption isotherms fit to the Freundlich model (FM) with a *r*² > 0.901. The heterogeneity index (1/*n*), which is an indication of how favorable is the adsorption process and of the degree of error from linearity, range from 1.01 to 7.26, with the exception of DCO adsorption on MWCNT, where values of even 0.85 are observed. When *n* > 1, it suggests favorable adsorption, as it is observed as general trend. The *n* < 1 values, less common, are justified by the aforementioned by the unfavorable DCO capacity of adsorption at very low adsorbate concentrations. This behavior, where *n* values are lower than one and adsorption isotherms could be approximate to upswept curves, have already been observed for the adsorption of NAL on CNF (Patiño et al., 2015). It is remarkable, in agreement with Langmuir isotherm, the highest affinity of NAL on MWCNT-NH₂ surface. This high affinity of the adsorbate with the adsorbent was also found in the adsorption of norfloxacin onto surface-modified carbon nanotubes (*n* values between 5 and 9) (Wang et al., 2009), whereas values of *n* slightly lower were reported for the recovery of bisphenol F on MWCNT, with *n* constants between 3.1 and 3.5, depending on the temperature (Zhang et al., 2013), phenolic compounds onto graphene oxides (1.26–3.47) (Wang et al., 2014), or pharmaceutical compounds onto activated carbons (1.5–5) (Rakic et al., 2014).

The saturated adsorption amount (*K_f*) follows the order DCO > NAL > MPET. For DCO and NAL, MWCNT shows the highest adsorption capacity, 380 and 111 mg g⁻¹, respectively; whereas the lowest values are for MWCNT-COOH, 248 and 79 mg g⁻¹, respectively, at 298 K. For MPET, the order followed is: N-CNT > MWCNT-NH₂ > MWCNT-COOH > MWCNT. The MPET is the least voluminous adsorbate (151.211 Å³), thus could enter easily in those pores that are not accessible for the rest of the adsorbates; in fact, the order followed by *K_f* is the order of decreasing surface area (Table 1). Concerning the behavior of NAL and DCO, both the mesoporous volume and the surface chemistry could be involved: MWCNT is the sample with the highest pore width and mesoporous volume, whereas MWCNT-COOH exhibits the lowest PZC.

The results obtained can be compared with those obtained in a previous work (Patiño et al., 2015) for the adsorption of DCO, NAL and MPET by conventional adsorbents as activated carbons (GF-40 and GC-900), carbon nanofibers (CNF) and high surface area graphite (HSAG-500). Comparing these supports with the reported in this work, it is observed that all the studied CNTs present poorer performance for DCO adsorption, being comparable for NAL, and performing the CNTs even better than the activated carbon for MPET adsorption.

3.3. Thermodynamic studies

The spontaneity and feasibility of the DCO, NAL and MPET adsorption on CNTs was studied by determination of thermodynamic parameters, by the following equations.

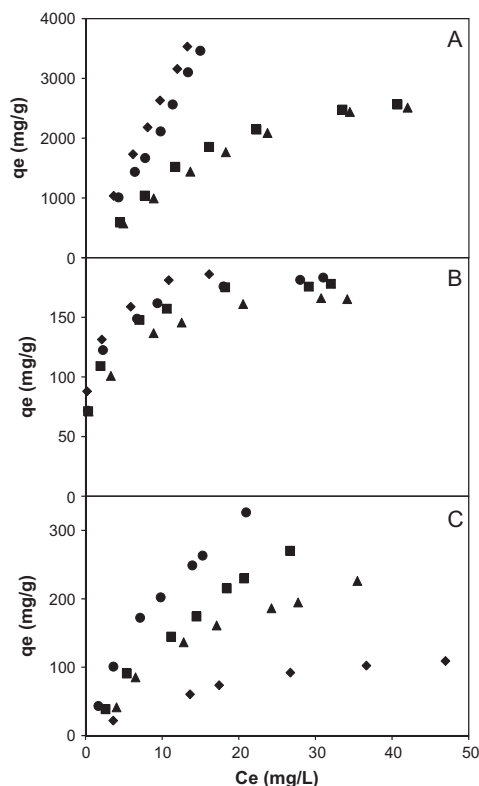


Fig. 1. Sorption isotherms for the adsorption of DCO (A), NAL (B) and MPET (C) on different CNT at 298 K (♦ MWCNT, ▲ MWCNT-COOH, ■ MWCNT-NH₂, ● N-CNT).

Table 2

Fitting results of isotherms for DCO, NAL and MPET on the four studied adsorbents.

Adsorbent	Temperature (K)	Langmuir model						Freundlich model						Langmuir model						Freundlich model					
		Langmuir model			Freundlich model			Langmuir model			Freundlich model			Langmuir model			Freundlich model			Langmuir model			Freundlich model		
		Q_0	k	r_1^2	K_F^a	n	r_2^2	Q_0	k	r_1^2	K_F^a	n	r_2^2	Q_0	k	r_1^2	K_F^a	n	r_2^2	Q_0	k	r_1^2	K_F^a	n	r_2^2
MWCNT (Patiño et al., 2015)	298	—	—	—	380.96	1.06	0.999	196.08	0.8	0.973	111.73	5.59	0.987	172.41	0.04	0.999	10.55	1.56	0.916						
	303	—	—	—	216.13	0.87	0.985	188.68	0.3	0.976	70.68	3.57	0.998	625.00	0.004	0.977	2.37	1.05	0.908						
	308	—	—	—	136.21	0.85	0.998	158.73	0.4	0.913	60.23	3.32	0.990	833.33	0.002	0.998	1.38	1.04	0.998						
	298	—	—	—	248.69	1.44	0.968	149.25	1.9	0.867	79.28	4.75	0.947	769.23	0.015	0.959	18.49	1.37	0.946						
	303	—	—	—	127.19	1.20	0.979	135.14	1.9	0.927	77.93	5.81	0.932	666.67	0.012	0.997	10.50	1.23	0.970						
MWCNT-COOH	308	—	—	—	91.74	1.12	0.979	117.65	0.6	0.894	59.31	5.37	0.918	588.24	0.007	0.999	5.52	1.18	0.987						
	298	—	—	—	308.65	1.54	0.942	163.93	1.8	0.934	98.09	5.75	0.951	909.09	0.018	0.997	19.94	1.23	0.985						
	303	—	—	—	186.12	1.44	0.919	144.93	2.8	0.911	94.97	7.26	0.925	769.23	0.015	0.999	12.64	1.14	0.997						
	308	—	—	—	185.73	1.55	0.901	125.00	5.7	0.905	62.09	5.18	0.947	1111.11	0.003	0.999	4.40	1.08	0.996						
	298	—	—	—	286.60	1.01	0.993	169.49	2.0	0.959	107.65	6.53	0.974	909.09	0.031	0.994	33.27	1.29	0.981						
N-CNT	303	—	—	—	252.35	1.09	0.996	151.52	1.7	0.960	92.35	6.47	0.983	714.29	0.016	0.995	13.59	1.20	0.981						
	308	—	—	—	137.08	1.09	0.992	142.86	0.4	0.939	59.51	4.17	0.961	909.09	0.008	0.994	10.22	1.22	0.962						

$$\Delta G^\circ = -RT \ln K_0, \text{ and} \quad (1)$$

$$\Delta G^\circ = \Delta H^\circ - T\Delta S^\circ \quad (2)$$

where T is temperature (K); K_0 the distribution coefficient (qe/Ce) (mg g^{-1}); R the universal gas constant ($8.314 \times 10^{-3} \text{ kJ mol}^{-1} \text{ K}^{-1}$); ΔG° the standard Gibbs free energy (kJ mol^{-1}); ΔH° the standard enthalpy (kJ mol^{-1}), and ΔS° the standard entropy ($\text{kJ mol}^{-1} \text{ K}^{-1}$). The Gibbs energy change ΔG° , was obtained by Eq. (1) and ΔH° and ΔS° were obtained from Eq. (2), taking the slope and intercept, respectively, of the linear plot of $\ln K_0$ versus $1/T$. The thermodynamic parameters were summarized in Table 3. The free energy change, ΔG , is negative, indicating a spontaneous process. The more negative the ΔG , the more spontaneous the adsorption was and, hence, it is expected a higher adsorption capacity. DCO and NAL have ΔG values between -11 and -14 kJ mol^{-1} , whereas MPET of only -5 kJ mol^{-1} ; accordingly, the K_F parameter from Freundlich isotherm decreases in the order

$\text{DCO} > \text{NAL} > \text{MPET}$. The enthalpies of adsorption are negative, indicative of an exothermic process. The magnitude of ΔH suggests a decreasing order of strength interaction: $\text{NAL} > \text{MPET} > \text{DCO}$, which is coincident with the n parameter of the Freundlich model, characteristic of the intensity of the adsorption. Values here reported are higher than obtained for the removal of Ciprofloxacin on carboxylated and graphitized MWCNTs ($80\text{--}10 \text{ kJ mol}^{-1}$ and -5 to -40 kJ mol^{-1} respectively (Li et al., 2014) or the retention of aromatic compounds on MWCNTs (9 to -13 kJ mol^{-1}) (Sheng et al., 2010). Finally, the negative values of the entropy suggest a decrease in randomness at the adsorbate/adsorbent interface during the adsorption. The values of entropy follow the same trend observed by the ΔH , since the highest strength of adsorption, the lowest degree of freedom at the interface.

3.4. Influence of CNTs functionalization and chemistry of the adsorbates on the adsorption

As it was deduced from both the enthalpy and the entropy of adsorption, the sorption affinity follows the order $\text{NAL} > \text{MPET} > \text{DCO}$, coincident with the decreasing order of the heterogeneity index of the Freundlich isotherm. This affinity sequence coincides with the increasing hydrophobicity of the adsorbates. The $\log K_{ow}$ parameter, octanol–water partition coefficient, shows that NAL has a higher affinity for water (0.228) than MPET (1.811) and DCO (4.086) (Molinspiration, 2014). Thus, the Van der Waals forces, usually predominant in the adsorption of organic molecules (Yan et al., 2014), are not the most prominent. In fact, it is observed that both the size and the molecular weight of the molecules are not the key parameters in the adsorption process. No clear trend is observed between the molecular volume of the adsorbates, NAL (229.762 \AA^3) $>$ DCO (174.121 \AA^3) $>$ MPET (152.19 \AA^3), and neither the strength of the interaction nor the adsorption capacity, K_F . And the same trend is observed if molecular weight is compared instead of the molecular volume. Thus, the molecular sieving is not the only factor in the adsorption phenomenon. However, the hydrophilic character, related also to the

Table 3
Thermodynamic parameters for the adsorption by CNTs.

		ΔG° (kJ/mol)	ΔH° (kJ/mol)	ΔS° (kJ mol $^{-1}$ K $^{-1}$)
DCO	MWCNT (Patiño et al., 2015)	-14.23	-36.79	-0.075
	MWCNT-COOH	-11.16	-41.54	-0.100
	MWCNT-NH ₂	-11.48	-48.21	-0.120
	N-CNT	-13.47	-71.87	-0.194
	MWCNT (Patiño et al., 2015)	-13.21	-132.21	-0.394
NAL	MWCNT-COOH	-12.46	-134.41	-0.406
	MWCNT-NH ₂	-12.78	-135.36	-0.408
	N-CNT	-12.51	-71.03	-0.193
	MWCNT (Patiño et al., 2015)	-1.85	-88.10	-0.285
	MWCNT-COOH	-4.78	-67.39	-0.208
MPET	MWCNT-COOH	-5.57	-101.7	-0.319
	MWCNT-NH ₂	-5.69	-97.77	-0.302

number of substituted groups seems to be determinant (Wang et al., 2014). At first insight, the $\pi-\pi$ interaction plays an important role, since NAL shows two aromatic rings, followed by MPET with one ring. The formation of electron donor-acceptor complexes between the surface of carbonaceous materials and the aromatic rings of, for example, toluene or phenolic compounds, was already widely reported; where the carbon surface electron rich regions act as donors and the aromatic ring of the adsorbate act as acceptor (Castillejos and Serp, 2010; Gotovac et al., 2007; Lin and Xing, 2008; Woods et al., 2007). Likewise, the substituted groups of the adsorbate could cause the aromatic/unsaturated moieties of the molecules to work as π -electron donor or π -electron acceptor (Wang et al., 2014). In this way, $-\text{CH}_3$ or $-\text{OH}$ groups can act as donors, whereas $-\text{Cl}$, $-\text{CHO}$ or amides as acceptors (Ren et al., 2011). The $\pi-\pi$ interactions, as well as the substituted groups, influence favorably the adsorption of the emerging pollutants tested on the MWCNTs (Woods et al., 2007). Concerning the effect of adsorbents characteristics, both the morphology and the surface chemistry could affect. From Fig. 1, it is observed the highest adsorption capacity of MWCNTs for DCO and NAL, whereas for MPET, N-CNT exhibits the highest value. N-CNT support has the highest surface area (Table 1), although the small pore diameter could hinder the adsorption on a higher extension of DCO and NAL, molecules with larger molecular volume than MPET. Among the other three supports, no significant morphological differences are observed that could justify the different adsorptive behavior. Likewise, the highest adsorption capacity of DCO and NAL on MWCNTs points out the negative effect of surface functional groups on the adsorption. This effect has already been described, being attributed to the blockage of pores by the functional groups (Cho et al., 2008; Díaz et al., 2007; Liao et al., 2008). What is more, the hydrophilic character of these groups could enhance the formation of H-bonds with water molecules, decreasing the sorption of organic compounds (Zhang et al., 2013), justifying the lowest capacity of adsorption on MWCNTs-COOH (Fig. 1). In addition, the oxygen surface groups seem to modify the electron density at the CNTs surface and/or to create positive holes in the conductive π -band of the curved graphene layer, hindering the $\pi-\pi$ interaction between adsorbent and adsorbate (Castillejos and Serp, 2010; Wang et al., 2014).

If both the strength of the adsorption (ΔH) and the affinity of the interaction (n parameter of the FM) are analyzed, different behaviors are observed. For the case of NAL, similar strengths are determined for MWCNTs and derived, whereas a reduction of even 46% has been obtained on CNT-N. Considering the adsorption capacity (Fig. 1), and the surface area of the adsorbents (Table 1), different adsorption sites among the adsorbents can be inferred (Agnihotri et al., 2005). For N-CNT adsorption on the external surface and the amorphous carbon deposits, whereas for the MWCNTs and derived, add to the cylindrical outer sidewall surface of the individual nanotubes, some of the small grooves of the aggregated CNTs or even the interior of the individual CNTs, as it was observed from TEM micrographs. Adsorption on these less accessible sites could contribute to the increasing enthalpy of adsorption.

In the case of DCO, similar enthalpies of adsorption were obtained for MWCNTs and derived (from -36.8 to -48.2 kJ/mol) and for N-CNT the enthalpy reaches the -71.9 kJ/mol . This increment could correspond to the increased surface area of N-CNT that could favor the adsorption of the adsorbate in some configurations; but also to the surface chemistry of the adsorbent. The highest PZC of N-CNT (Table 1) could imply a decreased negative charge of the surface, minimizing in this way the electrostatic repulsion forces with the $-\text{Cl}$ groups of DCO. Furthermore, the middle chain of the molecule could have higher affinity with the surface of the adsorbent, due to its hydrophobic character.

The strength of the interaction of MPET shows the highest values for MWCNTs-NH₂ and N-CNT, which could be attributed to specific interactions due to the different morphology of both adsorbents. The nitrogen content is more elevated for N-CNT (Table 1), as well as the presence of the both pyridinic and pyrrolic nitrogen, thus quaternary nitrogen could increase this affinity for MPET, acting as electron donor and the aromatic ring of the pollutant as receptor. This enhancement on the interaction of aromatic compounds with nitrogen-containing functional groups was already reported on activated carbons (Fan et al., 2011; Yan et al., 2014), being able to be applied also to the CNTs. Furthermore, the $-\text{OH}$ substitution on the aromatic compound and the nitrogen groups on the adsorbent surface may form hydrogen bonds (Li et al., 2006). On the other hand, MWCNT-COOH presents the most negative surface charge ($\text{pH}_{\text{PZC}} = 0.64$) at the operation conditions, which explains its poor behavior. Carboxylic groups on the surface of the adsorbent acted as electrons withdrawing groups localizing electron from π system of CNTs, interfering with $\pi-\pi$ dispersion forces between the aromatic rings of the adsorbate and the graphitic structure of CNTs (Castillejos and Serp, 2010).

4. Conclusions

The adsorption of three emerging pollutants was studied on four different CNTs, including functionalized CNTs with oxygen and nitrogen surface groups. Adsorption isotherms and thermodynamic parameters were estimated in order to determine the effect of CNTs functionalization on the adsorption process. The main conclusions obtained were:

- The capacity of CNT materials for DCO adsorption was one order of magnitude larger than for NAL and MPET, due to its hydrophobicity, and higher affinity for CNTs.
- The enthalpy and the sorption affinity according to Freundlich isotherm follow the order NAL > MPET > DCO, coincident with the increasing hydrophobicity of the adsorbates.
- Adsorption capacity of CNT materials for the three emerging pollutants is strongly conditioned by the morphology of the adsorbents, oxygen functionalities hindering the adsorption capacity.
- The strength of the adsorption increases mainly by the $\pi-\pi$ interactions of the aromatic rings with the carbonaceous support, being especially relevant the affinity of the aromatic rings with the quaternary nitrogen of the surface.

Acknowledgements

This work was supported by the Spanish Government (contract CTQ2011-29272-C04-01, -02 and -03). Y. Patiño thanks the Government of the Principality of Asturias for a Ph.D. fellowship (Severo Ochoa Program).

Appendix A. Supplementary material

Supplementary data associated with this article can be found, in the online version, at <http://dx.doi.org/10.1016/j.chemosphere.2015.04.089>.

References

- Adams, C., Wang, Y., Loftin, K., Meyer, M., 2002. Removal of antibiotics from surface and distilled water in conventional water treatment processes. *J. Environ. Eng.* 128, 253–260.
 Alahmad, W.R., Alawi, M.A., 2010. HPLC/UV/fluorescence detection of several pharmaceuticals in sewage treatment plant wastewaters of Jordan. *Fresenius Environ. Bull.* 19, 805–810.

- Agnihotri, S., Mota, J.P.B., Rostam-Abadi, M., Rood, M.J., 2005. Structural characterization of single walled carbon nanotube bundles by experiment and molecular simulation. *Langmuir* 21, 896–904.
- Bai, Y., Lin, D., Wu, F., Wang, Z., Xing, B., 2010. Adsorption of Triton X-series surfactants and its role in stabilizing multi-walled carbon nanotube suspensions. *Chemosphere* 79, 362–367.
- Boleda, M.R., Majamaa, K., Aerts, P., Gomez, V., Galceran, M.T., Ventura, F., 2010. Removal of drugs of abuse municipal wastewater using reverse osmosis membranes. *Desalin. Water Treat.* 21, 122–130.
- Carballa, M., Omil, F., Lema, J.M., Llompart, M.A., García-Járes, C., Rodríguez, I., Gómez, M., Ternes, T., 2004. Behavior of pharmaceuticals, cosmetics and hormones in a sewage treatment plant. *Water Res.* 38, 2918–2926.
- Carere, M., Polesello, S., Sollazzo, C., Gawlik, B.M., 2012. Chemical monitoring and emerging pollutants in the common implementation strategy of the water framework directive. *Trends Anal. Chem.* 36, 12–14.
- Castillejos, E., Serp, P., 2010. Carbon nanotubes for catalytic applications. In: Guidi, D.M., Martín, N. (Eds.), *Carbon Nanotubes and Related Structures: Synthesis, Characterization, Functionalization, and Applications*. Wiley-VCH Verlag GmbH & Co. KGaA, Weinheim, pp. 321–348.
- Chinthaginjal, J.K., Seshan, K., Lefferts, L., 2007. Preparation and application of carbon-nanofiber based microstructured materials as catalyst supports. *Ind. Eng. Chem. Res.* 46, 3968–3978.
- Cho, H.H., Smith, B.A., Wnuk, J.D., Fairbrother, D.H., 2008. Influence of surface oxides on the adsorption of naphthalene onto multiwalled carbon nanotubes. *Environ. Sci. Technol.* 42, 2899–2905.
- Choi, J.K., Kim, S.G., Kim, C.W., Kim, S.H., 2005. Effects of activated carbon types and service life on removal of endocrine disrupting chemical: amitrol, nonylphenol, and bisphenol-A. *Chemosphere* 58, 1535–1545.
- Díaz, E., Ordóñez, S., Vega, A., 2007. Adsorption of volatile organic compounds onto carbon nanotubes, carbon nanofibers, and high-surface-area graphite. *J. Colloid Interface Sci.* 305, 7–16.
- EU, 2000. Directive of the European Parliament and of the Council 2000/60/EC Establishing a framework for Community action in the field of water policy, Official Journal, 2000, C513, 23.10.2000.
- Dixon, M.B., Falconet, C., Ho, L., Chow, C.W.K., O'Neill, B.K., Newcombe, G., 2010. Nanofiltration for the removal of algal metabolites and the effects of fouling. *Water Sci. Technol.* 61, 1189–1199.
- Dongil, A.B., Bachiller-Baeza, B., Guerrero-Ruiz, A., Rodríguez-Ramos, I., Martínez-Alonso, A., Tascón, J.M.D., 2011. Surface chemical modifications induced on high surface area graphite and carbon nanofibers using different oxidation and functionalization treatments. *J. Colloid Interface Sci.* 355, 179–189.
- Eswaramoorthy, M., Sen, R., Rao, C.N.R., 1999. A study of micropores in single-walled carbon nanotubes by the adsorption of gases and vapors. *Chem. Phys. Lett.* 304, 207–210.
- Faba, L., Criado, Y.A., Gallegos-Suárez, E., Pérez-Cadenas, M., Díaz, E., Rodríguez-Ramos, I., Guerrero-Ruiz, A., Ordóñez, S., 2013. Preparation of nitrogen-containing carbon nanotubes and study of their performance as basic catalysts. *Appl. Catal. A* 458, 155–161.
- Fan, J., Yang, W., Li, A., 2011. Adsorption of phenol, bisphenol A and nonylphenol etheroxylates onto hypercrosslinked and aminated adsorbents. *React. Funct. Polym.* 71, 994–1000.
- Fang, Q.L., Chen, B.L., 2012. Adsorption of perchlorate onto raw and oxidized carbon nanotubes in aqueous solution. *Carbon* 50, 2209–2219.
- Gamage, J., Zhang, Z., 2010. Applications of photocatalytic disinfection. *Int. J. Photoenergy* 10, 1–11.
- Gotovac, S., Yang, C.-M., Hattori, Y., Takahashi, K., Kanoh, H., Kaneko, K., 2007. Adsorption of polycyclic aromatic hydrocarbons on single wall carbon nanotubes of different functionalities and diameters. *J. Colloid Interface Sci.* 314, 18–24.
- Gregg, S.J., Sing, K.S.W., 1982. *Adsorption, Surface Area and Porosity*. Academic Press, New York.
- Huerta-Fontela, M., Galceran, M.T., Ventura, F., 2011. Occurrence and removal of pharmaceuticals and hormones through drinking water treatment. *Water Res.* 45, 1432–1442.
- IRSTEA, 2014. Institut national de recherche en sciences et technologies pour l'environnement et l'agriculture, La recherche sur les polluants émergents à l'agenda européen <<http://www.irstea.fr/toutes-les-actualites/departement-eaux/PI-water-recherche-polluants-emergents-agenda-europeen>> (Accessed September 2014).
- Iwasaki, S., Fukuhara, T., Abe, I., Yanagi, J., Mouri, M., Iwashima, Y., Tabuchi, T., Shinohara, O., 2001. Adsorption of alkylphenols onto microporous carbons prepared from coconut shell. *Synth. Met.* 125, 207–211.
- Joseph, L., Heo, J., Park, Y.-G., Flora, J.R.V., Yoon, Y., 2011. Adsorption of bisphenol A and 17 α -ethinyl estradiol on single walled carbon nanotubes from seawater and brackish water. *Desalination* 281, 68–74.
- Kang, S., Mauter, S.M., Elimelech, M., 2008. Physicochemical determinants of multiwalled carbon nanotube bacterial cytotoxicity. *Environ. Sci. Technol.* 42, 7528–7534.
- Kinoshita, K., 1988. *Carbon: Electrochemical and Physicochemical Properties*. Wiley, New York.
- Kondratyuk, P., Yates Jr., J.T., 2007. Molecular views of physical adsorption inside and outside of single-wall carbon nanotubes. *Acc. Chem. Res.* 40, 995–1004.
- Li, H., Zhang, D., Han, X., Xing, B., 2014. Adsorption of antibiotic ciprofloxacin on carbon nanotubes: pH dependence and thermodynamics. *Chemosphere* 95, 150–155.
- Li, X.J., Chen, W., Zhan, Q.W., Dai, L.M., Sowards, L., Pender, M., Naik, R.R., 2006. Direct measurements of interactions between polypeptides and carbon nanotubes. *J. Phys. Chem. B* 110, 12621–12625.
- Liao, Q., Sun, J., Gao, L., 2008. The adsorption of resorcinol from water using multiwalled carbon nanotubes. *Colloid Surf. A* 312, 160–165.
- Lin, D.H., Xing, B.S., 2008. Adsorption of phenolic compounds by carbon nanotubes: role of aromaticity and substitution of hydroxyl groups. *Environ. Sci. Technol.* 42, 7254–7259.
- Majeau, J.-A., Brar, S.K., Tyagi, R.D., 2010. Laccases for removal of recalcitrant and emerging pollutants. *Bioresour. Technol.* 101, 2331–2350.
- Molinpiration, 2014. Cheminformatics on the web <<http://www.molinpiration.com>> (Accessed September 2014).
- NORMAN, 2014. Network of reference laboratories, research centres and related organisations for monitoring of emerging environmental substances <<http://www.norman-network.net/>> (Accessed September 2014).
- Nevskia, D.M., Guerrero-Ruiz, A., 2001. Comparative study of the adsorption from aqueous solutions and the desorption of phenol and nonylphenol substrates on activated carbons. *J. Colloid Interface Sci.* 234, 316–321.
- Omil, F., Suárez, S., Carballa, M., Reif, R., Lema, J.M., 2010. Criteria for designing sewage treatment plants for enhanced removal of organic micropollutants. In: Fatta-Kassinos, D. et al. (Eds.), *Xenobiotics in the Urban Water Cycle, Mass Flows, Environmental Process, Mitigation and Treatment Strategies*. Springer, pp. 283–306.
- Patiño, Y., Díaz, E., Ordóñez, S., 2015. Performance of different carbonaceous materials for emerging pollutants adsorption. *Chemosphere* 119, S124–S130.
- Peng, H., Pan, B., Wu, M., Liu, R., Zhang, D., Wu, D., Xing, B., 2012. Adsorption of ofloxacin on carbon nanotubes: Solubility, pH and cosolvent effects. *J. Hazard. Mater.* 211–212, 342–348.
- Rakic, V., Rac, V., Krmar, M., Otman, O., Auoux, A., 2014. The adsorption of pharmaceutically active compounds from aqueous solutions onto activated carbons. *J. Hazard. Mater.* <http://dx.doi.org/10.1016/j.jhazmat.2014.04.062>.
- Ren, X., Chen, C., Nagatsu, M., Wang, X., 2011. Carbon nanotubes as adsorbents in environmental pollution management: a review. *Chem. Eng. J.* 170, 395–410.
- Rigobello, E.S., Dantas, A.D.B., Di Bernardo, L., Vieira, E.M., 2013. Removal of diclofenac by conventional drinking water treatment processes and granular activated carbon filtration. *Chemosphere* 92, 184–191.
- Rivera-Utrilla, J., Sánchez-Polo, M., Ferro-García, M.Á., Prados-Joya, G., Ocampo-Pérez, R., 2013. Pharmaceuticals as emerging contaminants and their removal from water. A review. *Chemosphere* 93, 1268–1287.
- Ruiz, B., Cabrita, I., Mestre, A.S., Parra, J.B., Pires, J., Carvalho, A.P., Ania, C.O., 2010. Surface heterogeneity effects of activated carbons on the kinetics of paracetamol removal from aqueous solution. *Appl. Surf. Sci.* 256, 5171–5175.
- Sheng, G.D., Shao, D.D., Ren, X.M., Wang, X.Q., Li, J.X., Chen, Y.X., Wang, X.K., 2010. Kinetics and thermodynamics of adsorption of ionizable aromatic compounds from aqueous solutions by as-prepared and oxidized multiwalled carbon nanotubes. *J. Hazard. Mater.* 180, 505–516.
- Sipma, J., Osuna, B., Collado, N., Monclús, H., Ferrero, G., Comas, J., Rodriguez-Roda, I., 2010. Comparison of removal of pharmaceuticals in MBR and activated sludge systems. *Desalination* 250, 653–659.
- Wang, J., Chen, Z., Chen, B., 2014a. Adsorption of polycyclic aromatic hydrocarbons by graphene and graphene oxide nanosheets. *Environ. Sci. Technol.* 48, 4817–4825.
- Wang, X., Huang, S., Zhu, L., Tian, X., Li, S., Tang, H., 2014b. Correlation between the adsorption ability and reduction degree of graphene oxide and tuning of adsorption of phenolic compounds. *Carbon* 69, 101–112.
- Wang, X., Liu, Y., Tao, S., Xing, B., 2010. Relative importance of multiple mechanisms in sorption of organic compounds by multiwalled carbon nanotubes. *Carbon* 48, 3721–3728.
- Wang, Z., Yu, X., Pan, B., Xing, B., 2009. Norfloxacin sorption and its thermodynamics on surface-modified carbon nanotubes. *Environ. Sci. Technol.* 44, 978–984.
- Woods, L.M., Bădescu, S.C., Reinecke, T.L., 2007. Adsorption of simple benzene derivatives on carbon nanotubes. *Phys. Rev. B* 75, 155415.
- Yan, W., Yan, L., Duan, J., Jing, C., 2014. Sorption of organophosphate esters by carbon nanotubes. *J. Hazard. Mater.* 273, 53–60.
- Yang, K., Xing, B.S., 2010. Adsorption of organic compounds by carbon nanomaterials in aqueous phase: polanyi theory and its application. *Chem. Rev.* 110, 5989–6008.
- Yang, Q.-H., Hou, P.-X., Bai, S., Wang, M.-Z., Cheng, H.-M., 2001. Adsorption and capillarity of nitrogen in aggregated multi-walled carbon nanotubes. *Chem. Phys. Lett.* 345, 18–24.
- Yu, Z., Peldszus, S., Huck, P.M., 2008. Adsorption characteristics of selected pharmaceuticals and an endocrine disrupting compound-Naproxen, carbamazepine and nonylphenol-on activated carbon. *Water Res.* 42, 2873–2882.
- Zhang, L., Pan, F., Liu, X., Yang, L., Jiang, X., Yang, J., Shi, W., 2013. Multi-walled carbon nanotubes as sorbent for recovery of endocrine disrupting compound-bisphenol F from wastewater. *Chem. Eng. J.* 218, 238–246.
- Zhou, J.-H., Sui, Z.-J., Zhu, J., Li, P., Chen, D., Dai, Y.-C., Yuan, W.-K., 2007. Characterization of surface oxygen complexes on carbon nanofibers by TPD, XPS and FT-IR. *Carbon* 45, 785–796.

4.2. Estudios de adsorción-desorción en lecho fijo

En esta sección se lleva a cabo la pre-concentración de los contaminantes modelo mediante adsorción/desorción en lecho fijo. Según los resultados obtenidos en el apartado 4.1, se seleccionaron como adsorbentes los representativos de distintas familias que presentaron las tres mayores capacidades de adsorción. Por lo tanto la pre-concentración se llevó a cabo sobre carbón activo (GF-40), nanotubos de carbono (MWCNT) y grafito de alta superficie (HSAG-500).

La Figura 4.2 representa el procedimiento llevado a cabo, donde una disolución del contaminante a estudiar de concentración conocida, se hizo pasar a través de la columna en cuyo interior se encuentra el lecho de adsorción. A su paso se irá produciendo la adsorción hasta alcanzar la saturación del lecho. Una vez alcanzada la misma, se pasa agua a contracorriente (a mayor temperatura que el proceso de adsorción) con el fin de desorber el contaminante y concentrarlo en la corriente de salida.

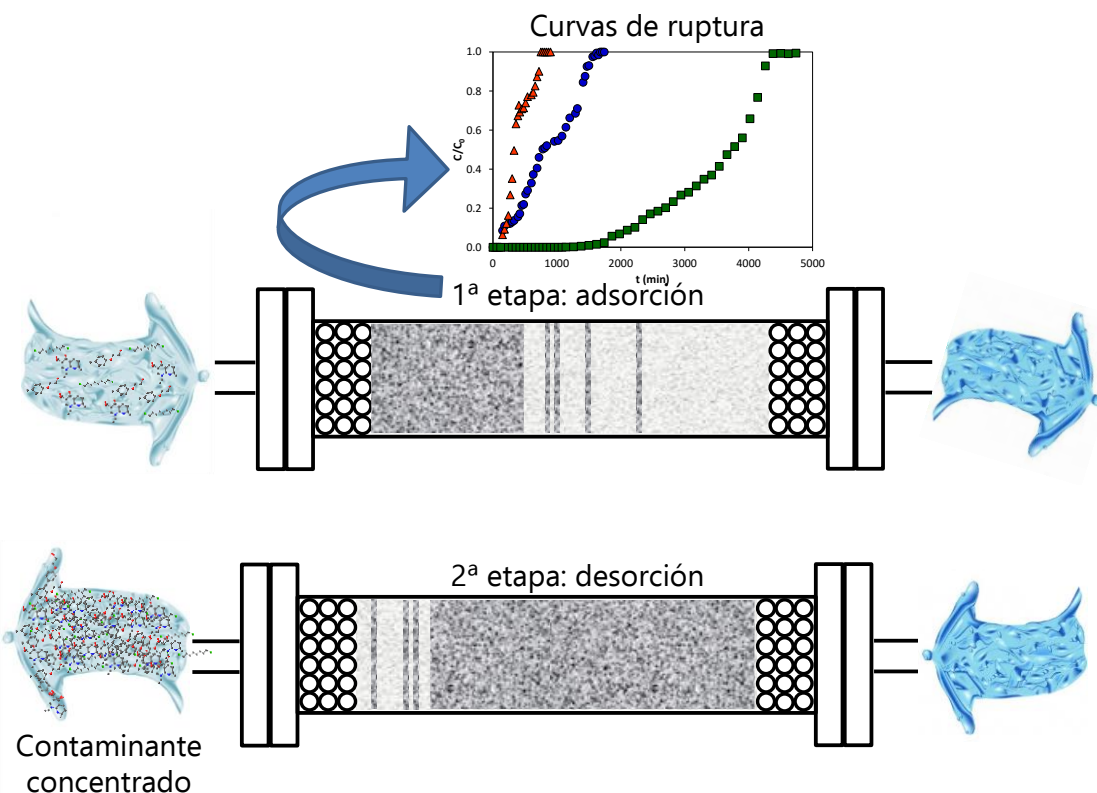


Figura 4.2. Gráfico conceptual del proceso de adsorción en continuo

Con los datos obtenidos a partir de la etapa de adsorción se obtienen las curvas de ruptura, las cuales son modelizadas mediante los modelos: *Bed depth service time* (BDST), Thomas y Yoon-Nelson.

Con los datos una vez completado el ciclo de adsorción/desorción se obtienen los factores de concentración y eficacia de regeneración, con el fin de poder obtener el adsorbente que proporciona una mayor pre-concentración y facilidad de regeneración. Así, una vez conseguida la pre-concentración del contaminante ya es posible llevar a cabo la degradación de los contaminantes partiendo de una concentración más elevada.

Los resultados obtenidos se presentan en los apartados 4.2.1 y 4.2.2, mediante las *Publicaciones III y IV* expuestas a continuación.

- Y. Patiño, E. Díaz, S. Ordóñez. Pre-concentration of nalidixic acid through adsorption-desorption cycles: Adsorbent selection and modelling, Chemical Engineering Journal 283 (2016) 486-494.
- Y. Patiño, E. Díaz, S. Ordóñez. Pre-concentration of a polychlorinated n-alkane and an alkylphenol on carbonaceous materials in fixed bed columns, Chemical Engineering Journal. En revisión.

4.2.1. Publicación III

**Pre-concentration of nalidixic acid through adsorption-desorption cycles:
Adsorbent selection and modelling**

Autores: Y. Patiño, E. Díaz, S. Ordóñez

Publicado en:

Chemical Engineering Journal

Volumen 283

Páginas 486-494

Año 2016





Pre-concentration of nalidixic acid through adsorption–desorption cycles: Adsorbent selection and modeling

Yolanda Patiño, Eva Díaz, Salvador Ordóñez*

Department of Chemical and Environmental Engineering, University of Oviedo, Faculty of Chemistry, Julián Clavería s/n, 33006 Oviedo, Spain

HIGHLIGHTS

- Nalidixic acid was pre-concentrated by adsorption/desorption cycles.
- Three adsorbents tested: activated carbon, carbon nanotubes and graphite.
- Experimental data fitted to various breakthrough curves models.
- Carbon nanotubes exhibits the lowest adsorption capacity losses after regeneration.
- Only carbon nanotubes are efficient for nalidixic acid pre-concentration.

ARTICLE INFO

Article history:

Received 6 May 2015

Received in revised form 27 July 2015

Accepted 30 July 2015

Available online 3 August 2015

Keywords:

Fixed bed adsorption

Breakthrough curve

Carbon materials

Adsorption modeling

Micropollutants

Emerging pollutants

ABSTRACT

A new approach is proposed for pre-concentrating emerging pollutants, taking nalidixic acid as representative. The approach consists of performing successive adsorption–desorption cycles in order to remove the pollutant from the main stream, generating a new stream with higher pollutant concentration during the adsorbent regeneration. For accomplishing these scopes (efficient removal and capability for pre-concentrate), adsorbents presenting both high adsorption capacity and regeneration easiness are needed. In this work, the performance of three different adsorbents is studied: activated carbon (GF-40), multi-walled carbon nanotubes (MWCNTs) and high surface area graphite (HSAG-500). Adsorption experiments were performed at 25 °C, whereas two different desorption temperatures (35 and 40 °C) were chosen in order to evaluate the ability of the materials for concentrating the NAL. The adsorption breakthrough curves were modeled considering different models: Bed Depth Service Time (BDST), Thomas and Yoon-Nelson. Although activated carbon largely presents the highest adsorption capacity, it is difficult to regenerate needing long regeneration times, leading to very dilute regeneration solutions. By contrast, MWCNTs present lower adsorption capacity, but they are more easily regenerated leading to higher NAL concentrations.

© 2015 Elsevier B.V. All rights reserved.

1. Introduction

In the last decades, pharmaceutical and personal care products (PPCPs), considered as emerging pollutants, have been released to the environment in large quantities. They enter into the ecosystems from personal, veterinary and aquaculture uses [1], and they are able to persist in the environment and to exhibit deleterious effects in organisms. Among the most prescribed drugs in human medicine, the analgesics/anti-inflammatories and antibiotics stand up [2]. Antibiotics are a group of compounds of especial harmful potential [3,4]. These compounds induce antibiotic resistance after chronic exposure in contaminated water, especially to quinolones

and sulfonamides [4–6]. Within the quinolones, nalidixic acid is the first antibacterial quinolone commercialized [7], being widely used in the treatment of gram-negative urinary tract infections [8] since it is more active against gram-negative than gram-positive bacteria [7]. Nalidixic acid has been selected in the present study because of its presence in hospital wastes, wastewater treatment plants effluents, environmental waters and soils [9–11]. It has serious effects on human health, such as chronic toxicity and carcinogenicity effect [12].

The antibacterial nature of this kind of antibiotics prevents effective removal in traditional wastewater treatment plants [13,14]. Thus, they have been frequently detected in surface, ground and drinking water in different countries worldwide [13,15–18]. For this reason, it is very important to develop effective techniques for removing this kind of compounds from

* Corresponding author. Tel.: +34 985 103 437; fax: +34 985 103 434.
E-mail address: sordonez@uniovi.es (S. Ordóñez).

wastewaters. Bioprocesses have been used to eliminate biodegradable pollutants, but in many cases, they are inefficient for the degradation of antibiotics, since most of them are bio-recalcitrant [19]. Dorival-García et al. [20] employed an activated sludge reactor for the degradation of six quinolone antibiotics in wastewaters with a percentage of removal from 14.9 to 43.8 in aerobic conditions and it increases to 36.2–60% under nitrifying conditions. Bendz et al. [21] reported that activated sludge treatment resulted in <50% removal efficiency of trimethoprim and sulfamethoxazole. Conventional process such as filtration, coagulation/flocculation or sedimentation achieve very low removal efficiencies [18,22]. Kimura et al. [23] studied the filtration of different endocrine disruptors and pharmaceutical by reverse osmosis with two different membranes. With a cellulose acetate membrane, most of the compounds exhibited retentions lower than 50%, and for a polyamide membrane, it increases to retentions between 75% and 90%. Adams et al. [24] studied the removal of different antibiotic (Carbadox, Trimethoprim and five different sulfonamide) employing aluminum sulfate and ferric sulfate as coagulant/flocculant without significant removal of any of these compounds. Although advanced oxidation process are effective to degrade antibiotics, the intermediates compounds can be even more toxic than the parent compounds. On the other hand, these processes are efficient at higher concentrations than the usually found in wastewaters [25,26]. Therefore, pre-concentration of the emerging pollutant using other techniques will be a very interesting previous step.

At this point, adsorption on carbon materials is one of the most usual alternatives for the treatment of wastewaters containing antibiotics. It presents several advantages: simple design and operation, low initial cost, and high potential for the removal of emerging pollutants due to the vast variety of adsorbents [27–29]. Activated carbons are effective to remove antibiotics from water, significant adsorption capacities being reported in the literature [30–32]. But for adsorption process, the possibility of regeneration, allowing the use of the adsorbent in subsequent adsorption-desorption cycles, is as important as the adsorption capacity [33]. In the same way, as the regeneration will be easier (needing milder conditions and lower regenerating solution flow rates), more concentrated solutions will be obtained during the regeneration, enabling further destructive treatments. At this point, activated carbons have demonstrated high adsorption capacities for this kind of pollutants, but their regeneration is usually difficult because of both their microporous character and the strong interaction with their active sites [33]. By contrast, carbon nanotubes (CNTs) or mesoporous graphites (such as High Surface Area Graphites, HSAG) can be used as effective adsorbents to remove organic contaminants because of their exceptional sorption properties. Their strong hydrophobic nature and their unique graphitic structure provide a high adsorption capability [34]. Previous studies have reported high adsorption capacity for organic pollutants including PPCPs. Yang et al. [35] studied the adsorption of norfloxacin on CNTs and Zhang et al. [36] studied the adsorption of tetracycline by CNTs under different conditions.

Most of the studies about the removal of pharmaceutic compound has been studied by batch sorption methods using in stirred devices, but fixed bed adsorption are easier to scale-up to industrial application. On the other hand, fixed bed column studies are necessary to predict the column breakthrough or the shape of the adsorption wave front and provide the most practical application for this process in wastewater treatment [37,38]. Likewise, regeneration behavior of the adsorbent should be optimized for subsequent uses of the adsorbent and for obtaining regenerating solutions concentrated enough. There are different methods for the regeneration such as extraction with different solvents, chemical regeneration or thermal treatments [32,39,40]. There are few studies focused on continuous adsorption/desorption of

pharmaceutical products with regeneration of the adsorbent. Yaghmaeian et al. [32], studied the removal of amoxicillin using activated carbon and the desorption was carried out by using ozonation. Otero et al. [41] studied the fixed bed adsorption and desorption of salicylic acid employing water at the same temperature than adsorption for the elution process while Tian et al. [5] realized the desorption of two sulfonamide antibiotics using a NaCl and NaOH solution to regenerate the column. most studies are focus on the study of the adsorption/desorption as removal methodology, but not in its use as pre-concentration technique. Our purpose at this point is the use of the adsorption technique for obtaining a most concentrated stream, but always using mild conditions.

In this study, adsorption/desorption of nalidixic acid on an activated carbon (AC), carbon nanotubes (MWCNT) and a high surface area graphite (HSAG) in a fixed bed column was investigated with the aim to obtain an adsorption/desorption methodology to pre-concentrate NAL. The main goals are: (i) evaluate the performance of nalidixic acid adsorption in continuous mode; (ii) develop a breakthrough curve model; and, (iii) evaluate the in-situ regeneration efficiency of the saturated adsorbent and their ability for obtaining concentrated regeneration solutions.

2. Materials and methods

2.1. Materials

Nalidixic acid (NAL) was purchased from Duchefa, Biochemie B.V. (>99.4%), and used in the experiments directly without any further purification. The physico-chemical properties of NAL are summarized in Table 1.

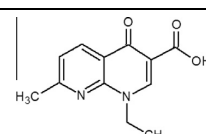
As adsorbents, three carbon materials have been used: activated carbon (Norit, GF-40), multi wall carbon nanotubes (Dropsens, MWCNT) and high surface area graphite (Lonza, HSAG-500). The adsorbent properties are given in Table 2.

2.2. Fixed bed column sorption experiments

The adsorption experiments were conducted in a fixed bed column. The experimental set-up consisted of a stainless steel column with an internal diameter of 3.3 mm and a total height of 500 mm. The column was packed with the carbon material – bed length of 1 cm-, and then filled with two layers of glass balls (250–355 µm diameter) to compact the column and prevent preferential channels and dead volumes. Standard solutions, with a concentration of 80 ppm, were pumped into the column through a perforated plate, fixed at the top of the column, using a HPLC pump (LabAlliance, serie II) at constant volumetric flow rate of 1 mL/min. The downward flow ensures that bed expansion does

Table 1
Physicochemical properties of nalidixic acid used as adsorbate.

Nalidixic acid (NAL)	
CAS number	389-08-2
Molecular weight (g/mol)	232.23
Polarizability	$23.8 \pm 0.5 \cdot 10^{-24} \text{ cm}^3$
Molecular volume	203.58 Å^3
Isoelectric point	5.28



www.chemspider.com.

Table 2

Textural parameters and chemical properties of the adsorbents used in this work.

Adsorbent	Abbreviation	S_{BET} ($\text{m}^2 \text{ g}^{-1}$)	V_{meso} ($\text{cm}^3 \text{ g}^{-1}$)	V_{micro} ($\text{cm}^3 \text{ g}^{-1}$)	PZC
Activated carbon	AC GF-40	1248 ^a	0.29 ^a	0.18	1.36 ^a
Multi wall carbon nanotubes	MWCNT	277 ^a	2.51 ^a	0.005 ^a	4.19 ^a
High surface area graphites	HSAG-500	580	0.75	—	3.16 ^a

^a Ref. [42].

not affect the hydrodynamics and performance of the adsorption bed.

The stock solutions were placed in a constant-temperature water bath ($25 \pm 1^\circ\text{C}$). The samples of the effluent were collected at different time intervals until saturation was reached, and analyzed by High Pressure Liquid Chromatography – HPLC – (Agilent 1200 with an UV-VIS detector and a 150 mm Zorbax SB-Aq column).

It was considered that the process reached the saturation when the effluent concentration is equal to the input concentration or when it was constant for a long period of time.

2.3. Column desorption and recycling

Desorption experiments were carried out when the column saturation was reached. Water was injected through the bed in counter flow to normal adsorption, at the same volumetric flow rate. The feasibility of performing the desorption of organic pollutants with liquid water has been previously demonstrated by Otero et al. [41] reporting complete elution of salicylic acid onto activated carbon using water as eluent. Adsorption is an exothermic process, slight increases of eluent temperature will enhance desorption process. Thus, two different temperatures, 35 and 40 °C were chosen. The samples of the effluent were analyzed until negligible or constant concentration. After the elution time, the adsorbent was reused in a second cycle for adsorption at the same conditions than the first cycle to evaluate the reusability of the adsorbent.

3. Results and discussion

3.1. Breakthrough curves and adsorption parameters

The obtained breakthrough curves are shown in Fig. 1. The breakthrough time increases in the order HSAG-500 < MWCNT < GF-40, whereas the slope of the curve follows exactly the opposite behavior, which indicates a slower mass transport due to decreased diffusion coefficient or decreased mass transfer coefficient from HSAG-500 to GF-40. This behavior contrasts with the favorable adsorption isotherms observed for this adsorbate on the studied adsorbents [42], especially for GF-40 and MWCNT; since, it is expected that favorable adsorption isotherms leads to sharper mass transfer areas into the column. Thus, as it was already observed by other authors, the concentration gradients in batch and continuous flow systems are different [31]. At this point, the adsorption process on porous solids can be split into three stages: (a) external mass transfer of the adsorbate through the liquid film to the external surface of the adsorbent (outer diffusion); (b) transport of the adsorbate from the exterior surface of the adsorbent to the pores of the internal structure of the adsorbent (intra-particle diffusion or inner diffusion); and (c) adsorption of the adsorbate onto the active sites on the inner and outer surfaces of the adsorbent [43]. Generally, the adsorption process is controlled by either the first or the second step, or a combination of both [44,45], and from the observed results, it is important to point out that activated carbon is the

most microporous material (Table 2), thus the diffusion of NAL from the bulk liquid to the mesopores and then into the micropores could take a longer time, leading to slower adsorption kinetics [31]. This internal diffusion can also explain the different shapes of the breakthrough curves for the three adsorbents, since the GF-40 curves exhibit the most early breakthrough and tailing. This effect, related to the intra-particle diffusion, is more evident as the bed height is increased.

From the breakthrough curves, important parameters of the adsorption process can be calculated, in order to provide information about the adsorption process (Table 3). The adsorption capacities at breakthrough time (q_{bk} for $C/C_0 = 0.05$ [31]) and at saturation time (q_s for the maximum C/C_0 obtained) were calculated according to the Gaoenkoplis' model [46]:

$$q_{\text{bk}} = \frac{C_0 Q}{W} \int_0^{t_{\text{bk}}} \left(1 - \frac{C}{C_0}\right) dt \quad (1)$$

$$q_s = \frac{C_0 Q}{W} \int_0^{t_s} \left(1 - \frac{C}{C_0}\right) dt \quad (2)$$

where C and C_0 are the NAL effluent and inlet concentration (mg/L); Q , the volumetric flow rate (L/h); W , the mass of adsorbent (g); and, t_s and t_{bk} the saturation and breakthrough times respectively (h).

Both, q_{bk} and q_s follow the order GF-40 > MWCNT > HSAG-500, as is also concluded from the breakthrough curves depicted in Fig. 1. The highest adsorption capacity was obtained by activated carbon, where both morphology and surface chemistry justify these differences in adsorption capacity. The values of the adsorption capacity for the different carbonaceous materials are higher than the obtained in other works for the adsorption of pharmaceuticals, which present a similar structure with aromatic rings, where $\pi-\pi$ interactions can take place. Many of the reported studies proposing activated carbon as adsorbent, estimate similar values for these parameters. For example, adsorption capacities lower than 100 mg/g were found for ibuprofen, naproxen and clofibric acid by Dubey et al. [47] and for tetracycline and chloroamphenicol by Liao et al. [48]. A bit higher adsorption capacity (35–222 mg/g) was obtained by Sotelo et al. [31] for flumequine removal. It should be noted that these compounds have higher molecular weight, which affects the adsorption process. Regarding to the adsorption on carbon nanotubes, Tian et al. [5] studied the adsorption of sulfonamide antibiotics, obtaining capacities from 11 to 123 mg/g, much lower than those obtained in this study.

The fractional bed utilization (FBU) was calculated following the Eq. (3). FBU represents the fraction of bed which is being used for the adsorption at the saturation concentration:

$$\text{FBU} = \frac{q_{\text{bk}}}{q_s} \quad (3)$$

The mass transfer zone (MTZ) is the length of the adsorbent that is gradually being saturated, where the mass transfer takes place. It can be calculated according to:

$$\text{MTZ} = \left(1 - \frac{q_{\text{bk}}}{q_s}\right)L \quad (4)$$

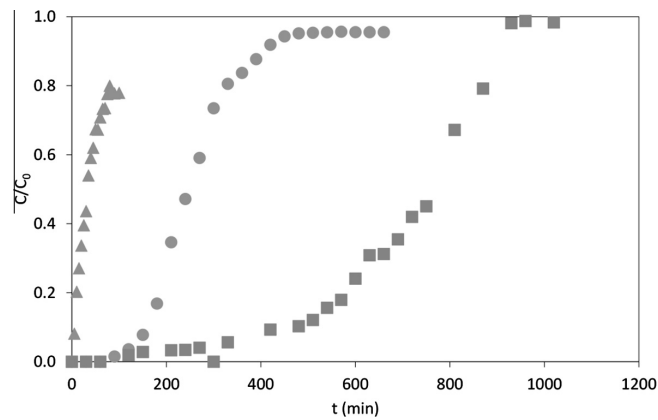


Fig. 1. Breakthrough curves representing NAL adsorption onto GF-40 (squares), MWCNT (circles) and HSAG-500 (triangles) at 25 °C.

Table 3

Adsorption capacities (q_{bk} , q_s), FBU, MTZ and area-normalized capacity for nalidixic acid adsorption.

	q_{bk} (mg g ⁻¹)	q_s (mg g ⁻¹)	FBU	MTZ (cm)	q_s/area (mg g ⁻¹ m ⁻²)
GF-40	449	1595	0.28	0.72	1.28
MWCNT	193	583	0.33	0.67	2.10
HSAG-500	5	62	0.07	0.93	0.17

where L is the bed length (cm). The MTZ value has been calculated for the maximum value that corresponds to the bed depth, where most of the mass transfer takes place [47]. The MTZ value decreases with increasing the mass transfer efficiency. The MTZ value increases as MWCNT < GF-40 < HSAG-500, so the mass transfer efficiency follows the reverse order, where MWCNT presents the highest value.

It is remarkable the similar values obtained for both parameters, FBU and MTZ, in the case of GF-40 and MWCNT, although the crystalline structure of these two materials is quite different (GF-40 is amorphous, whereas MWCNTs have graphitic structures). If the normalized adsorption capacity (mg_{NAL}/m²adsorbent) is calculated (Table 3), an increase is observed following the order MWCNT > GF-40 ≫ HSAG-500. The large difference observed for HSAG-500 cannot be explained exclusively from the point of view of the crystallographic characteristics or electrostatic interactions. In the first case, limitations could be due to steric constraints in the NAL adsorption due to the volume of the molecule, and these limitations should be more important as the entrance to the pores is reduced. Therefore, MWCNT, which presents the highest volume of mesopores, presents the higher normalized adsorption capacity. However, according to Table 2, the most microporous material (GF-40) and with the lowest mesopore volume exhibits the intermediate behavior, whereas the HSAG-500, mesoporous material, presents the worst normalized adsorption capacity. Concerning the electrostatic interactions, the three adsorbents present a negative surface charge at pH = 7, and also the adsorbate, since the isoelectric point of NAL is 5.28 (Table 1). Thus, the interaction could be more favored on the surface of MWCNT, which is the material with the highest PZC. But, once again, HSAG-500 does not follow the trend. At this point, it is remarkable that both HSAG-500 and MWCNT have graphitic structures (contrary to GF-40) and, between both of them, HSAG is the material most highly structured, whereas MWCNT presents higher surface reactivity (carbon atoms are in rolled layers, instead of in flat layers) [49]. Furthermore, whereas graphite is constituted by flat graphene layers, MWCNT consist of curved graphene

layers, distorting the sp^2 hybridization and therefore changing the nature of the chemical interaction with the adsorbate. This configuration of MWCNT improves the $\pi-\pi^*$ interactions, where the adsorbent acts as an electron donor and the solute benzene rings has an electron withdrawing character [41]. Similarly, Liao et al. [48] reported that the strongest adsorption of tetracycline and chloramphenicol using carbon materials was ascribe to the $\pi-\pi$ interaction; and Fan et al. [50] addressed that this kind of interactions enhances the adsorption of chloramphenicol on modified carbonaceous materials.

3.2. Application of breakthrough curve models

Different mathematical models have been used to predict the breakthrough curves and breakthrough adsorption parameters, very important for the design of fixed bed columns, especially for industrial scale where it is necessary a continuous treatment. Bed Depth Service Time (BDST), Thomas, and Yoon-Nelson models have been used to describe adsorption kinetics and the maximum adsorption capacity [32,38,51]. In the present study, these three models have been studied to find out the best model describing the adsorption in column. The Fig. 2 shows the experimental and theoretical breakthrough curves for NAL.

3.2.1. Bed Depth Service Time (BDST) model

The BDST model equation is given below:

$$t = \frac{N_0 z}{C_0 u} - \frac{1}{k C_0} \ln \left(\frac{C_0}{C} - 1 \right) \quad (5)$$

where t is the time (min), z is the bed height (cm), u is the linear flow rate (mL cm⁻² min⁻¹) and C_0 and C are the inlet and outlet adsorbate concentrations (mg L⁻¹). The adsorption rate constant (k , L mg⁻¹ min⁻¹) and the adsorption capacity (N_0 , mg L⁻¹) values were calculated from the slope and intercept of the plot between $\ln \left(\frac{C_0}{C} - 1 \right)$ versus time. BDST model was well-fitted with the data from test of columns adsorption capacity with a higher correlation

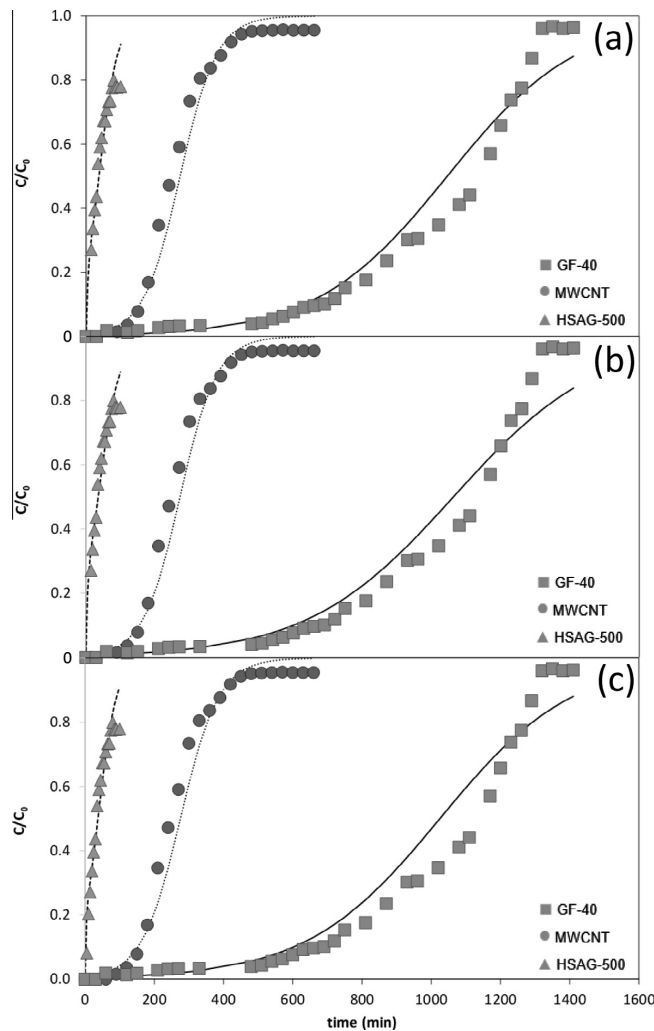


Fig. 2. Experimental and predicted breakthrough curves for NAL removal based on BDST model (a), Thomas model (b) and Yoon-Nelson model (c) for adsorption of NAL onto GF-40 (squares), MWCNT (circles) and HSAG-500 (triangles).

Table 4
Predicted parameters for BDST, Thomas and Yoon-Nelson models for NAL adsorption on carbonaceous materials.

	BDST			Thomas			Yoon-Nelson		
	$k \times 10^4$ ($\text{L mg}^{-1} \text{min}^{-1}$)	N_0 (mg L^{-1})	r^2	$k_{\text{TH}} \times 10^4$ ($\text{L min}^{-1} \text{mg}^{-1}$)	q_0 (mg g^{-1})	r^2	$K_{\text{YN}} \times 10^2$ (min^{-1})	τ (min)	r^2
GF-40	0.7	1077560	0.90	0.6	1654	0.92	0.5	1025	0.91
MWCNT	2.4	280615	0.96	2.4	424	0.96	1.8	275	0.95
HSAG-500	4.7	38465	0.93	4.2	56	0.93	3.7	37	0.95

coefficient ($r^2 > 0.9$). The obtained parameters are summarized in **Table 4**. The adsorption rate constant (k) decreases as the adsorption capacity increases (N_0), so it is related to the adsorption kinetics. Compared with other studies, the fitting of the experimental values here obtained present a correlation coefficient of 0.90 (GF-40), 0.96 (MWCNT) and 0.93 (HSAG-500), higher than obtained by Tian et al. [5] for the adsorption of two sulfonamide antibiotics for different bed depths, flow rates and initial concentration.

N_0 value obtained by the model, can be compared with the adsorption capacity calculated by the Eq. (2) (**Table 3**) expressed as mg g^{-1} . The trend obtained is the same GF-40 (1616 mg g^{-1}) > MWCNT (420 mg g^{-1}) > HSAG-500 (57 mg g^{-1}), whereas the values present a deviation lower than 10% for AC and HSAG, and around 35% for MWCNT. As can be seen in **Fig. 2**, the model fits well for the first area of the breakthrough curve, but not close to the saturation.

3.2.2. Thomas model

Thomas model assumes a Langmuir isotherm for equilibrium and a rate driving force accepting a second-order reversible reaction kinetics [52]. It is used to calculate the maximum solid phase concentration of the solute on the adsorbent and the adsorption rate constant for a continuous adsorption process. It is one of the most general and widely used. The Thomas model allows calculating the adsorption capacity of an adsorbent, needed for design the adsorption process. The linearized form is given as:

$$\ln \left(\frac{C_0}{C - 1} \right) = \frac{k_{TH} q_0 m}{Q} - k_{TH} C_0 t \quad (6)$$

where m is the mass of the adsorbent (g) and Q is the flow rate (L min^{-1}). The values of the Thomas rate constant (k_{TH} , $\text{L min}^{-1} \text{mg}^{-1}$) and the maximum adsorption capacity (q_0 , mg g^{-1}) can be determined for plotting $\ln \left(\frac{C_0}{C - 1} \right)$ versus t .

The different parameters are summarized in Table 4 where it can be seen that the breakthrough curves fit well for Thomas model with a $r^2 > 0.92$ being higher for MWCNT. Values of q_0 here obtained follow the same trend than for BDST method, with differences lower than 2.5%. The adsorption capacity values obtained by this model were compared with the experimental capacity, observing an error lower than 10% for GF-40 and HSAG-500, whereas in the case of MWCNT, this value increases to 27%, suggesting differences in the adsorption behavior. For GF-40 and HSAG-500 these errors are less than obtained in literature by Dubey et al. [47] with deviations until 16% for the adsorption of ibuprofen, naproxen and clofibric acid onto mesoporous carbon. Oppositely, these values are lower than the obtained in this work for MWCNT. Comparing these results in terms of correlation coefficient with the results obtained by Yaghmaeian et al. [32] for the removal of amoxicillin by NH_4Cl -activated carbon, the r^2 is in general terms, slightly higher than the reported in this study.

Although both, BDST and Thomas models fit well to predict the adsorption capacity ($r^2 > 0.9$), Thomas presents the higher r^2 value for the different adsorbents and it can predicted properly the adsorption capacity, being the most preferred to predicted the breakthrough curves for the adsorption of NAL using the adsorbents selected.

3.2.3. Yoon-Nelson model

The Yoon-Nelson model considers that the rate of decrease in the probability of adsorption for the adsorbate molecule is proportional to the probability of both adsorbate adsorption and breakthrough on the adsorbent [53].

The model equation is expressed as:

$$\ln \left(\frac{C}{C_0 - C} \right) = k_{YN} t - \tau k_{YN} \quad (7)$$

where the values of Yoon-Nelson rate constant (k_{YN} , min^{-1}) and the time needed for 50% of adsorbate breakthrough (τ , min) were estimated by the slope and intercept of $\ln \left(\frac{C}{C_0 - C} \right)$ versus time.

The Yoon-Nelson model fits the experimental data with a value of $r^2 > 0.91$ as can be seen in Table 4, where the different parameters are summarized. The τ obtained by the model are very close to the theoretical – GF-40 (900 min), MWCNT (285 min) and HSAG-500 (40 min) – and the deviations obtained follow the next order: MWCNT (3.5%) < HSAG-500 (7.5%) < GF-40 (13%). This can be justified since the activated carbon presents the slowest adsorption kinetic with a better fit at the first part of the curve, having greater differences in the middle and saturation zones. The model deviation respect to the experimental data is lower than those observed in Yaghmaeian et al. [32] with deviation from 24% to 52% and from 6% to 18% for amoxicillin adsorption onto NH_4Cl activated carbon and standard activated carbon respectively.

These deviations are also in general lower than the obtained by Dubey et al. [47] (1.5–21%) for the adsorption of pharmaceutical by mesoporous carbon.

3.3. Column regeneration

The elution curves were obtained at two different temperatures, 35 and 40 °C (Figs. 3–5). The elution curves obtained, present an asymmetric shape, which has a strong decrease at first, followed by a slight decrease. The strong decrease is more pronounced for MWCNT, obtaining a maximum effluent concentration of 6.5 C/C_0 at the initial time, so most of the NAL desorption takes place in the first part of the desorption curve. Contrary, HSAG-500 has the maximum at C equal to C_0 , whereas for activated carbon, the obtained maximum is about twice the initial concentration, decreasing the concentration more slightly with the time. Likewise, the MWCNT is the only material where the final effluent concentration is negligible. Thus, although the adsorption mechanism is mainly due to the $\pi-\pi$ interactions, as it was previously indicated, and these interactions were especially important for MWCNT, this adsorption is demonstrated to be fully reversible. Contrary, in the case of HSAG-500, the C/C_0 never reaches the null value, indicating that some chemisorption process should occur on the edges of the graphite structures. For the case of GF-40, due to the microporosity, desorption involves the empty of the filled pores [54] and the chemisorbed species are not considered free to move from the adsorption sites [55].

Desorption studies were followed by two cycles of adsorption (Fig. 6). The adsorption capacity of the fixed bed decreases after the regeneration, especially for the GF-40. In the case of the mesoporous adsorbent, the irreversibility of the first adsorption due to the pore filling process avoids that the second cycle could reach the initial breakthrough curve obtaining a regenerability close to 30% (Fig. 7). In the case of HSAG-500, due to the mesoporous character of the material, only the edges of the flat layer of graphite could contain chemisorption adsorption sites, for this reason although the adsorption sites decrease, the regenerability is around the 65% (Fig. 7). For both, GF-40 and HSAG-500, no differences were observed for regeneration at 35 or 40 °C. Concerning MWCNT, the predominant interactions of NAL are due to $\pi-\pi$ interactions between the aromatic ring of the adsorbate and the rolled layers of the graphitic CNTs. But, interactions between the NAL and the edges of the rolled layers could not be completely discarded, thus these sites would be analogous to the chemisorption sites of HSAG-500. In this case, the regenerability is ≈60% (Fig. 7) and differences were obtained by varying the temperature of regeneration obtaining a 10% more of regenerability at 40 °C.

Another factor to take into account is the bed volumes (BV) needed for the regeneration since the concentration factor increases as decreases the bed volume required for regeneration (Fig. 7). The worst results were obtained with GF-40, for which, the regeneration BV is higher than the 160% of the adsorption BV due to the difficulty of desorbing from the micropores. The best results were obtained for MWCNT where the regeneration BV was lower than 70%. The concentration degree can be measured according to the ratio ($BV_{\text{adsorption}}/BV_{\text{desorption}}$). When this ratio is higher than one, a concentration process is taking place, which was only obtained for MWCNT with a ratio equal to 1.15 for regeneration at 35 °C and 2.0 at 40 °C at the experimental conditions. Therefore with a regeneration at the higher temperature an effluent is obtained at a concentration twice the initial. Contrary in the case of GF-40 and HSAG-500 the ratio ($BV_{\text{adsorption}}/BV_{\text{desorption}}$) is in the range of 0.49–0.55 for GF-40 and 0.46–0.47 in the case of HSAG-500 without major difference for both desorption temperatures. Otero et al. [41] studied the adsorption/desorption of salicylic acid onto activated carbon using

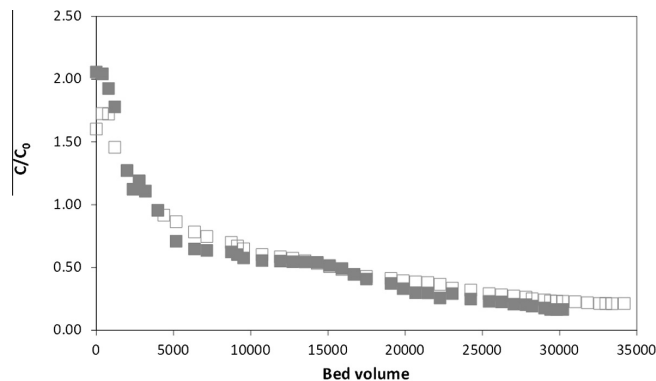


Fig. 3. Elution concentration profile for NAL column desorption by water using GF-40 as adsorbent at 35 °C (□) and 40 °C (■) with a volumetric flow rate of 1 mL/min.

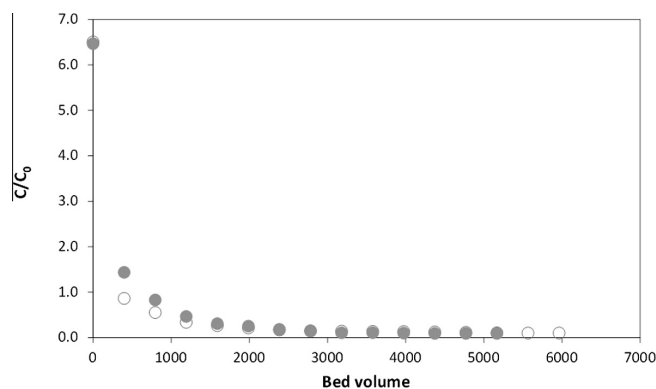


Fig. 4. Elution concentration profile for NAL column desorption by water using MWCNT as adsorbent at 35 °C (○) and 40 °C (●) with a volumetric flow rate of 1 mL/min.

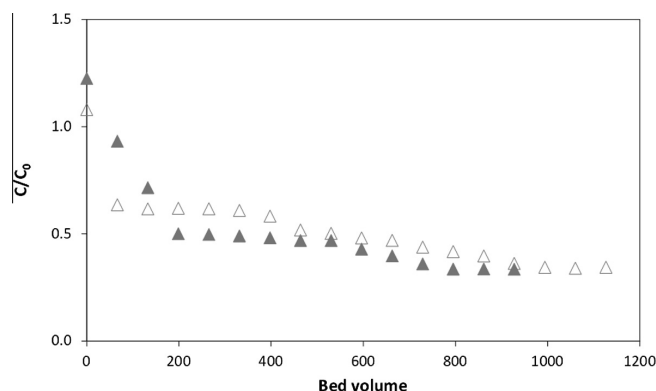


Fig. 5. Elution concentration profile for NAL column desorption by water using HSAG-500 as adsorbent at 35 °C (△) and 40 °C (▲) with a volumetric flow rate of 1 mL/min.

water for regeneration. The concentration factor obtained in this case was less than the obtained in this work (0.16–0.33). Besides this, the compound is different, the same temperature is used for adsorption and desorption so one of the two processes will be favored over the other according to the chosen temperature. Tian et al. [5] carried out desorption of two sulfonamide antibiotics onto CNT with a NaCl/NaOH solution. In this case, the concentration

factor obtained was less than one, so the concentration is not taking place contrary that the results obtained in this work with MWCNT.

Considering all results, although GF-40 presents the highest adsorption capacity, it presents the greatest loss of adsorption capacity after regeneration due to the irreversibility of the adsorption, for this reason it is not effective for pre-concentrate.

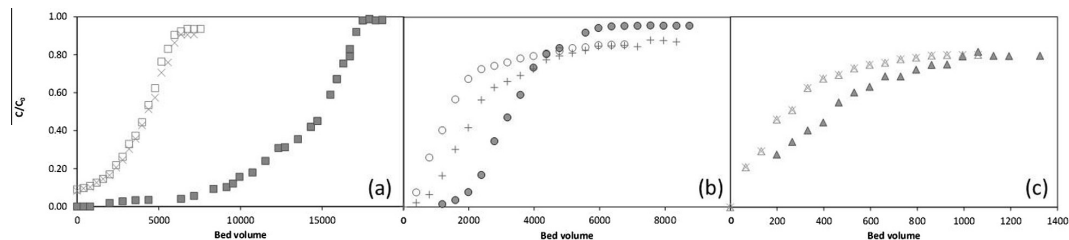


Fig. 6. Breakthrough curves for NAL column adsorption before and after regeneration on (a) GF-40, (b) MWCNT and (c) HSAG-500. Conditions: volumetric flow rate 1 mL/min and initial NAL concentration 80 ppm. First adsorption cycle (full symbol), second cycle after regeneration at 35 °C (empty symbol) and second cycle after regeneration at 40 °C (cross symbol).

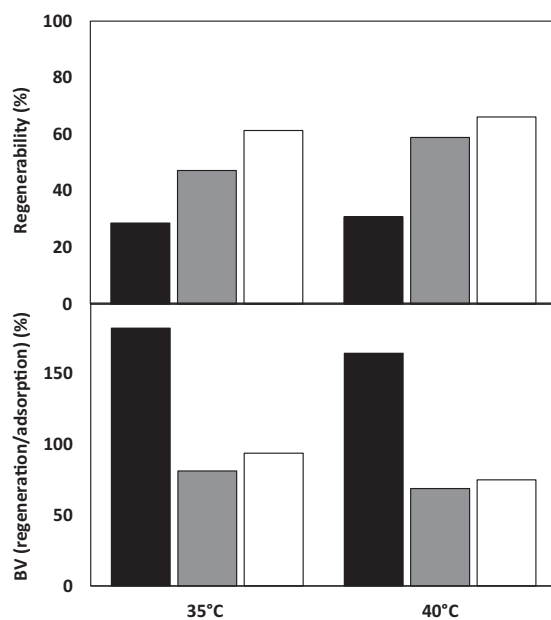


Fig. 7. Comparison column capacity after regeneration process at 35 and 40 °C in terms of regenerability and bed volume (BV) for GF-40 (black), MWCNT (gray) and HSAG-500 (white).

HSAG-500 is the worst adsorbent for NAL in water since it has a very low adsorption capacity, one and two order of magnitude lower than the others adsorbents and in the same way that the activated carbon it is not useful to obtain a more concentrated stream. Therefore, MWCNT is, among the studied materials, the best adsorbent for the adsorption and concentration of NAL, because it presents the highest normalized adsorption capacity, the highest desorption velocity and the lowest loss of adsorption capacity after the second adsorption cycle.

4. Conclusions

Adsorption of nalidixic acid on three different carbonaceous adsorbents, GF-40, MWCNT and HSAG-500, was tested in this work in a fixed bed, and the breakthrough curves were obtained, as well as the adsorption parameters. The adsorption capacity increases in the order HSAG-500 < MWCNT < GF-40. The normalized adsorption capacity at the breakthrough time follows the order MWCNT (2.10) > GF-40 (1.28) > HSAG-500 (0.17). Likewise, according to the MTZ value, the MWCNT is the material with the largest mass

transfer efficiency. This is attributed to the $\pi-\pi^*$ interactions between the curved graphene layers of the MWCNT and the aromatic ring of NAL.

Bed Depth Service Time (BDST), Thomas and Yoon-Nelson models were applied to the experimental data for the prediction of breakthrough curves. The three methods fitted with a correlation coefficient $r^2 > 0.9$, being especially accurate in the first part of the breakthrough curves. Likewise, in all the cases, the fit is better for GF-40 and MWCNT due to the fast adsorption kinetics.

Desorption experiments were performed using water at two different temperatures, performing a subsequent adsorption cycle. Adsorption capacity decreases after regeneration for the three materials. This decrease is more pronounced for the GF-40 where only 30% of regenerability was reached whereas MWCNT and HSAG-500 present a higher regenerability, 60% and 65%, respectively. After desorption cycle, a concentration factor equal to two is obtained with MWCNT while for both, GF-40 and HSAG this factor is less than one, not allowing NAL pre-concentration during the adsorption-desorption cycle.

Acknowledgments

This work was supported by the Spanish Government (contracts CTQ2011-29272-C04-02 and FC-15-GRUPIN14-078). Y. Patiño thanks the Government of the Principality of Asturias for a Ph.D. fellowship (Severo Ochoa Program).

References

- [1] D.W. Kolpin, E.T. Furlong, M.T. Meyer, E.M. Thurman, S.D. Zaugg, L.B. Barber, H.T. Buxton, Pharmaceuticals, hormones, and other organic wastewater contaminants in U.S. streams, 1999–2000: a national reconnaissance, *Environ. Sci. Technol.* 36 (2002) 1202–1211.
- [2] D. Barceló, M.J. López de Alda, Contaminación y calidad química del agua: el problema de los contaminantes emergentes. Instituto de Investigaciones Químicas y Ambientales-CSIC (Barcelona), 2008 <<http://www.unizar.es/fnca/varios/panel/15.pdf>> (Consultado: 8/12/2014).
- [3] E.R.E. Mojica, D.S. Aga, Antibiotics pollution in soil and water: potential ecological and human health issues, in: J.O. Nriagu (Ed.), *Encyclopedia of Environmental Health*, Elsevier, Burlington, 2011, pp. 97–110.
- [4] S. Park, K. Choi, Hazard assessment of commonly used agricultural antibiotics on aquatic ecosystems, *Ecotoxicology* 17 (2008) 526–538.
- [5] Y. Tian, B. Gao, V.L. Morales, H. Chen, Y. Wang, H. Li, Removal of sulfamethoxazole and sulfapyridine by carbon nanotubes in fixed-bed columns, *Chemosphere* 90 (2013) 2597–2605.
- [6] S. Schmid, J. Winter, C. Gallert, Long-term effects of antibiotics on the elimination of chemical oxygen demand, nitrification, and viable bacteria in laboratory-scale wastewater treatment plants, *Arch. Environ. Contam. Toxicol.* 63 (2012) 354–364.
- [7] G.Y. Leshner, E.J. Froelich, M.D. Gruett, J.H. Bailey, R.P. Brundage, 1,8-Naphthyridine derivatives. A new class of chemotherapeutic agents, *J. Med. Pharm. Chem.* 5 (1962) 1063–1065.
- [8] R. Gleckman, S. Alvarez, D.W. Joubert, S.J. Matthews, Drug therapy reviews: nalidixic acid, *Am. J. Hosp. Pharm.* 36 (1979) 1071–1076.
- [9] A.Y.-C. Lin, T.-H. Yu, C.-F. Lin, Pharmaceutical contamination in residential, industrial, and agricultural waste streams: risk to aqueous environments in Taiwan, *Chemosphere* 74 (2008) 131–141.

- [10] F. Tamtam, F. van Oort, B. Le Bot, T. Dinh, S. Mompelat, M. Chevreuil, I. Lamy, M. Thiry, Assessing the fate of antibiotic contaminants in metal contaminated soils four years after cessation of long-term waste water irrigation, *Sci. Total Environ.* 409 (2011) 540–547.
- [11] A.J. Watkinson, E.J. Murby, D.W. Kolpin, S.D. Costanzo, The occurrence of antibiotics in an urban watershed: from wastewater to drinking water, *Sci. Total Environ.* 407 (2009) 2711–2723.
- [12] R.E. Morrissey, S. Eustis, J.K. Haseman, J. Huff, J.R. Bucher, Toxicity and carcinogenicity studies of nalidixic acid in rodents, *Drug Chem. Toxicol.* 14 (1991) 45–66.
- [13] M. Carballa, F. Omil, J.M. Lema, M.A. Llopart, C. García-Járes, I. Rodríguez, M. Gómez, T. Ternes, Behavior of pharmaceuticals, cosmetics and hormones in a sewage treatment plant, *Water Res.* 38 (2004) 2918–2926.
- [14] S.K. Khetan, T.J. Collins, Human pharmaceuticals in the aquatic environment: a challenge to green chemistry, *Chem. Rev.* 107 (2007) 2319–2364.
- [15] B.A. Wilson, V.H. Smith, F. deNoyelles, C.K. Larive, Effects of three pharmaceutical and personal care products on natural freshwater algal assemblages, *Environ. Sci. Technol.* 37 (2003) 1713–1719.
- [16] X.-S. Miao, F. Bishay, M. Chen, C.D. Metcalfe, Occurrence of antimicrobials in the final effluents of wastewater treatment plants in Canada, *Environ. Sci. Technol.* 38 (2004) 3533–3541.
- [17] E.M. Golet, A.C. Alder, W. Giger, Environmental exposure and risk assessment of fluoroquinolone antibacterial agents in wastewater and river water of the Glatt Valley Watershed, Switzerland, *Environ. Sci. Technol.* 36 (2002) 3645–3651.
- [18] T.A. Ternes, M. Meisenheimer, D. McDowell, F. Sacher, H.-J. Brauch, B. Haist-Gulde, G. Preuss, U. Wilme, N. Zulei-Seibert, Removal of pharmaceuticals during drinking water treatment, *Environ. Sci. Technol.* 36 (2002) 3855–3863.
- [19] K. Kümmeler, The presence of pharmaceuticals in the environment due to human use – present knowledge and future challenges, *J. Environ. Manage.* 90 (2009) 2354–2366.
- [20] N. Dorival-García, A. Zafra-Gómez, A. Navalón, J. González-López, E. Hontrada, J.L. Vilchez, Removal and degradation characteristics of quinolone antibiotics in laboratory-scale activated sludge reactors under aerobic, nitrifying and anoxic conditions, *J. Environ. Manage.* 120 (2013) 75–83.
- [21] D. Bendz, N.A. Paxéus, T.R. Ginn, F.J. Loge, Occurrence and fate of pharmaceutically active compounds in the environment, a case study: Höje River in Sweden, *J. Hazard. Mater.* 122 (2005) 195–204.
- [22] M. Petrović, E. Eljarrat, M.J. López de Alida, D. Barceló, Analysis and environmental levels of endocrine-disrupting compounds in freshwater sediments, *TrAC 20* (2001) 637–648.
- [23] K. Kimura, S. Toshima, G. Amy, Y. Watanabe, Rejection of neutral endocrine disrupting compounds (EDCs) and pharmaceutical active compounds (PhACs) by RO membranes, *J. Membr. Sci.* 245 (2004) 71–78.
- [24] C. Adams, M. Asce, Y. Wang, K. Loftin, M. Meyer, Removal of antibiotics from surface and distilled water in conventional water treatment processes, *J. Environ. Eng.* 128 (2002) 253–259.
- [25] G. Moussavi, A. Alahabadi, K. Yaghmaeian, M. Eskandari, Preparation, characterization and adsorption potential of the NH4Cl-induced activated carbon for the removal of amoxicillin antibiotic from water, *Chem. Eng. J.* 217 (2013) 119–128.
- [26] R.F. Dantas, S. Contreras, C. Sans, S. Esplugas, Sulfamethoxazole abatement by means of ozonation, *J. Hazard. Mater.* 150 (2008) 790–794.
- [27] J. Rivera-Utrilla, G. Prados-Joya, M. Sánchez-Polo, M.A. Ferro-García, I. Bautista-Toledo, Removal of nitroimidazole antibiotics from aqueous solution by adsorption/biosorption on activated carbon, *J. Hazard. Mater.* 170 (2009) 298–305.
- [28] E.K. Putra, R. Pranowo, J. Sunarso, N. Indraswati, S. Ismadji, Performance of activated carbon and bentonite for adsorption of amoxicillin from wastewater: mechanisms, isotherms and kinetics, *Water Res.* 43 (2009) 2419–2430.
- [29] A.A. Ahmad, B.H. Hameed, Fixed-bed adsorption of reactive azo dye onto granular activated carbon prepared from waste, *J. Hazard. Mater.* 175 (2010) 298–303.
- [30] S.H. Kim, H.K. Shon, H.H. Ngo, Adsorption characteristics of antibiotics trimethoprim on powdered and granular activated carbon, *J. Ind. Eng. Chem.* 16 (2010) 344–349.
- [31] J.L. Sotelo, G. Ovejero, A. Rodríguez, S. Álvarez, J. García, Analysis and modeling of fixed bed column operations on flumequine removal onto activated carbon: pH influence and desorption studies, *Chem. Eng. J.* 228 (2013) 102–113.
- [32] K. Yaghmaeian, G. Moussavi, A. Alahabadi, Removal of amoxicillin from contaminated water using NH4Cl-activated carbon: continuous flow fixed-bed adsorption and catalytic ozonation regeneration, *Chem. Eng. J.* 236 (2014) 538–544.
- [33] L. Ji, F. Liu, Z. Xu, S. Zheng, D. Zhu, Zeolite-templated microporous carbon as a superior adsorbent for removal of monoaromatic compounds from aqueous solution, *Environ. Sci. Technol.* 43 (2009) 7870–7876.
- [34] X. Wang, Q. Li, J. Xie, Z. Jin, J. Wang, Y. Li, K. Jiang, S. Fan, Fabrication of ultralong and electrically uniform single-walled carbon nanotubes on clean substrates, *Nano Lett.* 9 (2009) 3137–3141.
- [35] W. Yang, Y. Lu, F. Zheng, X. Xue, N. Li, D. Liu, Adsorption behavior and mechanisms of norfloxacin onto porous resins and carbon nanotube, *Chem. Eng. J.* 179 (2012) 112–118.
- [36] L. Zhang, X. Song, X. Liu, L. Yang, F. Pan, J. Lv, Studies on the removal of tetracycline by multi-walled carbon nanotubes, *Chem. Eng. J.* 178 (2011) 26–33.
- [37] J. Goel, K. Kadivelu, C. Rajagopal, V. Kumar, Garg, Removal of lead(II) by adsorption using treated granular activated carbon: batch and column studies, *J. Hazard. Mater.* 125 (2005) 211–220.
- [38] K.S. Rao, S. Anand, P. Venkateswarlu, Modeling the kinetics of Cd(II) adsorption on *Syzygium cumini* L. leaf powder in a fixed bed mini column, *J. Ind. Eng. Chem.* 17 (2011) 174–181.
- [39] D.M. Nevskaia, A. Guerrero-Ruiz, Comparative study of the adsorption from aqueous solutions and the desorption of phenol and nonylphenol substrates on activated carbons, *J. Colloid Interface Sci.* 234 (2001) 316–321.
- [40] S.W. Nahm, W.G. Shim, Y.-K. Park, S.C. Kim, Thermal and chemical regeneration of spent activated carbon and its adsorption property for toluene, *Chem. Eng. J.* 210 (2012) 500–509.
- [41] M. Otero, M. Zabkova, C.A. Grande, A.E. Rodriguez, Fixed-bed adsorption os salicylic acid onto polymeric adsorbents and activated charcoal, *Ind. Eng. Chem. Res.* 44 (2005) 927–936.
- [42] Y. Patiño, E. Díaz, S. Ordóñez, Performance of different carbonaceous materials for emerging pollutants adsorption, *Chemosphere* 119 (Suppl.) (2015) S124–S130.
- [43] M. Basibuyuk, C.F. Forster, An examination of the adsorption characteristics of a basic dye (Maxilon Red BL-N) on to live activated sludge system, *Process Biochem.* 38 (2003) 1311–1316.
- [44] J. Ma, F. Yu, L. Zhou, L. Jin, M. Yang, J. Luan, Y. Tang, H. Fan, Z. Yuan, J. Chen, Enhanced adsorptive removal of methyl orange and methylene blue from aqueous solution by alkali-activated multiwalled carbon nanotubes, *ACS Appl. Mater. Interfaces* 4 (2012) 5749–5760.
- [45] F. Yu, J. Ma, S. Han, Adsorption of tetracycline from aqueous solutions onto multi-walled carbon nanotubes with different oxygen contents, *Sci. Rep.* 4 (2014).
- [46] M.L.G.M.G.A. Vieira, M.G.C.C. da Silva, Modeling of the process of adsorption of nickel in bentonite clay, *Chem. Eng. Trans.* 17 (2009) 421–426.
- [47] S.P. Dubey, A.D. Dwivedi, C. Lee, Y.-N. Kwon, M. Sillanpää, L.Q. Ma, Raspberry derived mesoporous carbon-tubules and fixed-bed adsorption of pharmaceutical drugs, *J. Ind. Eng. Chem.* 20 (2014) 1126–1132.
- [48] P. Liao, Z. Zhan, J. Dai, X. Wu, W. Zhang, K. Wang, S. Yuan, Adsorption of tetracycline and chloramphenicol in aqueous solutions by bamboo charcoal: a batch and fixed-bed column study, *Chem. Eng. J.* 228 (2013) 496–505.
- [49] P. Serp, M. Corrias, P. Kalck, Carbon nanotubes and nanofibers in catalysis, *Appl. Catal. A* 253 (2003) 337–358.
- [50] Y. Fan, B. Wang, S. Yuan, X. Wu, J. Chen, L. Wang, Adsorptive removal of chloramphenicol from wastewater by NaOH modified bamboo charcoal, *Bioresour. Technol.* 101 (2010) 7661–7664.
- [51] W.A. Cabrera-Lafaurie, F.R. Román, A.J. Hernández-Maldonado, Single and multi-component adsorption of salicylic acid, clofibric acid, carbamazepine and caffeine from water onto transition metal modified and partially calcined inorganic–organic pillared clay fixed beds, *J. Hazard. Mater.* 282 (2015) 174–182.
- [52] H.C. Thomas, Heterogeneous ion exchange in a flowing system, *J. Am. Chem. Soc.* 66 (1944) 1466–1464.
- [53] Y.H. Yoon, J.H. Nelson, Application of gas adsorption kinetics. I. A theoretical model for respirator cartridge service life, *Am. Ind. Hyg. Assoc. J.* 45 (1984) 509–516.
- [54] S.C.M.P. Somasundaran, X. Yu, S. Krishnakumar, *Handbook Of Surface and Colloid Chemistry*, Third Edition, Colloid Systems and Interfaces Stability of Dispersions through Polymer and Surfactant Adsorption, CRC Press, Boca Raton (FL), 2008.
- [55] T.X. Bui, H. Choi, Adsorptive removal of selected pharmaceuticals by mesoporous silica SBA-15, *J. Hazard. Mater.* 168 (2009) 602–608.

4.2.2. Publicación IV

**Pre-concentration of a polychlorinated n-alkane and an alkylphenol on
carbonaceous materials in fixed bed columns**

Autores: Y. Patiño, E. Díaz, S. Ordóñez

Enviada a:

Chemical Engineering Journal



Pre-concentration of a polychlorinated n-alkane and an alkylphenol on carbonaceous materials in fixed bed columns

Yolanda Patiño, Eva Díaz, Salvador Ordóñez*

Department of Chemical and Environmental Engineering, University of Oviedo, Faculty of Chemistry,
Julián Clavería s/n, 33006 Oviedo, Spain

E-mail: *sordonez@uniovi.es*, Tel: +34 985 103 437; Fax: +34 985 103 434

Abstract

Pre-concentration of emerging pollutants – endocrine disruptor and chlorinated paraffin – have been carried out by adsorption/desorption cycle onto carbonaceous materials – activated carbon (GF-40), multiwall carbon nanotube (MWCNT) and a high surface area graphite (HSAG-500) –. Desorption has been tested with water at two different temperatures (35 and 40 °C) in order to obtain an elution stream more concentrate than the starting. The breakthrough curves have been modeled by Bed Depth Service Time (BDST), Thomas and Yoon-Nelson models. The first two models can be used to predict the adsorption capacity and the last one to obtain the time requires for reach the 50% adsorbate breakthrough. Desorption process has been modeled following a first order kinetics. Normalized adsorption capacity, desorption efficiency and pre-concentration capacity are key parameters to obtain the best adsorbent. MWCNT presents for both, DCO and MPET the higher normalized adsorption capacity. Although GF-40 offers 100% of elution efficiency, no pre-concentration was obtained with this adsorbent. Contrary, pre-concentration was reached with MWCNT and HSAG-500, obtaining the best results for MWCNT, with a higher elution efficiency and a pre-concentration factor of 3.4 for DCO and 2.8 for MPET.

Keywords: alquilfenol etoxylate; chlorinated paraffin; fixed bed adsorption; pre-concentration; carbon materials; breakthrough curve

1. Introduction

Emerging pollutants (EPs) are synthetic or naturally occurring chemicals that are not commonly monitored in the environment but which have the potential to enter the environment and can cause adverse ecological and/or human health effects. Among these EPs, chlorinated paraffins (CPs) and endocrine disruptors (EDCs) are within the selected compounds by the U.S. Environmental Protection Agency (EPA) in its monitoring program of emerging pollutants, as they are considered substances which require priority actions and regulations. Although their origin and chemical properties are different, both families are a great risk for aquatic environmental and human health. Besides, these compounds are considered persistent, toxic and bioaccumulative [1, 2].

Chlorinated paraffin (CPs) are complex industrial formulations of polychlorinated n-alkanes (PCAs) used as additives in lubricants and cutting fluids for the metal working industry, in paints and sealants, as well as flame retardants in plastics [2-6]. Short Chain Chlorinated Paraffins (SCCPs) are the most dangerous CPs type, considered as possible carcinogenic compound to humans [5, 7].

EDCs are a wide kind of natural and synthetic chemicals, which interfere with the normal behaviour of the endocrine system [8, 9]. Within EDCs, the alkylphenols (APs) can be remarked for their riskiness and its common presence in wastewater effluents [8]. One of the most common AP is the Triton X-100 ($C_{14}H_{22}O(C_2H_4O)_n$).

Once the problematic of these pollutants is recognized, it is necessary to develop a methodology for their complete removal since conventional water treatment processes are rather ineffective [10-13]. It is important to note that these pollutants are presented in water at very low concentration ($ng \cdot L^{-1}$ to $\mu g \cdot L^{-1}$), so the amount of effluent to be treated to remove a large amount of pollutant it is very high, increasing the operation costs [14]. Therefore, a step of pre-concentration prior to destructive treatments is a good alternative. In this way, the technical feasibility of a pre-concentration approach based on adsorption-desorption cycle was demonstrated for a pharmaceutical EP, nalidixic acid (NAL). This work propose the use of fixed bed adsorption using three kinds of carbonaceous materials – activated carbon (GF-40), multiwall carbon nanotubes (MWCNT) and a high surface area graphite (HSAG-500) [15, 16]. From their performance in adsorption-desorption cycles, it was observed that the most promising material was the MWCNT, attributing this behavior to the influence of the p-p interaction between the graphene layers of the MWCNTs and the aromatic ring of the NAL. However, there is not in the literature any other work providing insights about the feasibility of this approach to other EPs.

The main aim of this work is to test this approach to model compounds resembling the behavior of CPs and EDCs. The two selected compounds, 1,8-dichlorooctane (DCO) and 2-(4-methylphenoxy)ethanol (MPET) were selected add to the different sources, because of the different chemical structure and lower molecular size than NAL. Likewise, from the discontinuous adsorption of these three emerging pollutants on carbon materials it was concluded that the capacity of adsorption of DCO was one order of magnitude larger than for NAL and MPET, being attributed to its hydrophobicity [18]. Thus, the continuous process should be studied in order to know the regenerability.

It should be also note that the implementation of these techniques requires the development of mathematical models for adsorption and desorption stages taking into account both adsorption equilibria, kinetics and mass transfer. At the same time, these parameters vary on the properties of both the adsorbate and the adsorbent. At this point, on three different carbonaceous materials – activated carbon (GF-40), multiwall carbon nanotube (MWCNT) and high surface area graphite (HSAG-500) –, whose discontinuous adsorption behaviour was previously studied [15], were considered. From the breakthrough curves different adsorption parameters were estimated, and the experimental results were fitted to different adsorption models: Bed depth service time (BDST), Thomas model and Yoon-Nelson model. The loss of the adsorption capacity after regeneration increasing the temperature is obtained by a second adsorption cycle.

Also in the case of chlorinated paraffins, there are numerous articles [5, 17-19] on the determination of chlorinated paraffin because it is difficult for being very complex mixtures, nevertheless the studies related to their adsorption are scarce.

2. Material and methods

2.1. Emerging pollutants.

Two different compounds have been used in this work: 1,8-dichlorooctane (DCO, Sigma-Aldrich, 98%) and 2-(4-methylphenoxy)ethanol (MPET, TCI Europe NV, 98%) and used in the experiments directly without any further purification. Their main properties are figured in Table 1.

Table 1. Main properties of adsorbates

Compound	1,8-dichlorooctane	2-(4-Methylphenoxy)ethanol
Symbol	DCO	MPET
Molecular volume (\AA^3) ^a	174.121	151.211
Log K_{ow} ^a	4.086	1.811
Water solubility ($\text{g}\cdot\text{L}^{-1}$) ^a	0.17 (293 K)	9.407 (298 K)

^aData obtained from <http://www.molinspiration.com>

2.2. Adsorbent materials.

Activated carbon (Norit, GF-40), multi wall carbon nanotubes (Dropsens, MWCNT) and high surface area graphite (Lonza, HSAG-500) have been used as adsorbents. Their textural parameters and chemical properties have been reported in a previous work [15]. For the experiments the adsorbent was dried at 100 °C at 24 h and a size fraction between 250-355 µm has been used, which has been previously optimized in order to obtain the maximum adsorption capacity [15].

2.3. Analytical technique.

Samples were analyzed by GC-MS in a calibrate Shimadzu GC/MS QP2010 Plus instrument, using a 30 m long TRB-5MS capillary column. The samples were, previous to the analysis, extracted in chloroform using a volume ratio (1:1).

2.4. Adsorption experiments.

A stainless steel column was used for the fixed bed adsorption under the same conditions as those used in a previous work, and for the same initial concentration (80 ppm). The samples of effluent were collected at intervals of 30 minutes for DCO and 5 minutes for MPET, and analyzed by GC-MS as stated in section 2.3 until the saturation was reached, when the effluent concentration is equal to the initial concentration or when the value is constant along the time.

2.5. Pre-concentration and regeneration of the saturated bed.

Pre-concentration takes place at the same time than the bed regeneration when the column saturation is reached. A water solution at two different temperatures – 35 and 40 °C – was passed through the bed in counter flow to normal adsorption, at the same conditions of flow. The analysis of the samples was developed in the same way as for adsorption until negligible or constant concentration.

2.6. Reusability of the adsorbent.

After regeneration of the column the adsorbent was reused in a second adsorption cycle under the same conditions in order to determine the reusability of the adsorbent.

3. Results and discussion

3.1. Fixed bed adsorption.

The obtained breakthrough curves of DCO and MPET adsorption are shown in Fig. 1. It is clear from this figure that the adsorption capacity of DCO is much greater than for MPET. The molecular volumes for both compounds are not so different, so the effect of the molecular size does not seem to be responsible of this difference. This behavior can be understood both by the highest octanol-water partition coefficient ($\log K_{ow}$) (Table 1) of DCO – indicating it is more hydrophobic than MPET-, and the lower DCO solubility than MPET. Thus, the presence of OH groups may produce an adverse effect on adsorption of MPET, because of the hydrogen bonds with the water molecule, making it less available to be absorbed onto the carbon materials[20]. The same trend has been observed by Sulaymon et al. [20], for the adsorption of furfural and phenolic compound onto activated carbons.

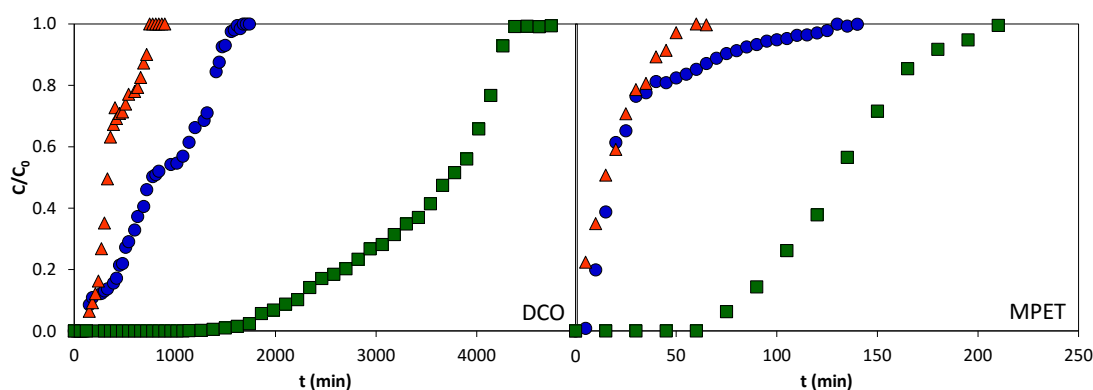


Figure 1. Breakthrough point curves for DCO and MPET adsorption onto (■) GF-40, (●) MWCNT and (▲) HSAG-500.

In both cases, the adsorption capacity of the different adsorbents follows the same order: GF-40 > MWCNT > HSAG-500, with the slope of the curve following the reverse order, as it was previously obtained for adsorption of nalidixic acid (NAL) under the same conditions [16]. The flattest profile corresponds to the microporous adsorbent (GF-40), which is indicative of a non-ideal transport within the pores, presenting the slowest adsorption kinetics [21]. The same relationship between the slope of the breakthrough curve and microporosity was obtained by Álvarez-Torrellas et al., [22] for the adsorption of two emerging pollutant onto carbonaceous materials. A lower slope is indicative of a slower mass transport due to a decreased diffusion coefficient or decreased mass transfer coefficient. The maximum adsorption capacity corresponds with the adsorbent with the highest S_{BET} [16]. However there is no a relationship between the adsorption capacity in the fixed bed and the S_{BET} for the other two adsorbents. In this case, the highest capacity of MWCNT may be due to the highest mesoporous volume [16],

more than three times the corresponding to HSAG-500 and eight times higher than the corresponding to GF-40. The same behaviour was obtained in the previous work for NAL [16]; in this case the adsorption in the micropores is further justified, since DCO and MPET have less molecular volume and the entrance and adsorption will be easier, especially for MPET. In the case of DCO, with an intermediate volume, more flat profile is observed, so steric hindrance effect can take place in the bed [22].

It should be pointed out that for MPET, HSAG-500 and MWCNT present the same adsorption profile until $C/C_0 \approx 0.8$, whereas the slope of the curve decreases dramatically for MWCNTs after this point, revealing the existence of two different adsorption processes. For the adsorption of benzene on CNTs, two different possibilities were already described, adsorption within CNTs (intra-adsorbate) and outside the nanotube cylinders. Gauden et al. [23] comparing the adsorption of benzene on both as received MWCNTs and opened MWCNTs by calorimetry observed that after opening the nanotube tips the adsorption at low relative pressure remains identical, whereas an enhancement was observed at higher values of relative pressure. Thus, up to $C/C_0 \approx 0.8$, adsorption on MWCNTs could be of similar nature than on the HSAG, which is formed by flat graphene layers. Over $C/C_0 \approx 0.8$, adsorption into the central canal could take place, but with a lower adsorption rate.

From the breakthrough curves the different adsorption parameters were estimated: adsorption capacities at breakthrough time (q_{bk}) and saturation time (q_s), length of the mass transfer zone (MTZ) and fractional bed utilization (FBU). These values are reported in Table 2. GF-40 presents the highest breakthrough and saturation time due to the contribution of microporosity in the adsorption, leading to a more unsharpened adsorption wave [22, 24].

The value of MTZ represents the zone where the mass transport takes place. The MTZ calculated is the maximum value that corresponds to the bed depth. As the mass transfer efficiency increases, this value leads to the ideal condition where MTZ is zero and the breakthrough curve corresponds with a step function [25, 26]. For DCO, this value is close to 1 in all cases, so the adsorption process takes place in each moment along the entire bed, away from the ideality. For MPET, the MTZ values are less than the total bed length and follows the order: GF-40 < MWCNT < HSAG-500. Concerning FBU, it relates the adsorption capacities at breakthrough and saturation time and it is inversely related to MTZ, so the highest values correspond to MPET, while DCO presents values close to zero.

Table 2. Adsorption parameters for DCO and MPET onto GF-40, MWCNT and HSAG-500.

	DCO			MPET		
	GF-40	MWCNT	HSAG-500	GF-40	MWCNT	HSAG-500
t_{bk} (min)	1800	200	66	54	10	2
t_s (min)	4380	1590	810	210	145	55
$q_{bk}(\text{mg g}^{-1}) = \frac{C_0 Q}{W} \int_0^{t_{bk}} \left(1 - \frac{C}{C_0}\right) dt$	117	114	103	87	15	3
$q_s(\text{mg g}^{-1}) = \frac{C_0 Q}{W} \int_0^{t_s} \left(1 - \frac{C}{C_0}\right) dt$	5533	1419	627	204	46	30
$MTZ = \left(1 - \frac{q_{bk}}{q_s}\right) L$	0.99	0.98	0.96	0.57	0.68	0.90
$FBU = \frac{q_{bk}}{q_s}$	0.015	0.018	0.037	0.43	0.32	0.10
$q_s/\text{area (mg m}^{-2}\text{)}$	4.4	5.1	1.1	0.16	0.16	0.05

C and C_0 are the effluent and inlet concentration (mg L^{-1})

Q is the volumetric flow rate (L h^{-1})

W is the mass of adsorbent (g)

t_s and t_{bk} are the saturation and breakthrough times respectively (h)

L is the bed length (cm)

Due to the importance of the adsorbent morphology and surface, it is more important the normalized adsorption capacity (q_s/area) to compare the maximum adsorption capacity of the three adsorbents. For DCO this ratio follow the order MWCNT > GF-40 >> HSAG-500, while for MPET the order is MWCNT = GF-40 > HSAG-500. The highest normalized adsorption capacity corresponds to MWCNT, which presents the highest mesoporous volume, trend not followed by the other two adsorbents. DCO normalized adsorption capacity has greater difference between the MWCNT and the other two adsorbents, which may be due to the CH- π interaction between the carbonaceous linear chain of DCO and the aromatic ring of MWCNT [27]. Due to its nature, CH- π interactions are mainly contributed by the dispersive interactions, and, although the CH- π interaction is quite weak ($1.82 \text{ kcal}\cdot\text{mol}^{-1}$), its effect can be additive [28]. So for a carbonaceous linear structure as DCO its influence can be pronounced with a final strength of $14.56 \text{ kcal}\cdot\text{mol}^{-1}$ for each DCO molecule. Besides, linear structure of DCO, allows it to enter more easily into the gaps generated in the nanotubes and between the different layers, increasing the probability of CH- π interaction.

The results here obtained for MPET are in good agreement with other observations previously reported in the literature. Choi et al., [29] for the nonylphenol adsorption onto activated carbons with similar S_{BET} , but with a higher V_{meso} , obtained normalized adsorption capacities in the interval: $0.008\text{-}0.15 \text{ mg}\cdot\text{m}^{-2}$. On the other hand, Vidal et. al., [30] in a study of the adsorption of endocrine disruptors onto nanoporous adsorbents, obtained normalized adsorption capacities from $0.12 \text{ mg}\cdot\text{m}^{-2}$ until $0.43 \text{ mg}\cdot\text{m}^{-2}$. These values are a bit higher than those obtained in this work, which can be due to the ability of the molecules under study to be introduced in the nanopores.

3.2. Application of breakthrough curve models.

It is important for the design of fixed bed columns to predict the behavior of breakthrough adsorption parameters, especially for continuous treatment in industrial plants. For this purpose three different adsorption models have been tested (Figures 2 and 3 and Table 3).

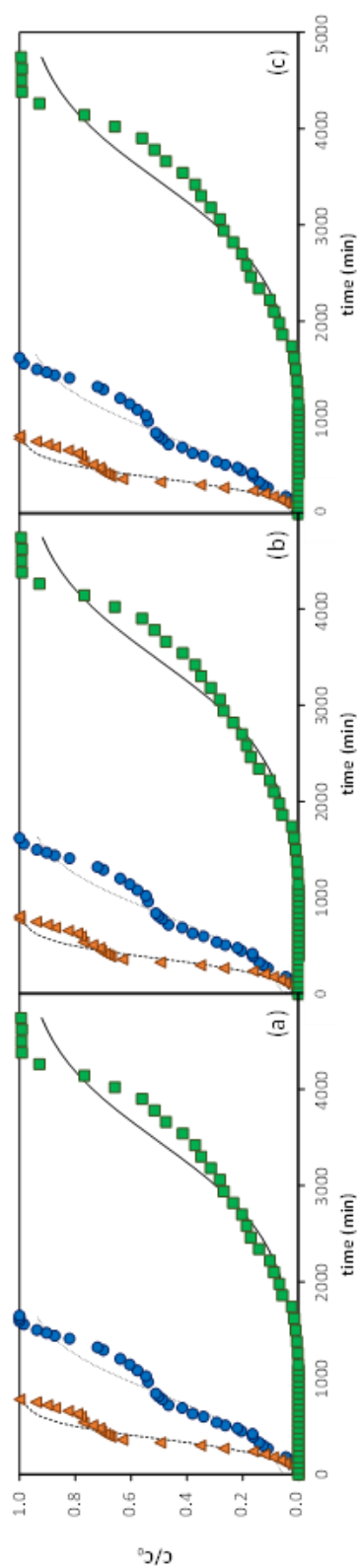


Figure 2. Experimental and predicted breakthrough curves for DCO removal based on BDST (a), Thomas (b) and Yoon-Nelson (c) models, for the adsorption onto (■) GF-40, (●) MWCNT and (▲) HSAG-500.

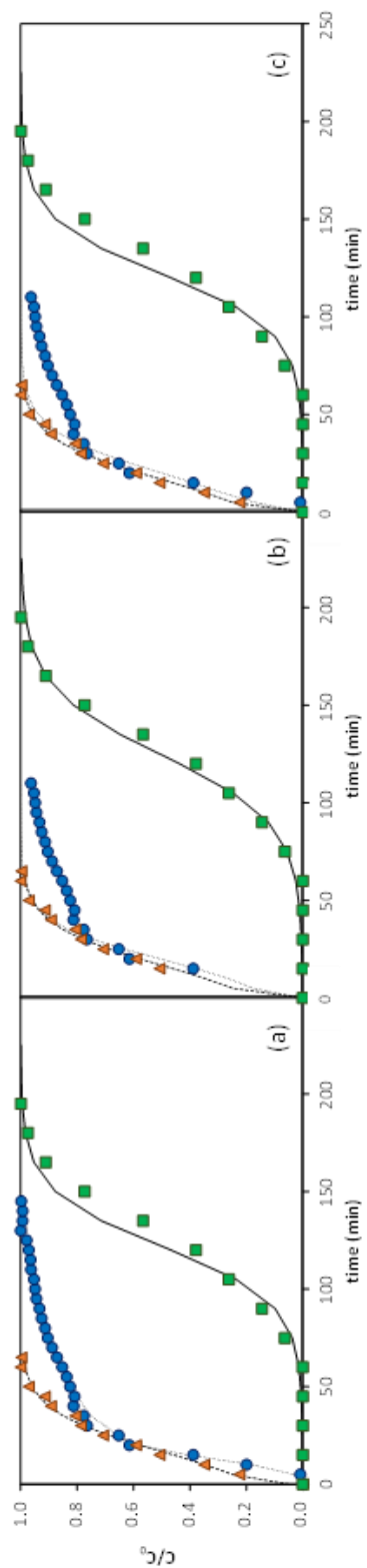


Figure 3. Experimental and predicted breakthrough curves for MPET removal based on BDST (a), Thomas (b) and Yoon-Nelson (c) models, for the adsorption onto (■) GF-40, (●) MWCNT and (▲) HSAG-500.

Table 3. Predicted parameters for BDST, Thomas and Yoon-Nelson models for DCO and MPET adsorption on carbonaceous materials.

		BDST				Thomas				Yoon-Nelson			
		$k_{AB} \times 10^4$ (L·mg ⁻¹ ·min ⁻¹)	N_0 (mg·L ⁻¹)	Q_0 (mg·g ⁻¹)	r^2	$k_{TH} \times 10^4$ (L·min ⁻¹ ·mg ⁻¹)	Q_0 (mg·g ⁻¹)	r^2	$K_{YN} \times 10^2$ (min ⁻¹)	τ (min)	r^2		
DCO	GF-40	0.18	3690000	5532	0.91	0.19	5595	0.91	0.19	3453	0.91		
	MWCNT	0.38	942154	1410	0.94	0.38	1423	0.94	0.34	840	0.94		
	HSAG-500	1.41	392253	581	0.92	1.34	591	0.92	1.07	370	0.92		
MPET	GF-40	7.9	143100	214	0.98	0.65	220	0.98	6.97	122	0.92		
	MWCNT	9.1	27020	40	0.94	13.41	37	0.90	9.06	20	0.90		
	HSAG-500	13	18160	27	0.97	13.57	27	0.97	9.44	17	0.97		
1													

3.2.1. Bed depth service time (BDST) model.

This model is used to describe the initial part of the breakthrough curve [31, 32]. The relation between service time and bed depth is as follows:

$$t = \frac{N_0}{C_0 \cdot U} Z - \frac{1}{C_0 \cdot K_{AB}} \ln \left(\frac{C_0}{C_t} - 1 \right) \quad \text{Ec. 1}$$

where C_0 and C_t are the inlet and effluent concentration of adsorbate ($\text{mg} \cdot \text{L}^{-1}$), N_0 is the dynamic adsorption capacity of the bed ($\text{mg} \cdot \text{L}^{-1}$), Z is the column length (cm), K_{AB} is the adsorption rate constant ($\text{L} \cdot \text{mg}^{-1} \cdot \text{min}^{-1}$) and t is the service time at breakthrough (min). N_0 and K_{AB} were obtained from the intercept and slope of the plot between $\ln \left(\frac{C_0}{C_t} - 1 \right)$ versus t . The obtained parameters are shown in Table 3 and for both compounds the model fit well, with $r^2 > 0.90$. N_0 , expressed in $\text{mg} \cdot \text{g}^{-1}$ (Q_0) can be compared to the adsorption capacity obtained in the previous section (Table 2 and 3). The values follow the same order for both compounds: GF-40 > MWCNT > HSAG-500, and the adsorption capacity value can be predict with a deviation lower than 8%, except in the case of the adsorption of MPET onto MWCNT, for which the deviation increase to 13%. The breakthrough curve predicted by the model for MPET, fits over the entire curve, contrary, for DCO, the model fit well into the first zone of the curve, with grater deviation in the saturation zone.

3.2.2. Thomas model.

This model is used to describe the adsorption kinetics and the maximum adsorption capacity (q_0). It is defined by the following equation:

$$\ln \left(\frac{C_0}{C_{t-1}} \right) = \frac{k_{TH} \cdot q_0 \cdot m}{Q} - k_{TH} \cdot C_0 \cdot t \quad \text{Ec. 2}$$

where k_{TH} is the Thomas rate constant ($\text{L} \cdot \text{min}^{-1} \cdot \text{mg}^{-1}$), m is the mass of adsorbent in the column (g) and Q is the volumetric flow rate ($\text{L} \cdot \text{min}^{-1}$).

The model assumed the Langmuir isotherm for equilibrium [25] and it is suitable for adsorption processes where the external and internal diffusion limitations are absent. It must take into account that application of this model leads to an error in adsorption processes [25, 33] with first order reaction kinetics.

Thomas model parameters were obtained by slop and intercept of $\ln \left(\frac{C_0}{C_{t-1}} \right)$ versus t . The result obtained are showed in Table 3. The Thomas model fit well with coefficients regression higher than 0.90. The values predicted by Thomas model for the maximum adsorption capacity of DCO are similar than the obtained by BDST model, with deviations less than 6%. Contrary, the

deviation to predict the value of the MPET adsorption capacity is slightly higher, less than 10% for GF-40 and HSAG-500, but it increases to 20% for MWCNT.

3.2.3. Yoon-Nelson model.

This model assumes that the rate of decrease in the probability of adsorption for each adsorbate molecule was proportional to the probability of adsorbate adsorption and the probability of adsorbate breakthrough on the adsorbent [25, 34]. The Yoon-Nelson equation is expressed as:

$$\ln\left(\frac{C_0}{C_0 - C_t}\right) = k_{YN} \cdot t - \tau \cdot k_{YN} \quad \text{Ec. 3}$$

where k_{YN} is the Yoon-Nelson rate constant (min^{-1}) and τ is the time required for reaching the 50% adsorbate breakthrough (min). The values k_{YN} and τ can be determined from slope and intercept of the plot of $\ln\left(\frac{C_0}{C_0 - C_t}\right)$ versus t . As seen in Table 3, the model could be well fitted, and the results also indicate that k_{YN} increases with decreases τ . The times needed for 50% adsorbate breakthrough from the experiments (Fig. 2 and 3) are close to the obtained by the model. The τ (min) obtained for DCO by the model presents deviations less than 6% comparing with the experimental data - GF-40 (3700), MWCNT (850) and HSAG-500 (325) - In the case of MPET the deviation obtained is less than 11% taking into account the following experimental values obtained: GF-40 (130), MWCNT (18) and HSAG-500 (16). The deviations are similar than the obtained in a previous work for NAL adsorption onto the same adsorbents [16]. Also, the variation between the model and experimental data, are similar than the obtained by Sotelo et al.,[25] (in most cases < 12%) for the adsorption of atenolol and isoproturon onto activated carbon. Contrary, Yaghmaeian et al., [35] obtained deviation around 24 – 52% for the adsorption of amoxicillin.

Both BDST and Thomas models can be used to predict the DCO and MPET adsorption capacities onto GF-40, MWCNT and HSAG-500. The capacity values predicted by BDST model are closer to the experimental data than those obtained by Thomas model (Tables 2 and 3). So, although both models can be used to predict the adsorption capacity, in this case is most recommendable BDST model. On the other hand, Yoon-Nelson model fits perfectly with the experimental data and allows the calculation of 50% adsorbate breakthrough.

3.3. Pre-concentration capacity and desorption studies.

The main goal of this study is to concentrate the pollutant, therefore, it was carried out desorption with water at two different temperatures -35 and 40 °C- to increase effluent concentration after desorption, comparing with the initial concentration. The obtained elution curves are depicted in Figs. 4 and 5.

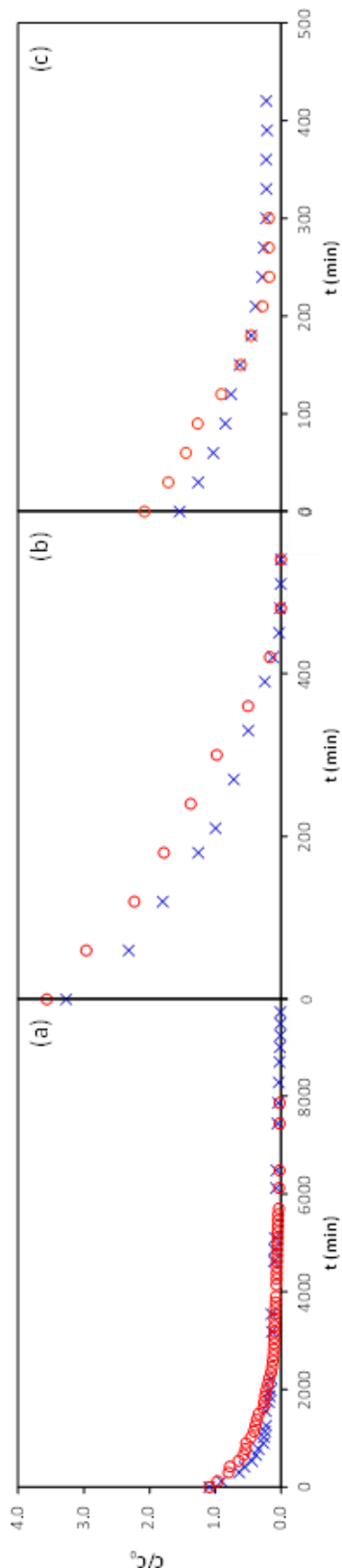


Figure 4. Elution profile for DCO desorption using water at 35 °C (x) and 40 °C (o) for the three adsorbents: GF-40 (a), MWCNT (b) and HSAG-500 (c)

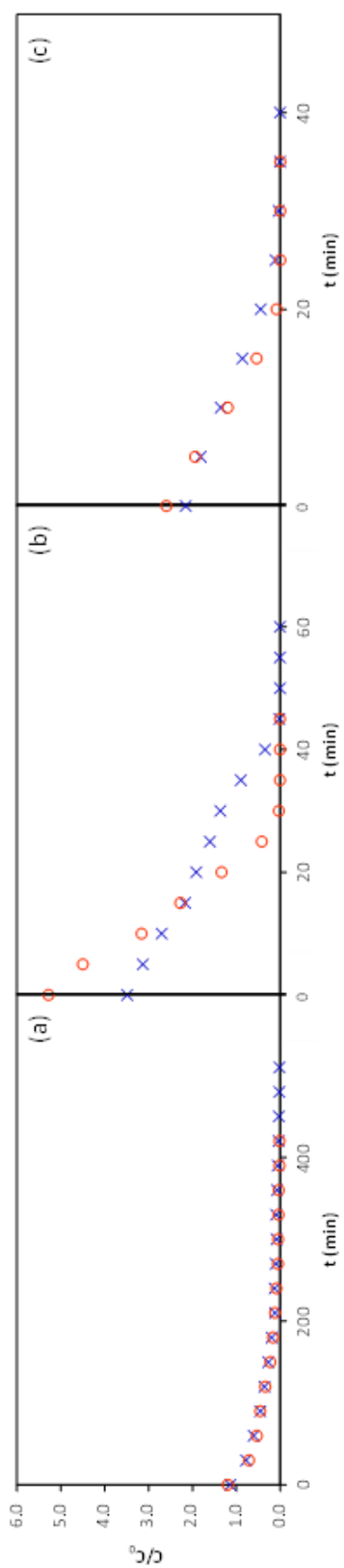


Figure 5. Elution profile for MPET desorption using water at 35 °C (x) and 40 °C (o) for the three adsorbents: (a) GF-40, (b) MWCNT and (c) HSAG-500.

The elution curve for both, DCO and MPET, presents the same profile, an initial zone at constant decrease in concentration follow by a zone with lower variation in the output concentration until it reaches a value practically negligible. Typical profiles have been obtained, similar to those obtained by other authors in elution of emerging contaminants employing analogous adsorbents [16, 21, 22].

Elution parameters have been obtained through the elution curve (Table 4). The relation between the mass desorbed (m_d) and the mass adsorbed (m_a), is the elution/desorption efficiency, calculated by the following equation:

$$E (\%) = \frac{m_d}{m_a} \cdot 100 \quad \text{Ec. 4}$$

Where m_d and m_a are calculated from numerical integration of the regeneration and adsorption curves from $t = 0$ to $t = t_d$ (time needed for desorption) and $t = t_s$ respectively.

Table 4. Elution parameters for DCO and MPET removal onto carbonaceous materials.

		E (%)		BV_a/BV_d		C_F	
		35 °C	40 °C	35 °C	40 °C	35 °C	40 °C
DCO	GF-40	100	100	0.5	0.6	162	130
	MWCNT	70	93	2.9	3.4	27	23
	HSAG-500	54	60	2	2.9	41	28
MPET	GF-40	100	100	0.4	0.5	205	158
	MWCNT	75	97	2.3	2.8	34	28
	HSAG-500	62	70	1.5	1.8	54	44

The elution efficiency increases for both DCO and MPET in the order: HSAG-500 < MWCNT < GF-40, and also it increases with increasing desorption temperature (Table 4). The effectiveness of desorption increases with the temperature around 20% for MWCNT and 10% for HSAG-500. The more important effect on the MWCNTs could be attributed to the more easy removal of the adsorbate within the CNT.

The most important factor to determine the concentration capacity is the ratio between the bed volumes required for the adsorption and desorption (BV_a/BV_d) (Table 4). This parameter give us the pollutant concentration obtained after desorption, and it is related to the final average concentration: C_F (Table 4).

Regarding the adsorbates, the pre-concentration is higher for DCO, compound for which the adsorption capacity is also more relevant. The high time required for MPET elution is probably due to its strong $\pi-\pi$ interactions with the carbon materials, makes more difficult its desorption, requiring more time to be desorbed implying a lower pollutant concentration [21, 36].

The trend for the (BV_a/BV_d) ratio is the same for both DCO and MPET: MWCNT > HSAG-500 > GF-40. Activated carbon not only presents the worst result, besides, the value obtained is less than one, so that, there is not pollutant concentration. Due to the large microporosity of GF-40, the molecules adsorbed inside the micropores could present more difficulties to be desorbed [37]. For both, MWCNT and HSAG-500 pre-concentration is achieved. Comparing these results here obtained for MPET and DCO preconcentration with the obtained in a previous work for NAL under the same conditions, the concentration factors obtained for DCO and MPET are higher than the obtained for NAL (2.0 for MWCNT after regeneration at 40 °C) [16]. The main interaction between NAL and the different adsorbents is by π - π interaction of the two benzene rings with the carbon materials [16], thus it could be stronger than even for MPET with just one ring.

Taking into account the different parameters obtained, MWCNT is presented as the best absorbent for the concentration of these contaminants. It not only has the highest normalized adsorption capacity, but it also achieves the highest pollutant concentration. Besides the desorption efficiency is higher than 90%, and close to 100% in the case of MPET, so the losses of adsorbent into the column are minimal. It is important to note at this point that studies about the concentration of these pollutants by adsorption on carbonaceous materials have not been obtained in the literature.

Taking into account that desorption process takes places by mass transfer from the adsorbent to the liquid, it can be considered that the process follows a first-order kinetic, according to the equation:

$$\ln \frac{C}{C_{d_0}} = -k_{des} \cdot t \quad \text{Ec. 5}$$

where C and C_{d_0} are the concentration with the time and the concentration at $t=0$ ($\text{mg}\cdot\text{L}^{-1}$), k_{des} is the desorption kinetic constant (min^{-1}) and t is the desorption time (min). From the slope of $\ln \frac{C}{C_{eq}}$ versus t, the k_{des} can be obtained. The obtained results are showed in Table 5.

Table 5. Desorption kinetic constant for DCO and MPET at two different temperatures

	DCO				MPET			
	35°C		40°C		35°C		40°C	
	k_{des} (min^{-1})	r^2						
GF-40	0.0015	0.984	0.0008	0.993	0.009	0.977	0.010	0.989
MWCNT	0.0056	0.997	0.0046	0.943	0.031	0.992	0.061	0.951
HSAG-500	0.0065	0.993	0.0076	0.955	0.055	0.945	0.093	0.939

It is remarkable that the k_{des} for MWCNT and HSAG-500 is higher for MPET than for DCO. As it was mentioned above, MPET presents the highest solubility in water, making easier its transfer to the aqueous phase in the desorption process. In the case of GF-40, desorption kinetics is similar for both compounds, suggesting that materials microporosity hinders both desorption process in a similar way.

3.4. Bed recycling.

After the elution process is important to determine the bed capacity for a second adsorption cycle. The change of column capacity in terms of regenerability is showed in Fig. 7 and 8. From these plots, it is concluded that, in general terms, column capacity decreases after reuse. It could be due to a reduction in the available adsorption sites or/and repulsion by the irreversible adsorbed compound in the first cycle [38]. It is important to note that MWCNT presents the lowest reduction in the adsorption capacity, followed by HSAG-500 and GF-40. Even for MPET, the bed regeneration with MWCNT is higher than 90% being minimal the reduction in the adsorption capacity. In the case of HSAG-500, a small part of the compounds are chemisorbed on the edges of the flat layer of graphite, so that regenerability is lower than for MWCNT for both, DCO and MPET [16]. The behavior for GF-40 is a little bit different. Desorption efficiency was equal to 100%, but the regenerability is lower than 50%. Although the adsorbent is free of adsorbate and ready for a second adsorption cycle, the adsorption sites have changed after desorption process, diminishing the concentration of adsorption sites or being these sites less accessible for a new adsorption. That is why GF-40 presents the greatest loss of adsorption capacity after regeneration.

Concerning the effect of temperature, no differences were observed for GF-40. The maximum efficiency was obtained at the lowest temperature, so the desorption efficiency cannot be improved by increasing desorption temperature. Contrary, in the case of MWCNT and HSAG-500 the regenerability and desorption efficiency are higher after elution at 40 °C, for both DCO and MPET. With increasing elution temperature, desorption of the physisorbed fraction increases, so that the efficiency improves and there are more available sites to a second desorption cycle.

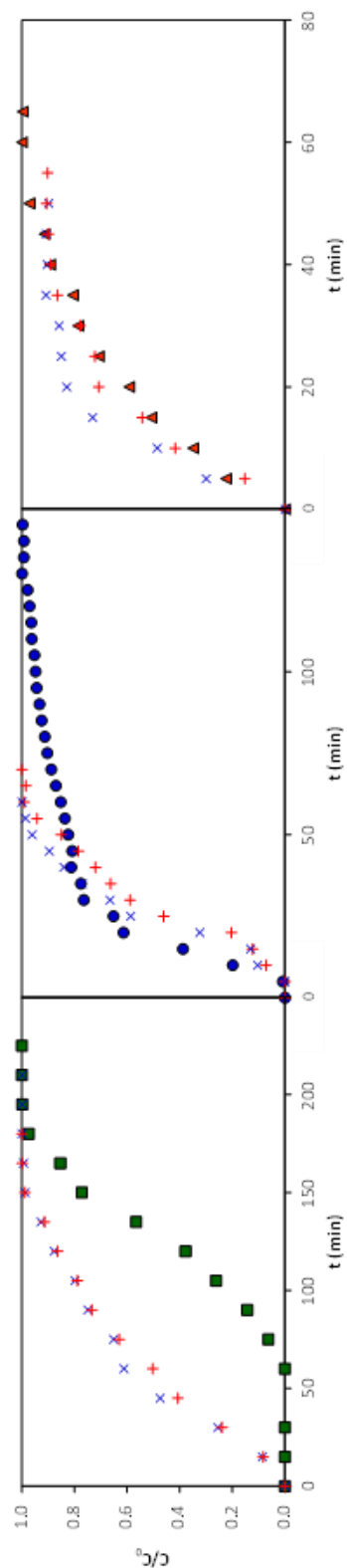


Figure 7. Breakthrough curves for MPET adsorption before and after regeneration with water at 35 °C (x) and 40 °C (+) for the three adsorbents: (■) GF-40 , (●) MWCNT and (▲) HSAG-500.

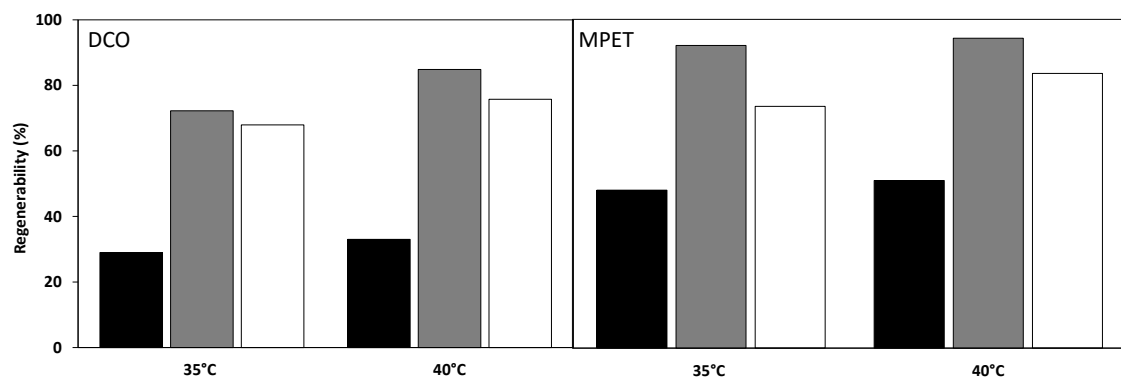


Figure 8. Adsorbent regeneration after desorption with water at 35 and 40 °C for both DCO and MPET using GF-40 (black), MWCNT (grey) and HSAG-500 (white)

4. Conclusions

DCO and MPET pre-concentration have been studied by adsorption-desorption cycles under different adsorbents: activated carbon (GF-40), multiwall carbon nanotubes (MWCNT) and high surface area graphite (HSAG-500).

The adsorption capacity of DCO is much higher than for MPET, due to its higher hydrophobicity. Besides, the –OH groups of MPET may form hydrogen bonding with the water making it less available to be absorbed onto the carbon materials. Regarding to the adsorbent, the normalized adsorption capacity (q_s/area) follows the order MWCNT > GF-40 > HSAG-500, where the highest adsorption capacity of MWCNT may be due to the higher mesoporous volume.

BDST and Thomas models fit well for the experimental data and both of them can be used to predict the adsorption capacities, with a less deviation by BDST model. Yoon-Nelson model predicts correctly the time needed for 50% of adsorbate breakthrough.

Desorption efficiency is favored at high temperatures, follows the order: GF-40 > MWCNT > HSAG-500, but no pre-concentration was obtained in the case of GF-40 after the elution process. However, pre-concentration was reached for the other two adsorbents follow the order: MWCNT > HSAG-500 for both DCO and MPET. Besides MWCNT presents the higher regenerability.

MWCNT are presented as the best adsorbent for both adsorbates taking into account its higher normalized adsorption capacity and the concentration factor obtained – 3.4 for DCO and 2.8 for MPET –.

Acknowledgements

This work was supported by the Spanish Government (contracts CTQ2011-29272-C04-02 and FC-15-GRUPIN14-078). Y. Patiño thanks the Government of the Principality of Asturias for a Ph.D. fellowship (Severo Ochoa Program).

References

- [1] J.R. Madeley, R.S. Thomson, D. Brown, The Bioconcentration of a Chlorinated Paraffin by the Common Mussel (*Mytilus edulis*), Imperial Chemical Industries PLC, Devon, UK, 1983, BL / B / 2531.
- [2] S. Bayen, J.P. Obbard, G.O. Thomas, Chlorinated paraffins: A review of analysis and environmental occurrence, *Environ. Int.* 32 (2006) 915-929.
- [3] Chlorinated Paraffins Industry Association (CPIA). Chlorinated paraffins: A status report. 2009; http://www.regnet.com/czia/status_report.html. December 2015.
- [4] G.T. Tomy, A.T. Fisk, J.B. Westmore, D.C.G. Muir, Environmental chemistry and toxicology of polychlorinated n-alkanes, *Rev. Environ. Contam. Toxicol.* 158 (1998) 53-128.
- [5] P. Castells, F.J. Santos, M.T. Galceran, Solid-phase microextraction for the analysis of short-chain chlorinated paraffins in water samples, *J. Chromatogr. A* 984 (2003) 1-8.
- [6] A.B. Mukherjee, The use of chlorinated paraffins and their possible effects in the environment, National board of waters and the environment, Helsinki, Finland, 1990.
- [7] Chlorinated Paraffins. Environmental and Risk Assessment, RM1 De-cision Package, US Environmental Protection Agency (EPA), Office of Toxic Substances, Washington, DC, 1991
- [8] V. Belgiorno, L. Rizzo, D. Fatta, C. Della Rocca, G. Lofrano, A. Nikolaou, V. Naddeo, S. Meric, Review on endocrine disrupting-emerging compounds in urban wastewater: occurrence and removal by photocatalysis and ultrasonic irradiation for wastewater reuse, *Desalination* 215 (2007) 166-176.
- [9] T. Tsuda, A. Takino, M. Kojima, H. Harada, K. Muraki, Gas chromatographic-mass spectrometric determination of 4-nonylphenols and 4-tert-octylphenol in biological samples, *J.Chromatogr. B: Biomed. Sci. and Appl.* 723 (1999) 273-279.

- [10] T.A. Ternes, M. Meisenheimer, D. McDowell, F. Sacher, H.J. Brauch, B. Haist-Gulde, G. Preuss, U. Wilme, N. Zulei-Seibert, Removal of pharmaceuticals during drinking water treatment, Environ. Sci. Technol. 36 (2002) 3855-3863.
- [11] S.A. Snyder, S. Adham, A.M. Redding, F.S. Cannon, J. DeCarolis, J. Oppenheimer, E.C. Wert, Y. Yoon, Role of membranes and activated carbon in the removal of endocrine disruptors and pharmaceuticals, Desalination 202 (2007) 156-181.
- [12] R. Broséus, S. Vincent, K. Aboufadel, A. Daneshvar, S. Sauvé, B. Barbeau, M. Prévost, Ozone oxidation of pharmaceuticals, endocrine disruptors and pesticides during drinking water treatment, Water Res. 43 (2009) 4707-4717.
- [13] F.J. Beltrán, A. Aguinaco, J.F. García-Araya, A. Oropesa, Ozone and photocatalytic processes to remove the antibiotic sulfamethoxazole from water, Water Res. 42 (2008) 3799-3808.
- [14] C.G. Daughton, T.A. Ternes, Pharmaceuticals and personal care products in the environment: agents of subtle change. Environ. Health Perspect. 107 Suppl (1999), pp. 907-938.
- [15] Y. Patiño, E. Díaz, S. Ordóñez, Performance of different carbonaceous materials for emerging pollutants adsorption, Chemosphere 119, Supplement (2015) S124-S130.
- [16] Y. Patiño, E. Díaz, S. Ordóñez, Pre-concentration of nalidixic acid through adsorption-desorption cycles: Adsorbent selection and modeling, Chem. Eng. J. 283 (2016) 486-494.
- [17] Z. Zencak, A. Borgen, M. Reth, M. Oehme, Evaluation of four mass spectrometric methods for the gas chromatographic analysis of polychlorinated n-alkanes, J. Chromatogr. A 1067 (2005) 295-301.
- [18] F. Pellizzato, M. Ricci, A. Held, H. Emons, W. Böhmer, S. Geiss, S. Iozza, S. Mais, M. Petersen, P. Lepom, Laboratory intercomparison study on the analysis of short-chain chlorinated paraffins in an extract of industrial soil, Trends in Analyt. Chem. 28 (2009) 1029-1035.
- [19] M.-L. Nilsson, S. Bengtsson, H. Kylin, Identification and determination of chlorinated paraffins using multivariate evaluation of gas chromatographic data, Environ. Pollut. 163 (2012) 142-148.
- [20] A.H. Sulaymon, K.W. Ahmed, Competitive Adsorption of Furfural and Phenolic Compounds onto Activated Carbon in Fixed Bed Column, Environ. Sc. Technol. 42 (2008) 392-397.
- [21] J.L. Sotelo, G. Ovejero, A. Rodríguez, S. Álvarez, J. García, Analysis and modeling of fixed bed column operations on flumequine removal onto activated carbon: pH influence and desorption studies, Chem. Eng. J. 228 (2013) 102-113.

- [22] S. Álvarez-Torrellas, A. Rodríguez, G. Ovejero, J. García, Comparative adsorption performance of ibuprofen and tetracycline from aqueous solution by carbonaceous materials, *Chem. Eng. J.* 283 (2016) 936-947.
- [23] P.A. Gauden, A.P. Terzyk, G. Rychlicki, P. Kowalczyk, K. Lota, E. Raymundo-Pinero, E. Frackowiak, F. Béguin, Thermodynamic properties of benzene adsorbed in activated carbons and multi-walled carbon nanotubes, *Chem. Phys. Lett.* 421 (2006) 409-414.
- [24] Wang, X. Yu, B. Pan, B. Xing, Norfloxacin Sorption and Its Thermodynamics on Surface-Modified Carbon Nanotubes, *Environ. Sci. Technol.* 44 (2010) 978-984.
- [25] J.L. Sotelo, G. Ovejero, A. Rodríguez, S. Álvarez, J. García, Removal of Atenolol and Isoproturon in Aqueous Solutions by Adsorption in a Fixed-Bed Column, *Ind. Eng. Chem. Res.* 51 (2012) 5045-5055.
- [26] S.P. Dubey, A.D. Dwivedi, C. Lee, Y.-N. Kwon, M. Sillanpaa, L.Q. Ma, Raspberry derived mesoporous carbon-tubules and fixed-bed adsorption of pharmaceutical drugs, *J. Ind. Eng. Chem.* 20 (2014) 1126-1132.
- [27] Y. Li, Z. Chen, XH/π (X = C, Si) Interactions in Graphene and Silicene: Weak in Strength, Strong in Tuning Band Structures, *J. Phys. Chem. Lett.* 4 (2013) 269-275.
- [28] S. Tsuzuki, K. Honda, T. Uchimaru, M. Mikami, A. Fujii, Magnitude and Directionality of the Interaction Energy of the Aliphatic CH/π Interaction: Significant Difference from Hydrogen Bond, *J. Phys. Chem. A* 110 (2006) 10163-10168.
- [29] K.J. Choi, S.G. Kim, C.W. Kim, S.H. Kim, Effects of activated carbon types and service life on removal of endocrine disrupting chemicals: amitrol, nonylphenol, and bisphenol-A, *Chemosphere* 58 (2005) 1535-1545.
- [30] C.B. Vidal, M. Seredych, E. Rodríguez-Castellón, R.F. Nascimento, T.J. Bandosz, Effect of nanoporous carbon surface chemistry on the removal of endocrine disruptors from water phase, *J. Colloid Interf. Sci.* 449 (2015) 180-191.
- [31] Z. Aksu, F. Gönen, Biosorption of phenol by immobilized activated sludge in a continuous packed bed: prediction of breakthrough curves, *Process Biochem.* 39 (2004) 599-613.
- [32] S.S. Baral, N. Das, T.S. Ramulu, S.K. Sahoo, S.N. Das, G.R. Chaudhury, Removal of Cr(VI) by thermally activated weed *Salvinia cucullata* in a fixed-bed column, *J. Hazard. Mater.* 161 (2009) 1427-1435.
- [33] S. Singh, V.C. Srivastava, I.D. Mall, Fixed-bed study for adsorptive removal of furfural by activated carbon, *Colloids Surf. A: Physicochem. Eng. Asp.* 332 (2009) 50-56.

- [34] W. Zhang, L. Dong, H. Yan, H. Li, Z. Jiang, X. Kan, H. Yang, A. Li, R. Cheng, Removal of methylene blue from aqueous solutions by straw based adsorbent in a fixed-bed column, *Chem. Eng. J.* 173 (2011) 429-436.
- [35] K. Yaghmaeian, G. Moussavi, A. Alahabadi, Removal of amoxicillin from contaminated water using NH₄Cl-activated carbon: Continuous flow fixed-bed adsorption and catalytic ozonation regeneration, *Chemi. Eng. J.* 236 (2014) 538-544.
- [36] D. Lin, B. Xing, Adsorption of Phenolic Compounds by Carbon Nanotubes: Role of Aromaticity and Substitution of Hydroxyl Groups, *Environ. Sci. Technol.* 42 (2008) 7254-7259.
- [37] T.X. Bui, H. Choi, Adsorptive removal of selected pharmaceuticals by mesoporous silica SBA-15, *J. Hazard. Mater.* 168 (2009) 602-608.
- [38] Y. Tian, B. Gao, V.L. Morales, H. Chen, Y. Wang, H. Li, Removal of sulfamethoxazole and sulfapyridine by carbon nanotubes in fixed-bed columns, *Chemosphere* 90 (2013) 2597-2605.



Capítulo V

Degradación electroquímica

En este capítulo se lleva a cabo la optimización de la degradación electroquímica de los contaminantes emergentes seleccionados, mediante técnicas voltamperométricas: voltamperometría de pulso diferencial (DPV) y voltamperometría cíclica (CV)

5.1. Publicación V

5.2. Publicación VI

V. Degradación electroquímica

Una vez que se ha obtenido la pre-concentración de los contaminantes modelo, se procede a su degradación mediante técnicas electroquímicas - voltamperometría diferencial de pulso (DPV) y voltamperometría cíclica (CV) -. Se selecciona un modelo de celda convencional con tres electrodos: electrodo de calomelanos saturado (SCE) como electrodo de referencia, electrodo de platino (Pt) como electrodo auxiliar, mientras que se variará el electrodo de trabajo.

Hay que tener en cuenta que, por lo general, estas técnicas presentan baja sensibilidad al emplear electrodos de trabajo convencionales. Una de las alternativas para mejorar la sensibilidad es mediante la modificación del electrodo con materiales carbonosos. Por ello, se empleará un electrodo comercial de carbón vítreo (glassy carbon electrode, GCE), así como modificaciones del mismo. Se modificará el GCE con nanotubos de carbono (CNT) ya que presentan un gran potencial en electroanálisis debido a sus particulares y excelentes propiedades, como pueden ser la elevada conductividad eléctrica, alta resistencia mecánica, buena estabilidad química, elevada área superficial, etc. Es importante estudiar también la influencia que posibles grupos funcionales presentes en los CNT tienen sobre el rendimiento electroquímico.

Por todo ello, se emplean cuatro electrodos de trabajo, el electrodo convencional (GCE), electrodo modificado con CNT (MWCNT-GCE), electrodo modificado con CNT con grupos funcionales carboxilo y amino (MWCNT-COOH-GCE y MWCNT-NH₂-GCE).

Un esquema general puede verse en la Figura 5.1, donde a partir de los electrodos seleccionados se lleva a cabo la degradación electroquímica de cada uno de los compuestos mediante voltamperometría de pulso diferencial (DPV) o voltamperometría cíclica (CV).

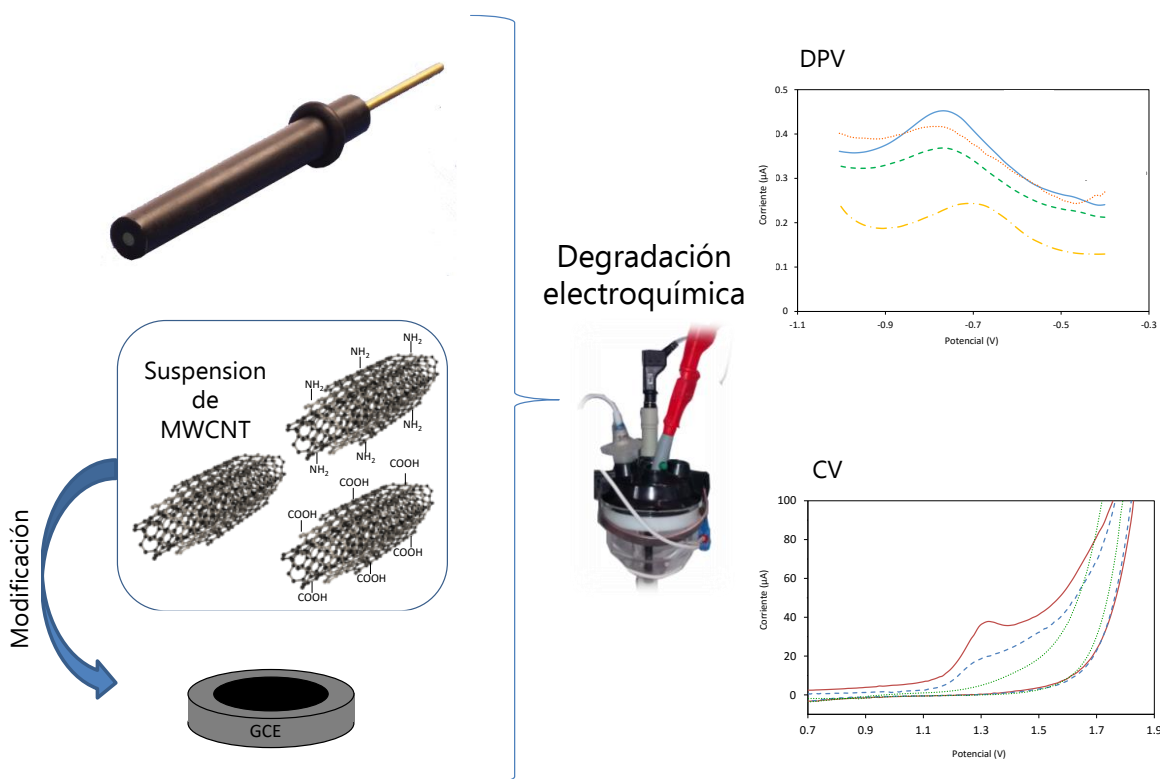


Figura 5.1. Gráfico conceptual del proceso de degradación electroquímica

Previo al estudio la degradación propiamente dicho, se llevó a cabo la optimización de las variables típicas que afectan a las técnicas electroquímicas, como son el pH, velocidad de barrido y agitación.

En el caso de la modificación del electrodo de trabajo, ésta se lleva a cabo mediante impregnación de una suspensión de los diversos nanotubos de carbono, sobre la superficie del electrodo. Por lo tanto es importante determinar la el volumen óptimo de las suspensiones de CNT a impregnar, para maximizar el rendimiento de la degradación.

Una vez optimizada la técnica se llevó a cabo la degradación empleando como electrodo de trabajo el que dio lugar a una mejor respuesta electroquímica. La degradación se llevó a cabo mediante la aplicación de ciclos sucesivos de la técnica electroquímica seleccionada, con el objetivo de degradar una nueva cantidad de contaminante con cada uno de los ciclos. Una vez fijado el electrodo de trabajo, se pudo maximizar el porcentaje de degradación variando tanto el número de ciclos, como el volumen a tratar, ya que el área de trabajo permanece constante. Asimismo, se ha perfeccionado la técnica obteniendo la relación volumen a tratar/área del electrodo óptima, así como el número de ciclos a aplicar para la cual se consigue la degradación completa del contaminante.

Los resultados obtenidos, así como la discusión de los mismos, se presentan en los apartados 5.1 y 5.2, mediante las *Publicaciones V y VI*, expuestas a continuación.

- Y. Patiño, S. Pilehvar, E. Díaz, S. Ordóñez, K. De Wael. Electrochemical reduction of nalidixic acid at glassy carbon electrode modified with multi-walled carbon nanotubes. En preparación.
- Y. Patiño, E. Díaz, S. Ordóñez. Carbon nanotube modified glassy carbon electrode for electrochemical oxidation of alkylphenol ethoxylate. En preparación.

Cabe destacar en este punto que no ha sido posible la degradación del 1,8-diclorooctano (DCO) mediante técnicas electroquímicas, probablemente debido a que la molécula del DCO no presenta grupos funcionales electroquímicamente activos, ya que es un alcano que cuenta además con dos grupos Cl en sus extremos. Por lo tanto sería interesante para futuros estudios, buscar una alternativa que permita la degradación del DCO.

5.1. Publicación IV

**ELECTROCHEMICAL REDUCTION OF NALIDIXIC ACID AT GLASSY
CARBON ELECTRODE MODIFIED WITH MULTI-WALLED CARBON
NANOTUBES**

Yolanda Patiño^a, Sanaz Pilehvar^b, Eva Díaz^a, Salvador^a Ordóñez, Karolien De

Wael^{b*}

^aDepartment of Chemical and Environmental Engineering, University of Oviedo, Faculty of Chemistry, Julián Clavería s/n, 33006 Oviedo, Spain

^bAXES research group, Department of Chemistry, University of Antwerp, Groenenborgerlaan 171, 2020 Antwerp, Belgium

E-mail: karolien.dewael@uantwerpen.be

Abstract

An electrochemical method has been optimized for the removal of nalidixic acid (NAL) from water samples, taking into account the great potential of multi-walled carbon nanotubes (MWCNT) in electroanalysis applications. MWCNT modified glassy carbon electrodes (MWCNT-GCE) were tested by cyclic voltammetry (CV) and differential pulse voltammetry (DPV) demonstrating the catalytic activity of MWCNT in reductive degradation of NAL. The effect of surface functional groups of MWCNT-COOH-GCE and MWCNT-NH₂-GCE were studied and compared with MWCNT-GCE and bare-GCE. The results indicate that the modification of GCE electrodes with MWCNTs leads to an improved performance for NAL reduction following the order of MWCNT > MWCNT-NH₂ > MWCNT-COOH. It has been shown that the obtained best response at MWCNT-GCE is mainly due to an increased i electrode active area, and also is due to the enhanced MWCNT adsorption properties.

The experimental condition were optimized according to pH, scan rate, deposition time and volume of MWCNT. The NAL degradation was carried out under optimal conditions using MWCNT modified GCE obtaining an irreversible reduction of NAL to less toxic products. The parameters of several DPV and volume/area (V/A) ratio were adjusted with the aim of obtaining the maximum degradation. It was observed that after 15 DPV and V/A=8, a complete reduction was obtained and two different sub-products were identified by HPLC-MS. The method was successfully utilized for the degradation of NAL with a 100% of removal employing a cheap and green technology.

1. Introduction

In recent years, pharmaceutical products have been produced in large quantities around the world, therefore with increasing consumption, also increases their released into environment, growing contamination of different water matrices [1]. Most of these antibiotics are not biodegradable, toxics, soluble, and resistant to degradation by conventional chemical processes or biological methods [2].

Nalidixic acid (NAL) is a non-biodegradable antibacterial agent synthesized by Lesher et al. in 1960s, used in the treatment of gram-negative urine tract infections, which has been frequently identified in surface water and wastewater [3-6]. Due to its release in water effluents and its inefficient removal in sewage treatment plants, the concerns about its effects on human health have increased. When it is present at low concentrations acts as bacteriostatic, inhibiting bacterial growth and reproduction, while at high concentrations it exhibit bactericidal effects [7]. Besides, it presents chronic toxicity and carcinogenicity effects [8].

Although there are many studies about the determination of nalidixic acid by several techniques, such us, spectroscopy [9], fluorescence [10, 11], phosphorescence [12] and chromatography [13-15], the studies on its degradation are much scarce. Sirtori et al. [5] studied its removal by solar photo-Fenton, Pollice et al. [7] Reported its degradation by an integrated MBR-ozonation system and the photodegradation of NAL has been considered by Petronella et al. [16] and Vargas et al. [17].

Due to the low concentration at which are present in water and in order to facilitate removal step, it would be interesting to have a two-step process by pre-concentration and removal. In a previous work the NAL pre-concentration was studied by adsorption onto carbon materials – activated carbon, high surface area graphite and multiwall carbon nanotubes – obtaining the best results with carbon nanotubes [18]. Once the contaminant is concentrated and the amount of water to be treated has been reduced, the stage of destruction of NAL takes place. Electrochemical treatment is an interesting method to remove pharmaceutical products since this technology offers relevant advantages such as instrumental simplicity, moderate costs, use of clean reagents – electrons- and possibility to operate at ambient temperature and pressure[19, 20]. Electrochemical methods present low sensitivity when conventional electrodes are used. It is an ongoing challenge in the electrochemical detection of water-contaminant to get proper material for electrode surface modification which can improve the sensitivity and selectivity of the method [21]. As an alternative for electrode modification, carbonaceous materials, and in particular carbon nanotubes (CNTs) presents a great potential in electroanalysis due to their small size, high electrical conductivity, high mechanical resistance, good chemical stability and high surface area [22, 23]. Increased electrode surface area improves the electrochemical response and induce electrode with an anti-fouling capability [23]. Other advantage of CNTs as an electrode modification material is their ability to promote electrode-

transfer reactions; the electrocatalytic effect has been attributed to the activity of edge-plane-like graphite sites at the CNTs ends [24, 25]. In addition, the electrochemical response of the CNT modified electrode is greatly influenced by the functional groups present in CNTs. Therefore, it is important to study the effect of different functional groups on the electroanalytical performance of modified electrode. Some similar studies have already taken into account the effect of functionalization [26, 27].

In this work, the electrocatalytic effect of multi-walled carbon nanotubes (MWCNT) modified glassy carbon electrode (MWCNT-GCE) on electrochemical reduction of NAL was investigated. Three kinds of MWCNT were used: without functionalized (MWCNT), functionalized with carboxylic (MWCNT-COOH) and amine (MWCNT-NH₂) groups. To our knowledge, electrochemical degradation of NAL using carbon nanotubes modified electrodes has not been reported yet.

The objective of this work is to develop a fast and sensitive method for the complete removal of NAL from water samples, by optimizing of variables which affect the process as well as the study of degradation products.

2. Materials and Methods

2.1. Chemicals and reagents. Nalidixic acid was purchased from Duchefa, Biochemie B.V. (purity > 99.4).

Three multi-walled carbon nanotubes have been used manufactured by DropSense: multi-walled non-functionalized carbon nanotubes (MWCNT) functionalized with –COOH groups (MWCNT-COOH) and functionalized with –NH₂ groups (MWCNT-NH₂).

Phosphate buffer (PBS) solutions of different pH were prepared by mixing the corresponding amounts of NaCl, KCl, KH₂PO₄ and Na₂HPO₄.

K₄[Fe(CN)₆] was purchased from Merck and K₃[Fe(CN)₆] was obtained from Sigma-Aldrich, Belgium.

2.2. Instrumentation. All electrochemical experiments, cyclic voltammetry and differential pulse voltammetry, were performed using a μ-Autolab Potentiostat/Galvanostat PGSTAT20, type II controlled by NOVA 1.10 software package (ECO Chemie, Utrecht, The Netherlands). The three electrodes system consist of a glassy carbon (GCE) as working electrode, saturated calomel (SCE) as the reference electrode and platinum (Pt) as an auxiliary electrode. Prior to the electrochemical measurements, the solution were purged for 20 min with purified nitrogen gas and a constant potential was applied to enable the deposition of NAL on the working electrode surface to increase the NAL reduction.

Cary 100 UV-Vis spectrophotometer (Varian Inc. USA) was employed for the detection of NAL at a wavelength of 258 nm. Calibration was established using 5 standards with the coefficient of determination r^2 higher than 0.995.

The degradation by-products were determined by high performance liquid chromatography with mass spectrometry detector (HPLC-MS), using a UPLC Agilent 6460.

2.3. Preparation of the modified electrodes. Before modification, the GCE was polished with 0.1 and 0.05 μm aluminum slurry, rinsed with distilled water and then ultrasonicated in water for a certain time and dried in the air.

MWCNTs solution was prepared by dispersing into dimethylformamide (DMF) at different concentrations 0.25 g L^{-1} by ultrasonication to obtain a well-dispersed suspension, according to the process developed by García-González et al. [28] Next, a 5, 10 or 15 μL aliquots of the suspension was deposited on the GCE area and then dried under room temperature before electrochemical measurements.

2.4. Electrode characterization. Scanning electron microscopy (SEM) was performed with a QUANTA 250 FEG SEM (FEI, Hillsboro, Oregon, USA). SEM was used to characterize the working electrodes modified with MWCNTs solutions.

The surface areas of the MWCNTs modified GCE and the bare GCE were obtained by cyclic voltammetry (CV) using $1 \text{ mM L}^{-1} \text{ K}_3[\text{Fe}(\text{CN})_6]$ solution at different scan rates.

3. Results and Discussion

3.1. Characterization of the modified electrodes.

The multi-walled carbon nanotube modified glassy electrodes were first characterized using scanning electron microscopy (SEM). Fig. 1 shows the SEM images obtained for the different working electrodes. As shown in Fig. 1 (B), the modified electrode presents an interwoven mesh of nanotubes, with different thin layers forming a porous structure. Functionalized MWCNT modified electrodes (Fig. 1 (C) and (D)), resulted in a more heterogeneous surface. In the case of MWCNT-COOH modified GCE (Fig. 1(C)), carbon nanotubes formed a bubble like structures, where the carbon nanotubes are clustered. For MWCNT-NH₂ (Fig. 1(D)), the MWCNT density presents differences between the perimeter zone, where the numbers of layers and therefore the density of MWCNT-NH₂ is less, and the central zone, where the density is higher. Thus, MWCNT modified GCE presents the most uniform surface, with different MWCNT layers where the electrocatalytic reduction of NAL can take place. The distributions obtained for the working electrodes correspond to those achieved in other works [26, 29, 30].

The active surface area of the different electrodes is estimated according to the Randles-Sevcik equation (Eq. 1) (at 20 °C) for a reversible process. [31]

$$i_p = 2.69 \times 10^5 n^{3/2} A C_0 D_R^{1/2} v^{1/2} \quad \text{Ec. 1}$$

Where i_p is the anodic peak current, n is the number of electron transfer ($n=1$), A is the surface area of the electrode, C_0 is the concentration of potassium ferrocyanide (1 mM), D_R is the diffusion coefficient ($D_R = 7.6 \times 10^{-6} \text{ cm}^2 \text{s}^{-1}$) and v is the scan rate. From the slope of the $i_p \text{ vs } v^{1/2}$, the value of A can be obtained.

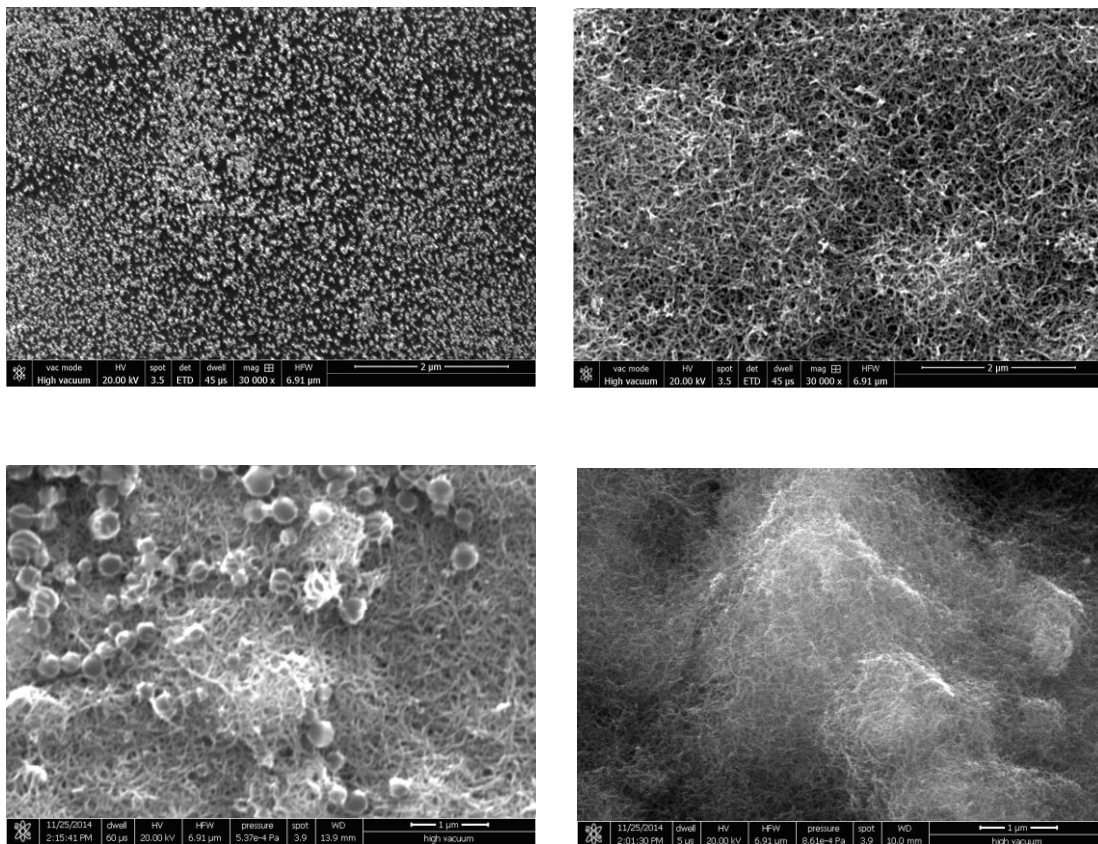


Figure 1. SEM images of working electrodes (A) Bare-GCE, (B) MWCNT modified GCE, (C) MWCNT-COOH modified GCE and (D) MWCNT- NH₂ modified GCE.

The electrode surface area obtained for bare GCE was 0.064 cm², 0.180 cm² for MWCNT-modified GCE, 0.069 cm² and 0.070 cm² for MWCNT-NH₂ and MWCNT-COOH, respectively. As it is clear from the values obtained for surface area for different electrodes, MWCNT-GCE presents the higher surface area, three times greater than the bare GCE. Modified GCE with functionalized MWCNT present a similar area between them, and a bit higher compare with

bare-GCE. Similar results were obtained by other authors, with the same ratio for Jain et al. [32] and a bit less and higher for Moyo at al. [33] and Rezaei et al. [29]. In all of the reported studies, the active surface area values after modification with carbon nanotubes was higher than the obtained values using bare GCE. The results showed an increase in the effective area after modification of GCE with MWCNT, which can produce a higher adsorption capability of the modified electrode surface. Higher adsorption properties of the modified surface can lead to the higher pre-concentrated amount of NAL at the surface of electrode. Consequently, higher amount of NAL can be electrochemically reduced and current response of NAL at modified electrode will be improved.

3.2. Electrochemical response by CV and DPV

The cyclic voltammetry responses of 1×10^{-5} M NAL in phosphate-buffered saline (PBS; pH=7) at bare GCE are shown in Fig. 2. A reduction/oxidation peak was not observed at GCE in blank solution. In the presence of 1×10^{-5} M NAL in the solution, a reduction peak appeared at -0.91 V (vs. SCE). The absence of the oxidative peak on the reverse scan suggests the irreversible nature of the electrode process [34].

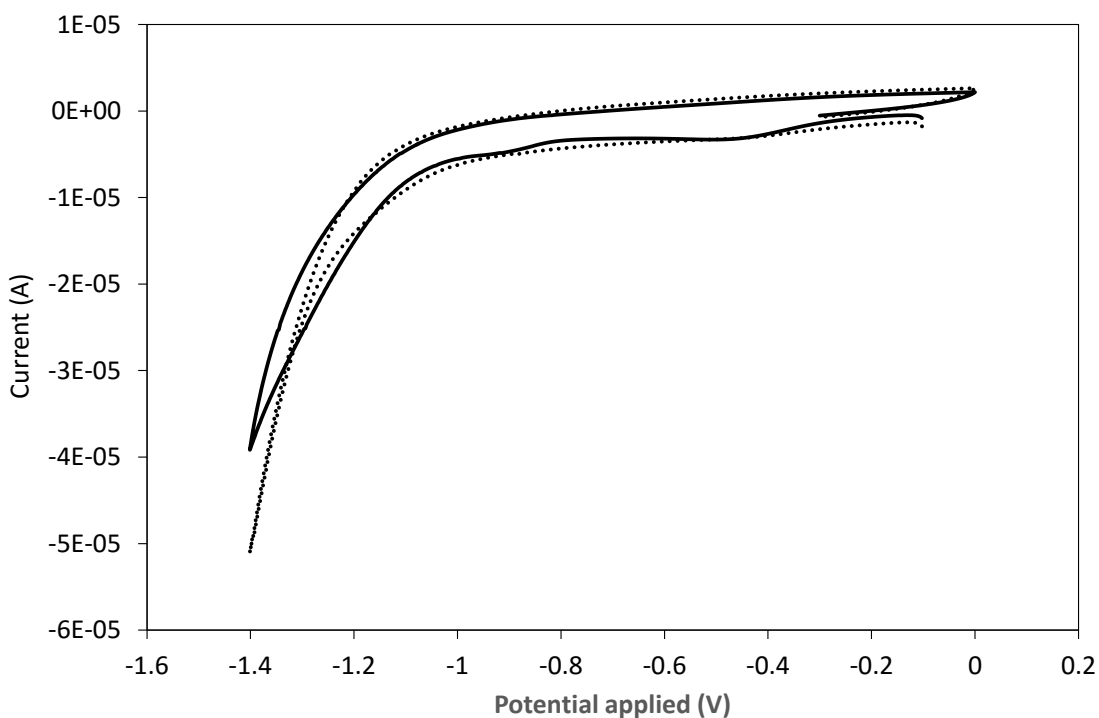


Figure 2. Cyclic voltammogram of bare GCE in blank solution (....) and in the presence of 1×10^{-5} M of NAL (—), both in PBS buffer (pH=7.0) and scan rate: 50 mVs⁻¹

To evaluate the electrocatalytic effect of MWCNT on NAL reduction, DPV scans were performed at bare GCE and MWCNT-GCE. As can be seen in Fig. 3, the peak current related to the NAL (1×10^{-5} M) improved when the surface of GCE is modified with MWCNTs, which indicates that MWCNTs possessed high activity toward NAL reduction. Same results were obtained by other studies about the electrochemical response of different antibiotics. For example, Rezaei et al., [29] did not obtain an oxidation peak for noscapine at the bare electrode, on the contrary, two oxidation peak were obtained using MWCNT modified electrode by cyclic voltammetry. Moyo et al., [33] obtained better results with MWCNT-GCE for the electro-oxidation of triclosan, with a peak area approximately twice bigger compared to that obtained at bare GCE by cyclic voltammetry and differential pulse voltammetry. In general terms, the increased surface area of the electrode after the modification with carbon nanotubes results in higher catalytic activity and adsorption capability of the surface and higher response.

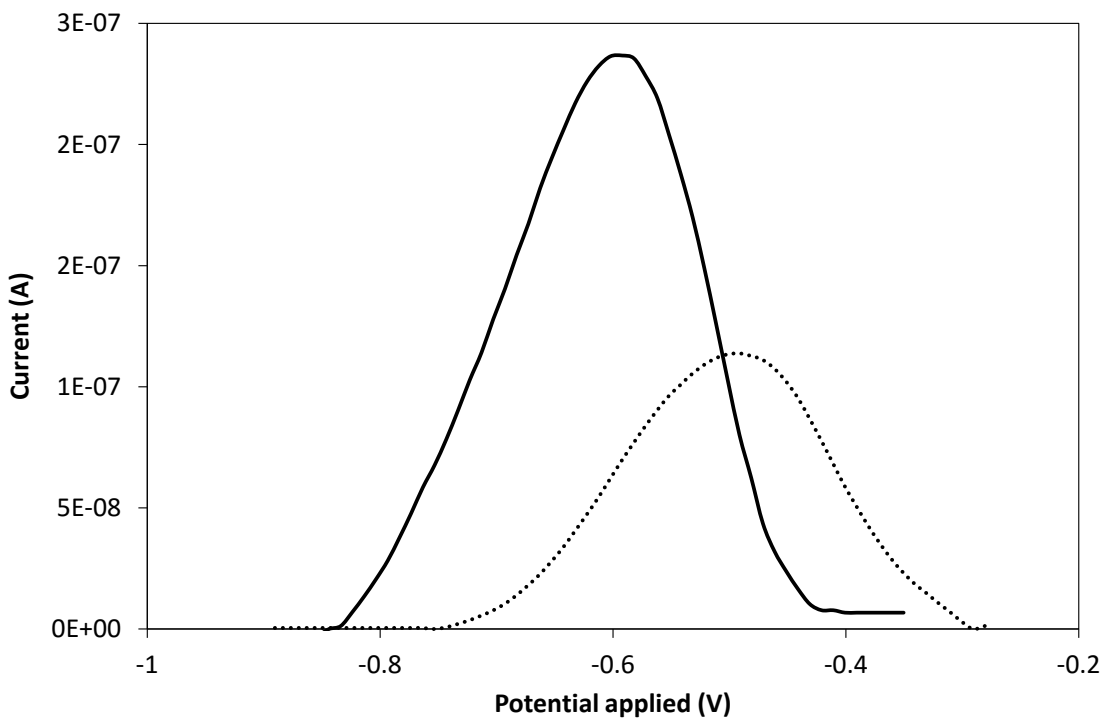


Figure 3. Electrocatalytic effect of GCE-MWCNTs on 1×10^{-5} M NAL by DPV on (----) bare GCE and (—) modified GCE with MWCNTs in PBS buffer (pH=7.0) and scan rate: 50 mVs⁻¹.

3.3. Optimization of experimental variables

Effect of the pH. The effect of pH on the DPV response was studied in PBS with different pH in the range of 3.0 - 9.0, to obtain the optimum pH value for NAL reduction using MWCNT-GCE as working electrode. Fig. 4 shows the DPV voltammograms obtained at different pH. The pH has

a significant influence on the reduction of NAL, reaching maximum value at pH 5.0, after that, the peak current decrease. In addition, the reduction peak potential shifted negatively as pH increase. Therefore, pH 5.0 was chosen as the optimum and it was used for the following experiments.

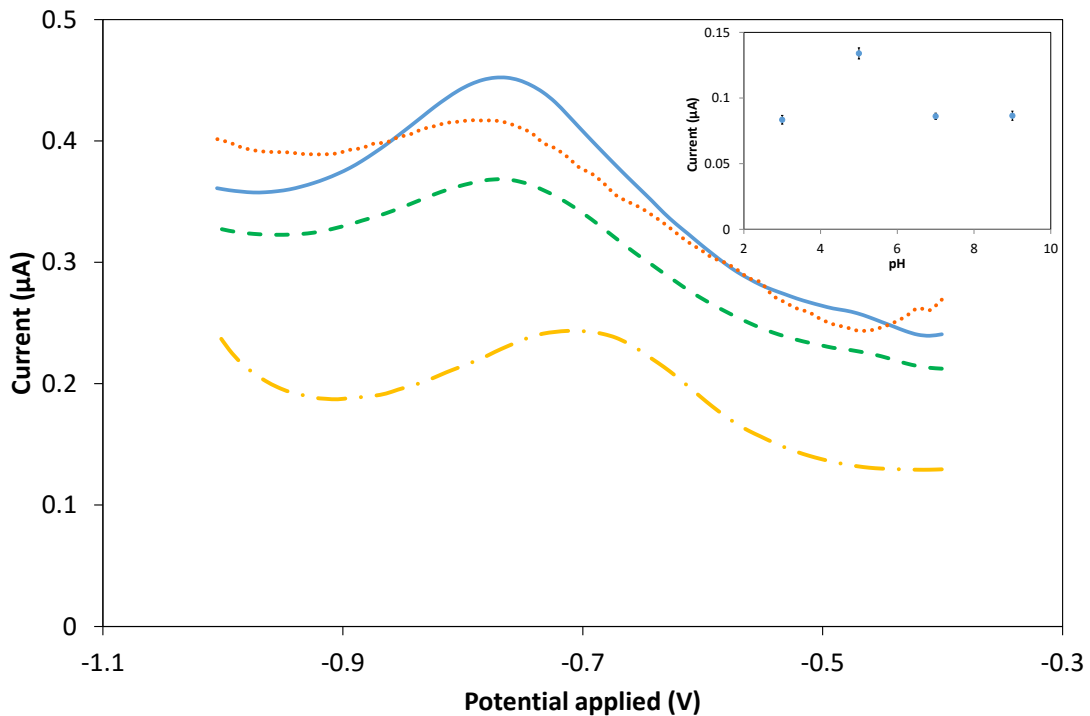


Figure 4. Effect of pH on peak current of 1×10^{-5} M NAL in PBS at the MWCNT-GCE electrode and scan rate of 50 mVs^{-1} . pH=3 - - -, pH=5 —, pH=7 - - -, pH=9 - · - .

Effect of Scan Rate. The effect of scan rate on the reductive peak currents of 1×10^{-5} M NAL at the MWCNT modified GCE in PBS buffer (pH 5.0) was studied with DPV at different scan rates from 10 to 60 mVs^{-1} (Fig. 5). As it is clear from figure, the peak potential shifts to more negative values with increase in scan rate, which confirms the irreversible nature of the reduction process [32, 35]. The reduction peak current increased slowly until scan rate of 50 mVs^{-1} , following by a sudden decrease in current at 60 mVs^{-1} . The peak current depends linearly on the square root of scan rate in the range of $10\text{-}50 \text{ mVs}^{-1}$ which shows that the electrode reaction is diffusion controlled process at modified GCE [32, 36].

The signal was reached to maximum value at scan rate of 50 mVs^{-1} , therefore it was chosen in the present study.

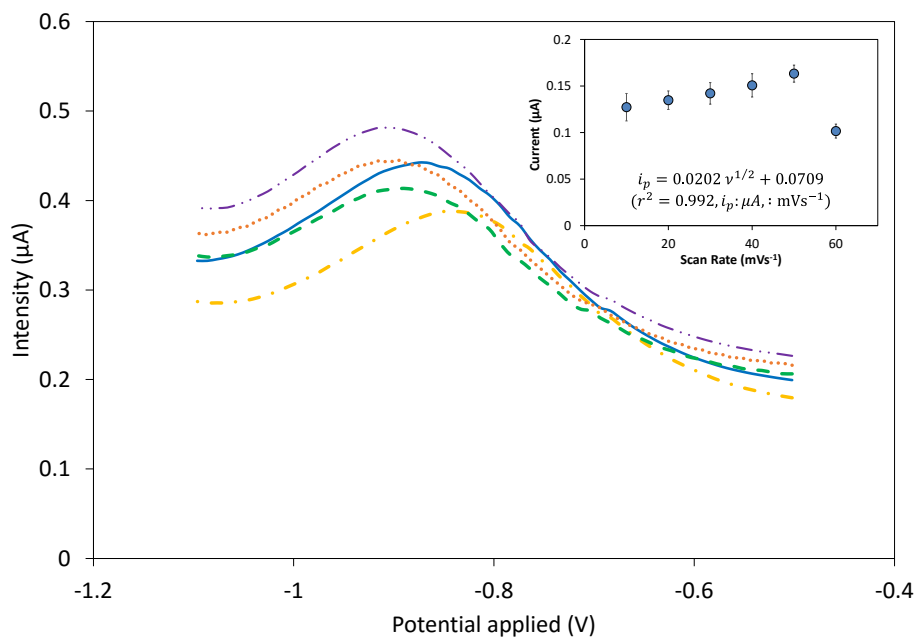


Figure 5. Effect of scan rate on DPV of 1×10^{-5} M NAL in PBS ($\text{pH}=5.0$) in different scan rates

from 10 mVs^{-1} to 60 mVs^{-1} . 10 mVs^{-1} — · · · · · , 20 mVs^{-1} — — — — — , 30 mVs^{-1} - - - - - , 40 mVs^{-1} · · · · · ,
 50 mVs^{-1} — · · · · · .

Effect of deposition time. Initially, a constant potential is applied in order to favor the NAL adsorption on the electrode surface. For this reason, the effect of deposition time was studied ranging from 10 to 1200 s. Fig. 6 shows that the peak current decrease for deposition time higher than 20 s. No further change in peak current was observed with the increasing time higher than 20 s, so, the adsorption of NAL on the film reaches a maximum due to the MWCNT layer at the electrode surface, which is not stable when a constant voltage is applied during the time. Due to the instability of the layer in time, part of the nanotubes can detach the electrode, decreasing the concentration of carbon nanotubes in the electrode surface.

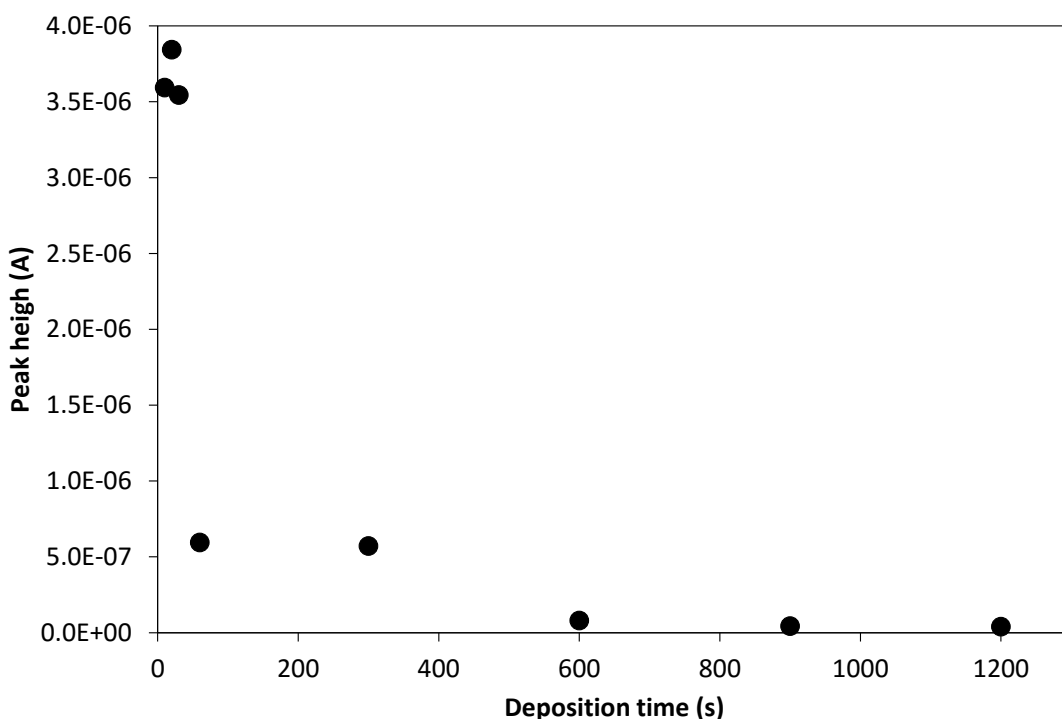


Figure 6. Effect of the deposition time on the peak height on DPV of 1×10^{-5} M NAL in PBS (pH=5.0) and 50 mVs^{-1} of scan rate

Effect of volume of MWCNT. The effect of varying volume of MWCNT suspension was studied in the range from 5 to 15 μL . It was observed that with increasing the MWCNTs volume, the reduction peak current increases until 10 μL and then, the current decrease drastically. This effect can be explained in relation to the thickness of film. When the film is too thin, the amount of NAL adsorbed is less and therefore, the reduction current is suppressed. When the film is too thick, the film conductivity reduced and the MWCNT film becomes unstable, resulting in a decreased peak current. Therefore, 10 μL of MWCNTs is chosen as the optimal dosage in the present study. The same trend was obtained in different studies for the detection of pharmaceutical products using GCE modified with MWCNTs [32, 37, 38].

After optimization of all the variables that can affect the process, the selected optimum conditions were: pH equal to five, 50 mVs^{-1} for scan rate, 20 s of deposition time and 10 μL of MWCNT to drop on the GCE surface. The rest of the experiments were done at optimal conditions.

3.4. Effect of functional groups of MWCNT

In order to study the effect of functional group of MWCNT on electrochemical reduction of NAL, MWCNT, MWCNT-COOH and MWCNT-NH₂ modified glassy carbon electrode were tested by DPV. The peak intensity of 1×10^{-5} M NAL obtained at different modified electrodes are compared and illustrated in Fig. 7. All electrodes modified with MWCNTs improved the peak current related to the reduction of NAL. However, MWCNT-GCE presents the highest peak current which can be due to the high adsorption capacity of NAL onto MWCNT. During the deposition step, NAL is adsorbed on the electrode surface, which is followed by the electrochemical removal. The deposition step is very important since the amount of reduced NAL increases as the amount of adsorbed NAL on the electrode surface increases. The adsorption of NAL onto these carbon nanotubes has been studied in previous works by batch and fixed bed adsorption, where the adsorption capacity obtained for the different MWCNT followed the order: MWCNT>MWCNT-NH₂>MWCNT-COOH,[39][18]coinciding with the results obtained in this work, which justifies that the adsorption stage during the constant potential plays an important role in reducing NAL. The negative effect of functionalized-MWCNT is because of functional groups onto MWCNT could block the pores where the NAL molecules can adsorb. Also they could form H-bonds with water molecules due to their hydrophilic character and decrease the NAL adsorption on the surface of modified electrode [39].

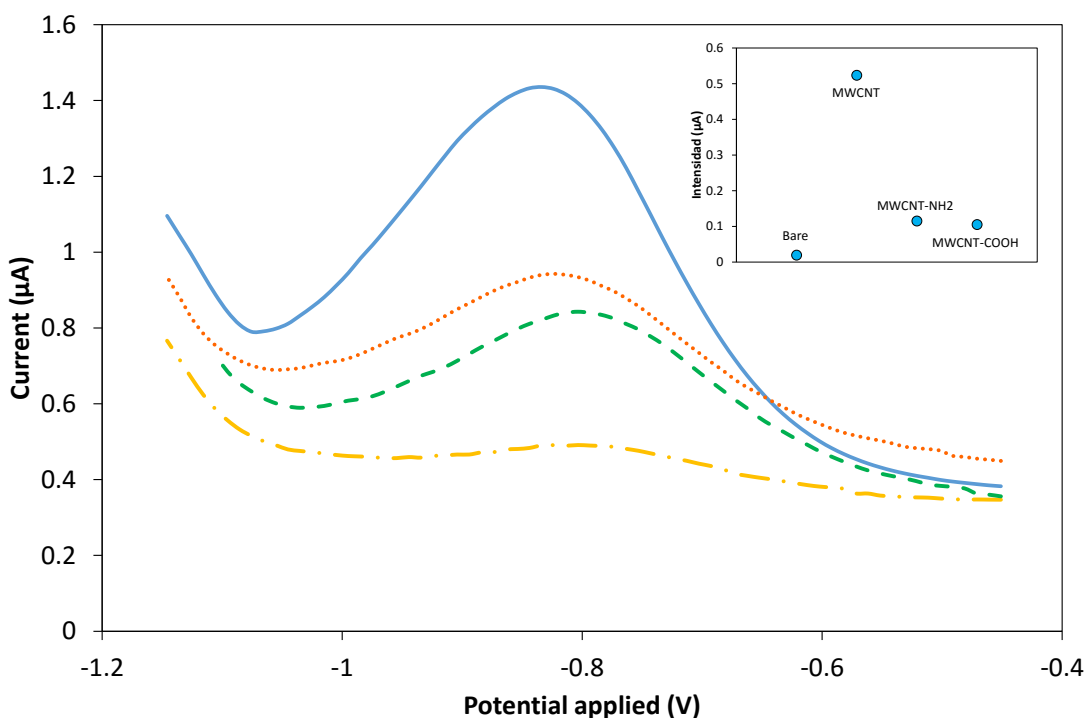


Figure 7. Electrocatalytic effect of GCE modified with functionalized-MWCNT of 1×10^{-5} M NAL in PBS (pH=5.0). Bare —·—·—, MWCNT ———, MWCNT-COOH -·---, MWCNT-NH₂ ······.

The intensity/area (i/A) ratio of different electrodes were compared in order to determinate whether the increment is only due to their higher area or not. The i/A ratio follow the order: MWCNT-GCE>MWNCT-COOH-GCE>MWCNT-NH₂-GCE>GCE, which confirms that the increase in the signal is not only due to the different area. The chemical nature of the nanotubes affects positively the NAL reduction, which indicates that modified GCE present an electro-catalytic effect for NAL reduction [40].

The peak potential of NAL reduction are all shifted to a small value for functionalized-MWCNT, in the order: MWCNT (-0.84 V) < MWCNT-NH₂ (-0.82 V) < MWCNT-COOH (-0.80 V) < Bare (-0.79 V), which proves the existence of electro-catalytic activity of these modified GCE [41]. Bi et al.,[40] obtained similar result in the study of the effect of functional groups of MWCNT for the detection of ascorbic acid, dopamine and uric acid. The study employed MWCNT, MWCNT-COOH and MWCNT-OH, where the highest electrocatalytic activity was obtained by MWCNT.

3.5. Response characteristics of the GCE-MWCNT electrode

The relation between the peak current and concentration of NAL was obtained by DPV technique under optimal experimental conditions, observing that the peak current increases with increase in the NAL concentration (Fig. 8). Two different ranges were obtained, the first linear range between 0.0001-0.05 μM and the second linear range from 0.1 μM to 50 μM, both with a regression coefficient, higher than 0.996. The same trend where two different trend exist, has been observed by other authors by different electrochemical techniques for paracetamol [42], ascorbic acid and caffeine [43]. This phenomena can be explained through the formation of a sub-monolayer in the first linear part, where NAL molecules are adsorbed inside pores and between the different layers , followed by the formation of a NAL monolayer in the second part of the calibration plot, after adsorption on the electrode surface [42].

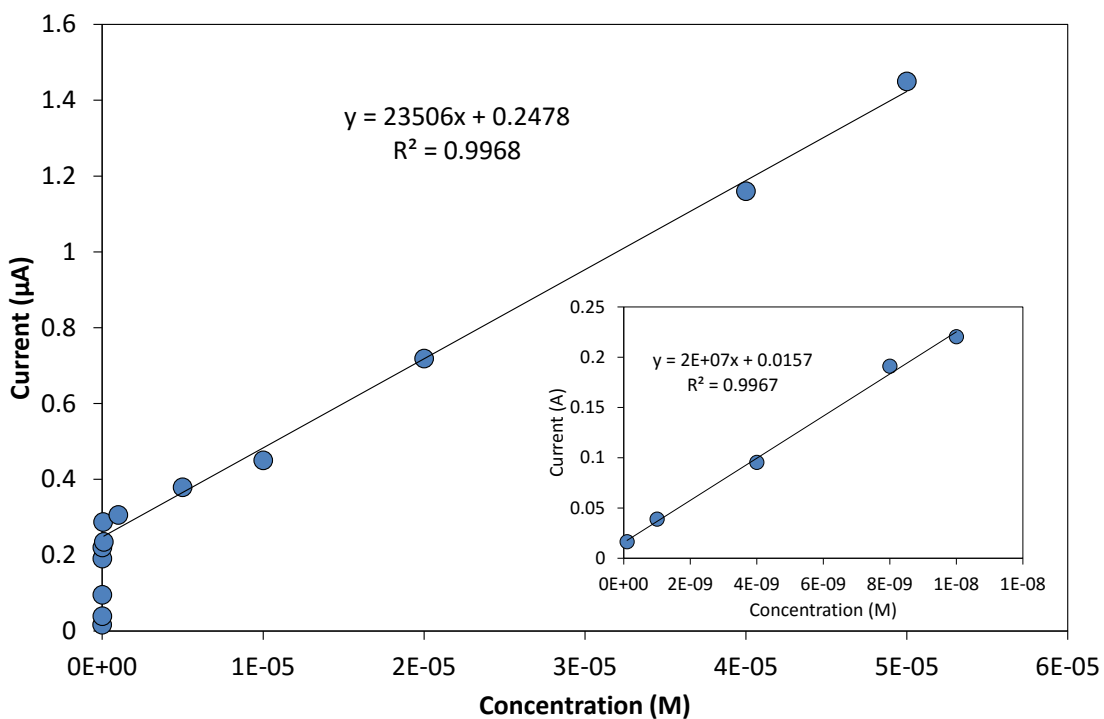


Figure 8. Plot between peak current versus concentration as obtained in reduction of NAL by DPV in the optimal conditions.

3.6. Degradation of NAL by DPV and degradation products

The electrochemical degradation of NAL was performed using DPV under the optimum operating conditions using potential range of -0.3 to -1.15 V, taking into account that the NAL reduction is an irreversible electrode process. The experiments were performed for 2, 3, 4, 5, 10 and 15 DPV scans and the final concentration was analyzed by UV-Vis spectrophotometer in order to estimate the NAL degradation in %. A V/A ratio equal to 28 and an initial NAL concentration of 1×10^{-5} M of NAL were selected. After one DPV, the degradation of NAL in the solution was calculated to be 12.5%. In order to increase the NAL removal, repetitive DPV were carried out. With increasing the number of DPVs, more NAL deposition on the electrode surface takes place, which could increase the amount of reduced NAL.

Fig. 9 (A) shows the effect of several DPV on the NAL degradation (%). The degradation increases linearly ($r^2 > 0.9$) from 12.5% to 80% as the number of DPV increase, up to 10 DPV. After 10 DPV, the final concentration remain constant without any increase in the NAL degradation, which may be due to the saturated electrode surface. If the electrode surface is saturated, the NAL adsorption onto the surface is not possible and as consequence, the MWCNT cannot act as electro-catalyst for its reduction.

In order to increase the NAL degradation, the V/A ratio was decreased until obtaining the maximum NAL reduction. By reducing the total volume (same initial concentration and electrode area), the mass of NAL in the solution decreases, therefore the saturation of the electrode will take place after more DPV. The same effect will takes places if the electrode area increases. Three different V/A ratio containing 28, 14 and 8 were tested at 15 DPV to ensure that the maximum NAL degradation is obtained. As can be seen in Fig. 9 (B) the maximum NAL degradation was obtained for a V/A ratio equal to eight, where all the NAL has been reduced to the sub-products.

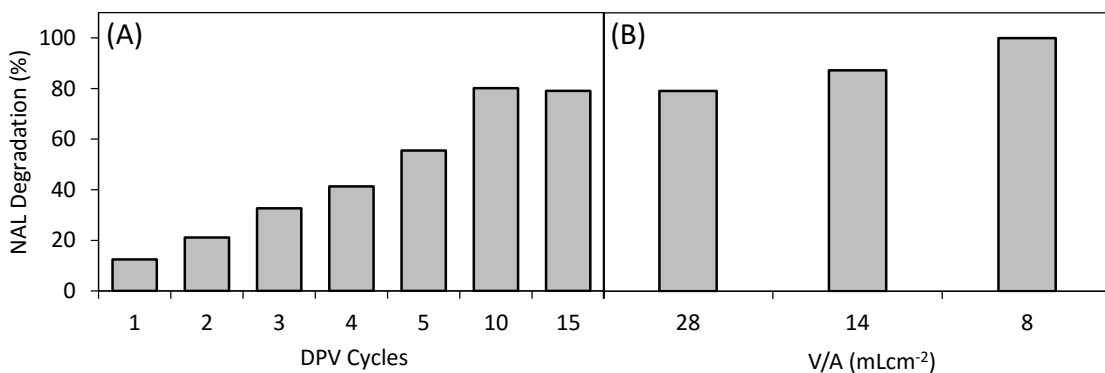


Figure 9. Electrochemical degradation of 1×10^{-5} M NAL, (A) constant V/A ratio and different DPV cycles and (B) 15 DPV and different V/A ratio, both at the optimum experimental conditions

The sub-products have been identified by HPLC-MS through the final solution under the conditions where a complete degradation was obtained. The disappearance of the peak corresponding to the nalidixic acid confirms its complete degradation. On the other hand, the appearance of two new peaks indicates the formation of transformation products where the higher intensity was obtained for a m/z ratio equal to 223 and 269. At this point, it is important to emphasize that there are not any studies reported about the sub-products resulted from the electrochemical reduction of NAL. Their identification was based on the elemental composition for the measured accurate m/z of the protonated molecules. The proposed structures and pathways are shown in Fig. 10. The methyl-pyridine ring remained unchanged in all of them. In the first step, the double bond cleavage of the second ring takes place by water addition in both cases. In the second step, a new water molecule causes the cleavage ring with the addition of an oxygen in C₂ or C₃ depending on the mechanism proposed. The products P₁ and P₃ are obtained by reduction of the less stable carbonyl group. The loss of the carboxylic group generates the products P₂ and P₄ corresponding with the m/z=222. In the pathway 1, the previous molecule has two carboxylic groups so that, this loss takes place in the less stable bond, corresponding with the C-N bond.

4. Conclusions

The electrochemical degradation of nalidixic acid at the surface of MWCNT-GCE was studied by differential pulse voltammetry.

The modified electrode with MWCNT shows superior electrocatalytic effect and the peak current increase in comparison with not modified glassy carbon electrode. MWCNT-GCE presents a nanostructure that allow the adsorption and pre-concentration of NAL on the electrode surface during the deposition step, which yield higher current responses by CV and DPV. Two modified GCE with MWCNT-COOH and MWCNT-NH₂ has been tested for their effect on NAL reduction, resulting in a higher current than for bare-GCE, but worst result in comparison with MWCNT-GCE due to a less adsorption on the electrode surface.

A complete reduction of NAL has been obtained with MWCNT modified GCE, under the optimal conditions after 15 DPV and V/A ratio equal to 8. The complete degradation has been confirmed by UV-VIS spectrophotometer and two different sub-products have been identified by LC-MS. This study shows the direct application of MWCNT modified GCE for the complete degradation of nalidixic acid.

The treatment of wastewater with NAL by this method presents a green alternative, a simple fabrication procedure and an easy regeneration of electrode surface, which only needs to be polished for a new use.

Acknowledgements

This work was supported by the Spanish Government (contract CTQ2011-29272-C04-01, -02 and -03). Y. Patiño thanks the Government of the Principality of Asturias for a Ph.D. fellowship (Severo Ochoa Program). S. P. and K. D. W. are thankful to UA for DOCPRO financial support.

References

- [1] V. Homem, L. Santos, Degradation and removal methods of antibiotics from aqueous matrices – A review, *Journal of Environmental Management*, 92 (2011) 2304-2347.
- [2] L. Feng, E.D. van Hullebusch, M.A. Rodrigo, G. Esposito, M.A. Oturan, Removal of residual anti-inflammatory and analgesic pharmaceuticals from aqueous systems by electrochemical advanced oxidation processes. A review, *Chemical Engineering Journal*, 228 (2013) 944-964.
- [3] S.A. R. Gleckman, D.W. Joubert, S.J. Mathews, *Am. J. Hosp. Pharm.*, p. 1071.
- [4] E.J.F. G.Y. Lesher, M.D. Gruett, J.M. Bailey, R.P. Brundage, *J. Med. Pharm. Chem.*, p. 1063.

- [5] C. Sirtori, A. Zapata, W. Gernjak, S. Malato, A. Lopez, A. Agüera, Solar photo-Fenton degradation of nalidixic acid in waters and wastewaters of different composition. Analytical assessment by LC-TOF-MS, *Water Research*, 45 (2011) 1736-1744.
- [6] L. Ge, J. Chen, X. Wei, S. Zhang, X. Qiao, X. Cai, Q. Xie, Aquatic Photochemistry of Fluoroquinolone Antibiotics: Kinetics, Pathways, and Multivariate Effects of Main Water Constituents, *Environmental Science & Technology*, 44 (2010) 2400-2405.
- [7] A. Pollice, G. Laera, D. Cassano, S. Diomede, A. Pinto, A. Lopez, G. Mascolo, Removal of nalidixic acid and its degradation products by an integrated MBR-ozonation system, *Journal of Hazardous Materials*, 203–204 (2012) 46-52.
- [8] M.S. Ibrahim, I.S. Shehatta, M.R. Sultan, Cathodic adsorptive stripping voltammetric determination of nalidixic acid in pharmaceuticals, human urine and serum, *Talanta*, 56 (2002) 471-479.
- [9] E.F. Salim, I.S. Shupe, Qualitative and quantitative tests for nalidixic acid, *Journal of Pharmaceutical Sciences*, 55 (1966) 1289-1290.
- [10] J.A.M. Pulgarin, A.A. Molina, P.F. López, Direct determination of nalidixic acid in urine by matrix isopotential synchronous fluorescence spectrometry, *Talanta*, 43 (1996) 431-438.
- [11] M.L. Wang, S.C. Chen, J.C. Lien, S.C. Kuo, Determination of nalidixic acid by fluorometry with sodium borohydride and hydrogen peroxide, *Journal of AOAC International*, 85 (2002) 572-575.
- [12] L.F. Capitán-Vallvey, F. Ojeda, M. Del Olmo, R. Avidad, A. Navalón, T. Vo-Dinh, Use of transmitted room-temperature phosphorescence to improve nalidixic acid determination, *Applied Spectroscopy*, 52 (1998) 101-105.
- [13] V.R. Bari, U.J. Dhorda, M. Sundaresan, Simultaneous estimation of nalidixic acid and metronidazole in dosage forms using packed column supercritical fluid chromatography, *Analytica Chimica Acta*, 376 (1998) 221-225.
- [14] T. Pérez-Ruiz, C. Martínez-Lozano, A. Sanz, E. Bravo, Separation and simultaneous determination of nalidixic acid, hydroxynalidixic acid and carboxynalidixic acid in serum and urine by micellar electrokinetic capillary chromatography, *Journal of Chromatography B: Biomedical Sciences and Applications*, 724 (1999) 319-324.
- [15] M. Horie, K. Saito, Y. Hoshino, N. Nose, E. Mochizuki, H. Nakazawa, Simultaneous determination of nalidixic acid, oxolinic acid and piromidic acid in fish by high-performance liquid chromatography with fluorescence and uv detection, *Journal of Chromatography A*, 402 (1987) 301-308.
- [16] F. Petronella, S. Diomede, E. Fanizza, G. Mascolo, T. Sibillano, A. Agostiano, M.L. Curri, R. Comparelli, Photodegradation of nalidixic acid assisted by TiO₂ nanorods/Ag nanoparticles based catalyst, *Chemosphere*, 91 (2013) 941-947.
- [17] F. Vargas, C. Rivas, R. Machado, M.A. Miranda, PHOTODEGRADATION OF NALIDIXIC AND TIAPROFENIC ACIDS AND NIFEDIPINE IN AEROBIC CONDITIONS, *Photodermatol. Photoimmunol. Photomed.*, 8 (1991) 218-221.

- [18] Y. Patiño, E. Díaz, S. Ordóñez, Pre-concentration of nalidixic acid through adsorption-desorption cycles: Adsorbent selection and modeling, *Chemical Engineering Journal*, 283 (2016) 486-494.
- [19] C. Carlesi Jara, D. Fino, V. Specchia, G. Saracco, P. Spinelli, Electrochemical removal of antibiotics from wastewaters, *Applied Catalysis B: Environmental*, 70 (2007) 479-487.
- [20] F.C. Walsh, Electrochemical technology for environmental treatment and clean energy conversion, *Pure and Applied Chemistry*, 73 (2001) 1819-1837.
- [21] V.K. Gupta, R. Jain, K. Radhapyari, N. Jadon, S. Agarwal, Voltammetric techniques for the assay of pharmaceuticals—A review, *Analytical Biochemistry*, 408 (2011) 179-196.
- [22] R.N. Goyal, M. Oyama, V.K. Gupta, S.P. Singh, R.A. Sharma, Sensors for 5-hydroxytryptamine and 5-hydroxyindole acetic acid based on nanomaterial modified electrodes, *Sensors and Actuators B: Chemical*, 134 (2008) 816-821.
- [23] L. Agüí, P. Yáñez-Sedeño, J.M. Pingarrón, Role of carbon nanotubes in electroanalytical chemistry: A review, *Analytica Chimica Acta*, 622 (2008) 11-47.
- [24] G. Liu, S.L. Riechers, M.C. Mellen, Y. Lin, Sensitive electrochemical detection of enzymatically generated thiocholine at carbon nanotube modified glassy carbon electrode, *Electrochemistry Communications*, 7 (2005) 1163-1169.
- [25] S.M. Ghoreishi, M. Behpour, E. Hajisadeghian, M. Golestaneh, Voltammetric determination of resorcinol on the surface of a glassy carbon electrode modified with multi-walled carbon nanotube, *Arabian Journal of Chemistry*.
- [26] H. Shin, J. Song, E. Shin, C. Kang, Ion-exchange adsorption of copper(II) ions on functionalized single-wall carbon nanotubes immobilized on a glassy carbon electrode, *Electrochimica Acta*, 56 (2011) 1082-1088.
- [27] L.Q. Hoa, M.d.C. Vestergaard, H. Yoshikawa, M. Saito, E. Tamiya, Functionalized multi-walled carbon nanotubes as supporting matrix for enhanced ethanol oxidation on Pt-based catalysts, *Electrochemistry Communications*, 13 (2011) 746-749.
- [28] R. García-González, A. Fernández-La Villa, A. Costa-García, M.T. Fernández-Abedul, Dispersion studies of carboxyl, amine and thiol-functionalized carbon nanotubes for improving the electrochemical behavior of screen printed electrodes, *Sensors and Actuators B: Chemical*, 181 (2013) 353-360.
- [29] B. Rezaei, S.Z. Mirahmadi Zare, Modified glassy carbon electrode with multiwall carbon nanotubes as a voltammetric sensor for determination of noscapine in biological and pharmaceutical samples, *Sensors and Actuators B: Chemical*, 134 (2008) 292-299.
- [30] L. Fotouhi, M. Alahyari, Electrochemical behavior and analytical application of ciprofloxacin using a multi-walled nanotube composite film-glassy carbon electrode, *Colloids and Surfaces B: Biointerfaces*, 81 (2010) 110-114.
- [31] L.R.F. A.J. Bard, E. Methods, N.Y.p. (second edition) Wiley, [M].

- [32] R. Jain, S. Sharma, Glassy carbon electrode modified with multi-walled carbon nanotubes sensor for the quantification of antihistamine drug pheniramine in solubilized systems, *Journal of Pharmaceutical Analysis*, 2 (2012) 56-61.
- [33] M. Moyo, L.R. Florence, J.O. Okonkwo, Improved electro-oxidation of triclosan at nano-zinc oxide-multiwalled carbon nanotube modified glassy carbon electrode, *Sensors and Actuators B: Chemical*, 209 (2015) 898-905.
- [34] A.G. Cabanillas, M.I.R. Cáceres, M.A.M. Cañas, J.M.O. Burguillos, T.G. Díaz, Square wave adsorptive stripping voltammetric determination of the mixture of nalidixic acid and its main metabolite (7-hydroxymethylnalidixic acid) by multivariate methods and artificial neural network, *Talanta*, 72 (2007) 932-940.
- [35] A.C. Pereira, A.d.S. Santos, L.T. Kubota, Electrochemical behavior of riboflavin immobilized on different matrices, *Journal of Colloid and Interface Science*, 265 (2003) 351-358.
- [36] F. Xiao, F. Zhao, J. Li, R. Yan, J. Yu, B. Zeng, Sensitive voltammetric determination of chloramphenicol by using single-wall carbon nanotube-gold nanoparticle-ionic liquid composite film modified glassy carbon electrodes, *Analytica Chimica Acta*, 596 (2007) 79-85.
- [37] J.A. Rather, K. De Wael, C60-functionalized MWCNT based sensor for sensitive detection of endocrine disruptor vinclozolin in solubilized system and wastewater, *Sensors and Actuators B: Chemical*, 171–172 (2012) 907-915.
- [38] R. Jain, J.A. Rather, Voltammetric determination of antibacterial drug gemifloxacin in solubilized systems at multi-walled carbon nanotubes modified glassy carbon electrode, *Colloids and Surfaces B: Biointerfaces*, 83 (2011) 340-346.
- [39] Y. Patiño, E. Díaz, S. Ordóñez, E. Gallegos-Suarez, A. Guerrero-Ruiz, I. Rodríguez-Ramos, Adsorption of emerging pollutants on functionalized multiwall carbon nanotubes, *Chemosphere*, 136 (2015) 174-180.
- [40] H. Bi, Y. Li, S. Liu, P. Guo, Z. Wei, C. Lv, J. Zhang, X.S. Zhao, Carbon-nanotube-modified glassy carbon electrode for simultaneous determination of dopamine, ascorbic acid and uric acid: The effect of functional groups, *Sensors and Actuators B: Chemical*, 171–172 (2012) 1132-1140.
- [41] B. Habibi, M.H. Pournaghi-Azar, Simultaneous determination of ascorbic acid, dopamine and uric acid by use of a MWCNT modified carbon-ceramic electrode and differential pulse voltammetry, *Electrochimica Acta*, 55 (2010) 5492-5498.
- [42] R.T. Kachoosangi, G.G. Wildgoose, R.G. Compton, Sensitive adsorptive stripping voltammetric determination of paracetamol at multiwalled carbon nanotube modified basal plane pyrolytic graphite electrode, *Analytica Chimica Acta*, 618 (2008) 54-60.
- [43] V.K. Gupta, A.K. Jain, S.K. Shoura, Multiwall carbon nanotube modified glassy carbon electrode as voltammetric sensor for the simultaneous determination of ascorbic acid and caffeine, *Electrochimica Acta*, 93 (2013) 248-253.

5.2. Publicación VI

**CARBON NANOTUBE MODIFIED GLASSY CARBON ELECTRODE FOR
ELECTROCHEMICAL OXIDATION OF ALKYLPHENOL ETHOXYLATE**

Yolanda Patiño, Eva Díaz, Salvador Ordóñez

*Department of Chemical and Environmental Engineering, University of Oviedo, Faculty of
Chemistry, Julián Clavería s/n, 33006 Oviedo, Spain*

E-mail: sordonez@uniovi.es

Abstract

The electrochemical oxidation of an alkylphenol ethoxylate (APE) from water has been studied by cyclic voltammetry (CV). Due to the extraordinary properties of multiwall carbon nanotubes (MWCNT) in electrochemistry, MWCNT modified glassy carbon electrode (GCE) has been checked. The results shows that MWCNT-GCE improves the electrochemical behavior, increasing the oxidation peak. The results exhibits a single peak reduction, so this would be an irreversible process. The effect of functional groups on MWCNT on the electrochemical oxidation of MPET has been studied with MWCNT-NH₂-GCE and MWCNT-COOH-GCE as working electrodes. The oxidation peak current follow the order MWCNT> MWCNT-NH₂> MWCNT-COOH, but taking into account the normalized peak current (I_p/A), MWCNT-NH₂ exhibits the best results due its strength interaction with MPET.

Under optimal conditions, the MPET degradation was studied for MWCNT-GCE and MWCNT-NH₂-GCE in order to obtain a total degradation. In the case of MWCNT-GCE, it took place for a volume/area (V/A) ratio equal to 19 after four CV cycles. Contrary, in the case of MWCNT-NH₂-GCE the maximum degradation achieved was around 90% for V/A=37, higher than the obtained for MWCNT-GCE in the same conditions. With both working electrodes, no by-products were obtained by GC-MS suggesting a complete mineralization of MPET.

1. Introduction

Alkylphenol ethoxylates (APEs) are the main components of nonionic surfactants, used to formulate products such as detergents, paints, antioxidants of plastic, pesticide, wetting products, and petroleum recovery chemicals [1-3]. APEs are considered an emerging organic pollutants, with endocrine disrupting activity [4, 5]. Their extensive use in industrial and commercial formulations has resulted in the increased of their presence as common environmental contaminants found in sewage sludge and sediments, wastewater, surface waters and treated drinking water [6-9]. Besides, the degradation of this kind of pollutants in sewage treatment plants leads to the formation of more toxic and resistant metabolites, responsible for feminization and carcinogenesis on various organisms [10, 11].

The European legislation by the Water Framework Directive 2000/60/EC includes some APEs in its priority list [12, 13]. In addition, the European Directive No. 2003/53/EC (2003) has forbidden the use of nonylphenol and its ethoxylates in the European Union, but some industrial applications cannot replace them by alternative chemicals due to technical and economic reasons and continue using these compounds [14]. For all that, there is really a need to find an efficient method for their removal.

Conventional treatments of water and effluents present difficulties to degrade APEs [15, 16]. Thus new technologies have been developed, such as advance oxidation process (AOPs) [7, 17-22] and electrochemical degradation [3, 7].

AOPs includes techniques like zonation, photocatalysis and Fenton, which employ a highly reactive oxidizing agent, such as hydroxyl radicals ($\text{HO}\cdot$) [23, 24]. Although AOPs are a good alternative and they are widely studied, they present some disadvantages: expensive process, excess consumption of chemicals and, in some cases, production of by-products of unknown effects, most of them, more harmful than the starting products.

On the other hand, although the electrochemical degradation has not been hardly studied, it presents several advantages, such as ease of operations, the option to work at ambient temperature and pressure and at the same time, it can produce a complete mineralization of the target compound [7, 25, 26]. All that make this technique as a good alternative for APEs degradation.

However it is necessary to take into account that these compounds are presented in water at very low concentration, in the order of $\mu\text{g}\cdot\text{L}^{-1}$ to $\text{ng}\cdot\text{L}^{-1}$, which is a disadvantage for their removal [27-31]. It would be necessary to treat a large volume of water to remove a small amount of pollutant. For this reason, a two stage process with a pre-concentration followed by electrochemical degradation is proposed.

In a previous work, the first step was proposed [32]. The pre-concentration of 2-(4-methylphenoxy)ethanol (MPET) as representative of APEs was carried out by adsorption/desorption cycles onto carbonaceous materials due to their good adsorption properties. The best results were obtained with multiwall carbon nanotubes (MWCNT), with a pre-concentration factor equal to 2.8.

After pre-concentration, the electrochemical degradation can be carried out with modified electrodes, which allow to accelerate electron transfer for the electrochemical oxidation [33]. Carbon based electrodes have been widely used, and recently, MWCNT are employed to modified electrodes because of their good properties including good porosity, enhance electronic properties and rapid electrode kinetics [34-36]. Although several authors have studied MWCNT modified electrodes in both electrochemistry and electroanalytical chemistry there are scarce studies on the degradation of APEs by this technique [7, 37-39].

The objective of this study is to develop an electrochemical method to remove MPET from aqueous solution based on the unique properties of glassy carbon electrode (GCE) modified with MWCNT. The electrochemical oxidation of MPET has been studied by cyclic voltammetry. The influence of several process properties such as pH, scan rate and amount of MWCNT have been studied. In order to determine the effect of functional groups on MWCNT, the electrochemical behavior under two functionalized MWCNT – MWCNT-NH₂ and MWCNT-COOH – was compared with MWCNT under optimal conditions. In this way, the best working electrode for a complete degradation of MPET by a green technology could be selected.

2. Materials and Methods

2.1. Chemicals and reagents. 2-(4-methylphenoxy)ethanol (MPET) was purchased from TCI Europe N.V., with a purity > 98% and used in the experiments directly without any further purification.

The chemicals employed for the phosphate buffer (PBS) (NaCl, KCl, KH₂PO₄ and Na₂HPO₄), K₄[Fe(CN)₆] and K₃[Fe(CN)₆] were obtained from Sigma-Aldrich.

The different multi-walled carbon nanotubes: MWCNT, MWCNT-NH₂ and MWCNT-COOH and have been used manufactured by DropSense.

2.2. Instrumentation. Cyclic voltammetry, were performed using a Zahner XPOT Potentiostat. The surface areas of the working electrodes were performed using a μ-Autolab Potentiostat/Galvanostat PGSTAT20.

Batch oxidation was performed in a undivided electrolytic cell with a conventional three electrode cell: bare and modified glassy carbon (GCE) as working electrode, saturated calomel (SCE) as reference electrode and platinum (Pt) as auxiliary electrode. The buffer solution was deoxygenated by passing purified nitrogen gas for 20 min.

The quantitative analysis of MPET and the by-products obtained were quantified by GC-MS in a calibrate Shimadzu GC/MS QP2010 Plus instrument, using a 30 m long TRB-5MS capillary column by prior extraction in chloroform using a volume ratio (1:1).

2.3. Preparation of the modified electrodes. MWCNTs suspensions were prepared by dispersing into dimethylformamide (DMF) until obtain a well-dispersed suspension.

A bare-GCE was polished with 0.3 and 0.05 µm aluminum slurry, and cleaning by ultrasonication in double distilled deionized water. After the electrode was dried in the air, it was dropped by depositing 5, 10 or 15 µL of the MWCNTs suspension on the GCE area and then dried under room temperature before electrochemical measurements.

3. Results and Discussion

3.1. Surface area electrode study

For an electrochemically reversible process the active surface area can be estimated according to Randles-Sevcik equation, which relates the oxidation peak current (I_p) to potential (v) at 20°C for a reversible process (Eq. 1).

$$I_p = 2.69 \times 10^5 n^{3/2} A C_0 D_R^{1/2} v^{1/2} \quad \text{Ec. 1}$$

where I_p is the anodic peak current, n is the number of electron transfer ($n=1$), A is the surface area of the electrode, C_0 is the concentration of species being oxidised, D_R is the diffusion coefficient ($D_R = 7.6 \times 10^{-6} \text{ cm}^2 \text{s}^{-1}$) and v is the scan rate. From the slope of the I_p vs $v^{1/2}$, the value of A can be obtained.

The surface areas were obtained by cyclic voltammetry (CV) using 1mML^{-1} $\text{K}_3[\text{Fe}(\text{CN})_6]$ solution in PBS buffer solution at different scan rates. The electrode surface area obtained follow the order: MWCNT (0.135 cm^2) > MWCNT-NH₂ (0.054 cm^2) > MWCNT-COOH (0.051 cm^2) > Bare (0.040 cm^2).

The electrochemical effective surface area increase after modification of GCE. This increase is less pronounced for MWCNT-COOH and MWCNT-NH₂, obtaining similar effective surface are between both of them, and just a bit greater than bare. However for MWCNT the effective surface area increases more than three times compared with bare, and more than two times

than for functionalized MWCNT. The effect of MWCNT on the electrode surface has been studied by other authors. Patil et al., [40] obtained a similar rise in the electrode surface after modification, while others authors as Dogan-Topal et al., and Rezaei et al., obtained a smaller increase. However, the final area after modification is always better than for bare-GCE.

3.2. Electrochemical behavior of MPET on GCE and MWCNT modified electrode

The cyclic voltammogram of 1×10^{-5} M MPET on bare-GCE and MWCNT-GCE at pH 5 in PBS buffer solution is shown in Fig. 1. The electrode response of MPET is typical of an irreversible electrode reaction, since no peak was observed in the reverse scan. Oxidation peaks were observed at 1.28 and 1.31, for bare-GCE and MWCNT-GCE, respectively. It is observed that the response increases at MWCNT-GCE with a shift in the peak potential to positive values, and an improvement in the peak current, which is indicative of the catalytic effect of MWCNT on the electrochemical oxidation of MPET [41, 42]. The reason of this improvement with MWCNT is due to the nanometer dimensions of MWCNT, the electronic structure and the topological defects of the surface as well as due to the higher effective area of the electrode [40, 42]

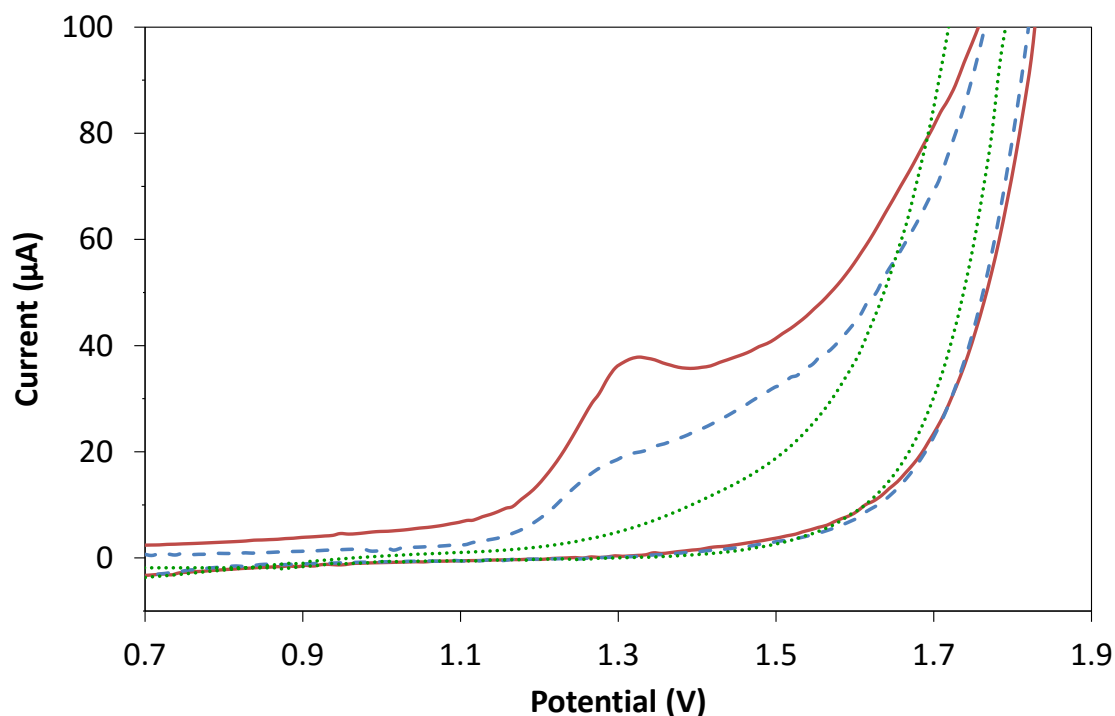


Figure 1. Electrocatalytic effect of MWCNT-GCE in 1×10^{-5} M MPET (CV, scan rate 50 mVs⁻¹) at (.....) blank (- - -), bare-GCE (—) and MWCNT-GCE

3.3. Influence of the amount of MWCNT

The amount of MWCNT can modified the properties and functions of the electrode surface, so the effect of different volumes of MWCNT was studied. Volumes of MWCNT between 5 and 15 μL was dropped to the electrode surface and dried at room temperature. The oxidation peak current increases with increases in the amount of MWCNT up to 10 μL , volume from which the peak current decrease. The peak current variation is related to the thickness of the film. If the film is too thin, the amount of MPET adsorbed on the electrode surface is small, which involves a small peak current. Contrary, when it is too thick, the MWCNT film is usually less stable could leave off the electrode surface, accompanied with a slower peak current [41, 43, 44]. Therefore, 10 μL was selected as the optimum amount of MWCNT suspension.

3.4. Effect of pH on the peak potential and peak currents

The electrochemical behavior is affected by the pH of the supporting electrolyte [33]. The voltammetric oxidation of MPET was studied in the range of 3 to 9. As shown in Fig. 2a the oxidation peak current reaches a maximum at pH 5, after that deceases. Considering this pH effect, a pH of 5 was chosen for the rest of experiments.

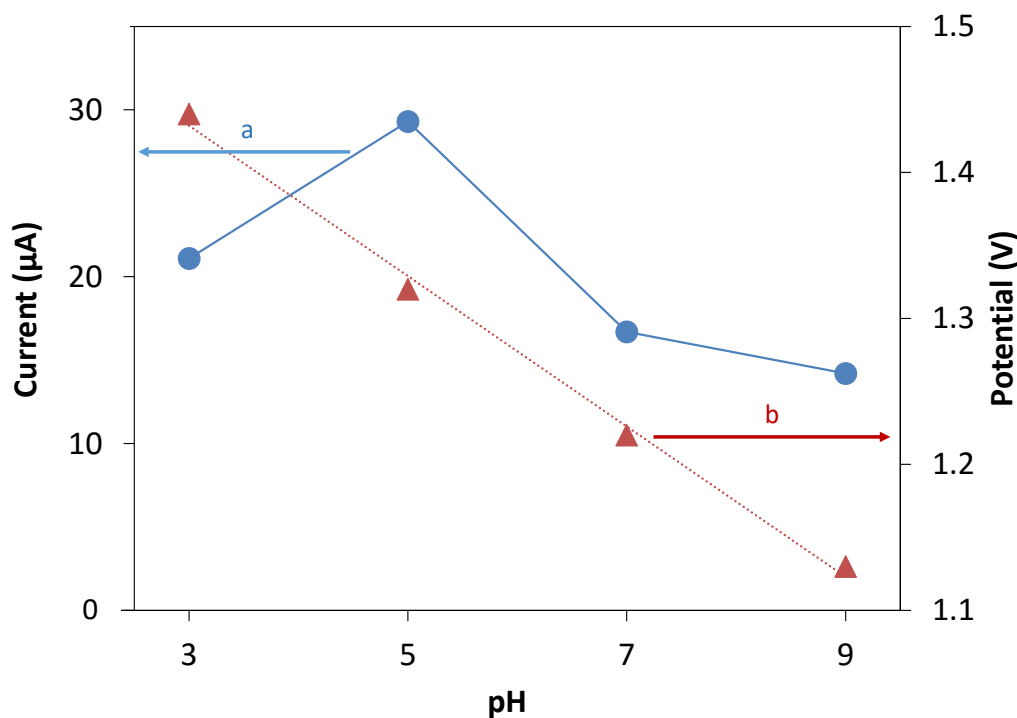


Figure 2. Dependence of (a) oxidation peak current and (b) oxidation peak potential, as a function of pH by cyclic voltammetry on MWCNT-GCE (1×10^{-5} M MPET and scan rate:

50 mVs⁻¹)

The relationship between the oxidation potential and pH is represented in Fig. 2b. It was found that peak potential shifted towards the negative potential with increasing pH, which indicates that protons are directly involved in the oxidation of MPET. The oxidation peak potential increased linearly with the pH, and the linear regression equation is:

$$E_p \text{ (V)} = 0.0515 \text{ pH} + 1.5865 \quad (r^2 = 0.995) \quad \text{Ec. 2}$$

The slope is close to the theoretical Nernstian value (0.059 V), indicating the participation of the same protons and electrons during the oxidation reaction[45].

3.5. Effect of scan rate

Cyclic voltammograms on MWCNT-GCE of 1×10^{-5} M MPET at different scan rates of 10 to 50 mVs⁻¹ were done in order to investigate the effect of scan rate. By increasing the scan rate, the peak current increases and also, peak potential shifted toward more positive values, typical effect with increasing scan rate [40, 43, 44].

Scan rate studies provide information about whether the process is controlled by diffusion or adsorption. It was found that the logarithm of peak current is linear to the logarithm of scan rate, according to the equation (2) (Fig. 3a). If the slope is 0.5, the process is under diffusion controlled, but contrary, when the slope is 1.0, the process is controlled by adsorption [44]. In this case, the slope has an interval value, which suggests a mixed control: diffusion-adsorption [46].

$$\ln I_p = 0.7608 \ln v + 0.387 \quad (r^2 = 0.991) \quad \text{Ec. 3}$$

A linear relationship between peak potential (E_p) and logarithm of v was also observed, and the expression is expressed as followed (Fig 3b):

$$E_p = 0.0501 \ln v + 1.1209 \quad (r^2 = 0.98) \quad \text{Ec. 4}$$

For an irreversible electrode process, according to Laviron [47], E_p is defined by the equation 4.

$$E_p = E^0 + \frac{R T}{\alpha n F} \ln \left(\frac{R T k^0}{\alpha n F} \right) + \frac{R T}{\alpha n F} \ln v \quad \text{Ec. 5}$$

where n is the number of electron transfer, α is the electron transfer coefficient, which is assumed to be 0.5 in totally irreversible electrode process [48], E^0 is the formal potential, k^0 is the standard rate constant of the reaction. R, T and F are gas-constant, temperature and Faraday constant respectively.

The calculated value of n is 1.02, therefore, the number of electrons (n) transferred in the oxidation of MPET is 1. It has been demonstrated in the previous section that the number of electrons and protons involved in the oxidation of MPET is the same, so the electrochemical oxidation of MPET at MWCNT-GCE is a one-electron and one-proton process.

The value of E^0 can be obtained from the intercept in the plot between E_p and v ($v = 0$). In our system the E^0 was obtained to be 1.1209 (Fig. 3c). Now, k^0 can be calculated from equation 4 taking into account the intercept of E_p vs $\ln v$, resulting in a value of 2.58 s^{-1} .

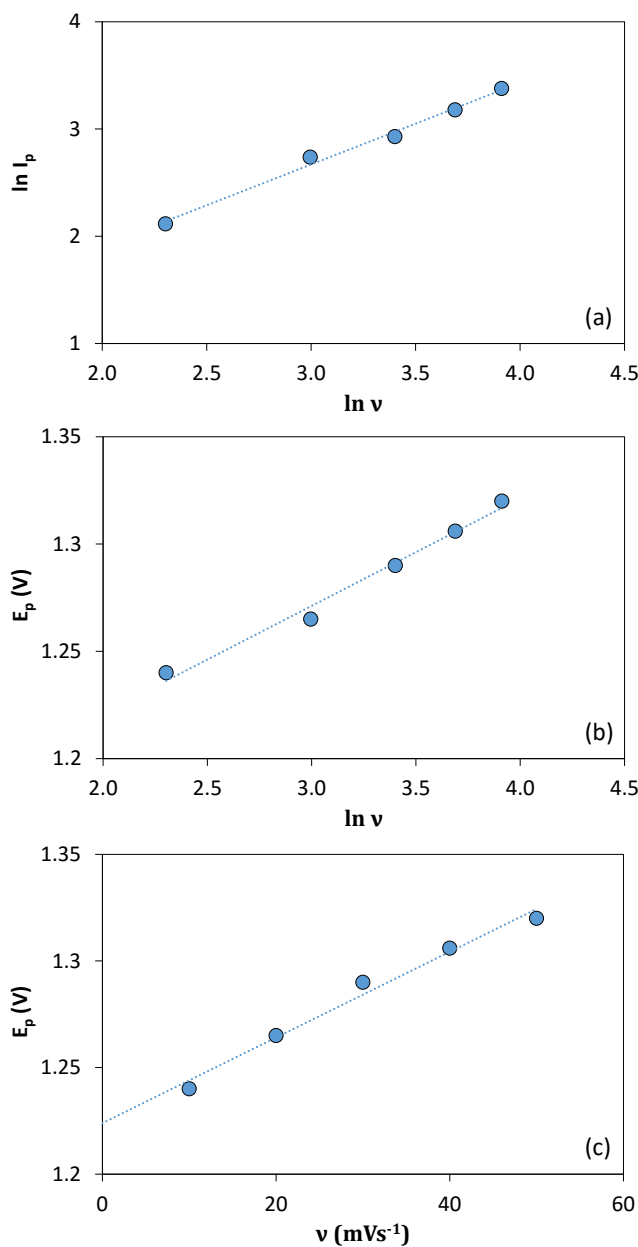


Figure 3. Effect of the scan rate on the peak current (I_p) and peak potential (E_p); (a) logarithm of peak current versus logarithm of scan rate, (b and c) variation of the peak potential versus logarithm of scan rate and scan rate respectively.

3.6. Effect of functional groups of MWCNT

The effect of the functionalization of MWCNT on the electrochemical oxidation of MPET, has been studied by CV under three different MWCNT modified GCE as working electrodes: MWCNT, MWCNT-NH₂ and MWCNT-COOH. The behavior is different for each working electrode, which can be seen from Fig. 4. The peak current increase in the order: MWCNT > MWCNT-NH₂ > MWCNT-COOH, coincident with the electrode surface area. However in the case of functionalized MWCNT where the effective area is very similar, there are major differences in the peak intensity obtained, suggesting that other factor affect to the oxidation process. During the electrochemical process, MPET is adsorbed on the electrode surface, where the electrochemical oxidation takes places, so the peak current trend may be affected also by the different strength of the adsorption due to the functionalization of MWCNT. The adsorption of MPET onto MWCNT and functionalized MWCNT was study in a previous work, by batch adsorption at three different temperatures (298, 303 and 308 K) [49]. The strength of the interaction was measured in terms of standard enthalpy (ΔH° , kJ·mol⁻¹) and follows the order MWCNT-NH₂ (101.7) > MWCNT (88.1) > MWCNT-COOH (67.4). In order to remove the factor "area" and with the aim to obtain how the adsorption affect to the electrochemical oxidation, the normalized peak current (I_p/A , measured in $\mu\text{A}/\text{cm}^2$) has been calculated. The normalized peak current decrease in te order: MWCNT-NH₂ > MWCNT > MWCNT-COOH, which is coincident with the strength of the interaction[49] (Fig. 5). As the strength of interaction increases, the stability of the MPET adsorbed increases and it has less tendency to leave the electrode surface. Thus, a higher strength implies a higher normalized peak current.

Besides, MWCNT-NH₂ presents the highest normalized peak current, since the nitrogen content in MWCNT could increase its affinity for MPET. In this case, the π - π interaction plays a key role, where the nitrogen present on the MWCNT acts as electron donor and the aromatic ring of MPET as electron receptor, favoring the adsorption of the pollutant on the electrode surface [49, 50].

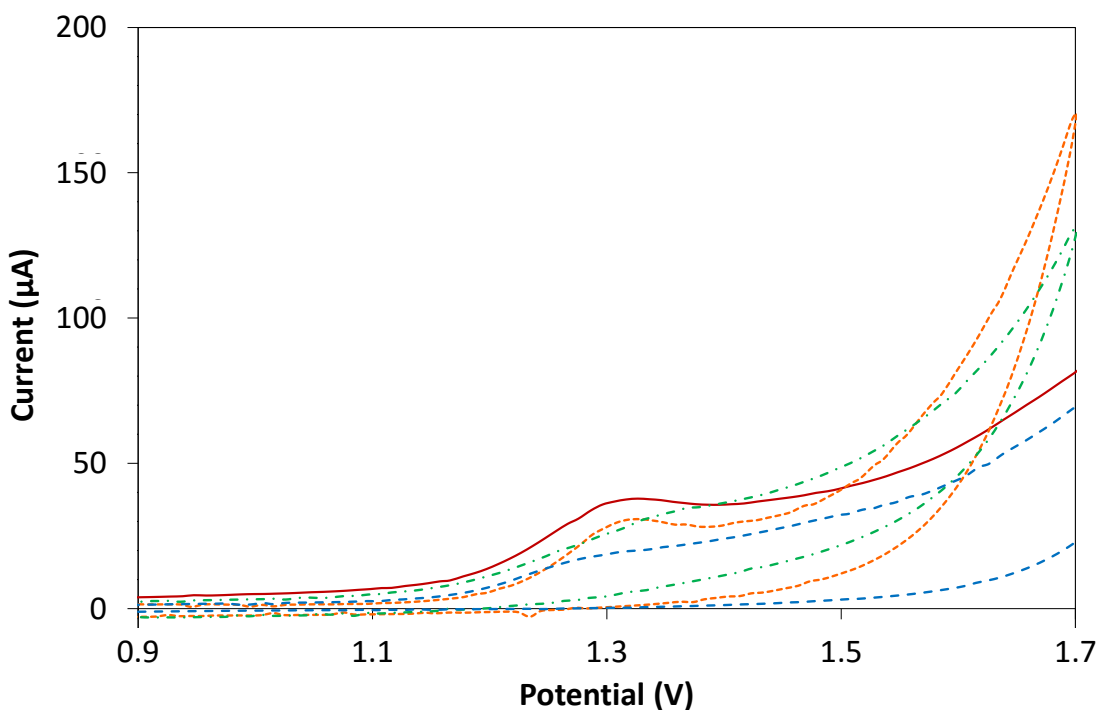


Figure 4. Effect of functionalized MWCNT on the electro-oxidation of MPET by CV (pH 5 and scan rate 50 mVs⁻¹). (—) MWCNT-GCE, (---) MWCNT-NH₂-GCE, (-·-) MWCNT-COOH-GCE and (---) Bare-GCE as working electrodes.

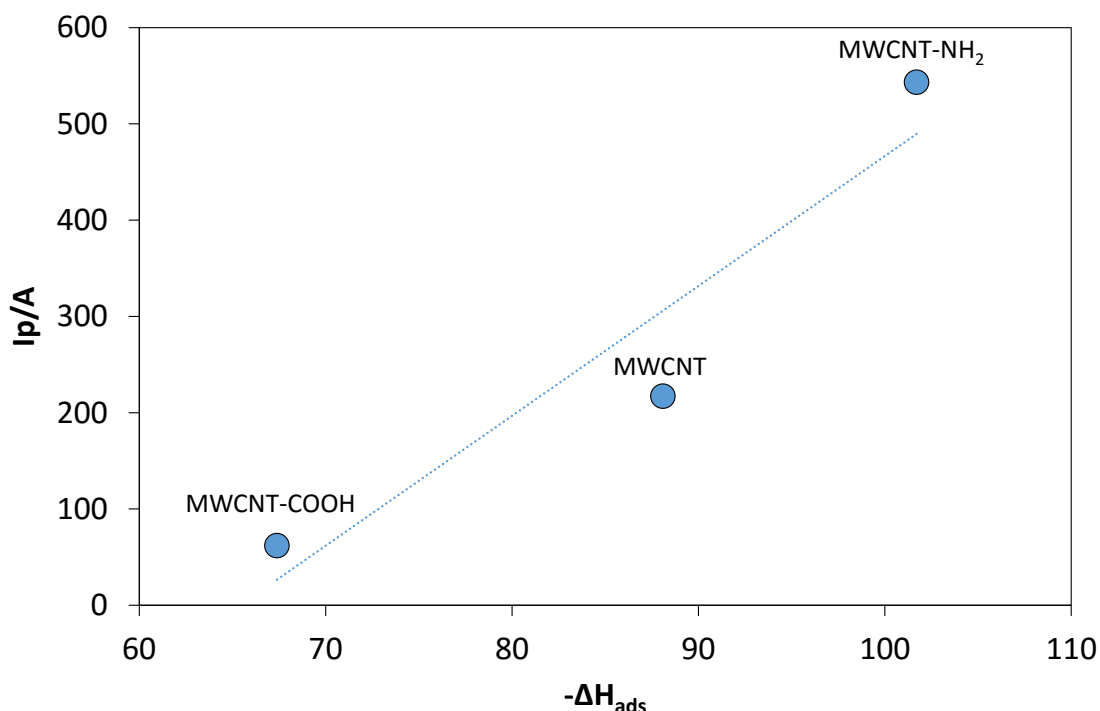


Figure 5. Influence of the enthalpy of adsorption (kJ·mol⁻¹) in the ratio (I_p/A) for electro-oxidation of MPET by CV under three different working electrodes: MWCNT-GCE, MWCNT-NH₂-GCE and MWCNT-COOH-GCE (pH 5 and scan rate 50 mVs⁻¹).

3.7. Degradation of MPET by CV

The MPET degradation has been studied by CV under two different working electrodes. Although MWCNT-NH₂ presents the highest normalized peak current, it is important to take into account that many times the electrode surface is a limiting factor. Therefore both, the effect of area and strength of interaction should be taken into account. For this reason, MWCNT and MWCNT-NH₂ modified GCE have been checked.

Both working electrode were tested by CV using a potential range of 0.9 to 1.7 V for an initial concentration of 1×10^{-5} M. The final concentration and possible intermediates were analyzed by GC-MS with the aim to estimate the percentage of degradation.

The surface area of the electrodes is a constant parameter after modification, so it is necessary to obtain the total volumen to be treated for which the maximum degradation is obtained. In this way, the optimum volumen/area (V/A) ratio will be obtained.

The oxidation of MPET was carried out initially in a total volumen of 5 mL for both working electrodes: MWCNT (V/A=37) and MWCNT-NH₂ (V/A=98) modified GCE. After one CV, the degradation of MPET was less than 31% for both working electrodes, so several cycles of CV were performed in order to degrade a new portion of pollutant at each new cycle, increasing the percentage of degradation (Fig. 6 empty symbols). With increasing the CV cycles, the degradation increases until saturation of the electrode. The maximum degradation obtained was 79 and 58% for MWCNT and MWCNT-NH₂ respectively (between 2.6 and 2.8 times greater than for one CV), keeping it constant after four CV cycles.

Since it is not possible to increase the MPET degradation by more CV cycles , the next step to increase it, is to decrease the total volume to be treated. In this way, the volume/area (V/A) ratio was modified in order to obtain a higher degradation (Fig. 6 full symbols). For MWCNT modified GCE, the degradation was carried out for a total volumen of 2.5 mL (V/A=19) and for one to five cyclic voltammetries. In this case, the degradation obtained after one CV is more than double compared with a total volume of 5 mL, and a total degradation was achieved after four CV. In the case of MWCNT-NH₂ modified GCE , the total volumen was decrease to 1.9 mL (V/A=37.3), because it is the smallest volumen that supports the experimental device and it is coincident with the first V/A ratio employed for MWCNT. In this case the maximum degradation is around 85 - 90% and more or less constant after three CV. For this working electrode there was no possible to reach a complete degradation due to the experimental constraints.

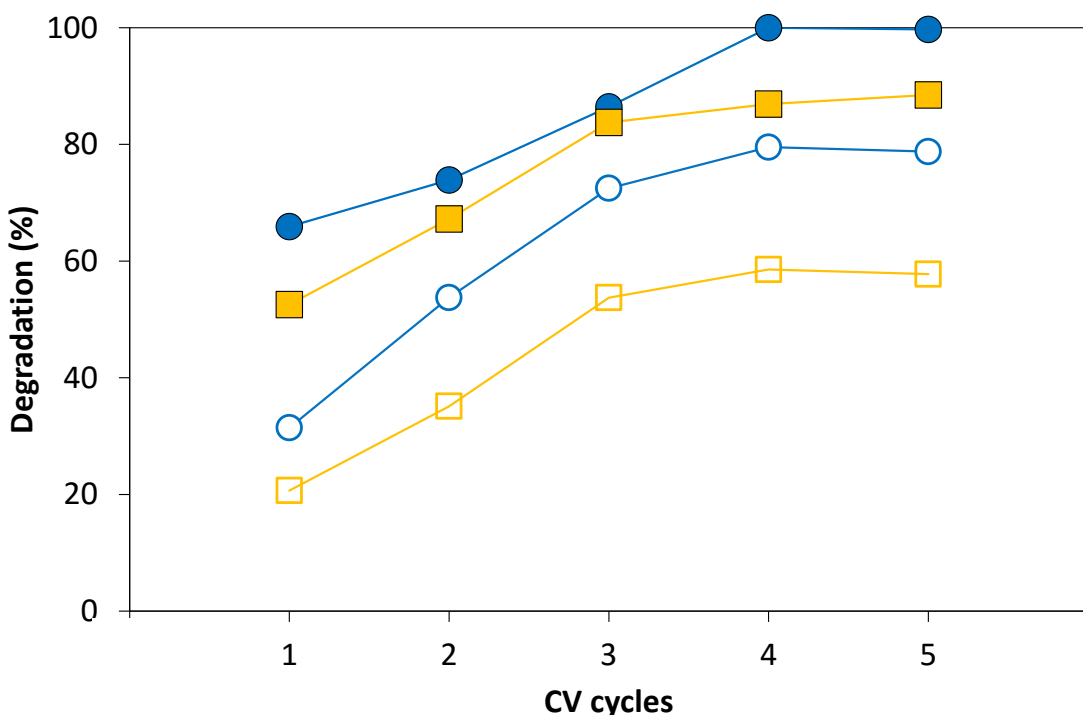


Figure 6. Degradation of MPET by CV (pH 5 and scan rate 50 mVs⁻¹) under different working electrodes and V/A ratio: (●) MWCNT-GCE, VT/A = 19, (○) MWCNT-GCE, VT/A = 37, (□) MWCNT-NH₂-GCE, VT/A = 98, (■) MWCNT-NH₂-GCE, VT/A = 37

When the V/A ratio is the same for both electrodes, the degradation is a bit higher for MWCNT-NH₂-GCE than for MWCNT-GCE, which is due to the high strength of interaction. The MPET adsorbed on the electrode surface is more stable in this case, making it more difficult to leave the electrode surface during the degradation process. However, when the volume to be treated is a limiting factor, MWCNT-GCE provides better results.

The results can be compared with the obtained by Kuramitz et al.,[3] for the electrochemical removal of p-nonylphenol with a carbon fiber electrode as working electrode. In this case, the removal efficiency was also 100%. Besides, the results obtained by electrochemical degradation, can be compared with those obtained by other authors using AOPs. Nagarnaik et al., [6] studied the degradation of APEs by UH – UV/H₂O₂, FH – Fe/H₂O₂, UFH – Fe/UV/H₂O₂. The maximum removal efficiency follow the order: UH – UV/H₂O₂ (97.1%) > UFH – Fe/UV/H₂O₂ (85.8%) > FH – Fe/H₂O₂ (95.5%) with values less or similar than the obtained in the present work. Karci et al., [14] studied the oxidation of an nonionic surfactant (NP-10) by three AOPs, whose oxidation efficiency decreases in the order: UV/H₂O₂ (100%) > Photo-Fenton (100%) > Fenton (20%). Although in some cases, a total oxidation could be obtained by AOPs, electrochemical oxidation provides a low cost and clean technology.

The final concentration and sub-products formation was analyzed by GC-MS after each test. The peak corresponding to MPET decreases after the electrochemical degradation, which confirms that oxidation takes place. On the other hand, no new peaks were observed, which suggests that complete degradation takes place, leading to the formation of carbon dioxide. The MPET adsorbed on the electrode surface in each CV cycle is completely oxidized to carbon dioxide, allowing a new amount of compound to be deposited and oxidized, until saturation of the electrode. This way provide a total mineralization of MPET by a green methodology without producing more toxic compound.

4. Conclusions

The results obtained offer an alternative for the degradation of MPET from water by cyclic voltammetry.

MWCNT modified GCE exhibits an electrocatalytic effect on the electrochemical oxidation of MPET, with a peak intensity four times higher than bare-GCE.

Different parameters were optimized in order to obtain an improved oxidation. The amount of carbon nanotubes to drop (10 µL), the pH (5.0) and the scan rate (50 mV·s⁻¹).

Functionalized MWCNT were checked in order to obtain how the functional groups on MWCNT affect to the electrochemical oxidation process. The peak current (I_p) increase in the order: MWCNT > MWCNT-NH₂ > MWCNT-COOH, coincident with the electrode surface area. The order for the normalized peak intensity (I_p/A) changes: MWCNT-NH₂ > MWCNT > MWCNT-COOH. This trend is coincident with the strength of adsorption on the electrode surface and in addition, the nitrogen presents on MWCNT-NH₂ increases the affinity for MPET through π-π interaction.

A total oxidation was obtained with MWCNT-GCE after four CV cycles under optimal conditions and V/A ratio equal to 19. In the case of MWCNT-NH₂ the maximum degradation obtained was around 90% for a V/A = 37. It was not possible to obtain complete degradation due to the restrictions of the experimental methodology. The sub-products analysis by GC-MS shows a complete mineralization of MPET.

Acknowledgements

This work was supported by the Spanish Government (contract CTQ2011-29272-C04-01, -02 and -03). Y. Patiño thanks the Government of the Principality of Asturias for a Ph.D. fellowship (Severo Ochoa Program).

References

- [1] N. Måansson, L. Sörme, C. Wahlberg, B. Bergbäck, Sources of Alkylphenols and Alkylphenol Ethoxylates in Wastewater—A Substance Flow Analysis in Stockholm, Sweden, *Water, Air, & Soil Pollution: Focus*, 8 (2008) 445-456.
- [2] M. Petrović, D. Barceló, Fate and Occurrence of Surfactants-Derived Alkylphenolic Compounds in Conventional and Membrane Bioreactor (MBR) Wastewater Treatment Plants, in: D. Fatta-Kassinos, K. Bester, K. Kümmeler (Eds.) *Xenobiotics in the Urban Water Cycle*, Springer Netherlands, 2010, pp. 375-385.
- [3] H. Kuramitz, J. Saitoh, T. Hattori, S. Tanaka, Electrochemical removal of p-nonylphenol from dilute solutions using a carbon fiber anode, *Water Research*, 36 (2002) 3323-3329.
- [4] P.C. Lee, W. Lee, In vivo estrogenic action of nonylphenol in immature female rats, *Bull. Environ. Contam. Toxicol.*, 57 (1996) 341-348.
- [5] R. White, Jobling, S., Hoare, S.A., Sumpter, J.P., Parker, M.G., Environmentally persistent alkylphenolic compounds are estrogenic. *Endocrinology*, 135 (1994).
- [6] P.M. Nagarnaik, B. Boulanger, Advanced oxidation of alkylphenol ethoxylates in aqueous systems, *Chemosphere*, 85 (2011) 854-860.
- [7] J. Kim, G.V. Korshin, A.B. Velichenko, Comparative study of electrochemical degradation and ozonation of nonylphenol, *Water Research*, 39 (2005) 2527-2534.
- [8] A. Soares, B. Guiyesse, B. Jefferson, E. Cartmell, J.N. Lester, Nonylphenol in the environment: A critical review on occurrence, fate, toxicity and treatment in wastewaters, *Environment International*, 34 (2008) 1033-1049.
- [9] G.-G. Ying, B. Williams, R. Kookana, Environmental fate of alkylphenols and alkylphenol ethoxylates—a review, *Environment International*, 28 (2002) 215-226.
- [10] B. Shao, J. Hu, M. Yang, Nonylphenol Ethoxylates and Their Biodegradation Intermediates in Water and Sludge of a Sewage Treatment Plant, *Bull. Environ. Contam. Toxicol.*, 70 (2003) 0527-0532.
- [11] A. Zgoła-Grześkowiak, T. Grześkowiak, R. Rydlichowski, Z. Łukaszewski, Determination of nonylphenol and short-chained nonylphenol ethoxylates in drain water from an agricultural area, *Chemosphere*, 75 (2009) 513-518.

[12] D.N.E.o.t.E.P.a.o.t.C.o.N.e.t.l.o.p.s.i.t.f.o.p.a.a. EC.

[13] D.o.t.E.P.a.o.t.C.E.e.a.f.f.c.a.i.t.f.o.w.p. EC, Official Journal of the EC C513 (2000) 23.10.2000.

[14] A. Karcı, I. Arslan-Alaton, M. Bekbolet, G. Ozhan, B. Alpertunga, H₂O₂/UV-C and Photo-Fenton treatment of a nonylphenol polyethoxylate in synthetic freshwater: Follow-up of degradation products, acute toxicity and genotoxicity, *Chemical Engineering Journal*, 241 (2014) 43-51.

[15] M. Catapane, C. Nicolucci, C. Menale, L. Mita, S. Rossi, D.G. Mita, N. Diano, Enzymatic removal of estrogenic activity of nonylphenol and octylphenol aqueous solutions by immobilized laccase from *Trametes versicolor*, *Journal of Hazardous Materials*, 248–249 (2013) 337-346.

[16] J.P.A. De Weert, M. Viñas, T. Grotenhuis, H.H.M. Rijnaarts, A.A.M. Langenhoff, Degradation of 4-n-nonylphenol under nitrate reducing conditions, *Biodegradation*, 22 (2011) 175-187.

[17] B. Ning, N.J.D. Graham, Y. Zhang, Degradation of octylphenol and nonylphenol by ozone – Part I: Direct reaction, *Chemosphere*, 68 (2007) 1163-1172.

[18] B. Ning, N.J.D. Graham, Y. Zhang, Degradation of octylphenol and nonylphenol by ozone – Part II: Indirect reaction, *Chemosphere*, 68 (2007) 1173-1179.

[19] Z. Qiang, Y. Nie, W. Ben, J. Qu, H. Zhang, Degradation of endocrine-disrupting chemicals during activated sludge reduction by ozone, *Chemosphere*, 91 (2013) 366-373.

[20] H. Dzinun, M.H.D. Othman, A.F. Ismail, M.H. Puteh, M.A. Rahman, J. Jaafar, Photocatalytic degradation of nonylphenol using co-extruded dual-layer hollow fibre membranes incorporated with a different ratio of TiO₂/PVDF, *Reactive and Functional Polymers*.

[21] Y. Xin, M. Gao, Y. Wang, D. Ma, Photoelectrocatalytic degradation of 4-nonylphenol in water with WO₃/TiO₂ nanotube array photoelectrodes, *Chemical Engineering Journal*, 242 (2014) 162-169.

[22] A. Dulov, N. Dulova, M. Trapido, Photochemical degradation of nonylphenol in aqueous solution: The impact of pH and hydroxyl radical promoters, *Journal of Environmental Sciences*, 25 (2013) 1326-1330.

[23] H. Suzuki, S. Araki, H. Yamamoto, Evaluation of advanced oxidation processes (AOP) using O₃, UV, and TiO₂ for the degradation of phenol in water, *Journal of Water Process Engineering*, 7 (2015) 54-60.

- [24] A. Asghar, A.A. Abdul Raman, W.M.A. Wan Daud, Advanced oxidation processes for in-situ production of hydrogen peroxide/hydroxyl radical for textile wastewater treatment: a review, *Journal of Cleaner Production*, 87 (2015) 826-838.
- [25] Y.J. Feng, X.Y. Li, Electro-catalytic oxidation of phenol on several metal-oxide electrodes in aqueous solution, *Water Research*, 37 (2003) 2399-2407.
- [26] A.M. Polcaro, S. Palmas, Electrochemical Oxidation of Chlorophenols, *Industrial and Engineering Chemistry Research*, 36 (1997) 1791-1798.
- [27] A.C. Mariel, B.P. Alejandra, P.C.C. Silvia, Developmental toxicity and risk assessment of nonylphenol to the South American toad, *Rhinella arenarum*, *Environmental Toxicology and Pharmacology*, 38 (2014) 634-642.
- [28] P.A. Babay, E.E. Romero Ale, R.F. Itria, E.T. Becquart, B. Thiele, D.A. Batistoni, Simplified determination of lipophilic metabolites of nonylphenol ethoxylates: method development and application in aqueous samples from Buenos Aires, Argentina, *Journal of Environmental Monitoring*, 10 (2008) 443-452.
- [29] C.-D. Dong, C.-W. Chen, C.-F. Chen, Seasonal and spatial distribution of 4-nonylphenol and 4-tert-octylphenol in the sediment of Kaohsiung Harbor, Taiwan, *Chemosphere*, 134 (2015) 588-597.
- [30] M. Kanaki, A. Nikolaou, C.A. Makri, D.F. Lekkas, The occurrence of priority PAHs, nonylphenol and octylphenol in inland and coastal waters of Central Greece and the Island of Lesvos, *Desalination*, 210 (2007) 16-23.
- [31] S. Esteban, M. Gorga, M. Petrovic, S. González-Alonso, D. Barceló, Y. Valcárcel, Analysis and occurrence of endocrine-disrupting compounds and estrogenic activity in the surface waters of Central Spain, *Science of The Total Environment*, 466–467 (2014) 939-951.
- [32] E.D. Y. Patiño, S. Ordóñez, Pre-concentration of a polychlorinated n-alkane and an alkylphenol on carbonaceous materials in fixed bed columns, *Chemical Engineering Journal*, Submitted (2016).
- [33] M. Moyo, L.R. Florence, J.O. Okonkwo, Improved electro-oxidation of triclosan at nano-zinc oxide-multiwalled carbon nanotube modified glassy carbon electrode, *Sensors and Actuators B: Chemical*, 209 (2015) 898-905.
- [34] C.B. Jacobs, M.J. Peairs, B.J. Venton, Review: Carbon nanotube based electrochemical sensors for biomolecules, *Analytica Chimica Acta*, 662 (2010) 105-127.

[35] S. Iijima, Helical microtubules of graphitic carbon, *Nature*, 354 (1991) 56-58.

[36] M. Moyo, J.O. Okonkwo, N.M. Agyei, A Novel Hydrogen Peroxide Biosensor Based on Adsorption of Horseradish Peroxidase onto a Nanobiomaterial Composite Modified Glassy Carbon Electrode, *Electroanalysis*, 25 (2013) 1946-1954.

[37] Q. Zheng, P. Yang, H. Xu, J. Liu, L. Jin, A simple and sensitive method for the determination of 4-n-octylphenol based on multi-walled carbon nanotubes modified glassy carbon electrode, *Journal of Environmental Sciences*, 24 (2012) 1717-1722.

[38] J.J. Gooding, A. Chou, J. Liu, D. Losic, J.G. Shapter, D.B. Hibbert, The effects of the lengths and orientations of single-walled carbon nanotubes on the electrochemistry of nanotube-modified electrodes, *Electrochemistry Communications*, 9 (2007) 1677-1683.

[39] N. Alexeyeva, T. Laaksonen, K. Kontturi, F. Mirkhalaf, D.J. Schiffrin, K. Tammeveski, Oxygen reduction on gold nanoparticle/multi-walled carbon nanotubes modified glassy carbon electrodes in acid solution, *Electrochemistry Communications*, 8 (2006) 1475-1480.

[40] R.H. Patil, R.N. Hegde, S.T. Nandibewoor, Electro-oxidation and determination of antihistamine drug, cetirizine dihydrochloride at glassy carbon electrode modified with multi-walled carbon nanotubes, *Colloids and Surfaces B: Biointerfaces*, 83 (2011) 133-138.

[41] R. Jain, S. Sharma, Glassy carbon electrode modified with multi-walled carbon nanotubes sensor for the quantification of antihistamine drug pheniramine in solubilized systems, *Journal of Pharmaceutical Analysis*, 2 (2012) 56-61.

[42] R. Jain, J.A. Rather, Voltammetric determination of antibacterial drug gemifloxacin in solubilized systems at multi-walled carbon nanotubes modified glassy carbon electrode, *Colloids and Surfaces B: Biointerfaces*, 83 (2011) 340-346.

[43] L. Fotouhi, M. Alahyari, Electrochemical behavior and analytical application of ciprofloxacin using a multi-walled nanotube composite film-glassy carbon electrode, *Colloids and Surfaces B: Biointerfaces*, 81 (2010) 110-114.

[44] B. Dogan-Topal, B. Bozal-Palabıyık, B. Uslu, S.A. Ozkan, Multi-walled carbon nanotube modified glassy carbon electrode as a voltammetric nanosensor for the sensitive determination of anti-viral drug valganciclovir in pharmaceuticals, *Sensors and Actuators B: Chemical*, 177 (2013) 841-847.

- [45] T. Łuczak, Preparation and characterization of the dopamine film electrochemically deposited on a gold template and its applications for dopamine sensing in aqueous solution, *Electrochimica Acta*, 53 (2008) 5725-5731.
- [46] D.K.G. Jr., *Cyclic Voltammetry, Simulation and Analysis of Reaction Mechanisms*, New York, 1993.
- [47] E. Laviron, Adsorption, autoinhibition and autocatalysis in polarography and in linear potential sweep voltammetry, *Journal of Electroanalytical Chemistry and Interfacial Electrochemistry*, 52 (1974) 355-393.
- [48] C. Li, Electrochemical determination of dipyridamole at a carbon paste electrode using cetyltrimethyl ammonium bromide as enhancing element, *Colloids and Surfaces B: Biointerfaces*, 55 (2007) 77-83.
- [49] Y. Patiño, E. Díaz, S. Ordóñez, E. Gallegos-Suarez, A. Guerrero-Ruiz, I. Rodríguez-Ramos, Adsorption of emerging pollutants on functionalized multiwall carbon nanotubes, *Chemosphere*, 136 (2015) 174-180.
- [50] J. Fan, W. Yang, A. Li, Adsorption of phenol, bisphenol A and nonylphenol ethoxylates onto hypercrosslinked and aminated adsorbents, *Reactive and Functional Polymers*, 71 (2011) 994-1000.



Capítulo VI

Conclusiones

En este capítulo se encuentran las principales conclusiones derivadas del presente trabajo

VI. Conclusiones

En esta Tesis se propone una nueva metodología para la eliminación de contaminantes emergentes. El método se basa en un proceso en dos etapas: pre-concentración mediante ciclos de adsorción-desorción, sobre materiales carbonosos – carbones activos, nanofibra de carbono, nanotubos de carbono y grafito de alta superficie – seguido por un tratamiento electroquímico de la disolución resultante, cuya viabilidad ha sido estudiada mediante voltamperometría diferencial de pulso (DPV) y voltamperometría cíclica (CV). La metodología ha sido probada con tres compuestos modelo, como representativos de contaminantes emergentes: ácido nalidíxico (NAL), 1,8-diclorooctano (DCO) y 2-(4-metilfenoxi)etanol (MPET).

La principal conclusión derivada de esta Tesis Doctoral es la validez de la metodología propuesta para la eliminación de NAL y MPET como representativos de productos farmacéuticos y alquilfenoles etoxilados, respectivamente. En el caso del DCO, aunque se obtuvo la pre-concentración del compuesto, no fue posible llevar a cabo la degradación electroquímica, debido a la ausencia de grupos funcionales electroquímicamente activos.

Las conclusiones específicas obtenidas para ambos procesos, pre-concentración y degradación, se explican a continuación.

6.1. Pre-concentracion

6.1.1. Experimentos en discontinuo

Se llevaron a cabo experimentos en discontinuo para determinar el equilibrio de adsorción. se seleccionaron diferentes materiales carbonosos como adsorbentes: carbones activos (GC-900 and GF-40), nanofibra de carbono (CNF), nanotubos de carbono (MWCNT) y grafito de alta superficie (HSAG-500). Se probaron además tres nanotubos de carbono funcionalizados: MWCNT-COOH, MWCNT-NH₂ and N-CNT, para obtener el efecto de la química superficial en el proceso de adsorción. Las conclusiones a partir de los resultados obtenidos son las siguientes:

- Para todos los adsorbentes, la capacidad de adsorción es un orden de magnitud superior para DCO que para MPET y NAL. Esto es debido a la hidrofobicidad del DCO que aumenta su afinidad por los materiales carbonosos. Teniendo en cuenta los distintos adsorbentes, la capacidad de adsorción sigue por lo general el orden: GC-900 > GF-40 > HSAG-500 > MWCNT > CNF, coincidente con el área superficial de los materiales, con excepción de los carbones activos (los cuales presentan la mayor área superficial, pero con una accesibilidad limitada por su carácter microporoso). Los resultados muestran por lo tanto que la capacidad de adsorción depende de ambos, las propiedades del adsorbato y la morfología del adsorbente.
- La funcionalización de los nanotubos de carbono influye en el mecanismo de adsorción. para el NAL y DCO, los nanotubos de carbono presentan la mayor capacidad de adsorción, lo que resalta el efecto negativo de los grupos funcionales en la superficie del adsorbente. Para el MPET, la tendencia es diferente: N-CNT > MWCNT-NH₂ > MWCNT-COOH > MWCNT. N-CNT tiene la mayor área superficial, pero su pequeño diámetro de poro dificulta la adsorción de NAL y DCO debido a su volumen molecular, mayor que el del MPET.
- La adsorción de NAL y MPET se ajusta a los modelos propuestos de Freundlich y Langmuir, pero en el caso del DCO, el modelo de Langmuir no resulta válido para predecir la adsorción.
- Se ha demostrado la naturaleza exotérmica del proceso de adsorción mediante la obtención de la entalpía estándar, la cual indica una fuerte interacción entre el adsorbente y el compuesto modelo. Los valores de la energía estándar de Gibbs, muestran la naturaleza espontánea del proceso. En el caso de la entropía estándar, su valor negativo y cercano a cero, implica que la adsorción prácticamente no afecta al orden de las especies adsorbidas.
- La fuerza de la adsorción aumenta cuando tienen lugar interacciones π-π entre los anillos aromáticos del adsorbente (NAL y MPET) y el material carbonoso, especialmente con N-CNT, debido a su alto contenido en nitrógeno, remarcado por la presencia de nitrógeno cuaternario.

6.1.2. Experimentos de adsorción en lecho fijo

Se llevó a cabo la pre-concentración de los compuestos modelo mediante ciclos de adsorción-desorción en una columna de lecho fijo, sobre tres materiales carbonosos – carbón activo (GF-40), nanotubos de carbono (MWCNT) y grafito de alta superficie (HSAG-500) -. Se obtuvieron las curvas de ruptura y se ajustaron a los modelos BDST, Thomas y Yoon-Nelson.

- Los tiempos de ruptura y saturación obtenidos a partir de la curva de ruptura aumentan según el orden: HSAG-500 < MWCNT < GF-40. La pendiente de la curva sigue el orden inverso, lo que indica un lento transporte de masa debido la disminución del coeficiente de difusión o transferencia de masa.
- Las capacidades de adsorción siguen el orden: GF-40 > MWCNT > HSAG-500, justificado por la morfología y superficie química. la tendencia de la capacidad de adsorción normalizada ($\text{mg adsorbato}/\text{m}^2 \text{ adsorbente}$) es: MWCNT > GF-40 > HSAG-500, ya que MWCNT es el adsorbente con mayor volumen de mesoporos.
- En todos los casos las curvas de ruptura fueron ajustadas por los modelos BDST, Thomas y Yoon-Nelson, los cuales permiten estimar los parámetros de adsorción. Los modelos BDST y de Thomas permiten predecir la capacidad de adsorción, presentando menores desviaciones respecto a los datos experimentales el modelo BDST. El modelo de Yoon-Nelson puede usarse para predecir el tiempo necesario para alcanzar el 50% de la curva de ruptura.
- La concentración obtenida para los tres compuestos sigue el orden: DCO > MPET > NAL. Este orden es debido a las interacciones $\pi-\pi$ entre el MPET y dificulta la desorción, especialmente para el NAL que presenta dos anillos aromáticos, frente a uno del MPET.
- Aunque GF-40 presenta la mayor capacidad de adsorción, no es posible llevar a cabo la pre-concentración con este adsorbente. Por el contrario se obtuvo la pre-concentración de los compuestos con MWCNT y HSAG-500 como adsorbentes, alcanzándose los mejores resultados con MWCNT:
- Los MWCNT se presentan como el mejor adsorbente para la pre-concentración de los tres compuestos modelo, ya que presenta la mayor capacidad de adsorción normalizada y el mayor poder de pre-concentración. El factor de pre-concentración obtenido sigue el orden: DCO (3.4) > MPET (2.8) > NAL (2.1).

6.2. Electrochemical degradation

Tras la pre-concentración, se lleva a cabo la degradación mediante técnicas electroquímicas. Se estudió la degradación electroquímica de NAL y MPET mediante voltamperometría de pulso diferencial (DPV) y voltamperometría cíclica (CV) respectivamente, en un electrodo de trabajo de carbón vítreo (GCE) y electrodo de carbón vítreo modificado - MWCNT-GCE, MWCNT-COOH-GCE and MWCNT-NH₂-GCE -.

- La degradación es irreversible para ambos, NAL y MPET, ya que no se obtienen picos reducción/oxidación. Para el NAL tiene lugar una reducción irreversible, mientras que tiene lugar una oxidación irreversible para el MPET.
- El GCE modificado con MWCNT, presenta efecto electrocatalítico para ambos compuestos, aumentando la corriente de pico al emplear los MWCNT. La nanoestructura de los MWCNT permite la adsorción y pre-concentración del contaminante en la superficie del electrodo.
- Las condiciones óptimas de operación son: pH 5.0 y velocidad de barrido 50 mVs⁻¹. La cantidad óptima de MWCNT a impregnar en la superficie del electrodo es igual a 10 µL.
- En el caso del NAL los MWCNT funcionalizados presentan mejores resultados que GCE, pero peores en comparación con los MWCNT sin funcionalizar. Por el contrario, para el MPET, la intensidad de pico normalizada (I_p/A) varía en el orden: MWCNT-NH₂ > MWCNT > MWCNT-COOH, coincidente con la fuerza de adsorción en la superficie del electrodo, añadiendo que el nitrógeno presente en MWCNT-NH₂ aumenta su afinidad por el MPET a través de interacciones π-π.
- Se obtiene la degradación completa del NAL con GCE modificado con MWCNT, bajo las condiciones óptimas, tras 15 DPV y una relación volumen/área (V/A) igual a 8. Se confirmó la completa degradación y se identificaron dos sub-productos diferentes.
- Se alcanzó la oxidación completa del MPET bajo las condiciones óptimas con GCE modificado con MWCNT tras 4 CV y una relación V/A de 19. Con GCE modificado con MWCNT-NH₂, la máxima degradación obtenida fue del 90% con una relación V/A de 37. No fue posible una completa degradación debido a las restricciones de la metodología experimental. El análisis de los subproductos de oxidación muestran una completa mineralización del MPET.

Capítulo VII

Conclusions

The main conclusions drawn from the present research are summarized in this chapter

VII. Conclusions

A new methodology for the removal of emerging pollutants has been proposed in this Thesis. The method is based on a two-steps process: a pre-concentration by adsorption-desorption cycles onto carbonaceous materials - activated carbons, carbon nanofiber, carbon nanotubes and high surface area graphite - followed by an electrochemical treatment of the resulting solution, whose feasibility has been studied by differential pulse voltammetry (DPV) and cyclic voltammetry (CV). The methodology has been tested with three model compound as representative of emerging pollutants: nalidixic acid (NAL), 1,8-diclorooctane (DCO), and 2-(4-methylphenoxy)ethanol (MPET).

The main conclusion derived from this PhD Thesis is the validity of the proposed methodology for the removal of NAL and MPET as representative of pharmaceutical products and alquilphenol ethoxylates, respectively. In the case of DCO, although the pre-concentration was achieved, its electrochemical degradation was no possible due to the absence of electrochemically active functional groups.

The specific conclusions obtained for both process, pre-concentration and degradation are explained below.

7.1. Pre-concentration

7.1.1. Batch adsorptions experiments

Batch adsorption experiments were carried out in order to determine adsorption equilibria. Different carbonaceous materials have been selected as adsorbent: activated carbons (GC-900 and GF-40), carbon nanofiber (CNF), multiwall carbon nanotube (MWCNT) and high surface area graphite (HSAG-500). Three functionalized carbon nanotubes were tested: MWCNT-COOH, MWCNT-NH₂ and N-CNT, in order to study the effect of surface chemistry on the adsorption process. The following conclusions have been withdrawn from the obtained data:

- For all the adsorbents, the adsorption capacity is one order of magnitude higher for DCO than for MPET and NAL. This is so because of the DCO hydrophobicity which increases its affinity for carbonaceous materials. Taking into account the different adsorbents, the adsorption capacity, in general, follows the order: GC-900 > GF-40 > HSAG-500 > MWCNT > CNF, coincident with the external surface area of the materials, with the exception of the activated carbons (which present the highest surface area, but with limited accessibility because of their microporous character). The results show that the adsorption capacity depends on both, the adsorbate properties and the adsorbent morphology.
- The functionalization of carbon nanotubes influences on the adsorption behaviour. For NAL and DCO, MWCNT exhibits the highest adsorption, which points out the negative effect of surface functional groups. For MPET the trend is different: N-CNT > MWCNT-NH₂ > MWCNT-COOH > MWCNT. N-CNT has the highest surface area, but its small pore diameter hinders the adsorption of NAL and DCO due to their molecular volume, larger than MPET.
- The adsorption of NAL and MPET fit well for both Freundlich and Langmuir models, but in the case of DCO Langmuir model is not able to predict adsorption performance.
- Concerning to the thermodynamic parameters, the exothermic nature of the adsorption process has been corroborated by obtaining the standard enthalpy (ΔH°), which indicates a stronger interaction between the adsorbents and the model compounds. The values of the standard Gibbs free energy (ΔG°), shows the spontaneous nature of the adsorption process. In the case of the standard entropy (ΔS°), the negative values are close to zero, indicates that the adsorption practically does not affect in the order of the adsorbed species.
- The strength of the adsorption is higher when $\pi-\pi$ interactions take place between the aromatic rings of the adsorbent (NAL and MPET) and the carbonaceous materials, especially with N-CNT due to its higher nitrogen content, highlighting the presence of quaternary nitrogen.

7.1.2. Fixed bed adsorption experiments

The pre-concentration of the model compounds were carried out by adsorption-desorption cycles in a fixed bed column, onto three different carbonaceous materials – activated carbon (GF-40), multiwall carbon nanotube (MWCNT) and high surface area graphite (HSAG-500) -. The breakthrough curves were obtained and modeled by BDST, Thomas and Yoon-Nelson models.

- The breakthrough time and saturation time obtained from the breakthrough curves increase in the order: HSAG-500 < MWCNT < GF-40. The slope of the curve follows the reverse order, which indicates a slower mass transport due to decrease diffusion coefficient or mass transfer.
- The adsorption capacities follow the order: GF-40 > MWCNT > HSAG-500, justified by the morphology and chemistry surface. The trend for the normalized adsorption capacity ($\text{mg adsorbate}/\text{m}^2 \text{ adsorbent}$) is: MWCNT > GF-40 > HSAG-500, since MWCNT is the adsorbent with the highest mesoporous volume.
- In all cases the breakthrough curves can be modeled by BDST, Thomas and Yoon-Nelson models allowing to estimate the adsorption parameters. BDST and Thomas models can be used to predict the adsorption capacity, with a less deviation by BDST model. Yoon-Nelson model can be applied in order to predict the time needed for 50% of adsorbate breakthrough.
- The concentration obtained for the three adsorbents follow the order: DCO > MPET > NAL. It can be due to the π - π interaction of MPET and NAL with the carbon materials since this interaction hinders desorption, especially for NAL with two aromatic ring against MPET, which have one aromatic ring.
- Although GF-40 presents a high adsorption capacity, the pre-concentration was not achieved with this adsorbent. Contrary, the pre-concentration was reached with MWCNT and HSAG-500 as adsorbents, with better results for MWCNT.
- MWCNT is the best option to pre-concentrate the three model compounds, since it presents the highest normalized adsorption capacity and the greatest concentration powder. The pre-concentration factor follows the order: DCO (3.4) > MPET (2.8) > NAL (2.1).

7.2. Electrochemical degradation

After pre-concentration, the degradation is carried out by electrochemical techniques. The electrochemical degradation of NAL and MPET was studied by differential pulse voltammetry (DPV) and cyclic voltammetry (CV) respectively by commercial glassy carbon electrode (GCE) and modified-GCE – MWCNT-GCE, MWCNT-COOH-GCE and MWCNT-NH₂-GCE - as working electrode.

- The degradation is irreversible for both NAL and MPET, since no reduction/oxidation peaks were obtained. For NAL, an irreversible reduction peak was obtained, whereas an irreversible oxidation peak was observed for MPET.
- The MWCNT modified GCE shows an electrocatalytic effect for both NAL and MPET, since the peak current improves comparing with bare-GCE. The nanostructure of MWCNT allows the adsorption and pre-concentration of the pollutant on the electrode surface.
- The optimal operating conditions are pH 5.0 and scan rate of 50 mVs⁻¹. The ideal amount of carbon nanotubes to drop results in 10 µL.
- In the case of NAL, functionalized MWCNT results in a higher peak current than for bare-GCE, but worst result in comparison with MWCNT-GCE. Contrary, for MPET the normalized peak intensity (I_p/A) changes: MWCNT-NH₂ > MWCNT > MWCNT-COOH coincident with the strength of adsorption on the electrode surface and in addition, the nitrogen presents on MWCNT-NH₂ increases the affinity for MPET through π-π interaction.
- A complete degradation of NAL was obtained with MWCNT modified GCE, under optimal conditions after 15 DPV and a volume/area (V/A) ratio equal to 8. The complete degradation has been confirmed and two different sub-products have been identified.
- A total oxidation of MPET was obtained with MWCNT-GCE after 4 CV under optimal conditions and V/A ratio equal to 19. Using MWCNT-NH₂ modified GCE, the maximum degradation obtained was around 90% for V/A ratio=37 and a complete degradation was not possible due to the restrictions of the experimental methodology. The sub-products analysis shows a complete mineralization of MPET.